

**NIR Based Process Analytical Technology:
In-line Residual Moisture Determination for a
Complete Batch Inspection
of Lyophilized End-Products**

Inauguraldissertation

zur

Erlangung der Würde eines Doktors der Philosophie
vorgelegt der
Philosophisch-Naturwissenschaftlichen Fakultät
der Universität Basel

von

Lars Sukowski

aus Tübingen, Deutschland

Basel, 2003

Genehmigt von der Philosophisch-Naturwissenschaftlichen Fakultät auf Antrag von

Prof. Dr. Hans Leuenberger

PD Dr. Michel Ulmschneider

PD Dr. Stephan Marrer

Basel, den 18. November 2003

Dekan Prof. Dr. Marcel Tanner

To my parents

Heide and Ingolf

Acknowledgements

I would like to thank the conductors of this thesis Prof. Dr. Hans Leuenberger of the Pharmacenter of the University of Basel and PD Dr. Michel Ulmschneider of the Quality Control department of the F. Hoffmann-La Roche Ltd. in Basel. They were the scientific supervisors who provided their expertise, constructive criticism, and guidance for the emergence of this current work.

Dr. Gerhard Paulini initiated this study in collaboration with PD Dr. Stephan Marrer, who simultaneously acted as co-referee. The thesis was carried out under the direction of Dr. Rainer Schmidt and Dr. Alfred Humm. I would like to deeply thank them especially for their unreserved support and confidence. Their cordial company and the unrestricted possibilities and liberty granted to me made the two years an unforgettable time.

Furthermore, I was allowed to take advantage of the resources of the Quality Control department presided over by Dr. Rolf Altermatt, to whom my thanks are especially due for his social fellowship.

The good esprit de corps among colleagues led to many personal friendships. Some supported my activity with their direct help, ideas, attention or others just gave me their company. In particular I would like to mention my fellow dissertation colleague Frauke Russell, who definitely contributed to a pleasant working atmosphere and was truly enriching. Thanks go to Pascal Chalus who showed serious commitment to the project and was a pleasant fellow. Of course, all the other team members must be mentioned as well, such as Florence Piétrain, Aurélie Edmond, Dr. Yves Roggo, and Dr. Christoph Roeseler, who supported me with their company, man power, feedback and revisions during the editorial of this thesis.

My general thanks go to F. Hoffmann-La Roche Ltd. in Basel for the generous disposal of financial and non-financial resources to render this work possible.

Additionally, I extend my thanks to Dipl. Ing. Meinhard Missbach, who not only put equipment to my disposal sometimes through unconventional means, but also offered his time of assistance for case related and other questions.

Last but not least, I would like to express my sincere gratitude to my parents Heide and Ingolf Sukowski for their support during almost three decades of training and education. They have, beyond any doubt, made a major contribution to all I have been able to achieve so far.

Table of contents

SUMMARY	11
ZUSAMMENFASSUNG	15
RESUME	19
ABBREVIATIONS	23
CHAPTER A: PREFACE	27
A.1 INTRODUCTION	27
A.1.1 <i>The production line</i>	28
A.1.2 <i>Quality control</i>	28
CHAPTER B: THEORETICAL BACKGROUND	31
B.1 REGULATORY CONTEXT	31
B.1.1 <i>Current Good Manufacturing Practice (cGMP)</i>	31
B.1.2 <i>Process analytical technology</i>	35
B.2 LYOPHILIZATION	44
B.2.1 <i>Phase diagram of water</i>	44
B.2.2 <i>Freeze drying process cycle</i>	45
B.2.3 <i>Meltback</i>	50
B.2.4 <i>Process control</i>	50
B.2.5 <i>Discussion</i>	51
B.3 NEAR-INFRARED SPECTROSCOPY (NIRS)	56
B.3.1 <i>NIR - historical review</i>	56
B.3.2 <i>NIR theory</i>	58
B.3.3 <i>NIR sampling modes</i>	65
B.3.4 <i>Instrumentation</i>	67
B.3.5 <i>Chemometrics and multivariate data analysis (MVDA)</i>	76
B.3.6 <i>MVDA applied to NIR spectroscopy</i>	89
B.3.7 <i>Discussion</i>	93
B.4 KARL FISCHER TITRATION	98
B.4.1 <i>Theoretical background</i>	98
B.4.2 <i>Volumetric KF titration</i>	100
B.4.3 <i>Coulometric titration</i>	101
B.4.4 <i>Sources of error</i>	102

CHAPTER C: EXPERIMENTAL PART	105
C.1	SCOPE
C.2	ORIGINAL SITUATION
C.2.1	<i>Measurement parameters</i>
C.2.2	<i>Preparation of the samples</i>
C.2.3	<i>Determination of water content</i>
C.2.4	<i>Baseline Situation, Product A</i>
C.3	EVALUATION OF THE APPROPRIATE ANALYSIS SYSTEM
C.3.1	<i>Preselection of spectrometers</i>
C.3.2	<i>Assessment parameters</i>
C.3.3	<i>Assessment oriented on the European Pharmacopoeia</i>
C.3.4	<i>Comparison of model performance</i>
C.3.5	<i>Conclusions</i>
C.4	STATIC SCAN MODE EVALUATION
C.4.1	<i>Procedure</i>
C.4.2	<i>Discussion and conclusions</i>
C.5	VALIDATED QUALIFICATION OF PRODUCT B VIALS
C.5.1	<i>Control and calibration</i>
C.5.2	<i>External validation</i>
C.5.3	<i>Results and discussion</i>
C.5.4	<i>Conclusions</i>
C.6	THE PROCESS SIMULATOR
C.6.1	<i>Dynamic scan mode evaluation</i>
C.6.2	<i>Conclusions</i>
C.7	VALIDATED QUANTITATIVE MODEL PRODUCT B
C.7.1	<i>Preconditions</i>
C.7.2	<i>Method development</i>
C.7.3	<i>Robustness testing</i>
C.7.4	<i>Conclusions</i>
C.8	QUANTITATIVE MODEL PRODUCT C 150 MG
C.8.1	<i>Scope</i>
C.8.2	<i>Control and calibration</i>
C.8.3	<i>At-line inspection</i>
C.8.4	<i>Discussion</i>
CHAPTER D: BUSINESS CASE	193
D.1	INVESTMENT ACCOUNTING IN PHARMACEUTICAL PRODUCTION
D.1.1	<i>Methods of investment appraisal</i>
D.1.2	<i>Business case in-line PAT</i>
D.1.3	<i>Conclusions</i>

CHAPTER E: OVERALL CONCLUSIONS	203
E.1 DISCUSSION AND CONCLUSIONS	203
<i>E.1.1 Scope.....</i>	<i>203</i>
<i>E.1.2 Original situation.....</i>	<i>203</i>
<i>E.1.3 Evaluation of the appropriate analysis system</i>	<i>204</i>
<i>E.1.4 The process simulator</i>	<i>205</i>
<i>E.1.5 Investment accounting.....</i>	<i>206</i>
E.2 OUTLOOK	207
CHAPTER F: APPENDICES.....	211
F.1 GLOSSARY OF TERMS.....	211
<i>F.1.1 Spectroscopic definitions</i>	<i>211</i>
<i>F.1.2 Statistics.....</i>	<i>214</i>
F.2 TABLES AND FIGURES	220
<i>F.2.1 Sample preparation.....</i>	<i>220</i>
<i>F.2.2 Evaluation of the appropriate analysis system</i>	<i>222</i>
<i>F.2.3 Static scan mode evaluation.....</i>	<i>223</i>
<i>F.2.4 Qualitative model Product B.....</i>	<i>224</i>
<i>F.2.5 Dynamic scan mode evaluation</i>	<i>229</i>
<i>F.2.6 Validated quantitative model Product B.....</i>	<i>235</i>
<i>F.2.7 Quantitative model Product C 150 mg.....</i>	<i>240</i>
F.3 CONVERSION OF WAVELENGTH UNITS	246
CURRICULUM VITAE.....	247

Summary

The social welfare systems of financially strong countries have come under increasing pressure in recent years. The factors responsible included, not least of all, the demographic trend which led to a steady increase in the elderly, a section of the population which is expensive in welfare terms. At the same time, drug manufacturers' lucrative patent rights ran out and numerous generics manufacturers rushed onto the market. Research and development, which was becoming increasingly expensive, did not however produce a corresponding increase in the number of commercial successes to make up for the lost sales. Instead, over time a chasm opened up between the investment costs and the number of pharmaceuticals brought to market by the research-based industry. Also, the authorities made increasingly stringent quality demands, particularly of companies operating worldwide.

Consequently, pharmaceutical industry managers had to increase both capacity and quality, whilst active substances and the corresponding drug forms became increasingly complex and expensive to process. In the past it has been possible to make only inadequate improvements in this situation by means of traditional quality control in accordance with the current pharmacopoeia. Instead, a need arose for modern monitoring systems which the US health authority FDA intended to meet by supporting 'process analytical technologies' (PAT). PAT was regarded as a generic term for production-based systems for monitoring critical quality and performance parameters. The aim was firstly to increase the quality of the finished products and secondly to reduce manufacturing costs in the long term.

Within the Galenical Bulk Operations department at F. Hoffmann-La Roche Ltd. in Basel this approach was to be investigated in a feasibility study. The example used was a freeze-drying line, since lyophilization is by nature a technique with complex process stages affecting quality which are difficult to monitor. The residual moisture content is recognized as being one of the most critical parameters besides product sterility. Traditionally, the residual water content on release was determined by quality control performed using random Karl Fischer (KF) titrations. If the mean of these determinations did not meet the specifications, the entire batch had to be destroyed,

with isolated outliers occasionally causing large numbers of rejects. The ability to reject individual containers that lay outside the specifications therefore offered considerable potential for financial savings, although this could be done only if a complete inspection was made for this test criterion.

The aim of this study was to develop an in-line analytical method for determining the residual water content. One of the biggest challenges was the line speed of up to 270 objects to be analyzed per minute. In a first stage a non-destructive residual water analysis was to be demonstrated on a laboratory scale using the various lyophilizates. Then, to check the applicability of this method in a dynamic inspection, a prototype was to be used to simulate the production line. If feasibility was established, account was also to be taken of cost-effectiveness in the investments needed to implement the program.

Near-infrared (NIR) spectroscopy was used as non-destructive method since in principle it allows the residual moisture content to be determined in line. The starting situation and any special product characteristics were investigated in an initial evaluation phase. Two spectrometers from different suppliers which used different techniques were compared as regards use in an in-line application. The most suitable AOTF device was used to perform further studies on a laboratory scale. This allowed the feasibility of residual water determination compared to KF titration to be established with good accuracy.

Collaboration with a mechanical engineering company was necessary from the outset in order to design a future process automation system in accordance with the specific requirements. A simulator was developed on the basis of this process unit which allowed all the existing formats to be fed to the NIR sensor at process speed. Another tool was created at the same time which might later be used for the development and validation of lyophilization cycles. In addition, rapidly changing regulatory requirements necessitated customer-specific modifications to the software. Dynamic calibrations were produced and in this way NIR analysis was performed successfully with moving samples.

Manual and semi-automatic off-line and at-line inspections of whole batches were performed on the basis of validated NIR models and provided a better insight into individual product characteristics. Qualitative and quantitative chemometric calibration methods were used, based on principal components analysis (PCA) and partial least squares (PLS), and compared as regards their advantages and disadvantages. It emerged that qualitative models were better suited to routine operation.

The findings of these analyses were used for an investment calculation which showed that amortization could be achieved in less than two years and thus supported the decision for in-line implementation of the analytical technique.

This successful feasibility study was used as a reference for other PAT projects which were then to be run at F. Hoffmann-La Roche Ltd. at earlier stages in product development.

Zusammenfassung

In den letzten Jahren ist das Sozialsystem der finanziell starken Länder immer stärker unter Druck geraten. Verantwortlich dafür war nicht zuletzt die demographische Entwicklung, die zu einem stetig anwachsenden Anteil der älteren und damit kostenintensiven Bevölkerungsschicht führte. Gleichzeitig liefen lukrative Lizenzrechte pharmazeutischer Unternehmen aus und zahlreiche Generika Hersteller drängten in den Markt. Die immer teurer werdende Forschung und Entwicklung führte aber nicht gleichermaßen zu gesteigerten Erfolgen, um diese Umsatzeinbußen auszugleichen. Stattdessen liefen mit der Zeit die Investitionskosten und die Anzahl der zur Marktreife gebrachten Pharmaka der forschenden Industrie scherenförmig auseinander. Dazu kam, daß die Behörden besonders an weltweit agierende Unternehmen immer höhere Qualitätsanforderungen stellten.

Demzufolge mußte das Management der pharmazeutischen Industrie sowohl Kapazität als auch Qualität steigern, während die Wirkstoffe und deren Arzneiformen immer komplexer und aufwendiger zu verarbeiten wurden. In der Vergangenheit konnten mithilfe der traditionellen Qualitätskontrolle entsprechend der gültigen Pharmakopöe diesbezüglich nur unzureichende Verbesserungen erzielt werden. Stattdessen entstand der Bedarf nach modernen Überwachungssystemen, dem die U.S. amerikanische Gesundheitsbehörde FDA mit der Unterstützung sogenannter Process Analytical Technologies (PAT) gerecht zu werden wollte. PAT wurde als ein Oberbegriff für produktionsnahe Monitoringsysteme von kritischen Qualitäts- und Leistungsparametern verstanden. Hierdurch sollten einerseits die Qualität der Endprodukte gesteigert und andererseits langfristig die Herstellungskosten gesenkt werden.

Innerhalb der Abteilung Galenical Bulk Operations der F. Hoffmann-La Roche AG, Basel, sollte dieser Ansatz in einer Machbarkeitsstudie überprüft werden. Als Beispiel wurde eine Gefriertrocknungslinie herangezogen, da die Lyophilisation naturgemäß eine Technik mit komplexen qualitätsrelevanten Prozessschritten ist, die schwierig zu überwachen sind. Neben der Produktsterilität wurde der Gehalt der Restfeuchte als einer der kritischsten Parameter erkannt. Traditionell fand die Freigabebestimmung des

Restwassergehalts der Qualitätskontrolle mit stichprobenweisen Karl Fischer (KF) Titrationen statt. Entsprechend der Mittelwert dieser Bestimmungen nicht den Spezifikationen, so mußte die gesamte Charge vernichtet werden und verursachte von Zeit zu Zeit durch einzelne Ausreißer hohen Ausschuss. Die Möglichkeit einzelne Behältnisse außerhalb der Spezifikationen auszusortieren bot daher ein umfangreiches Potential an finanziellen Einsparungen, die nur durch eine Totalinspektion dieses Prüfkriteriums erreicht würde.

Ziel dieser Arbeit war es, eine in-line Analysenmethode für die Bestimmung des Restwassergehalts zu entwickeln. Eine der größten Herausforderungen stellte die Liniengeschwindigkeit von bis zu 270 zu analysierenden Objekten pro Minute dar. In einem ersten Schritt sollte eine nicht destruktive Restwasseranalyse in den verschiedenen Lyophilisaten im Labormaßstab bewiesen werden. Um anschließend die Anwendbarkeit dieser Methode in einer dynamischen Inspektion überprüfen zu können, sollte mit einem Prototyp die Produktionslinie simuliert werden. Bei gegebener Machbarkeit sollte auch die Wirtschaftlichkeit der bei einer Implementierung anfallenden Investitionen berücksichtigt werden.

Die Nah-Infrarot (NIR) Spektroskopie wurde als nicht destruktive Methode herangezogen, die prinzipiell eine in-line Restfeuchtebestimmung erlaubt. In einer ersten Evaluationsphase wurden die Ausgangslage und spezielle Produkteigenschaften untersucht. Zwei Spektrometer verschiedener Lieferanten und Techniken wurden auf ihre Leistungsfähigkeit im Hinblick auf eine in-line Applikation miteinander verglichen. Das am besten geeignete AOTF Gerät wurde verwendet, um weitere Studien im Labormaßstab durchzuführen. Hierbei konnte die Machbarkeit der Restwasserbestimmung im Vergleich zur KF Titration mit guter Genauigkeit belegt werden.

Von Anfang an war eine Zusammenarbeit mit einer Maschinenbaufirma notwendig, um eine zukünftige Prozessautomation entsprechend den spezifischen Anforderungen zu konzipieren. In Anlehnung an eine solche Prozessanlage wurde ein Simulator entwickelt, der es erlaubte alle vorkommenden Formate in Prozessgeschwindigkeit dem NIR Sensor zuzuführen. Gleichzeitig entstand ein weiteres Werkzeug, das später zur Entwicklung und Validierung von Lyophilisationszyklen verwendet werden könnte.

Darüber hinaus machten sich schnell verändernde Behördenanforderungen kundenspezifische Anpassungen der Software notwendig. Dynamische Kalibrationen wurden erstellt und die NIR Analyse mit bewegten Proben konnte so erfolgreich durchgeführt werden.

Auf Basis von validierten NIR Modellen wurden manuelle und halbautomatische off- und at-line Inspektionen ganzer Chargen durchgeführt und ermöglichten einen besseren Einblick in die individuelle Produktbeschaffenheit. Dabei sind qualitative und quantitative chemometrische Kalibrationsansätze basierend auf Principal Components Analysis (PCA) bzw. Partial Least Squares (PLS) verfolgt und entsprechend ihrer Vor- und Nachteile miteinander verglichen worden. Es stellte sich heraus, daß qualitative Modelle für den Routinebetrieb besser geeignet waren.

Die Erkenntnisse dieser Analysen wurden für eine Investitionsrechnung herangezogen, die eine Amortisation in weniger als zwei Jahren ergab und damit die Entscheidung für eine in-line Implementierung der Analysentechnik unterstützte.

Diese erfolgreiche Machbarkeitsstudie diente als Referenz für weitere PAT Projekte, die anschließend in der F. Hoffmann-La Roche AG zu früheren Zeitpunkten in der Produktentwicklung unternommen werden sollten.

Résumé

Depuis quelques années, le système social des pays développés est l'objet de pressions croissantes, liées entre autres, au développement démographique, à savoir l'accroissement constant du nombre de personnes âgées, une catégorie de la population particulièrement exigeante en termes de prestations sociales. Dans le même temps, l'expiration des brevets des produits majeurs des compagnies pharmaceutiques dominantes le marché a provoqué une affluence de fabricants de médicaments génériques. Les activités de recherche et développement – dont le coût ne cesse d'augmenter – n'ont malheureusement pas abouti à une hausse des succès commerciaux, susceptible de compenser les pertes de chiffre d'affaires. Bien au contraire, l'écart entre les frais d'investissement et le nombre de spécialités pharmaceutiques commercialisées s'est creusé, sans oublier des exigences de qualité de plus en plus rigoureuses imposées par les autorités, notamment aux compagnies d'envergure internationale

Ainsi, les dirigeants de l'industrie pharmaceutique sont dans l'obligation d'accroître à la fois la capacité de production et la qualité, alors que les principes actifs et leurs formes galéniques deviennent de plus en plus complexes et chers à fabriquer. En l'occurrence, le contrôle de qualité classique tel qu'on le concevait par le passé, en conformité avec la pharmacopée en vigueur, ne permet plus des améliorations satisfaisantes. C'est pourquoi la mise en place de systèmes de surveillance modernes a été nécessaire. Ainsi l'administration américaine Food and Drug Administration (FDA), a tenté d'anticiper ce besoin en encourageant les «technologies analytiques des procédés» (Process Analytical Technologies ou PAT). PAT a été défini comme un terme générique pour désigner l'ensemble des systèmes de contrôle des paramètres critiques de qualité et de rendement, implantés directement la chaîne de production. En premier lieu, l'objectif est l'amélioration de la qualité des produits finaux et dans un second temps, la réduction des coûts de fabrication à long terme.

Cette nouvelle approche a fait l'objet d'une étude de faisabilité au sein de la division Galenical Bulk Operations de la société F. Hoffmann-La Roche SA à Bâle. La chaîne de lyophilisation a été retenue à titre d'exemple. Par nature, la lyophilisation implique des

étapes complexes ayant une incidence sur la qualité finale et qui sont difficiles à surveiller. Outre la stérilité des produits, la teneur en humidité résiduelle constitue ici l'un des paramètres les plus critiques. En contrôle qualité, l'analyse de la teneur en eau résiduelle est déterminée habituellement par la méthode titrimétrique de Karl Fischer (KF), sur la base d'échantillons prélevés au hasard. Si la valeur moyenne des titrages n'est pas conforme aux spécifications, un lot complet peut être détruit, suite à des anomalies isolées. Ainsi, la possibilité de rejeter individuellement les produits hors spécifications représente un véritable gain. Cela impose toutefois le contrôle de l'ensemble des échantillons du lot fabriqué.

L'objectif de ce travail était le développement d'une méthode d'analyse «in-line» pour la détermination de la teneur en eau résiduelle. Le défi majeur provenait de la vitesse de la chaîne de production, pouvant atteindre jusqu'à 270 échantillons à analyser par minute. Il s'agissait dans un premier temps, d'établir la faisabilité d'une analyse non destructive de l'eau résiduelle dans les différents lyophilisats, à l'échelle du laboratoire. Ensuite, il fallait simuler la chaîne de production à l'aide d'une installation prototype pour pouvoir vérifier l'applicabilité de cette méthode lors d'une inspection dynamique «in-line». Une fois la faisabilité technologique établie, il s'agissait également de faire entrer en ligne de compte la rentabilité des investissements nécessaires à la mise en œuvre opérationnelle.

La spectroscopie proche infrarouge (PIR) a été envisagée, dès le départ, car elle permet la détermination non destructive et rapide de l'humidité résiduelle. Une première phase d'évaluation a consisté en l'analyse de la situation de départ puis de l'inventaire des caractéristiques particulières ou critiques des produits concernés. Les performances de deux spectromètres de fabricants différents, n'employant pas la même technique, ont été confrontées en vue d'une application «in-line». Le système le mieux adapté, utilisant la technologie AOTF, a été retenu pour la conduite des études à l'échelle du laboratoire. La faisabilité du dosage de l'eau résiduelle par PIR a pu être établie puis la méthode validée avec une bonne précision par rapport au titrage KF.

Dès le départ, il a fallu collaborer avec un fabricant reconnu de lignes de production pour concevoir l'automatisation ultérieure du procédé, conformément aux exigences de Roche. Un simulateur a été mis au point pour reproduire les vitesses de défilement des

échantillons de la ligne de production actuellement en place. Il a également permis de soumettre à la mesure PIR l'ensemble des formats possibles de contenants. A l'avenir le simulateur pourra être utilisé pour le développement et la validation de cycles de lyophilisation d'autres produits. Les exigences fréquemment réactualisées des autorités relatives aux logiciels ont, par ailleurs, imposé une adaptation permanente du programme d'application «in-line». Enfin, la réalisation de calibrations dynamiques a permis la mise en œuvre de l'analyse PIR sur les échantillons en mouvement avec les vitesses de défilement requises.

Des inspections «off-line» et «at-line» manuelles et semi-automatiques de lots entiers comprenant des dizaines de milliers d'échantillons, ont été effectuées avec succès sur la base des modèles PIR validés. Des modèles de calibration qualitatives et quantitatifs, reposant sur l'analyse en composantes principales (ACP) et la régression des moindres carrés partiels (PLS, Partial Least Squares), ont été appliqués puis comparés du point de vue de leurs avantages et de leurs inconvénients. Ainsi les modèles qualitatifs se sont révélés particulièrement adaptés en usage de routine.

Les résultats accumulés au cours de cette étude ont été pris en compte pour une estimation de la rentabilité et du retour sur investissement. Ainsi, un amortissement sur moins de deux ans peut être envisagé, plaidant en faveur d'une mise en œuvre «in-line» de cette technologie.

L'étude de faisabilité ainsi couronnée de succès servira de référence aux projets PAT futurs, qui concerneront principalement des médicaments encore dans un stade précoce de leur développement galénique.

Abbreviations

ABC	A utomatic B aseline C orrection
AOTF	A cousto O ptical T unable F ilter
API	A ctive P roduct I ngredient
CDER	C enter for D rug E valuation and R esearch
CFR	C ode of F ederal R egulations
SF	S wiss F rancs
CSV	C omputerized S ystem V alidation
DR	D eviation R eport
EC	E uropean C ommunity
EMA	E uropean M edicines E valuation A gency
FCV	F ull C ross V alidation
FDA	F ood and D rug A dministration
FT	F ourier T ransformation
cGMP	c urrent G ood M anufacturing P ractice
GxP	Collective term for G ood C linical / L aboratory / M anufacturing P ractice
ICH	I nternational C onference on H armonisation of Technical requirements for Registration of Pharmaceuticals for Human Use
IR	I nvestigation R eport
IRR	I nternal R ate of R eturn
KF	K arl F ischer

ME	M oney E quivalent
MSC	M ultiplicative S catter C orrection
MVDA	M ultivariate D ata A nalysis
NIR	N ear- I nfrared
NIRA	N ear- I nfrared A nalysis
NIRS	N ear- I nfrared S pectroscopy
NIST	N ational I nstitute for S tandardization
NPV	N et P resent V alue
OOS	O ut of S pecification
ORA	O ffice of R egulatory A ffairs
PAT	P rocess A nalytical T echnology
PATRIOT	PAT Review, I nspection, and O ffice of Pharmaceutical Science Policy T eam
PC	P inciple C omponent
PCA	P rincipal C omponent A nalysis
PIC	P harmaceutical I nspection C onvention
PICS	P harmaceutical I nspection C ooperation S cheme
PLS	P artial L east S quares
PTFE	P oly- T etra- F luoro- E thylen (Teflon [®])
QA	Q uality A ssurance
QC	Q uality C ontrol

R&D	R esearch and D evelopment
RF	R adio F requency
RMSEC/P	R oot M ean S quares E rror of C alibration / P rediction
SD	S tandard D eviation
SD_{rel}	R elative S tandard D eviation
SECV	S tandard E rror of C ross V alidation
SEP	S tandard E rror of P rediction
SG	S avitzky- G olay
SIMCA	S oft I ndependent M odeling of C lass A nalogy
S / N	S ignal to N oise
SOP	S tandard O peration P rocedure
Swissmedic	Swiss health authority, formerly known as Schweizerisches Heilmittelinstitut (SHI)
TGA	T hermogravimetry
USP	U nited S tates P harmacopoeia
UV	U ltra V iolet
VIS	V isible
WHO	W orld H ealth O rganization

The following names are trademarks of:

Luminar Freespace 3030 [®]	Brimrose Corporation of America, Baltimore, MD, USA
MB160D [®]	ABB Bomem, Québec, Canada
Rapid Content-Analyzer [®]	FOSS NIRSystems, Inc., Silver Spring, MD, USA
The Unscrambler [®]	CAMO ASA, Oslo, Norway
Snap! [®]	Brimrose Corporation of America, Baltimore, MD, USA
Grams / 32 AI [®]	Thermo Galactic's, Salem, NH, USA
Vision [®]	FOSS NIRSystems, Inc., Silver Spring, MD, USA
Spectralon [®]	Labsphere, Sutton, NH, USA
Dosimat 701 KF Titrino [®]	Metrohm AG, Herisau, Switzerland
Hydranal [®]	Sigma-Aldrich Laborchemikalien GmbH, Seelze, Germany

Chapter A: Preface

A.1 Introduction

In order to raise the claim of continuously improving the quality control and quality assurance in an operating environment largely dominated by regulatory requirements, economic factors, and scientific research the F. Hoffmann-La Roche Ltd. was open to introduce technical innovations to their production environment. This study was conducted by the Galenical Bulk Operations department located at Basel with the aim of increasing the productivity of the lyophilization line and to raise the quality of its output.

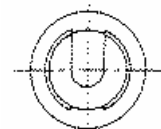
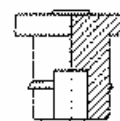
The residual moisture in lyophilized products is a critical quality parameter influencing not only the product's appearance and solubility but the shelf life as well. For that reason the moisture limits are registration relevant and this feature is considered in batch release.

Based on their responsibility towards patients and their customers the pharmaceutical industries utilize all technical options to face safety issues. Only a small spot check was required by the European authorities to prove the conformity and the pharmaceutical quality of a product. In order to control the production stream as best as possible and to increase the productivity a lot of samples were drawn and analyzed in certain intervals. Nevertheless the test procedure still relied on random testing, because it was up to now the only way to assure the quality of thousands of products produced in a day. Clusters of products deviating in water content caused by momentary production problems could not always be detected. Although the production is strictly controlled by GMP guidelines a latent uncertainty is still present and still OOS products are sold. This can lead to health risks and expensive product recalls accompanied by a substantial loss of image.

A.1.1 The production line

Initially glass vials were washed, then sterilized in a heating tunnel and transferred into the sterile room. The bottles were filled with the product solution and afterwards special stoppers were put on the bottleneck. These stoppers had a side opening and two rasters. The first raster allowed to fix the stopper on the vial without covering the opening completely.

After filling the vials were automatically gathered upon trays and then transferred to one of the four freeze dryers. The lyophilization procedure was followed by temperature and conductivity probes positioned in some vials in critical areas. The vacuum in the cabinet was broken with pure nitrogen once the entire drying cycle was completed. In a first step the pressure was raised up to 700 mbar and the shelves were moved up in order to push the stoppers into the bottle neck, and close the vials completely. Then the cabinet pressure was balanced to atmospheric pressure. Due to the pressure gradient from the outside to the inside, the vials were sealed very tightly. The trays were unloaded from the dryers and crimped directly. As a last step, the vials were either controlled visually by operators or after being washed inspected optically by an automated camera system to detect defects of the crimping, the glass or the cake appearance.



A.1.2 Quality control

Under routine conditions three samples per dryer were drawn and sent to the Quality Control (QC) department. The legally registered analysis method for residual moisture determination in lyophilizates was the widely used volumetric Karl Fischer (KF) titration. The average result of the three samples was considered as the release value for the entire lot.

High costs incurred as this method was time consuming, sample destructive, and required environment polluting reagents. Depending on the product the QC department invoiced per batch release between 30 to 240 minutes. Already some years ago this fact induced a change request for the most frequent product at that time. Furthermore a non-destructive near-infrared (NIR) determination with a laboratory

grating spectrometer was registered as official release method. Excluding any preparative step, one measurement took no more than one minute and reduced the costs by two-thirds.

Occasionally, out of specification (OOS) vials were detected. Apparently some of the thousands of vials in each dryer load got shut between their neighbors leading to an insufficient shelf contact and thereby a worse thermal conductivity. This caused unsatisfactory drying results for rare exceptions in comparison to the total number of vials. Some unsuccessful studies were conducted to reproduce such supposed phenomena. Due to natural process variations differences in water content of the end product seemed to be unavoidable. Two resulting scenarios were possible. Either the outliers were not detected, but delivered with the rest of the compliant product bearing potential health risks and expensive product recalls. Or the whole batch had to be destroyed due to the bad results of the outliers being randomly sampled. The latter caused equally a high loss of money, a decrease of the service level, and an increase of the workload for the production staff.

The aim was to prevent both scenarios: the delivery of any OOS vial and the destruction of an entire batch. Obviously the narrow random sampling did not really allow a valuable evaluation for a representative batch average.

A total in-line inspection of the crimped product instead, would offer the opportunity to check the batch for OOS vials and to reject them simultaneously. By this way it could be guaranteed that the remaining and finally delivered charge meets the specifications. This could only be performed by a non-invasive, non-destructive, and thereby precise and reliable method.

Near-infrared analysis (NIRA) fulfills these requirements since NIR radiation penetrates glass and no further sample preparation like dilution is necessary. The feasibility of this determination on a laboratory scale concerning one product was already proven.

With regard to a process analytical technology (PAT), it had to be demonstrated that the NIR measurement was also feasible for the other products of the department as well. In the following chapters only the synonyms of the products' names given in Table A-1 were used. To allow an in-line measurement without slowing down the production

line's speed, much higher measurement velocities would be required than in the laboratory application. Given that the line's maximum speed was 270 vials per minute and the automated analyzer should be integrated directly behind the crimping machine, the performance in speed and accuracy of NIRA had to be evaluated. For security reasons a further margin of about 10 % was added to the maximum velocity. Accordingly a spectrometer able to perform 5 accurate sample analyses per second had to be identified.

Synonym	Product A		Product B	Product C (cooling product)		Product D
Description	non-steroidal, analgesic, anti-inflammatory agent		antiviral fusion inhibitor	monoclonal antibody for cancer therapy		antiviral agent
Dosage [mg]	20	40	90	150	400	500
Target fill mass [mg] (anhydrous)	100	100	108	300	500	500
Max. water content	2 %		3 %	3 %		3 %
Vial diameter [mm]	16.25		16.25	26.5	42.5	22.0
Max. stream velocity [objects / min]	270		270	150	65	150
Lot size	37,000		37,000	14,000	3,500	20,000

Table A-1: Attributes and registered values of the freeze-dried products in question. Product C 400 mg and Product D were either under development or revalidation and were just mentioned for completeness.

To calibrate a quantitative or qualitative NIR model much preparatory work had to be conducted. A reference method was needed to provide the actual values in relation to the acquired spectra. Obviously this work could not be done in an operative area; otherwise the whole production would be interrupted. Subsequently such an apparatus had to be maintained in a laboratory and then transferred to the in-line application.

The final decision about the realization of the PAT project should be considered with regard to financial aspects.

Chapter B: Theoretical background

B.1 Regulatory context

Pharmaceuticals are products that need to comply with highest demands in terms of quality, efficacy and safety. In the last decades the pharmaceutical quality systems went through a great development. The driver of this process was to a high extend the body of cGxP rules and regulations, a collective term for current Good Manufacturing, Laboratory and Clinical Practices.

As these regulations are binding requirements for any new installation in a pharmaceutical production especially the GMP should be presented structurally and textually concerning NIR spectroscopy.

The application of these rules is regularly verified by the administrative authorities. From the point of view of an internationally operating Swiss pharmaceuticals company especially the Swissmedic, the U.S. American Food and Drug Administration (FDA), and the European Medicines Evaluation Agency (EMA) are of relevance. The applied standards for the inspections are oriented at the 'best practices' of the competitors, and the technological progress.

B.1.1 Current Good Manufacturing Practice (cGMP)

In order to ensure the quality of medicines, various pharmacopoeias provide guidelines concerning the development, production, storage, and analytics of medical products.^{1, 2, 3, 4} These guidelines are of a statutory nature and ensure uniform quality of medicines and test methods.

In 1969 the World Health Organization (WHO) published for the first time basic principles of an advisory nature⁵ for good practice in the manufacture and quality control of drugs with the aim of improving the quality of medicines.⁶ Since then, various organizations^{7, 8, 9} have published additional, in some cases expanded principles. These

cGxP guidelines are now mandatory for pharmaceuticals manufacturers. Figure B-1 illustrates the geographic scope of GMP guidelines.

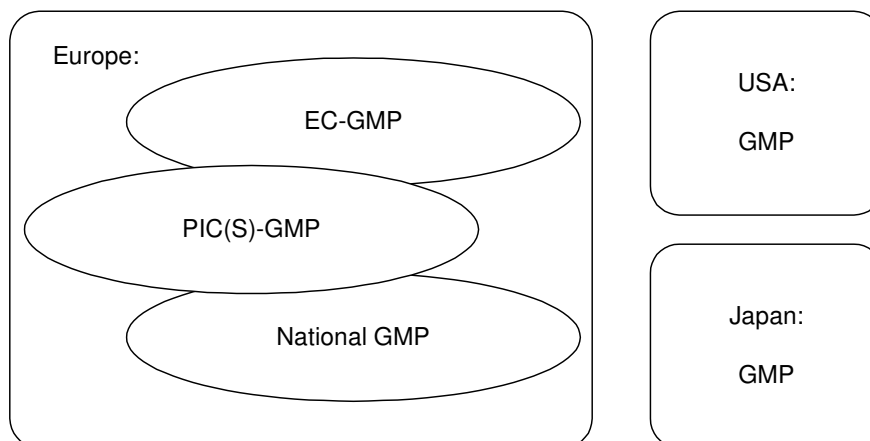


Figure B-1: Overview of relevant GMP guidelines. GMP = Good Manufacturing Practices, EC = European Community, PIC = Pharmaceutical Inspection Convention, and its successor organization PICS = Pharmaceutical Inspection Cooperation Scheme.

All GMP guidelines are based on pharmaceutical quality by prior verification of the correct functioning of equipment (qualification) and manufacturing methods (validation). The term qualification here means proof of correct operation of equipment and apparatus. In accordance with EC / PIC GMP guidelines, validation is generally taken to mean provision of proof that methods, procedures and processes together with the physical facilities necessary for this purpose actually give rise to the expected results.⁵ By rights, validation may only be performed on previously qualified equipment. However, care must be taken in quality assurance that validation and qualification processes do not generate costs which exceed the benefit of the minimized risk of error.¹⁰

The International Conference in Harmonization of Technical Requirements for Registration of Pharmaceuticals for Human Use (ICH) founded in 1990 is a unique project that brings together the regulatory authorities and experts from the pharmaceutical industry of Europe, Japan and the United States to discuss scientific and technical aspects of product registration. The purpose is to make recommendations on ways to achieve greater harmonization in the interpretation and application of technical guidelines and requirements for product registration in order to reduce or obviate the need to duplicate the testing carried out during the research and

development of new medicines. The objective of such harmonization is a more economical use of human, animal, and material resources, and the elimination of unnecessary delay in the global development and availability of new medicines. In meantime safeguards on quality, safety and efficacy, and regulatory obligations to protect public health should be maintained.⁵

B.1.1.1 Validation of analytical methods

The validation of analytical methods is a complex technical matter of confirming the trustworthiness of the method. Validation ensures that, under routine conditions, the method yields predictive, reproducible, and accurate results. Depending on the application of the analytical method the parameters indicated in the following table must be taken into account.

Parameter	Definition
Accuracy	Determination of the deviation from the true value
Precision	A measure of the degree of reproducibility. Mathematically, precision is expressed by the standard deviation of a number of measurements
Linearity	Proportionality between measurement result and quantity of substance
Robustness	Susceptibility of failure or resistance to outside influences and changes to measurement parameters
Specificity	An indication of the extend to which the method used is capable to distinguish the compound to be detected and other constituents
Detection limit	The smallest signal that can still be detected with adequate reliability
Limit of quantification	The smallest quantity of the substance to be determined that can still be quantitatively detected with adequate accuracy and precision

Table B-1: Parameters used to evaluate analytical methods.^{6, 11}

The acceptance criteria for validation of a method should be specified in advance in accordance with current practice. Details of actual international criteria are given in the references.¹²

B.1.1.2 Qualification of analytical apparatus

Qualified laboratory apparatus must be used to validate analytical methods. The purpose of qualifying analytical apparatus is to test and guarantee the proper functioning of the apparatus by means of appropriate testing. Depending on the principle of measurement (e.g. UV / VIS), the pharmacopoeias state limits which must be achieved.

New purchases and development of instruments should proceed in accordance with the V-model.⁵ Subsequent routine conditions determine user requirements, which are then used to define system specifications and the technical design. Design qualification provides proof that the system has been planned in accordance with user requirements and with relevant standards. User and supplier often agree a performance specification for this purpose. After purchase or development, installation qualification is performed. This is taken to mean documented proof that the system in question has been delivered in its entirety and correctly installed. Proper functioning of the apparatus is ensured in the context of operational qualification, while performance qualification provides proof that the corresponding apparatus operates according to plan in routine use.

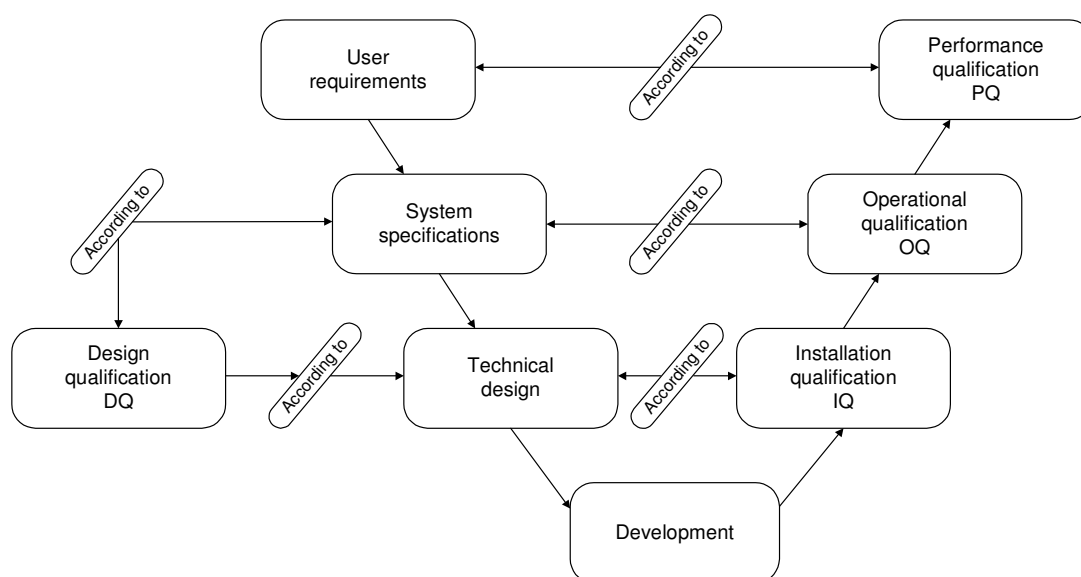


Figure B-2: V-model for the purchase and development of analytical devices. The terms are defined in the accompanying text.

B.1.1.3 Computerized system validation

Nowadays, computer systems are used in virtually every area of a pharmaceutical company. The authorities require validation for all systems in areas relevant to GMP, such as process control or laboratory data acquisition. The effort involved in validation is determined by the nature of the software used. While unmodified standard software packages which have been tried and tested by common use require little validation effort, more is required for customized or client-configurable software. Development of a customer specific software package demands the greatest validation extend.

Especially in newly developed programs, validation should be seen as an all-embracing quality assurance approach and is also performed in accordance with the V model shown in Figure B-2.

B.1.2 Process analytical technology

As demonstrated above, the pharmaceutical industry manufacturing sector is highly regulated and the responsible authorities demand review and approval of process, documentation, and facility prior to official approval of any facility or product. Subsequent process changes often require a new review and approval before institution. Thus even the ongoing manufacturing process is continuously subject to inspection and GMP standards conformance. On the other hand GMP standards are mostly empirical, and not science based. This system evolved about 30 - 40 years ago, when the different sectors of industry lacked rigorous SOPs.

Nevertheless, manufacturers observe an increasing trend toward manufacturing-related problems. Recalls, disruption of manufacturing operations, loss of availability of essential drugs, negative impact on new drug approvals, and low manufacturing and Quality Assurance (QA) process efficiency are the consequences. In combination all this ends up in a loss of image and to increased cost implications. The performance expectations keep on being unmet. While utilization levels decrease to 15 % or less 5 - 10 % of the products are scrapped and need to be reworked, and the costs of quality is in excess of 20 %.

During the last years, innovation and modernization enabled a technical progress on a large scale of application areas, e.g. in information science. But the technologies did not evolve as quickly in pharmaceutical industry as in other sectors and the high regulation slowed down the adoption of new technologies.

Significant potential and needs exist to improve the efficiency of pharmaceutical manufacturing and related regulatory processes. The technological opportunities are available to achieve this potential and the industry is reluctant to take advantage of such opportunities.

One approach for modern process management and improvement is the Six Sigma concept as a tool to achieve total quality. After very successful application in companies such as General Electric, Motorola, and Boeing, Six Sigma became widely known as a tool to increase productivity and cost effectiveness in a global competitive environment. Six Sigma is a strategy of a company-wide process optimization allowing no more than 3.4 errors per million possibilities. This principle can be applied to any area, industry, commerce, and service. Typically pharmaceutical industry ranges between 2 and 3 σ , rather than 5 and 6. Adopting the 'DMAIC' procedure according to the Six Sigma concept in both design of new procedures and improvement of existing processes involves more measurements and analysis to identify the sources of non-quality (see Figure B-3).

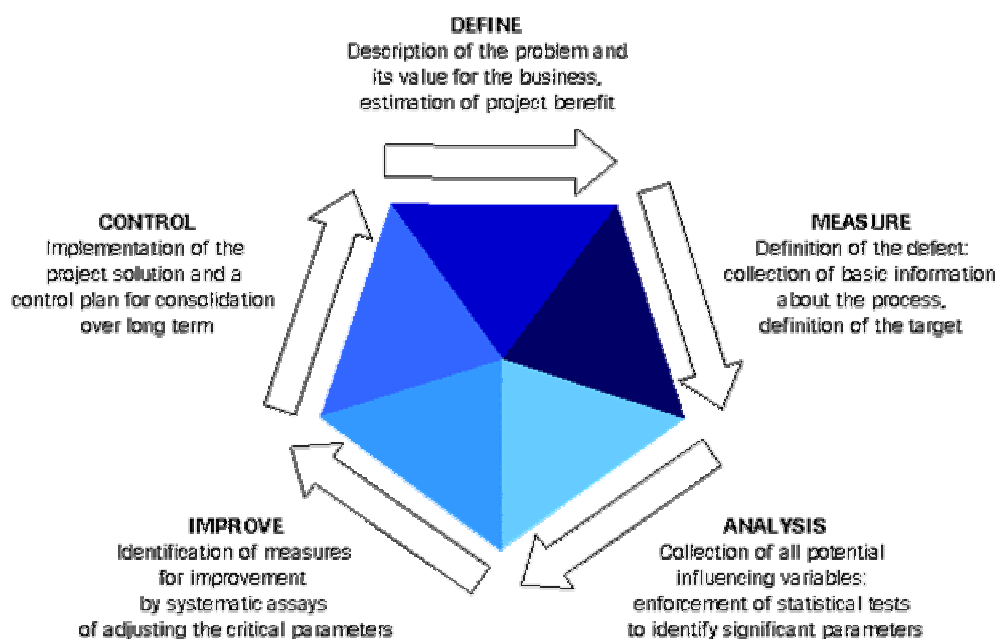


Figure B-3: Illustration of the 'DMAIC' procedure according to the Six Sigma concept.

Pharmaceuticals are complex, multivariate, physico-chemical systems, which are often treated like a univariate system (one-factor-at-a-time, trial and error experimentation). The raw materials are not always well characterized physically and the development of a formulation is performed with serious time restrictions due to shortening exclusivity periods on the competitive market. The equipment selection follows often traditional concepts and the process factors during manufacture are not completely understood. Within an established quality system and for a particular manufacturing process, there

is an inverse relationship between the level of process understanding and the risk of producing a poor quality product. But, due to 'regulatory uncertainties' and a number of scientific and technical issues, the pharmaceutical industry sometimes prefers to adopt a 'don't use' or 'don't tell' approach even if they had better analysis and production technology to implement, which is an undesirable situation for both industry and public health.

Sigma	Defects [ppm]	Yield	Cost of Quality
2 σ	308,537	69.2 %	25 - 35 %
3 σ	66,807	93.3 %	20 - 25 %
4 σ	6,210	99.4 %	12 - 18 %
5 σ	233	99.98 %	4 - 8 %
6 σ	3.4	99.99966 %	1 - 3 %

Figure B-4: Higher sigma indicates better processes. The pharmaceutical industry is typically located between two and three σ which is a sign for poor productivity.

B.1.2.1 PAT definition and options

The FDA process analytical technologies (PAT) initiative is an effort to facilitate the introduction of new technologies to the manufacturing sector of the pharmaceutical industry. PAT provides an opportunity to move from the current 'testing to document' paradigm to a 'continuous quality assurance' paradigm that can improve the industry's ability to ensure that quality was built in. This represents the ultimate realization of the true spirit of cGMP.¹³

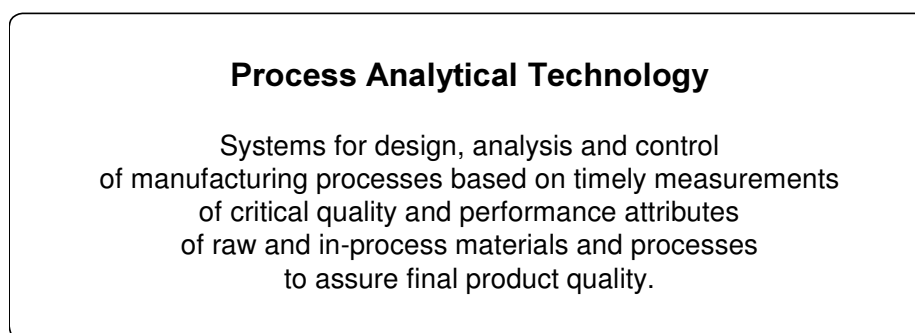
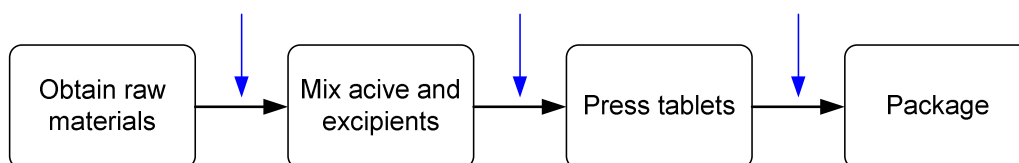


Figure B-5: Definition of PAT proposed by the CDER.¹⁴

(a) Conventional approach - laboratory based



(b) PAT approach - process based, at- / on- and in-line

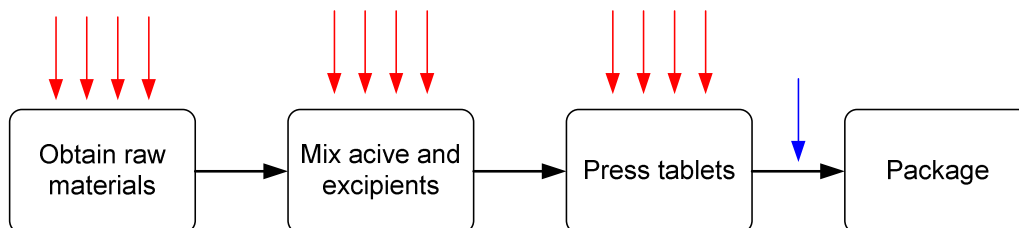


Figure B-6: Paradigm shift to the process control philosophy considering tablet manufacturing as an example: (a) end of phase testing of quality, to reduce the risk in moving to the next stage, (b) continuously or more frequently quality testing during each phase, to recognize deviations right in time to take measures. The amount of classical laboratory control can be reduced.

PAT involves optimal applications of process analytical chemistry tools already designed in the development phase, feedback process control strategies, and information management tools and / or product / process optimization strategies to the manufacture of pharmaceuticals. It can apply to all of the manufacturing sub-processes, such as inbound logistics, active ingredient manufacture, bulk formulation, fill and finish, packaging, and outbound logistics as well.

Such systems can be used to improve the efficiency of pharmaceutical manufacturing processes. The public health, as well as the pharmaceutical industry and the FDA could thereby benefit.

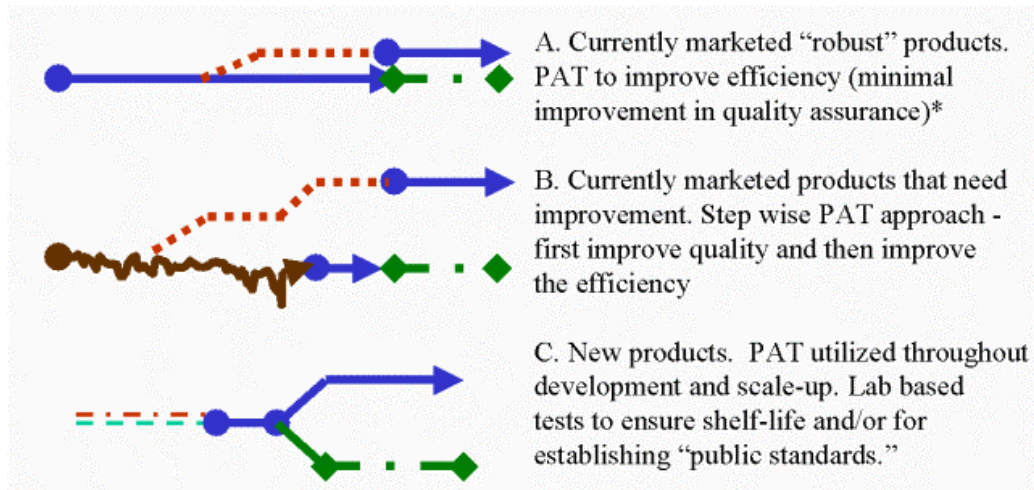


Figure B-7: Options for introducing PAT. *A step-by-step approach, one unit operation at a time similar to option B, is also an option.¹⁵

B.1.2.2 Definition of terms

In the context of PAT different terms are used very commonly, but the precise meaning sometimes appears to be obscure. For this work the following definitions of the CDER were adopted.¹⁶

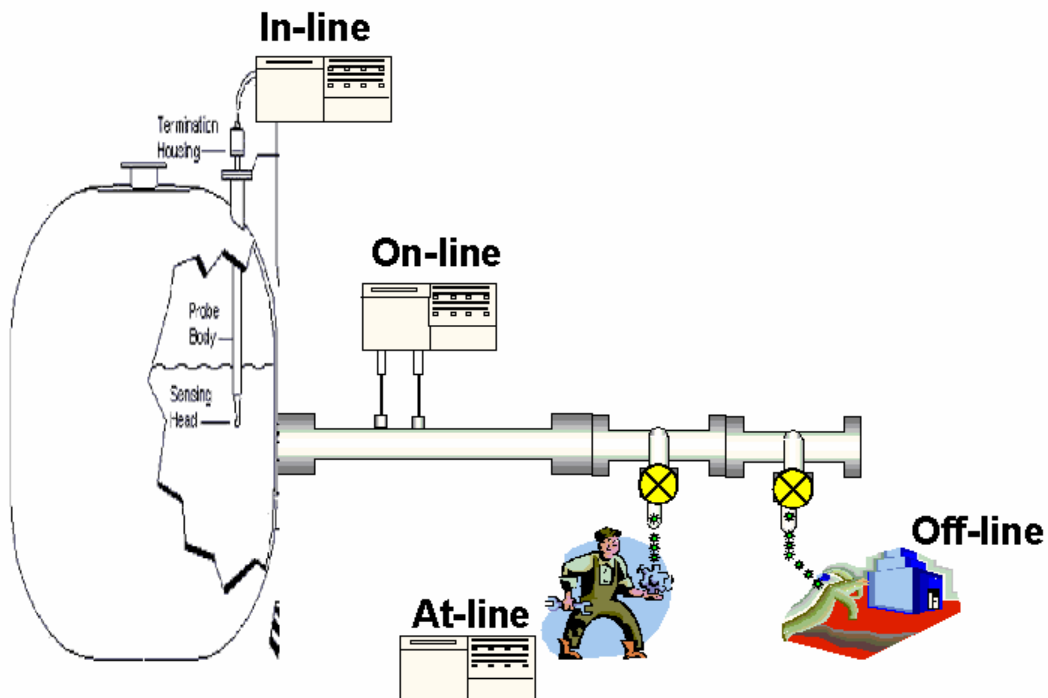


Figure B-8: Illustration of the meaning of the terms in-line, on-line, at-line, and off-line.

- **In-line**

The term in-line describes measurements made with PAT whereas the sensor is installed in direct contact with the process and measurements are performed in real time. The process stream may be disturbed. Examples: pH sensor, fiber optic sensor.

- **On-line**

Measurements made with PAT connected to the process through a sampling system are on-line. Typically this will be an analyzer requiring sample conditioning prior to analysis or a sensing technique that cannot be in direct contact with the process or be used in the process area. The sample may be returned to the process stream after measurement. Example: HPLC requires sample to be withdrawn from the process and moved into the analyzer.

- **At-Line**

Measurements made with PAT located close to the process, but not in direct contact with it are at-line. The samples are removed from the process and brought to the instrument. Example: normal laboratory type instrument such as a pH meter, gas chromatograph, or spectrophotometer located in a manufacturing area control room.

- **Off-line**

Analysis performed in a laboratory.

All these sampling techniques can be **non-invasive**, whenever the sensor is not in direct contact with the material and the process stream is not disturbed.

B.1.2.3 Discussion

PAT enables at- / on- / in-line measurements of 'performance' attributes in real time. Rapid feedback controls focus on prevention of the 'point of no return'. They offer the potential for significant reduction in production (and development) cycle time due to greater insight and understanding of processes. In long term they may reduce regulatory concerns and provide the possibility for remote inspection strategies.

On the other hand it can not be ignored that PAT will take significant financial and personnel resources to be developed and implemented. Currently there is still a lack of guidance for the pharmaceutical industry, being supposed to invest in this new trend. There is a need to clarify the general principles and terminology, the regulatory process of review and inspection. In the meantime this guide would serve as a tool for building a within-company consensus and to promote research and development activities in the pharmaceutical PAT area. The guidance should imply to be used in an environment of continuous improvement without undue regulatory burden.

Knowing that all products have critical quality attributes, process variables have to be found that can be controlled to maintain these critical parameters within acceptable limits. For this objective innovation is required and the selection of new and developing measurement tools should not be limited.

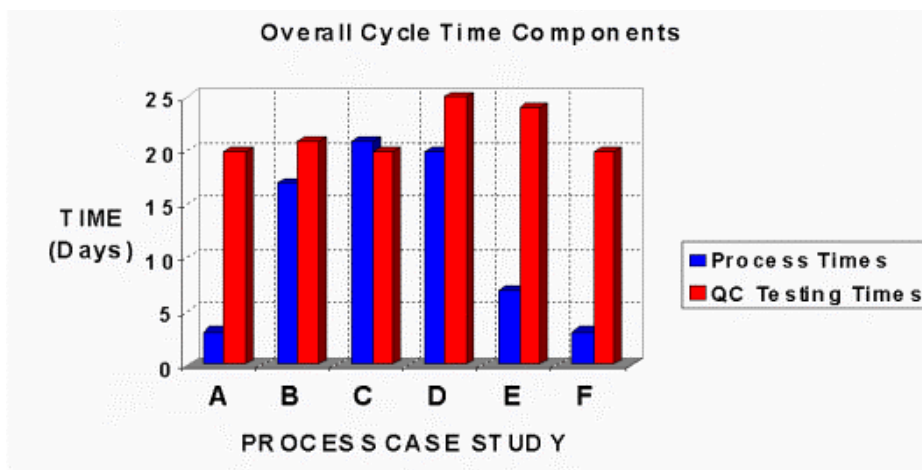


Figure B-9: Example of overall cycle times: without respect to the product, QC testing times are significant.¹⁷

The companies intend to move away from current univariate prescriptive testing according to pharmacopoeia monographs to multivariate process focused measurements. The regulation of PAT has to recognize that new insight into the process, which does not affect the quality of the product for its intended use, and should not require mandated changes in process. The replacement of current or classical methods with PATs for routine testing methods should be allowed. Furthermore, PAT offers the potential to reduce in large measure current validation

requirements. As frequent in- / on-line measurements produce a lot of data volume it is also required to define explicitly which records have to be kept and for how long.

For the successful development of new PAT the industry will require collaboration with academia to support new research areas. Simultaneously the FDA's CDER together with the ORA builds up a PAT steering committee called PATRIOT (= PAT Review, Inspection, and Office of Pharmaceutical Science Policy Development Team) with the intention to supply the required regulatory guidance. Only well defined preconditions will encourage the industry to submit future PAT projects.

References B.1 Regulatory context

- ¹ European Pharmacopoeia, 3rd edition, Deutscher Apotheker Verlag, Stuttgart, Govi Verlag - Pharmazeutischer Verlag GmbH, Eschborn 1997
- ² USP 24 NF 19, United States Pharmacopoeial Convention, Inc., Rockville, MD, 1999
- ³ The Japanese Pharmacopoeia (English Version), 13th Edition, Society of Japanese Pharmacopoeia, Tokyo, 1996
- ⁴ Pharmacopoeia Helvetica, 8th edition, EDMZ, Bern, 1997
- ⁵ WHO, Good practices in the manufacture and quality control of Drugs, Geneva, 1969
- ⁶ Marrer S., Obertüfer H., Inäbrit S., Qualitätssicherung in der Forschung, Entwicklung und Herstellung von Arzneimitteln [Quality assurance in pharmaceutical research, development and production], manuscript of lecture, ETH Zürich, 1999
- ⁷ Commission Directive of 13 June 1991 laying down the principles and guidelines of good manufacturing practice for medicinal products for human use (91/356/EEC)
Marrer S., Revised guidelines for good manufacturing practice (GMP) for pharmaceutical products, World Health Organisation (WHO) - a comparison with PIC-GMP guidelines, Pharm. Ind., 55 808-820, 1993
- ⁸ U. S. Food and Drug Administration, Rockville, MD, USA, Good Manufacturing Practice for Finished Pharmaceuticals, 21 CFR Parts 210 and 211
- ⁹ GMP Regulations of Japan, 4th Edition, 1992
- ¹⁰ Kromidas S., Validierung in der Analytik [Validation in Analytics], Wiley-VCH, Weinheim, New York, Chichester, Brisbane, Singapore, Toronto, 1999
- ¹¹ Rücker G., Neugebauer M., Willems G. G., Instrumentelle pharmazeutische Analytik [Instrumental pharmaceutical analysis], Wissenschaftliche Verlagsgesellschaft mbH, Stuttgart, 1992
- ¹² International Conference on Harmonization, Validation of Analytical Procedures: Methodology, ICH Harmonized Tripartite Guideline Q2B, 1995
Pharma Switzerland, Quality Assurance and Quality Control, Guideline, Validation of Analytical Methods, F. Hoffmann-La Roche Ltd., Basel, 1998
- ¹³ Hussain A., Current status of the PAT Initiative, Eighth Arden House European Conference, The Key for Achieving New Standards of Manufacturing Excellence and Regulatory Compliance: Process Analytical Technology, Royal Pharmaceutical Society, London, UK, March 24 - 26, 2003
- ¹⁴ U.S. Food and Drug Administration, Center for Drug Evaluation and Research, Homepage
- ¹⁵ Hussain A. S., The Process Analytical Technology (PAT) Initiative: Progress Report and Next Steps, FDA Science Board Meeting, April 9, 2002
- ¹⁶ Guidance for Industry, PAT - A Framework for Innovative Pharmaceutical Manufacturing and Quality Assurance, Draft Guidance, FDA, August 2003
- ¹⁷ Raju G. K., M.I.T. FDA Science Board Meeting, November 16, 2001

B.2 Lyophilization

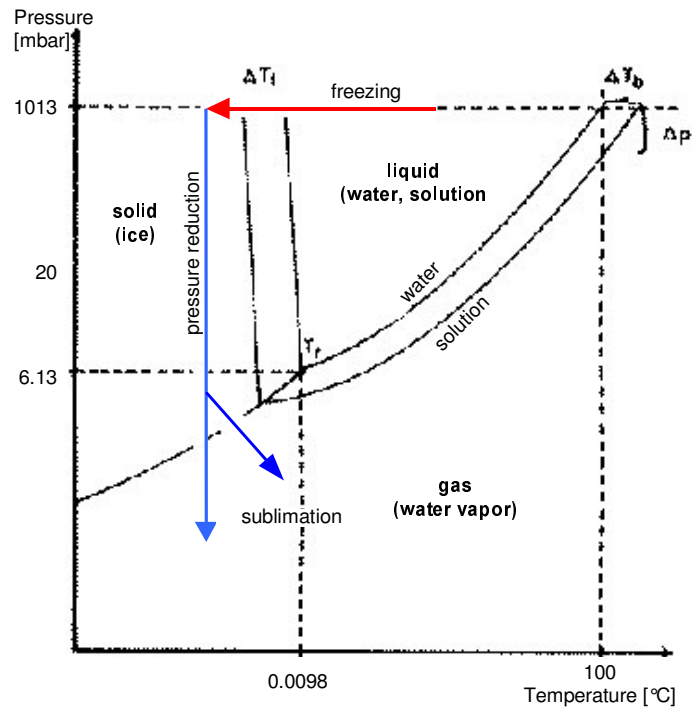
Freeze drying obtained relevance mainly during the Second World War to produce penicillin and blood plasma in the USA.^{1, 2} As any new technology, the field of freeze-drying opened more and more and became strongly rooted in the biological, pharmaceutical, food, and cosmetic industries.^{3, 4}

Lyophilization or freeze drying is a process in which the major portion of water and solvents in the frozen product is reduced by sublimation and desorption. First the product is frozen and then placed under a vacuum, allowing the ice to change directly from solid to vapor without passing through a liquid phase. The target is to remove carefully water out of solutions, dispersions and mixtures, especially when thermo labile substances are present, to limit biological and chemical reactions at the designated storage temperature.

Usually after freeze drying highly porous cakes or powders come into existence being very hygroscopic (lyophilization: Greek 'lyein' dissolve + 'philos' loving) due to their hydrophilic surface and the low vapor pressure above the capillaries. Hence the product has to be isolated hermetically to the atmosphere and even the inner surface protected by a dried gas like nitrogen.

B.2.1 Phase diagram of water

The relation of the different physical state of water and the parameters of pressure and temperature emerges out of the phase diagram where water and a solution of water are compared. The triple point (T_t) where ice, liquid water, and vapor coexist is by 6.13 mbar and 273.16 K.⁵ Due to dissolved substances the phase borders are moving, while the freezing point decreases of ΔT_f , the boiling point increases of ΔT_b , and the vapor pressure above the solution decreases of Δp .



Vapor pressure above ice:

[°C]	0	-18	-40	-58
[mbar]	6.11	1.25	0.13	0.014

Figure B-10: The phase diagram of water and a water solution illustrating the process steps of freeze drying with ΔT_f = freezing point depression, Δp = vapor pressure depression, ΔT_b = boiling point increase, ΔT_t = triple point (not according to measuring units).⁶

B.2.2 Freeze drying process cycle

The production of lyophilizates consists of separate, unique, and interdependent process steps. First of all the drug and excipients need to be dissolved in a suitable solvent, generally water for injection. The bulk solution is then sterilized by passing it through a 0.22 micron bacteria-retentive filter and filled into individual sterile containers. After partially stoppering the containers under aseptic conditions they are transported to the lyophilizer and loaded into the chamber. Here the containers are placed on cooled shelves and the solution is frozen. Once the entire solution became frozen a high-vacuum is applied to the cabinet and it is started to heat the shelves in order to sublimate and to desorb the water, in primary and secondary drying respectively. As soon as the drying procedure is completed the vials are entirely

stoppered, usually by hydraulic or screw rod stoppering mechanisms installed in the lyophilizers. After breaking the vacuum the containers can be discharged and crimped.

B.2.2.1 Freezing

The freezing usually takes place by atmospheric pressure. The end temperature has to be low enough (red arrow in Figure B-10) to pass the phase frontier solid / gas when the vacuum is performed in the second step (blue arrow in Figure B-10). During freezing an aqueous solution is gradually concentrated, but the solutes either precipitate incompletely or not at all. As the freeze-concentration increases a stage is reached where ice crystallization practically ceases, although the water in the mixture has not completely frozen. This is the glass transition temperature, where the properties of the amorphous mixture change from those typical of an elastic solid to those of a deformable, viscoelastic rubber.⁷ Above the glass-transition temperature viscosity drops and the freeze concentrate becomes sensitive to mechanical deformation (and chemical and microbiological deterioration). In freeze-drying terminology this process is known as collapse.⁸ Beyond others, Carpenter and Pikal showed that developing a glassy matrix during freezing could substantially reduce the osmotic and mechanical strains to the molecules. Unfortunately this might also be contrary to the requirements of the drying process itself which is easier to carry out from a non amorphous state. Thus, it might be necessary to mitigate between the conventional freezing and a 'thermal treatment', most often referred as an annealing process: double freezing with intermediate re-warming (Figure B-11).

The chemical changes that can occur during freezing are mainly due to freeze-concentration of all water-soluble constituents during the crystallization of ice as a pure water phase. Such concentration changes are dramatic. E.g. the freezing of an isotonic saline solution (0.15 M, 0.9 % w / w) to its eutectic temperature of - 21 °C is accompanied by a 24-fold increase in its concentration. Such high salt concentrations are partly responsible for the activity losses commonly observed during the freeze-drying of labile proteins. Furthermore enhanced reaction rates, changes in medium composition, precipitation of buffer salts and severe pH shifts can appear resulting in protein denaturation, aggregation, precipitation or reconstitution problems. These phenomena are prevented in practice by the addition of so-called cryo-protectants.

These sugars, sugar alcohols, and their oligomers or derivatives do not crystallize from aqueous solution during freezing, but tend to stabilize for example proteins in solution.

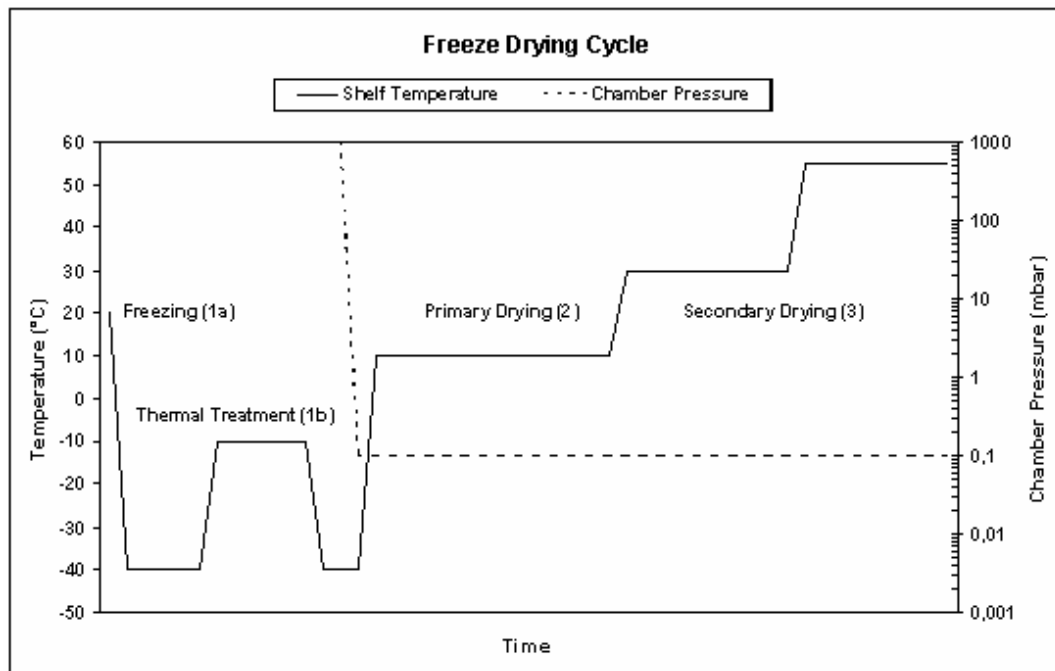


Figure B-11: The temperature and the pressure characteristics of a typical freeze drying cycle.⁹

B.2.2.2 Primary drying

Primary drying takes place when ice directly sublimates to vapor. Precondition therefore is to be below the triple point and to load the energy necessary for sublimation including among others the heat of the drying goods and the water, and supplementary the heat of fusion and evaporation.

➤ Condensation

At temperatures widely below 0 °C the water partial pressure is lowered by condensing vapor and the shelves are heated. A low total pressure favors a fast sublimation because the vapor pressure of ice decreases very much the lower the temperature. Consequently a water vapor saturated gas atmosphere still contains 4 g water / kg air at 0 °C, but only 0.65 g / kg at - 20 °C.² On the other hand 1 g water steam expands from 1.2 l at 1,013 mbar to about 1,000 l in vacuum at 1.3 mbar and approx. 10,000 l at 0.13 mbar.¹⁰ To pump off these amounts of gas would be absolutely uneconomic. That is the reason why condensers with lower temperatures than the frozen cargo are used

- between - 50 to - 80 °C. These surfaces should be as close as possible to the shelves because this temperature gradient of the condenser's and the product's surface are the precondition for the drying procedure.

➤ Energy addition

By thermal conduction, convection and radiation the energy input happens in the dryer, while the first two take the major part. Potential problems are shown by the schematic Figure B-12.

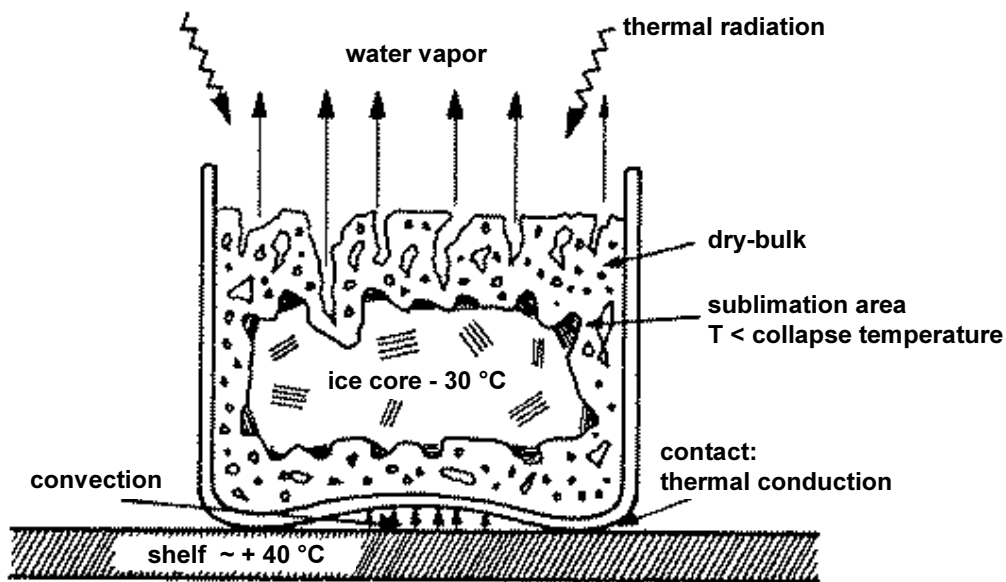


Figure B-12: Heat transfer and vapor transport during sublimation.¹¹

Thermal conduction occurs where the bottle's bottom is in touch with the shelf, convection in the gas space between shelf and container. In the beginning of the sublimation the heat transfer between vessel wall and product is effective. After a given time an ice free, porous and isolating area will appear.

Primary in case of inhomogeneous product structure and thick layers locally high temperatures can appear - e.g. above the collapse or the eutectic temperature - causing irreversible damage and bloating.¹ In this phase up to the end of ice sublimation energy input by convection in the interior of the product increases in importance. Now the pore structure of the cake determines the access to the ice core.¹²

If the pressure is below 10^{-1} mbar the sublimation velocity reduces strongly. On the first view this is surprising because one would expect a fast degradation of vapor according to the ad- / desorption isotherm of water. But the convection in the gas phase is overbalanced, being interrupted if pressures of 10^{-2} mbar are undershot. By periodically changing the pressure each heat transfer and vapor transport can be optimized.

If the performance of the dryer (ice capacity, temperature of condenser, heat supply to the shelf) is given, several system components are decisive for the energy transfer and the vapor transport. Concerning the product vessel (primary packaging) there are to mention its dimensions, the contact to the footprint, and the heat conductivity of the material including the stoppers. With regard to the dry-cargo the layer thickness, the heat conductivity of the already dried cake and its porosity have an impact.

B.2.2.3 Secondary drying

The operational definition of the beginning of secondary drying is frequently taken as the time when all ice has sublimated (i.e. the end of primary drying). However, from a mechanistic viewpoint, secondary drying begins in a local region of the product as soon as the ice is removed from that region¹³, but between 5 - 30 % of the original water still remains.² This water is physically or chemically adsorbed as hydrate or constitution water. It is attached to hydrophilic functional groups about hydrogen bridges and ion dipole interactions or electrostatic charges at ionic structures.

Accordingly the balanced vapor pressure above the drying good depends now on the adsorptivity of the solvent, whereby on micro porous structures (pores < 10 nm) capillary condensation is observed. Nevertheless to remove this water a very low water vapor partial pressure is necessary, varying between 0.01 - 0.001 mbar related to a low condenser temperature of about $- 80$ °C.^{14, 15} During secondary drying temperatures up to 50 °C can be tolerated without any observable loss of product quality, because after main drying already a stable state has been achieved.

To minimize hydrolysis and oxidation during storage a low water content has to be aspired in case of substances of low molecular weight or simple polymers. In practice the moisture content is reducible down to 0.1 %. In complex materials like proteins or

cell textures usually a certain amount of residual moisture must remain. In case of over drying mostly water unsolvable, irreversibly destroyed products may result.^{1, 15, 16}

B.2.3 Meltback

Meltback is a form of cake collapse and is caused by the change from the solid to liquid state. This happens if there is an incomplete sublimation in the vial. Associated with this problem is a change in the physical form of the drug substance and / or a pocket of moisture. These may result in greater instability and increased product degradation. Another problem may be poor solubility. Increased time for reconstitution at the user stage can result in partial loss of potency if the drug is not completely dissolved. Furthermore for some products the crystalline form is more stable than the amorphous form of lyophilized product. The amorphous form may exist in the meltback portion of the cake where incomplete sublimation occurs. Obviously the stability of lyophilized products which exhibit partial or complete meltback is corrupted.

B.2.4 Process control

The following shall only provide a short general introduction to technical realization or measuring methods.

➤ Freezing

Electrical conductivity is used for the validation of the freezing process. There is no more conductivity when the whole product is frozen. Afterwards the vacuum can be built up.

➤ Pressure

In lyophilization an exact pressure measurement is essential because of its influence of energy input and sublimation rate. Often heat conductivity manometers and capacitive manometers are applied. Mercury manometers are not used due to their contamination risk. The measurement range of mechanical manometers is too narrow and thereby unsuitable for this application.

➤ Temperature

Parts of the equipment consisting out of metal can be controlled precisely. A temperature measurement inside of the product with a probe supposes a homogenous

structure and heat conductivity. In huge plants many probes should be used with respect to the different temperature conditions at various areas on the shelves. Usually the average of the probes is calculated and compared with the shelves' temperature. The drying procedure is prolonged until the product reached the predefined temperature interval.

Due to heat conductivity caused by the thermo-element, probe bottles dry faster than the others. In addition to the difficulty to place the probes optimally and uniformly in small filling volumes, the contamination risk of sterile medicinal forms during the action is not negligible. Furthermore the probe system is very accident sensitive, breakage of wires, resolution of probe spikes or humidity in the connections necessitate a regular verification.¹¹ In the already dried porous parts of the sample the received values are no more representative and very often the probe's end does not stick in the sample where ice remains the longest.

During secondary drying a barometric temperature measuring is recommended. The method is based on the correlation of the partial water vapor pressure above the ice and the temperature of the interface between ice and gas. The principle consists in measuring the increasing pressure caused by water vapor while the gas room is separated from the condenser and vacuum pump. If ice is still present, a typical saturation vapor pressure appears. The end of primary drying is reached if the pressure does not rise more than 0.1 mbar in 2 minutes.^{15, 17}

➤ End point detection

The end point of the entire drying cycle is usually detected by a vacuum stability test. While the drying zone is physically separated from the condenser, the pressure increase within a defined time interval is controlled. If it is not higher than a certain threshold limit value, the product is supposed to be dry enough. Otherwise secondary drying can be continued and this test repeated. The secondary drying is ended by wincing the shelves together to seal the vials.

B.2.5 Discussion

The advantages of lyophilization include the ease of processing a liquid, which simplifies aseptic handling. The product stability is enhanced in a dry state and the

declared shelf life can be extended. The solvent is removed without excessive heating of the product, which makes this technique applicable for thermo-labile substances. Lyophilization affords a rapid and easy dissolution of the reconstituted product.

On the other hand complex equipment costs appear and high amounts of energy are required. Even more important, due to the limited energy transfer rates, increased handling and processing times are the consequence, varying between several hours up to a couple of days. Depending on the products, there might be very narrow margins to the tolerated process parameters and the end-points' temperatures. Velocities of cooling and re-warming need to be known very accurately by extensive previous laboratory determinations.

The traditional lyophilization process is a non-continuous cycle, but a batch per batch production. Depending on the position of the vials within the cabinet none is comparable to another and by definition a heterogeneous product results. Continuous processes should be more economical in power consumption because, unlike with the batch process, the plant does not require periodic cooling and heating back to room temperature.⁸ Meanwhile they are easier to control and give manufactured products a standard equal quality. Thus, some efforts were attempted to switch to a semi-continuous or continuous process as this is done in the food industry. Different approaches are under development such as 'vibrating heated trays' or 'spray freeze-drying' under atmospheric pressure. Both techniques have in common that the initial solution is distributed as individual droplets frozen into spherical granules. Then the bulk is continuously fed into differently conditioned (vacuum) chambers for sublimation in primary, and desorption in secondary drying. Finally, the population of granules enters an ultimate lock and can be numbered and bottled into sterile vials under dry neutral atmosphere. The result would be a batch of identical vials containing freeze dried granules instead of a more or less regular cake. Due to higher efficiency of these techniques the drying times drop by more than one order of magnitude in comparison to the classical lyophilization. Not yet resolved issues with these possibly future techniques is mainly that individual freezing of small homogeneous droplets is difficult, maybe mechanically the granules will not prove resistance to the process, and last but not least the sterility of the product is not easily guaranteed.

B.2.5.1 Quality control in lyophilization

It is commonly recognized that a complex technology is associated with the manufacturing and control of lyophilized pharmaceutical dosage forms. Some of the important aspects of these operations include: the formulation of solutions, filling of vials and validation of the filling operation, sterilization and engineering aspects of the lyophilizer, scale-up and validation of the lyophilization cycle, and testing of the end product. Inspections have disclosed potency, sterility and stability (storage and reconstitution) problems associated with the manufacture and control of lyophilized products.

Probably the most critical factor is the residual moisture with impact on other quality parameters such as the stability, dose uniformity, and sterility. This discussion addresses the residual moisture problem of a finished lyophilized dosage form.

➤ Optimum residual moisture

A critical issue is the determination of the optimum residual moisture, understanding that it could result from the drying process itself obviously, but also from release by the stoppers of water picked up during the sterilization process. Fran DeGrazio, Maninder Hora⁸, and others did show that this phenomenon definitely influences the storage ability of the freeze-dried products which depends, among other issues, on the quality of fit between the vial and the stopper which, in turn, depends on how tight the manufacturers can guarantee the dimensional tolerance of their products.

Formally regulated by the different responsible agencies, the residual moisture is quite difficult to grasp with exactitude. Neither Karl Fischer titration nor thermogravimetry (TGA) could determine the true value. Moreover, the first two techniques being destructive, they prevent any follow-up analysis of the sample over the shelf life. They titrate the 'total water' as a chemical, without discriminating between the part which is free to move and exchange between the stopper and the cake and the one, bound to the cake, which is often essential to maintain within the freeze-dried active substance, the three-dimensional structure which is at the root of its potency. The equilibrium water vapor pressure solves the follow-up issue since it is a non-intrusive, non-destructive technique but it gives only an indirect reading of the water content. Finally, in the dry product itself and without any interference from the container-closure

system, there are movements of water with time. Additionally during storage, the ratio between free and the different types of bound water changes and might impact the final potency.¹⁸

Despite of the elaborate design proposed by equipment manufacturers and the care that the drug companies take of their freeze-drying operations, they are still facing the recurrent problem of potential heterogeneity between vials and ampoules within a same single batch. The spatial distribution of 10,000 to 100,000 vials in a multi-shelf freeze-drying cabinet remains a problem. Some sit close to the door, some right in the middle, others near the condenser, some in the upper shelves, others down and they do not dry in the same way.

The above described phenomena explain why a widely used narrow random sampling of only few samples out of huge batches cannot provide representative results. But typically the average result of such a sampling is taken as estimated content for the entire batch and thereby as release criterion. If any deviation occurs within these samples measures need to be taken, and in the worst case it necessitates the destruction of the entire lot.

➤ Application of PAT

According to the USP it is good pharmaceutical practice to perform a 100 % inspection of parenteral products, including sterile lyophilized powders. Critical aspects would not only include the quality of the crimping, the presence of stoppers or of correct volume of cake and the cake appearance, but also the content of residual moisture. With the aid of a total inspection all the vials being out of specification could be recognized and rejected. In mean time the loss of an entire lot could be avoided. For an in-line control of lyophilized vials some preconditions are required from the applied analysis method. In contrast to established methods like KF titration and TGA, it must be non-invasive and non-destructive. Furthermore the production line should not be slowed down by a supplementary inspection step. Thus, the method must be reliable and as fast as the production speed. Near-Infrared (NIR) spectroscopy was considered to fulfill these requirements.

References B.2 Lyophilization

- ¹ Snowman J. W., Sterile Pharmaceutical Manufacturing, Vol. 1 Ed.: Groves M. J., Olsen W. P., Anisfeld M. H., Interpharm Press, Prairie View, 79ff., 1990
- ² Mumenthaler M., Sprüh-Gefreitrocknung bei Atmosphärendruck: Möglichkeiten und Grenzen in der Pharmazeutischen Technologie und in der Lebensmitteltechnologie; Dissertation Universität Basel, 1990
- ³ Keitel S., Herstellung und Eigenschaften von Chlortalidon- und Chlorttalidon/Mannitol-Lyophilisaten, Dissertation FU Berlin, 1987
- ⁴ Stricker H. (Ed.), Martin Swarbrick, Cammarata, Physikalische Pharmazie, Wissenschaftliche Verlagsgesellschaft mbH Stuttgart, 1987
- ⁵ Neumüller O. A., Römpps Chemie Lexikon Vol 6, 8. Aufl., Frank'sche Verlagshandl. Stuttgart, 1988
- ⁶ Oetjen G.-W., Gefriertrocknen, VCH Verlag, Weinheim, Germany, 1997
- ⁷ Levine H., Slade L., Water Science Reviews, 5, 79 - 185, 1988
- ⁸ Franks F., Freeze Drying: From Empiricism to Predictability, Cryo-Letters, 11, 93-110, 1990
- ⁹ Kramer M., Innovatives Einfrierverfahren zur Minimierung der Prozesszeit von Gefriertrocknungszyklen, Dissertation University of Erlangen, Germany, 1999
- ¹⁰ Barnickel H.; Formulierung, Abfüllung und Lyophilisierung von Proteinwirkstoffen; Pharm. Ind. 52, 912 1990
- ¹¹ Essig D., Oschmann R., Lyophilisation (Ein Seminar der APV vom 23. - 24. November 1992 in Würzburg, Wissenschaftliche Verlagsgesellschaft mbH, Stuttgart, 1993
- ¹² Levine H., Slade L., Water as a Plasticiser: Physico-chemical Aspects of Low-Moisture Polymeric System; Water Science Rev. 3, Water dynamics; Ed. Frank F., Cambridge Univ. Press, New York, pp. 79, 1985
- ¹³ Pikal J. M., Shah S., Intervial Distribution of Moisture during the Secondary Drying Stage of Freeze Drying, PDA Journal of Pharmaceutical Science & Technology, Vol. 51, No. 1, 1997
- ¹⁴ Gölker C., Gefriertrocknung biotechnologischer Produkte, Pharm. Technol. J. 10, 30, 1989
- ¹⁵ Willemer H., Grundlagen der Gefriertrocknung, Finn. Aqua 00.03.01/02.92.50 GK, 1992
- ¹⁶ Pikal J. M., Freeze Drying of Proteins I, Pharm. Technol. J. 10, 14, 1989
- ¹⁷ Leybold-Heraeus, Pharmazeutische Gefriertrocknung, 13.1.1. HV 200, Part 13, 1976
- ¹⁸ Rey L., Some Leading Edge Prospects in Lyophilization, Keynote Address from 2002 Lyophilization Conference, 2002

B.3 Near-infrared spectroscopy (NIRS)

B.3.1 NIR - historical review

Already in the year 1800 William Herschel discovered warming radiation beyond the visible red light, that he presented the Royal Society under the title 'Experiments on the Refrangibility of the invisible Rays of the Sun'. Today we know it must have been NIR, because the legendary telescope constructor used usual glass, which is not penetrable for longer wavelengths as infrared light. Hence the NIR area is also called 'Herschel-region'.¹

But it was necessary to wait until 1881 when Abney and Festing recorded the spectra of a couple of organic liquids realizing the importance of atomic groupings in the NIR spectrum and hydrogen bonding in particular. Coblentz identified the characteristics of CH-bonds in 1905 and postulated the bands could be part of a harmonic sequence.

The evolution of spectrographic instruments was underway, the diffraction grating (initially produced by winding a thin wire around a pair of fine threads) had been developed and the prism was well established. Christiansen and Rayleigh both produced relatively narrow-band optical filters, using index-matching and dyes. Just as Max Plank rounded off the 19th century with his radiation law, in 1891, Michelson published a paper describing the two-beam interferometer. Only one year later Rowland produced large ruled gratings and invented the concave diffraction grating, which became later the mainstay of spectrometer design.²

Prior to the Second World War the near-infrared region was not considered to be particularly useful for the spectroscopy of organic compounds.^{3,4} It was observed that NIR bands are severely overlapped, difficult to resolve and to interpret. If samples were not dried before NIRA the changes in hydrogen bonding due to the effects of sample temperature, ionic strength, and analyte concentration also would complicate the interpretation of mainly overlapping spectral bands. Changes in hydrogen bonding produce real and apparent band shifts as well as flattening and broadening of band shapes. The molecular absorptions found within the NIR region have significantly lower intensity in comparison to the fundamental infrared absorptions. Thus, the changes in

absorbance in the NIR region would be very small with regard to concentration changes. The relatively low extinction coefficients would place severe restrictions on the allowable noise levels and stability for any NIR instrument if quantitative work is carried out. Besides, sample presentation and the more or less obvious measurements by reflectance involve aspects which were not conceivable with the traditional infrared spectroscopy.

By the mid-50s Karl Norris had drifted into the very near-infrared but was limited by detectors to $< 1,000$ nm. At the U.S. Department of agriculture he demonstrated the potential value of this region for quantitative work by making measurements of agricultural products in the 1960s.⁵ The growing need to provide research facilities for fast, quantitative determination of moisture, protein, and oil provided the impetus for developing reliable calibrations.

The only commercially available instruments at that time were those developed to optimize measurements in the ultraviolet and visible regions, with the NIR capability only as an added feature. Adequate measurements without modifications were not possible, so that Norris decided to launch a new instrument specifically designed for recording NIR spectra. This instrument introduced tungsten halogen light sources, interference filters and uncooled lead sulfide detectors. The first operational unit was presented at the 1971 Illinois State Fair. Subsequently a first manufacturer designed a rotating filter grain quality analyzer. These instruments were non-user friendly dedicated systems with analog circuitry. The first dedicated on-line NIR analyzer appears to have been produced by Pier-Instrument in Germany in the late 1960s. It was vacuum tube based and employed two interference filters for the measurement of moisture. In the mid-1970s another manufacturer offered instruments for food analysis. This new instrument included features like dust-proof sealed optics and internal temperature control, thus improving the ruggedness and long term wavelength stability of the instrument. It also utilized the integrating sphere to give both reference reading and signal integration for each measurement. Many improvements of the commercially available instruments succeeded. The competition was initially very intense to win a large order for instrumentation from the U.S. Federal Grain Inspection Service which had adopted NIR initially as an approved method for analysis.

Obviously, the late 60s and early 70s saw the birth of what was to become the laboratory instrument sector of NIR analysis. By 1985, instruments had embedded microprocessors, memory was still expensive but there was a new versatility. Sets of calibrations could be stored, input data could be powerfully manipulated and results could be analyzed. Several new manufacturers appeared on the scene and a new group arose; the third party software vendors.

With personal computers rapidly dropping in price and massively increasing in performance, powerful data analysis software became available for data treatments, such as smoothing, curve fitting, regression etc. At last, principal components analysis and cluster analysis, with their origins in the 1930s, could be harnessed. Chemometrics, the name given to this expanding field by Svante Wold, had been born.⁶ Full wavelength instruments challenged wavelength pre-selection and the relative merits of the two methods have been the subject of much controversy. New optical techniques have also arisen with wavelength selection by non-linear optical crystals, acousto optical tunable filters (AOTF) and wavelength specific emitting diodes and laser diodes. The use of fiber-optical delivery means that in some applications a laboratory instrument can operate in the production environment or in hazardous areas. Over the last two decades, NIR technology has gained wide acceptance, deepening market penetration and maturity. The implementation of more powerful processors, better algorithms representing improved NIR modeling will lead to easier and more robust calibrations.²

B.3.2 NIR theory

B.3.2.1 Spectral regions

Out of a spectroscopist's view NIR describes the transition between absorption of light energy due to transfer of electrons in the visible range (400 – 800 nm or 25,000 – 12,500 cm^{-1}) and absorption due to molecular vibration in the mid-range infrared region (2,500 to 5,000 nm or 4,000 to 200 cm^{-1}).¹ In the area of NIR (780 – 2,500 nm, 12,821 – 4,000 cm^{-1} respectively)^{7, 8} overtones and combinations of the vibration of CH, OH, SH and NH bonds are mainly observed. All the absorption bands are the result of overtones or combinations of overtones originating in the fundamental mid-IR.

	0.1	0.4	0.8	2.5	50	500	3,000	μm
	UV	VIS	infrared (IR)			micro-waves		
			near	middle	far			
	10^5	25,000	12,500	4,000	200	20	3.3	cm^{-1}

Figure B-13: Illustration of different spectral ranges: from the ultra-violet (UV) about the visible (VIS) and the infrared (IR) to the microwaves.

Due to absorption of light energy stretching and deformation of bonding angles are caused. The consequences are molecular vibrations. The difference between NIR and mid-IR is only the frequency of these vibrations. Whereas in mid-IR primarily fundamental vibrations are induced, the more powerful NIR provokes first, second or higher overtones. Partially combinations of fundamentals and overtones are resulting. They are due to strongly overlapping absorption bands.¹

B.3.2.2 Physical background

Vibrational spectroscopy is based on the concept that atom-to-atom bonds within molecules vibrate with frequencies that may be described by the laws of physics and are therefore subject to calculation. When these molecular vibrators absorb light of a particular frequency, they are excited to a higher energy level. At room temperature, most molecules are at their rest or zero energy levels. That is, they are vibrating at the least energetic state allowed by quantum mechanics.⁹ The lowest, or fundamental, frequencies of any two atoms connected by a chemical bond may be roughly calculated by assuming that the band energies arise from the vibration of a diatomic harmonic oscillator and obey Hooke's law.¹⁰

$$\nu = \frac{1}{2\pi} \sqrt{\frac{k}{\mu}}$$

Equation B-1: Hooke's law valid for an ideal diatomic harmonic oscillator, with ν = vibrational frequency, k = classical force constant, μ = reduced mass of the two atoms.

This works fairly well for diatomic molecules and is not far from the average value of two-atom stretch within a polyatomic molecule. This approximation gives the average or center frequency of the band. Because the reduced masses of the involved atoms CH, OH and NH are 0.85, 0.89, and 0.87, respectively (these constitute the major

absorption bands in the near-infrared spectrum) the 'ideal' frequencies would be quite similar. But in actual molecules, the electron-withdrawing or donating properties of neighbors determine bond strength, length and thus frequency, so that an average value is of little use in structural determinations. These differences underline the development of a real spectrum. The k values (bond strengths) vary widely and create energy differences, which can both be calculated and used in spectral interpretation.

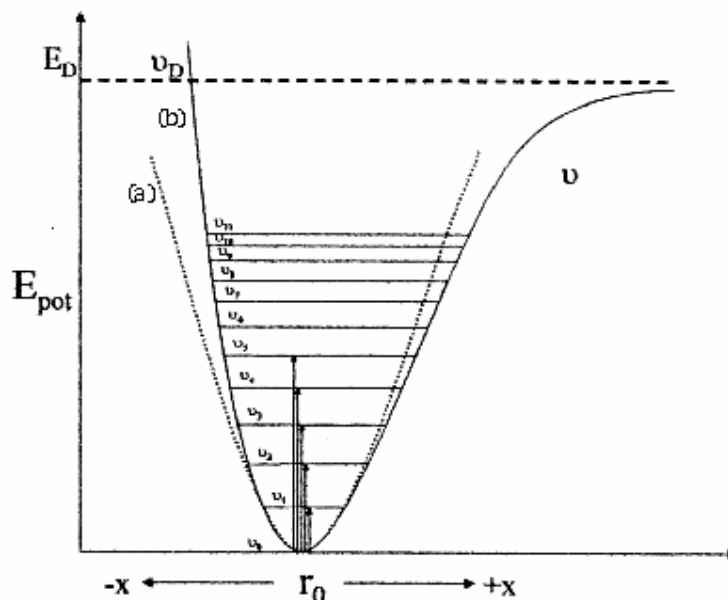


Figure B-14: Potential energy diagram of vibrational mode calculated as (a) an ideal harmonic diatomic oscillator, and (b) an actual anharmonic diatomic oscillator (E_{pot} = potential energy, E_D = dissociation energy, r_0 = interatomic distance, ν_x = energy level).¹⁰

➤ Fundamental frequencies

Unlike the classical spring model for molecular vibrations, there is no infinite number of energy levels. Instead of a continuum of energies, there are discrete energy levels described by the quantum theory. The time independent Schrödinger equation is solved using the vibrational Hamiltonian for a diatomic molecule. Somewhat complicated values for the ground state ($\nu = 0$) and succeeding excited states are obtained upon solving the equation. Absorption of a photon of suitable energy can cause the molecule to change between vibrational energy levels. At room temperature only the ground state has a significant population, so that transitions due to absorption at these temperatures occur from the ground state.¹⁰

A simplified version of these levels may be written for the energy levels of diatomic molecules, where the Hooke's law terms can be seen (Equation B-2).

$$E_v = \left(v + \frac{1}{2} \right) \frac{h}{2\pi} \sqrt{\frac{k}{\mu}}$$

Equation B-2: Valid for $v = 0, 1, 2, \dots$ and $h = \text{Planck's constant}$.

Rewritten using the quantum term $h\nu$, the equation reduces to Equation B-3:

$$E_v = \left(v + \frac{1}{2} \right) \cdot h\nu$$

Equation B-3: Valid for $v = 0, 1, 2, \dots$ and $h = \text{Planck's constant}$.

In case of a non-linear molecule with N atoms, there is a considerable number of energy levels. Ideally, one can treat such a molecule as a series of diatomic, independent, harmonic oscillators and the above equation can be generalized to Equation B-4:

$$E(v_1, v_2, v_3, \dots) = \sum_{i=1}^{3N-6} \left(v_i + \frac{1}{2} \right) \cdot h\nu_i$$

Equation B-4: Valid for $v_1, v_2, v_3, \dots = 0, 1, 2, \dots$ and $h = \text{Planck's constant}$.

Transition between ground state and excited energy level one ($v = 1$) gives the fundamental absorption if this leads to change in molecular dipole moment allowed by selection rules. Transitions between ground state and excited energy level two ($v = 2$) or higher ones ($v > 2$) give overtones. Transitions between multiple states can occur and give rise to combination bands. NIR spectra contain these overtones and combinations derived from the fundamental vibrations which appear in the mid-IR. From the selection rules viewpoint, overtones and combinations are not allowed, but appear as weak bands due to anharmonicity or Fermi resonance.

➤ Anharmonicity and overtones

In practice the so-called ideal harmonic oscillator has limits. As the mass approaches the point at which the spring is attached to the ceiling, real compression forces that counteract the bulk of the spring are often disregarded in calculations. As the spring stretches, it eventually reaches a point where it loses its shape and fails to return to its original coil. This ideal case is shown in part (a) of the potential energy diagram

(Figure B-14). The barriers at each end of the cycle are approached in a smooth and orderly fashion. In molecules, likewise, the respective electron clouds of the two boundary atoms restrict the approach of the nuclei during the compression step, thus, creating an energy barrier. On extension of the stretch, the bond eventually breaks when the vibrational energy level reaches the dissociation energy. The barrier at smaller distances increases at a rapid rate, while at the far end of the stretch it slowly approaches zero (shown in part (b) of the potential energy diagram). The energy levels in the anharmonic oscillator are not equidistant, but slightly closer as the energy increases. This phenomenon is expressed by the following formula:

$$E_v = \left(v + \frac{1}{2} \right) \cdot h\omega_e - \left(v + \frac{1}{2} \right)^2 h\omega_e x_e + \text{higher terms}$$

Equation B-5: The anharmonic oscillator, where $\omega_e = (1/2 \pi) (k_e / \mu)^{1/2}$ = vibrational frequency, x_e = anharmonicity constant, k_e = anharmonicity force constant, and μ = reduced mass of the two atoms.

In practice, the anharmonicity constant is between 1 and 5 %, thus, the first overtone wavelength of a fundamental of 3,500 nm would be:

$$\lambda = \frac{3,500}{2} (1 + x_e + 3x_e^2 + \dots)$$

Equation B-6: Computation of the first overtone wavelength of an exemplary fundamental.

Depending on structural or ambient conditions, the number may range from 1,768 nm to 1,850 nm for this example. However, it would generally appear at 1,750 nm plus a relatively small shift to a longer wavelength. Due to forbidden transitions, the overtones are between 10 and 1,000 times weaker than the fundamental bands. Thus, a vibration band would have to be in their third or fourth overtone to appear in the NIR region of the spectrum. For example, a fundamental carbonyl stretching vibration at $1,750 \text{ cm}^{-1}$ or 5,714 nm would have a first overtone at about 3,000 nm, a weaker second overtone at about 2,100 nm, and a third very weak one at about 1,700 nm. The fourth overtone, at approximately 1,400 nm, could be left out. These are based on an example 5 % anharmonicity constant¹

As a rule, overtones occur at half and third of the fundamental absorption wavelength i.e. 2 and 3 times the fundamental frequency. Most overtone peaks arise from the

stretching and bending modes because the dipole moment is high: OH, CH, SH and NH are strong NIR absorbers and form most NIR bands.

➤ Combination bands

Another prominent feature of the near-infrared spectrum is the large number of combination bands. In addition to the ability of a band to be reproduced at twice or threefold the frequency of the fundamental, here is a tendency for two or more vibrations to combine (via addition or subtraction of the energies) to give a single band.

A simple system containing combination bands is the gas sulfur dioxide (SO₂). From the simple theory of allowed bands there should be three absorption bands (refer to Equation B-7).

$$\text{Number of bands} = 3 \cdot N - 6$$

Equation B-7: Calculation of the degrees of freedom.

These are the symmetric stretch (found at 1,151 cm⁻¹), the asymmetric stretch (found at 1,361 cm⁻¹), and the O-S-O bend (found at 519 cm⁻¹). The three bands mentioned are the allowed bands according to group theory. However, bands also appear at 606, 1,871, 2,305, and 2,499 cm⁻¹. As discussed earlier, it is impossible for the molecule characterized as a harmonic oscillator to acquire energy to be promoted from the ground state to a second level (first overtone) or higher. For the anharmonic oscillator, although a first overtone of twice the frequency of the symmetric stretch is possible. This band occurs at 2,305 cm⁻¹, with the 3 cm⁻¹ difference arising from an exact doubling of the frequency accounted for by the anharmonicity.

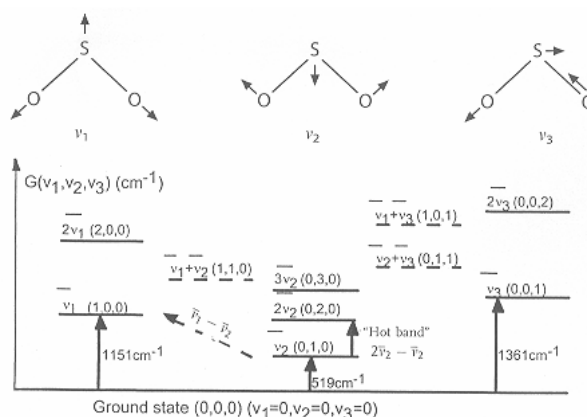


Figure B-15: Illustration of the anharmonic vibrations of SO_2 .¹¹

This still leaves three bands to be explained. If the possibility exists that two bands may combine as $\nu_a - \nu_b$ or $\nu_a + \nu_b$ to create a new band, then the remaining three bands are easy to assign arithmetically. The total bands for SO_2 can be assigned as seen in Table B-2. In the same manner, any unknown absorption band can, in theory, be deduced from first principles. When the bands in question are CH, NH, and OH ($4,000 - 2,500 \text{ cm}^{-1}$), the overtones and combinations make up much of the NIR spectrum.

$\nu \text{ (cm}^{-1}\text{)}$	Assignment
519	ν_2
606	$\nu_1 - \nu_2$
1,151	ν_1
1,361	ν_3
1,871	$\nu_2 + \nu_3$
2,305	$2 \nu_1$
2,499	$\nu_1 + \nu_3$

Table B-2: Band assignments for the infrared spectrum of SO_2 .¹²

While readily apparent in the better-resolved mid-IR, these effects, like fundamentals, overtones, and combinations of these two, is somewhat difficult to observe in the NIR region, often hidden under the broad, overlapping peaks associated with this region. Adding Fermi resonance to the overlapping combination and overtone bands already seen in the NIR, it is easy to understand why the region was dismissed for so many years as unusable. With current computers and chemometric software, however, these broad, undistinguished bands are merely non-esthetic while eminently usable. The NIR

signal measured is a complex function of physical and chemical parameters that has to be resolved chemometrically.¹³

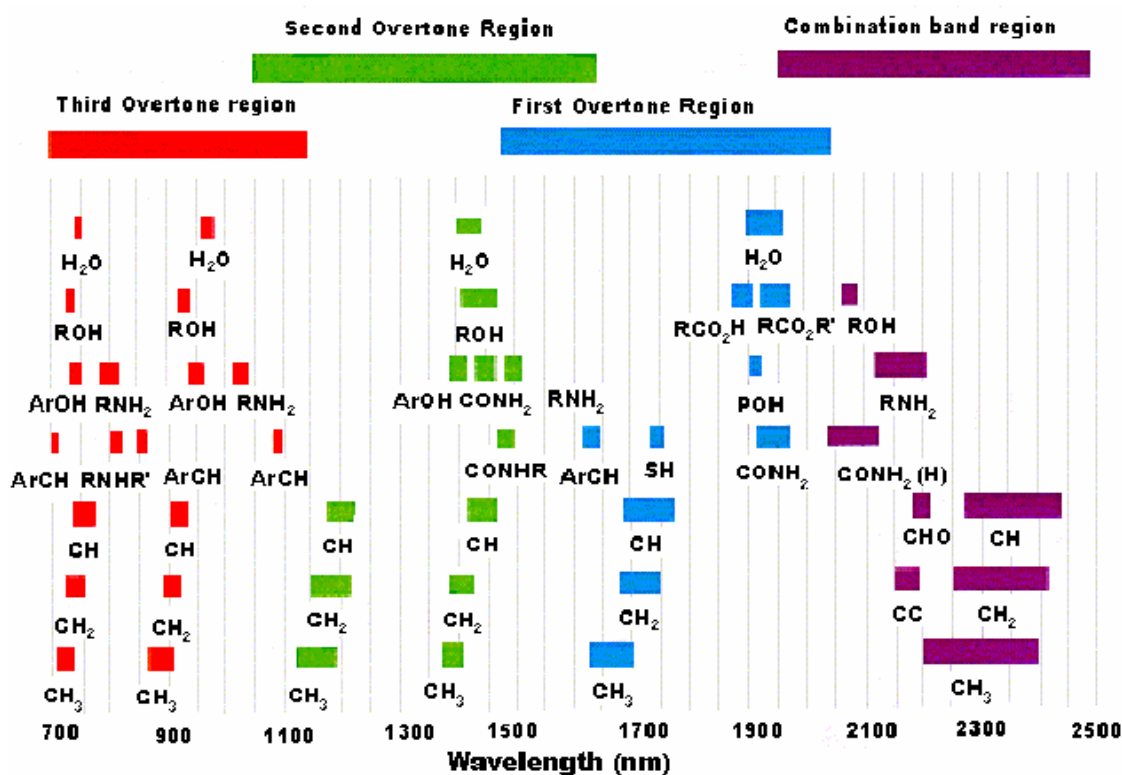


Figure B-16: Table of near-infrared absorption bands of common functional chemical groups assigned to overtones and combinations.¹⁴

B.3.3 NIR sampling modes

Different sampling techniques are leading to diverse results. Depending on the interest of information an adequate illumination mode has to be selected.

B.3.3.1 Transmittance

In case of liquids, solutions, goods in bulk, solids and tablets or capsules transmittance measurements are very common. The light source and the detector are positioned opposite of each other and the incident light has to cross the whole sample to be detected. Thus the spectrum contains a sum of information about surface and core of the sample. On the other hand this technique is only applicable if light intensity is high enough to penetrate the sample depending on the absorption coefficient and the sample thickness.

B.3.3.2 Diffuse reflectance

In contrast to the prior the diffuse reflectance mode is used for solid substances and requires a different spectrometer configuration. Whereas source and detector are on the same side in an angle of 45° to each other, the light reaches the surface of the sample. Depending on its structure it penetrates some millimeters and the majority is absorbed. The rest is reflected but reaches only partially the detector. The deeper zones of the sample are not regarded. If the physical properties of the surface, like e. g. the particle size, vary a lot the corresponding spectrum may be dominated by these influences rather than the chemical information. If the surface is a 100 % reflector like Spectralon virtually no absorbance will be recognized.

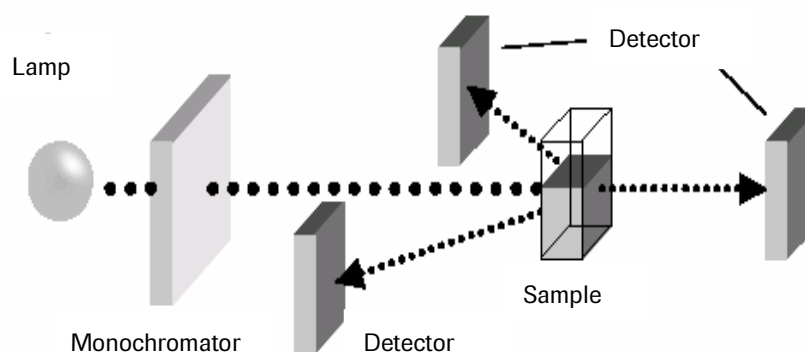


Figure B-17: Illustration of NIR measurements in diffuse reflectance and transmittance mode.

B.3.3.3 Transflectance

Transflectance combines both transmittance and reflectance modes and can be used for both, solid and liquid substances. Behind the sample a mirror is installed to reflect the light back on the detector being on the same side as the source where diffusely reflected and transmitted light is detected in mean time. While the incident light has to cross the sample even twice, here the restrictions of transmittance measurements are especially relevant.

All of these sampling modes can be combined with in some cases even very long fiber optic probes out of quartz glass, guiding the incident light to the sampling zone or leading the reflected light back to the detector.

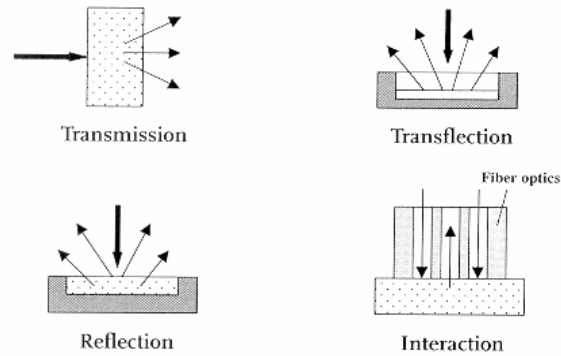


Figure B-18: Overview of the different sampling modes that can also be combined.

B.3.4 Instrumentation

Perhaps the strongest impetus for the development in NIR spectroscopy in pharmaceutical applications has been the explosive growth in both the types and sophistication of NIR equipment and software. Established manufacturers develop new NIR equipment yearly and new manufacturers appear regularly.

The different spectrometer types can be classified in dispersive and non-dispersive instruments. Filter, Grating, and AOTF instruments belong to the dispersive ones, while FT spectrometers and diode array systems are non-dispersive and collect all the wavelengths simultaneously. Without respect to the type of spectrometer usually a tungsten halogen lamp is installed, with a high light intensity in the desired wavelength range. Various cooled semi-conductive photo cells made of Ge, Si, PbS, InSb, InAs, and InGaAs (sorted according to increasing sensitivity) are used as detectors. For the choice of the detector the specific characteristics of the spectroscopic technique have to be considered, like light intensity and measuring velocity. The NIR measurements are performed against scans of reference standards of high reflective materials, usually ceramics or Teflon.

This chapter deals primarily with the three types of spectrometers that were deployed during the current work: an ABB Bomem FT NIR, a Brimrose AOTF NIR and a FOSS NIRSystems grating spectrometer as laboratory reference.

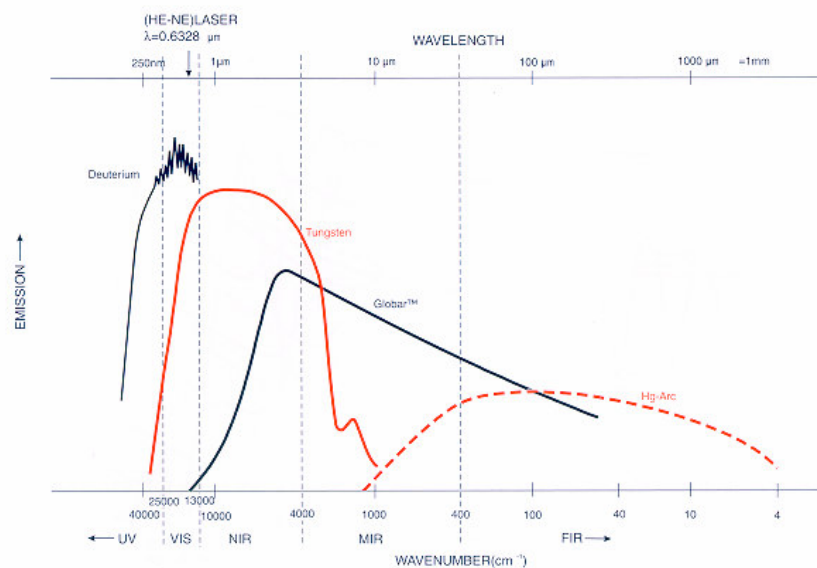


Figure B-19: Emission intensities of light sources used in spectroscopy.¹⁵

B.3.4.1 Fourier transform (FT) spectrometer

Developed in the late 19th century by Michaelson, the moving mirror interferometer was initially designed to determine the speed of light. While using the instrument, Michelson noticed some difference in the interference pattern when various materials were placed in the beam. However, it was not until roughly 1960 when the mathematical treatment of Fourier was applied to the interferogram produced by the device that an infrared spectrum was seen. The speed and advantages of the Fourier transform infrared (FT-IR) instrument rapidly made it a clear choice over either the prism or grating models for most laboratory applications in the mid- and far-infrared regions.

➤ Background

Any well-behaved periodic function (such as a spectrum) can be represented by a Fourier series of sine and cosine waves of varying amplitudes and harmonically related frequencies. A typical NIR spectrum may be defined mathematically by a series of sine and cosines in the following Equation B-8.

$$\begin{aligned}
 f(\lambda) = & a_0 + (a_1 \sin \omega\lambda + b_1 \cos \omega\lambda) \\
 & + (a_2 \sin 2\omega\lambda + b_2 \cos 2\omega\lambda) \\
 & + \dots (a_n \sin n\omega\lambda + b_n \cos n\omega\lambda)
 \end{aligned}$$

Equation B-8: Fourier transformation, with a_0 = average of the spectrum (mean term), a_i and b_i = weighting factors (or coefficient pairs), for $n = 1, 2, 3, \dots$ is the Fourier index.

This equation turns the interferogram into a spectrum or can convert a spectrum into workable pieces. This Fourier-factor concept was explored by McClure with data from NIR spectra. For instance, the first factor has the largest sine wave. Since the 'sloping baseline' associated with diffuse reflection is caused largely by scattering, this piece of the spectrum could be discarded by reconstructing the spectrum without the first Fourier term. Often, the later Fourier terms describe the instrument noise (high frequency signals versus broad, low frequency absorbance bands), and dropping them from the reconstructed spectrum has a smoothing effect.¹⁰

➤ Principle of measurement

A Michelson interferometer is seen in Figure B-20. The light from the source is split into two segments by the beam splitter. One portion travels to a fixed mirror and is reflected back to the splitter. The second impinges on a moving mirror and returns recombined with the first portion of the light. The pattern of peaks and valleys (caused by constructive and destructive interferences hence the name interferometer) is called an interferogram. A spectrum evolves when this interferogram is deconvoluted by some mathematical means, e.g. a Fourier transform. The resolution of an FT spectrometer depends on the covered distance of the mirror. The longer the way, the higher the resolution, but the more time is necessary per scan either. Without respect to the required wavelength range, the mirror (or wishbone) always accomplishes an entire movement. One scan is defined as the way back and forth.

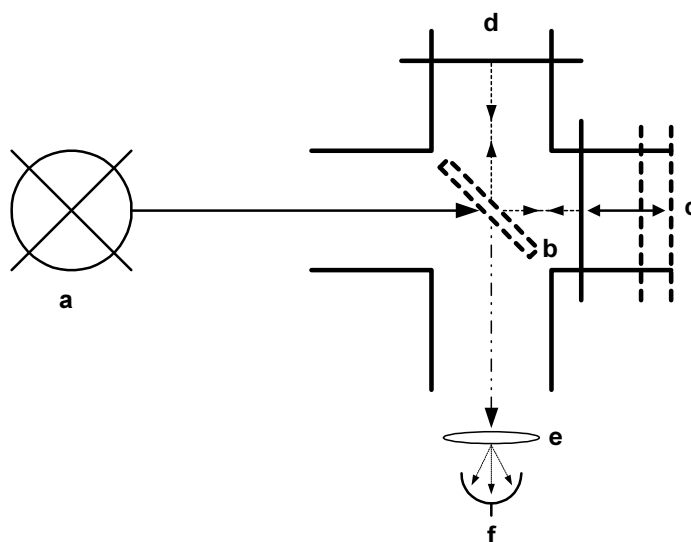


Figure B-20: Michelson interferometer (a = light source, b = beam splitter, c = moving mirror, d = fixed mirror, e = sample, f = detector). The resolution of the scan is dependent on the moving distance of the mirror c.

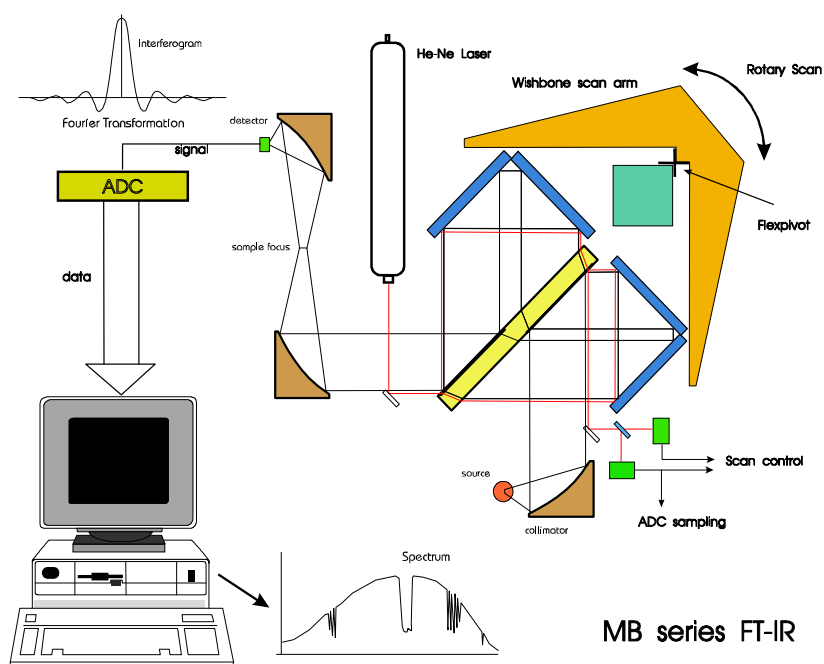


Figure B-21: The Bomem Michelson Interferometer, an interference-type spectrometer with moving wishbone scan arm and cubic mirrors. The helium-neon laser serves as wavelength reference for self-readjustment.¹⁶

➤ Discussion

The popularity of interferometers in mid-infrared has carried over to NIR. Speed and high resolution spectra are the strengths of FT instrumentation.

They are fast with the highest possible resolution, although the scan-averaging required for adequate S / N-ratio may provide ultimate scan times that are similar to other instrumentation. They are the best bet for analyzing gases or materials where resolution is critical (due to sharp λ_{\max}). Many active pharmaceutical ingredients (APIs) are crystalline and have sharp peaks, even in the NIR. In such cases, the resolution of a FT instrument is a plus.

The usual advantages of FT-IRs do not necessarily apply in the NIR, however. With NIR the source is quite strong, the absorbance very weak, and the detector(s) quiet and sensitive. The extra energy can, in some cases, burn the sample. Lactose is an example of a pharmaceutical excipient browned by the energy of FT-NIR. In addition, since most NIR peaks are broad and relatively featureless high resolution usually adds noise, which is, by nature, high frequency.

B.3.4.2 Acousto optical tunable filter (AOTF) spectrometer

The basic construction of a conventional single beam spectrometer splits the light with a dispersive element (prism or grid) and the desired spectral portion is then passed through the sample. The total spectrum is obtained through the mechanical movement of the dispersion element. However, the mechanics of the system limits the absolute wavelength reproducibility. Traditional instruments have relatively slow data-acquisition rates and issues of absolute wavelength calibration. Also, they are usually too delicate to deploy in direct process-control applications on the plant floor. These disadvantages are overcome by the AOTF technology through the use of a precise electronic scanning of a spectrum.

➤ Background

Acousto-optic interaction occurs in all optical mediums when an acoustic wave is launched into the optical medium. It generates a refractive index wave that behaves like a sinusoidal grating. An incident laser beam passing through this grating will diffract into several orders. With appropriate design, the first order beam has the

highest efficiency. Its angular position is linearly proportional to the acoustic frequency: the higher the frequency, the larger the diffracted angle.

$$\Theta = \frac{f_a \cdot \lambda}{V_a}$$

Equation B-9: Computation of the refractive angle, where λ = optical wavelength in air, f_a = acoustic frequency, V_a = acoustic velocity, Θ = angle between the incident and the diffracted laser beam.

The intensity of light diffracted (deflected) is proportional to the acoustic power (P_{ac}), the material figure of merit (M_2), geometric factors (L / H) and inversely proportional to the square of the wavelength. This is seen in Equation B-10.

$$D.E. = \eta = \sin^2 \left[\frac{\pi}{\lambda} \sqrt{\frac{M_2 \cdot P_{ac} \cdot L}{2 \cdot H}} \right]$$

Equation B-10: Computation of the intensity of the diffracted light.

With acousto-optics both deflection and modulation of the amplitude of the beam is possible. Also, in the acousto-optic interaction the laser beam frequency is shifted by an amount equal to the acoustic frequency.¹⁷

➤ Principle of measurement

The AOTF module is most commonly based on a mono-crystal of tellurium dioxide (TeO_2) provided with a thin piezo-electric mono-crystal plate. When a high-frequency electric field is applied to this piezo crystal (LiNbO_3) by vapor-coated electrodes, the piezo plate generates a high-frequency acoustic wave (ultra-sonic) propagating in the tellurium dioxide crystal.

As these acoustic waves pass through the TeO_2 , they cause the crystal lattice to be alternately compressed and relaxed. The resultant refractive index variations act like a transmission diffraction grating or Bragg diffracter. However, unlike a classical diffraction grating, the AOTF only diffracts one specific wavelength of light, according to the frequency of an applied RF source, so that it acts more like a filter than a grating. This is a result of the fact that the diffraction takes place over an extended volume, not just at a surface or plane, and that the diffraction pattern is moving in real time.¹⁸

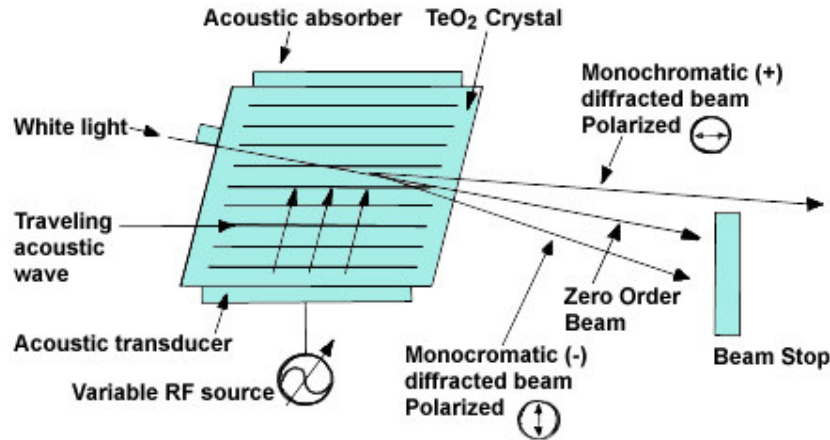


Figure B-22: Schematic drawing of the AOTF crystal.¹⁹

In case of the collinear AOTFs, the RF transducers are mounted on the crystal so that acoustic waves travel longitudinally through the crystal, that is, in the same direction as the light waves. A non-linear interaction in the crystal leads to an effect similar to frequency mixing, used to shift the frequency of laser beams. In simple terms, a photon of light (ν_1) combines with an acoustic phonon to generate a new photon (ν_2) of different energy: $\nu_1 \pm \nu_{aq}$. This energy shift is extremely small given that ν_1 is typically 10^7 larger than ν_{aq} .

Because the shifting takes place over a large path through the crystal (typically 1 cm), the incident light and diffracted light must have the same phase velocity (that is, they must be phase-matched). Otherwise the diffracted waves generated at different points along the transmission path will be out of phase and interfere destructively. The incident and diffracted light have slightly different frequencies, however, because they will naturally travel at different velocities because of dispersion. The collinear AOTF takes advantage of birefringence. The geometry of this crystal interaction is set up so that the diffracted light has its polarization rotated 90° with respect to the incident light. For a given RF value (phonon energy), there is only one wavelength of light in which the velocities of the incident and shifted light are equal because of their orthogonal polarization (the phase-matching condition). The only other thing necessary to make a functioning AOTF is to place appropriate polarizers on either end of the device so that light traveling through the crystal is plane-polarized.²⁰

➤ Discussion

The AOTF offers several significant advantages compared to conventional monochromator systems. The solid state tunable filter transmits selected monochromatic radiation without moving parts thus calibration can not be affected by orientation changes or even vibrations and it functions well even in harsh industrial environments.

The AOTF is also a high speed programmable device capable of randomly accessing thousands of wavelengths in less than a second. In fact, the wavelength of the transmitted light depends only on the applied RF; in most instances, this signal is digitally generated and controlled for very fast repeatable precision and accuracy. It is able to record a complete spectrum or portion of the NIR absorption spectrum or can allow the user to select discrete single wavelengths to observe the NIR absorption.²⁴ Programmable wavelength control gives a high flexibility, allowing the spectrometer to be readily adapted for custom analytical applications. Furthermore the throughput is not limited by slits, and exposure of the sample to white light, as with a diode array or an FT instrument, is avoided.²¹ Low energy light sources are suitable and have a longer lifetime than traditional sources. This enables a high light throughput, and in many application areas no fiber optic probes are required.

In spite of the apparent advantages, the AOTF does have some severe limitations. For example, the design of the crystal forces an angular input with a narrow field of view (low f_a number in Equation B-9). This makes them less attractive for applications in which the optical information (or signal) is weak, particularly for imaging processes. Increasing the bandpass of these devices beyond 10 - 20 μm is difficult if not impossible; thus many broadband applications are excluded.²²

In comparison to other spectrometer concepts like FT or gratings the spectral resolution of AOTF crystals is relatively low, decreasing to longer wavelengths.²³ Nevertheless, overall it can be stated that AOTF spectrometers are well suited for high speed applications and installations in critical areas, being easy to achieve and maintain. It can be incorporated in a sealed system using fiber optics for measuring remote samples or for use in extremely hostile conditions.²⁴

B.3.4.3 Scanning grating monochromator spectrometer

Holographic grating monochromators are among the largest selling type of NIR instruments today. Replacing the prism instruments of the 1950s and 1960s, gratings are easily made, inexpensive, and long-lived.

➤ Background

Modern gratings are interference based. A new grating is usually copied of a 'master' grating. It is manufactured by the interference pattern of two lasers impinging on a photosensitive surface (thus, the term holographic). This creates lines of very specific spacing on a reflective (aluminum, silver or gold) surface. When the polychromatic light from a source strikes the surface, it acts like thousands of prisms, dispersing the light according to Bragg's law.

$$m\lambda = 2d \sin \Theta$$

Equation B-11: Bragg's law, with m = order of diffraction, λ = wavelength (of light emitted), d = distance between lines of the grating, θ = angle of diffraction.

➤ Principle of measurement

Depending on the angle at which the grating is rotated, monochromatic light is emitted. The major difference between prisms and gratings is the order of diffraction. White light striking a diffraction grating separates into many orders of radiation, each comprising a spectrum dispersed across a certain angle. A characteristic of this diffraction is the partial overlap of orders. As a result, different wavelengths originating from different orders occur in the same position. For example, the wavelengths 2,400 nm, 1,200 nm, and 800 nm from the 1st, 2nd, and 3rd orders, respectively, might be superimposed.

Preferably, only first order radiation is used for spectrophotometry, as it is the most intense. Radiation from other orders must be blocked from the exit slit to prevent 'contaminating' the first order radiation used for spectral analysis. This is accomplished with order sorter filters, a set of high pass filters, with different short wavelength cutoffs. These filters are mounted in a paddle whose position is cycled through the beam in concert with grating rotation.²⁵ This coordinated effort allows the pure order of light to emerge and impinge on the sample.

Wood's anomaly describes a grating artifact. Wood's anomaly is an area where the polarity of monochromatic light changes, creating a peak in the reference spectrum. It can not be eliminated, so it has to be positioned, where it has minimum effect on spectral data.

➤ Discussion

To produce a workable, high S / N-ratio spectrum, the analyst usually co-adds a number of single spectra (32 or 64 scans are typical) to reduce the noise apparent in an individual scan. In practice this means that a typical laboratory grating instrument can scan one sample per minute. This is fast when compared with the first scanning spectrometers, but may be too slow for real-time quality control analyses. Since most classical equations have been generated on grating instruments, there is a wealth of information available for the user of a grating spectrometer. The better instruments are quite low in noise and have excellent reproducibility.

However, on the negative side the moving grating can be knocked out of calibration by vibrations in process environment. Indeed, any moving part will by definition wear out with time.

B.3.5 Chemometrics and multivariate data analysis (MVDA)

Chemometrics can be defined as the chemical discipline that uses mathematical, statistical, and other methods to design or select optimal measurement procedures and experiments to provide maximum relevant chemical information by analyzing chemical data, such as entire NIR spectra.²⁶ A data table starts to become incomprehensible to a superficial overview once the number of variables exceeds about five. Using chemometric regression methods, the attempt is made to find a statistical relationship between the spectral data and known characteristic values (e.g. active ingredient or moisture content) of the samples tested and to create a calibration function. If this connection is systematic, the characteristic values of unknown samples may be predicted by recording the NIR spectrum and then performing a computer analysis.²⁷

Multivariate data analysis (MVDA) provides a toolbox of flexible and versatile data analytical tools. There are three basic problem types to which these multivariate tools can be applied: (1) overview of a data table, (2) classification and / or discrimination

among groups of observations, and (3) regression modeling between two blocks of data (X and Y). Depending on the problem the appropriate tool must be chosen.

A simple overview of the information in a data table can be obtained with principal component analysis (PCA). PCA produces a summary showing how the observations are related and if there are any deviations in the data. In addition PCA identifies the relationships among the variables: which variables contribute similar information to the PCA model, and which provide unique information about the observations.

SIMCA classification method is based on disjoint PCA models. SIMCA focuses on modeling the similarities between members of the same class. A new sample will be recognized as a member of a class if it is similar enough to the other members, else it will be rejected.

Regression is a generic term for all methods attempting to fit a model to observed data in order to quantify the relationship between two groups of variables. In NIRS these groups of variables are spectra (X-matrix) being related by a regression method to constituents (Y-matrix). Building a regression model involves collecting data of common samples and fitting a predefined mathematical relationship to the collected data.

Univariate regression uses only a single predictor, which is often not sufficient to model a property precisely. Multivariate regression takes into account several predictive variables simultaneously, thus modeling the property of interest with more accuracy. One method of multivariate data analysis is the so-called partial least squares (PLS) being generally applicable to any kind of data without respect to its origin.²⁸

B.3.5.1 Principal component analysis (PCA)

PCA forms the basis for multivariate data analysis.^{29, 30} It goes back to the French mathematician Cauchy, but was first formulated in statistics by Pearson, who described the analysis as finding lines and planes of closest fit to systems of points in space. The most important use of PCA is to represent a multivariate data table as a low dimensional space. Statistically, PCA finds lines, planes, and hyper-planes in a K-

dimensional space that approximate the data as well as possible in the least squares sense.

The starting point for PCA is a data matrix (X) with N rows (observations) and K columns (variables). The observations can be analytical samples with measured properties being reflected in the variables of spectral origin. Each X -variable defines a coordinate axis in a K -dimensional space. The principle of representing rows as points in a space makes it possible to convert a data table to graphical representation. All the observations of X are displayed in K -space as a swarm of points.

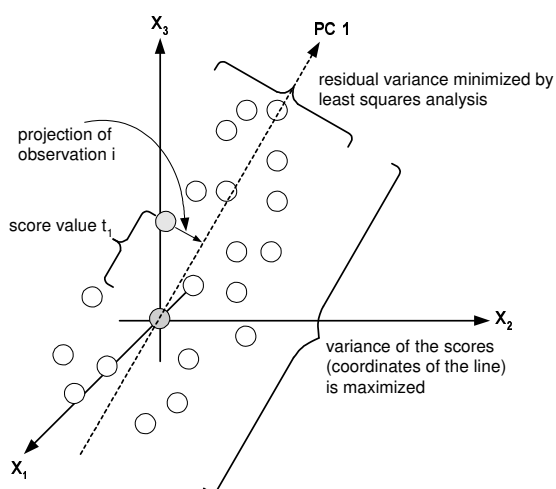


Figure B-23: PCA derives a model that fits the data as well as possible in the least squares sense. Alternatively, PCA may be understood as maximizing the variance of the projection coordinates. Each observation is projected onto this line in order to get a coordinate value along the PC-line. This value is known as a score.

After mean centering and scaling to unit variance, the data is set ready for computation of the first principal component (PC 1). This component is the line in the K -dimensional space that best approximates the data in the least squares sense. This line goes through the average point. Each observation may now be projected onto this line in order to get a coordinate value along the PC-line. This new coordinate value is known as a score.

Usually one component is insufficient to model the systematic variation of a data set. Thus, a second principal component (PC 2) is calculated. The second PC is also represented by a line in the K -dimensional variable space, which is orthogonal to the

first PC. This line also passes through the average point, and improves the approximation of the X-data as much as possible.

When two principal components have been derived they together define a plane, a window into the K-dimensional variable space. By projecting all the observations onto this low dimensional sub-space and plotting the results, it is possible to visualize the structure of the investigated data set. The coordinate values of the observations on this plane are called scores, and hence the plotting of such a projected configuration is known as a scores plot and represents a tool for geometric interpretation of the relationships of the variables.

The scores are accompanied by the corresponding loadings. Geometrically, the principal component loadings express the orientation of the model plane in the K-dimensional variable space. The direction of PC 1 in relation to the original variables is given by the cosine of the angles. These values indicate how the original variables load into, or contribute to the principal component. The loadings are used for interpreting the meaning of the scores.

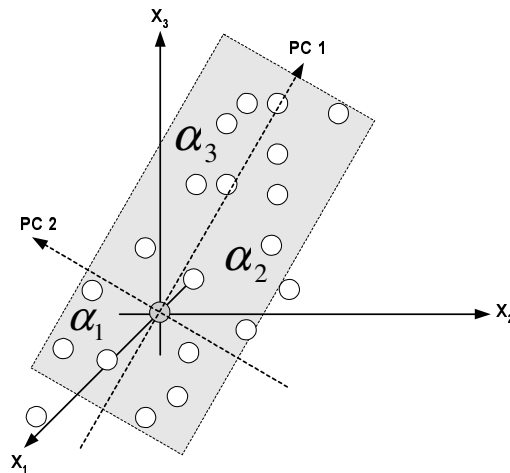


Figure B-24: The principal component loadings uncover how the PC model plane is inserted in the variable space. The loadings are used for interpreting the meaning of the scores.

By using PCA a data table X is modeled as:

$$X = 1\bar{x}' + TP' + E$$

Equation B-12: The first term represents the variable averages and originates from the preprocessing step. The second term is the matrix product and models the structure. The third term, the residual matrix E , contains the noise.

The principal component scores of the applied components (t_1, t_2, t_3, \dots) are columns of the score matrix T . These scores are the coordinates of the observations in the model (hyper-)plane. Alternatively, these scores may be seen as new variables which summarize the old ones. In their derivation, the scores are sorted in descending importance.

The meaning of the scores is given by the loadings. The loadings of the components (PC 1, PC 2, PC 3, ...) build up the loading matrix P (Figure B-25). The loadings define the orientation of the PC plane with respect to the original x -variables. Algebraically the loadings inform how the variables are linearly combined to form the scores. The loadings unravel the magnitude (large or small correlation) and the manner (positive or negative correlation) in which the measured variables contribute to the scores.

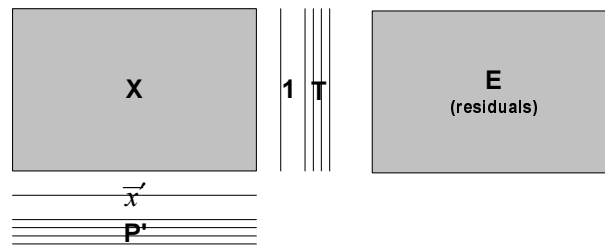


Figure B-25: A matrix representation of how a data table X is modeled by PCA.

Loadings and scores are sufficient to give a satisfactory description of each of the variables in the K -dimensional space. If a high number of observations is involved but only few PCs necessary to lead to low residuals, a severe data reduction has taken place by the projection of the individual observations on the lines, planes, or hyperplanes.

B.3.5.2 Partial least squares (PLS)

PLS stands for projection of latent structures by means of partial least squares. PLS is a method for relating two data matrices, X and Y , to each other by a linear multivariate model. This technique models both the X - and Y -matrices simultaneously to find the latent variables in X that will predict the latent variables in Y the best. In order to find the regression model PLS uses both, the independent and the dependent variables, switching between X and Y iteratively to find the PCs.

The basics of PLS are explained in geometric terms.³¹ This example with N observations (samples), 3 x -variables (wavelengths) is correlated to $M = 1$ response or y -variable (constituent). Whenever an X -matrix is correlated to only one y -value it is question of a PLS 1 (PLS 2 in case of multiple constituents).

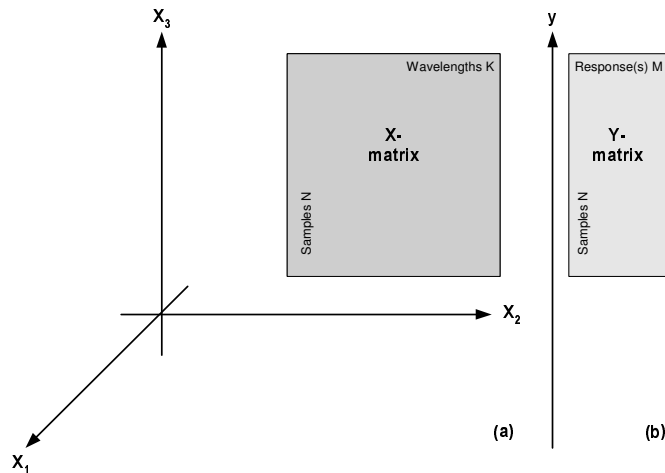


Figure B-26: A regression situation with K wavelengths (X -matrix) and M response(s) (Y -matrix). The length of each coordinate axis has been standardized by scaling to unit variance.

Each row of a data table corresponds to two points, one in the X - and another one in the Y -space. Consequently, with many observations in the data set, two point swarms are situated in these spaces (Figure B-27). The task for the data analysis is to describe the relationship between positions of the observations in the predictor space (X) and their positions in the response space (Y).

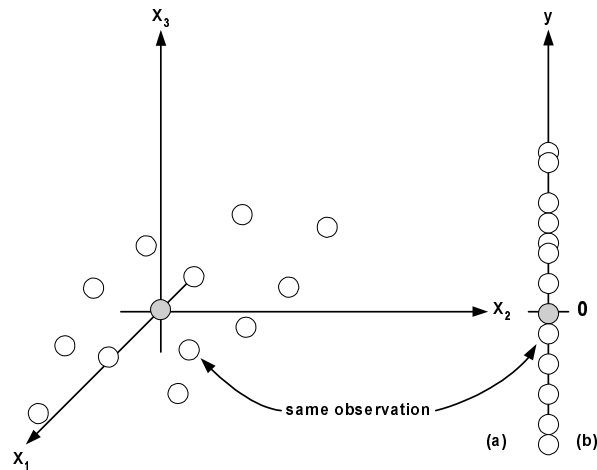


Figure B-27: In a regression problem, the observations can be understood as two point swarms, one in the predictor (X) space and one in the response (Y) space.

To simplify the problem, only a single response variable is considered, rather than a Y -matrix. All the data have been mean-centered. Thus, the coordinate system in X and the coordinate vector in y pass through the average point (in dark gray) of each point-swarm.

➤ The first PLS component

PLS components are lines in the X -space which well approximates the point swarm and provides a good correlation with the y vector. The coordinate of an observation along this line is obtained by projecting the sample onto the line. Similar to the procedure in PCA, this coordinate is termed the score, t_{i1} of observation i . The scores of all the observations from the first X -score vector t_1 .

The score vector t_1 can be thought of as a new variable, a latent variable, which reflects the information in the original x -variables that is of relevance for modeling and predicting the response variable. Subsequently, this score can be used to acquire an estimate of y , $\hat{y}_{(1)}$, after the first PLS component, which is t_1 multiplied by the weight of the y -vector, the so-called loading c_1 . This is explained in the (b) part of Figure B-28.

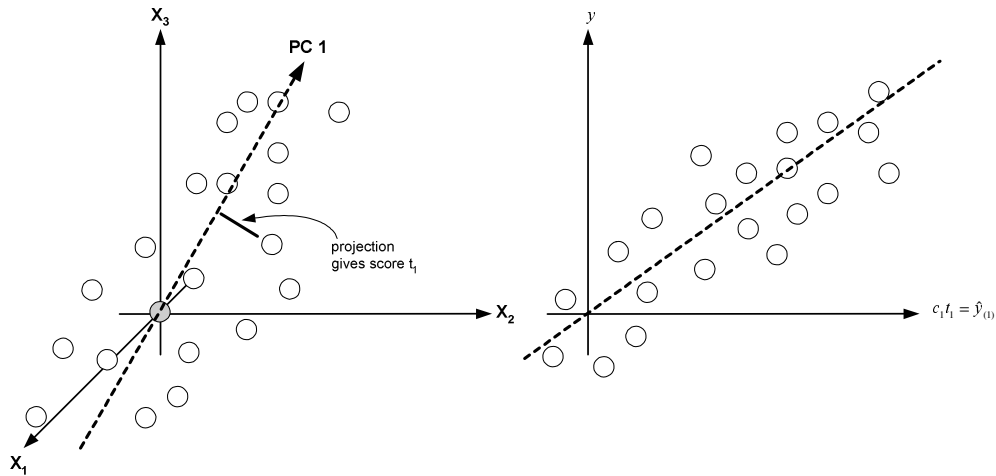


Figure B-28: With a single y -variable, the Y -space reduces to a one dimensional vector. The first component of the PLS model will therefore orient itself so that it well describes the point swarm in the X -space while at the same time giving a good correlation with the y -vector. The projections of the observations onto the line in the X -space give the score of each observation. These are new coordinate values of the observations and they form the score vector t_1 . This vector summarizes the information in the original x -variables.

The differences between measured and estimated response data are called residuals. The y -residuals represent the variation that is left unexplained by the first PLS component. A good model has small residuals. The scatter of the points around the diagonal in Figure B-28 (b) is a graphical way to assess the model performance. When all points are situated on the diagonal, the model is (though not very realistic) ideal of the response data with zero residuals.

Another way to look at the residuals of the response vector is presented in Figure B-29 where the residual vector f_1 , derived as $y - \hat{y}_{(1)}$, is plotted in the (b) part. This residual vector is much shorter than the parent vector of observed y -values. This implies that the first PLS component has accounted for a large part of the variation in y .

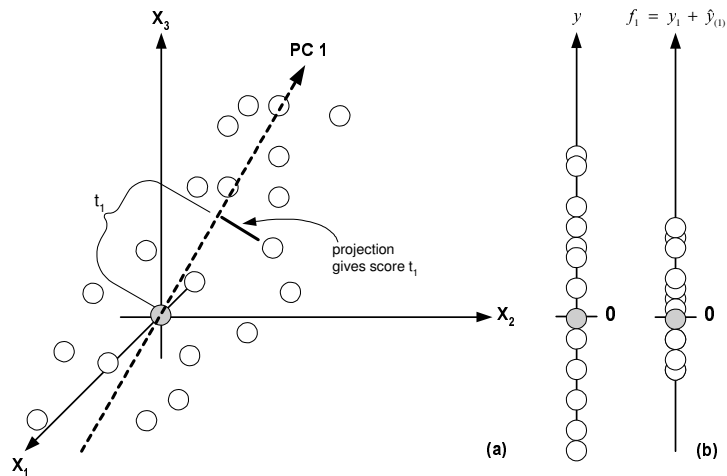


Figure B-29: An illustration of the y -residuals remaining after the first PLS component. The residual vector f_1 , obtained by subtracting $\hat{y}_{(1)}$ from y , is shorter than the vector consisting of the measured data. Therefore the first component has explained a large part of the response variation.

➤ Extending the model with the second component

If one component is insufficient to adequately model the variation in the y data, in almost the same manner as the PCA, the descriptive ability of the PLS model is improved by expanding it with a second component. This component finds the direction in the X -space that improves the description of the x -data as much as possible, while providing a good correlation with the y -residuals f_1 , remaining after the first component.

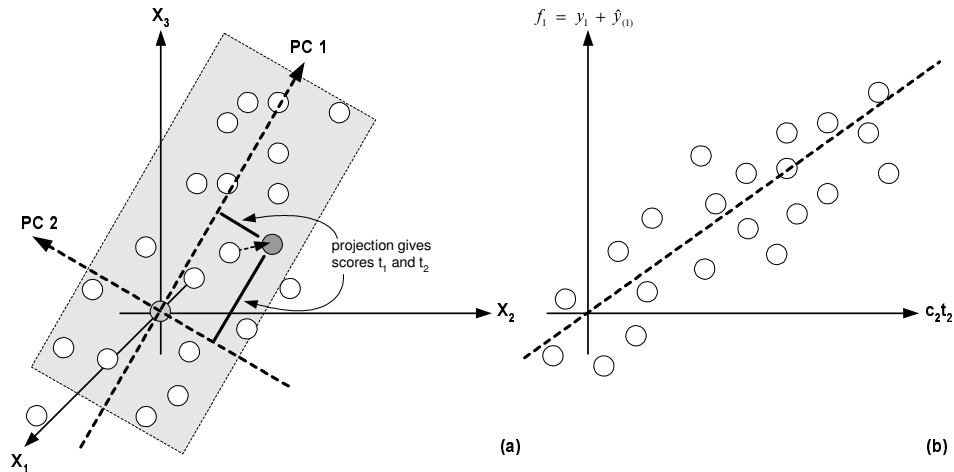


Figure B-30: The second projection coordinate (i.e. the second latent variable) in the X-space is orthogonal to the first one. By projecting the observations onto this line one obtains the score vector t_2 . In part (b) of the figure, we can see how the second score vector times the second loading c_2 , correlates with the y-residual f_1 , after the first dimension. The two components together define a plane in the X-space.

As shown in the (a) part of Figure B-30, the second set of score values of the observations arises from the coordinates along the second projection direction in the X-space. This second score vector is denoted t_2 . Part (b) of Figure B-30 illustrates how t_2 times the second loading, c_2 , correlates with the y-residual, f_1 , after the first dimension. The interpretation is similar to that of Figure B-28. Thus, the tighter the scatter around the dotted diagonal, the stronger is the correlation between X and y in the second PLS model dimension.

The combined power of t_1 and t_2 in modeling and predicting y can be examined. An estimate of y after two model components $\hat{y}_{(2)}$, is obtained through computing $c_1 t_1 + c_2 t_2$. By comparing the (b) parts of Figure B-28 and Figure B-31 it is realized that the y variable is better modeled by two components than by one. This is because the agreement between observed and estimated y-data is better with two components. Geometrically, this more precise estimate of y, $\hat{y}_{(2)}$, is interpretable as the vector addition of PC 1 to PC 2 in the X-space.

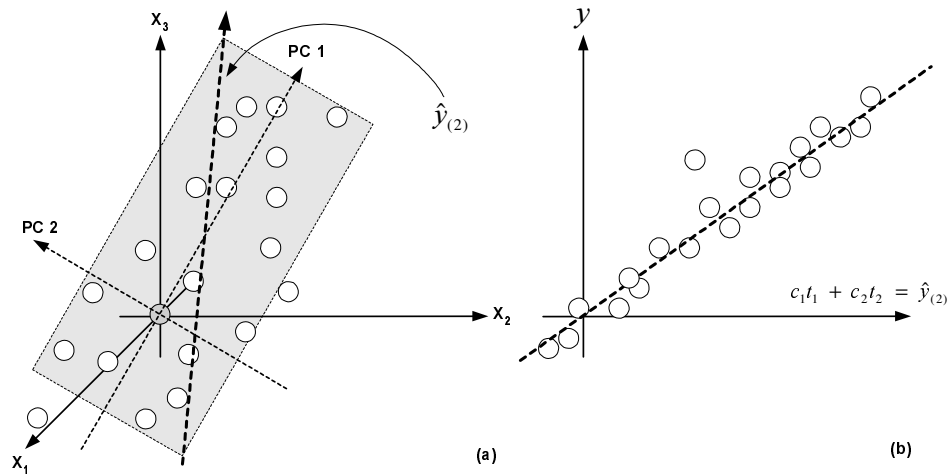


Figure B-31: A comparison of Figure B-28 and Figure B-31 indicates that the y -variable is better modeled with two components than when using only one component. Geometrically, $\hat{y}_{(2)}$ is interpretable as the result of the vector addition of PC 1 and PC 2 in the X -space.

This impact of the second model dimension is illustrated in Figure B-32. The first component explains much of the y -variation, and only a fraction remains in the residual f_1 . The situation is further improved after the inclusion of the second component, as the residual f_2 is smaller than f_1 .

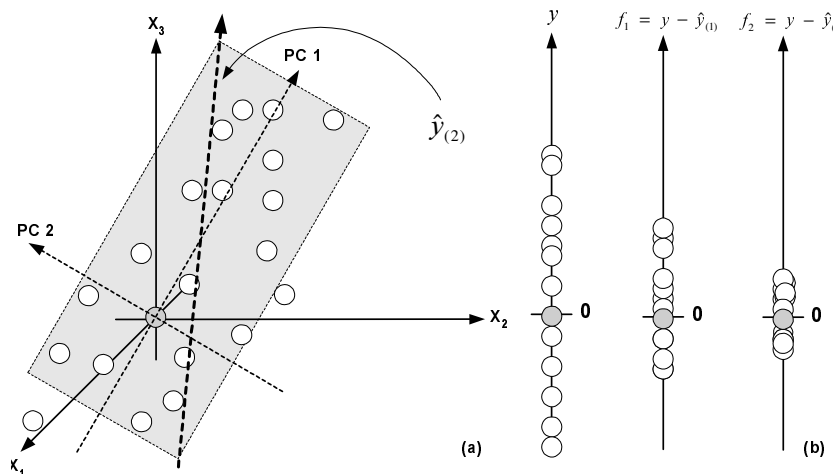


Figure B-32: Schematic illustration of the explanatory power of a PLS. After one PC, the y -residual f_1 , is significantly smaller than the spread of the measured variable. The situation is even better after the inclusion of the second component, and the residual f_2 .

The objectives are first to model the X - and Y -matrix, and then to predict Y from X according to Equation B-13.

$$X = 1\bar{x}' + TP' + E$$

$$Y = 1\bar{y}' + UC' + F = 1\bar{y}' + TC' + G$$

Equation B-13: Due to inner relation there are two formulas leading to Y .

In these expressions, the first terms $1\bar{x}'$ and $1\bar{y}'$, represent the variable averages and originate from the preprocessing step. The information related to the observations are stored in the scores-matrices T and U . The information related to the variables are stored in the X -loading matrix P' and the Y -loadings matrix C' . The variation in the data was left out of the modeling from the E and F residual matrices.

PLS is a maximum covariance model of the relationship between X and Y . A graphical representation of the matrix relationship of PLS is shown in Figure B-33.

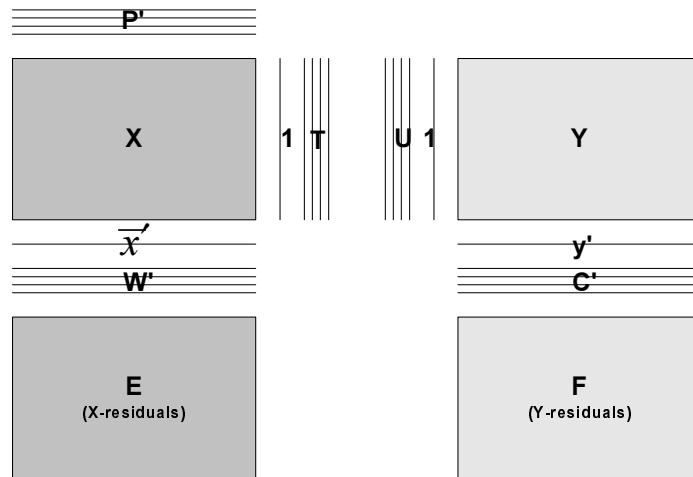


Figure B-33: Illustration of the matrix relationships in PLS, described by the PLS scores T and U , the X -loadings P' , the X -weights W' , and the Y -weights C' . The variation in the data that was left out of the modeling forms the E and F residual matrices.

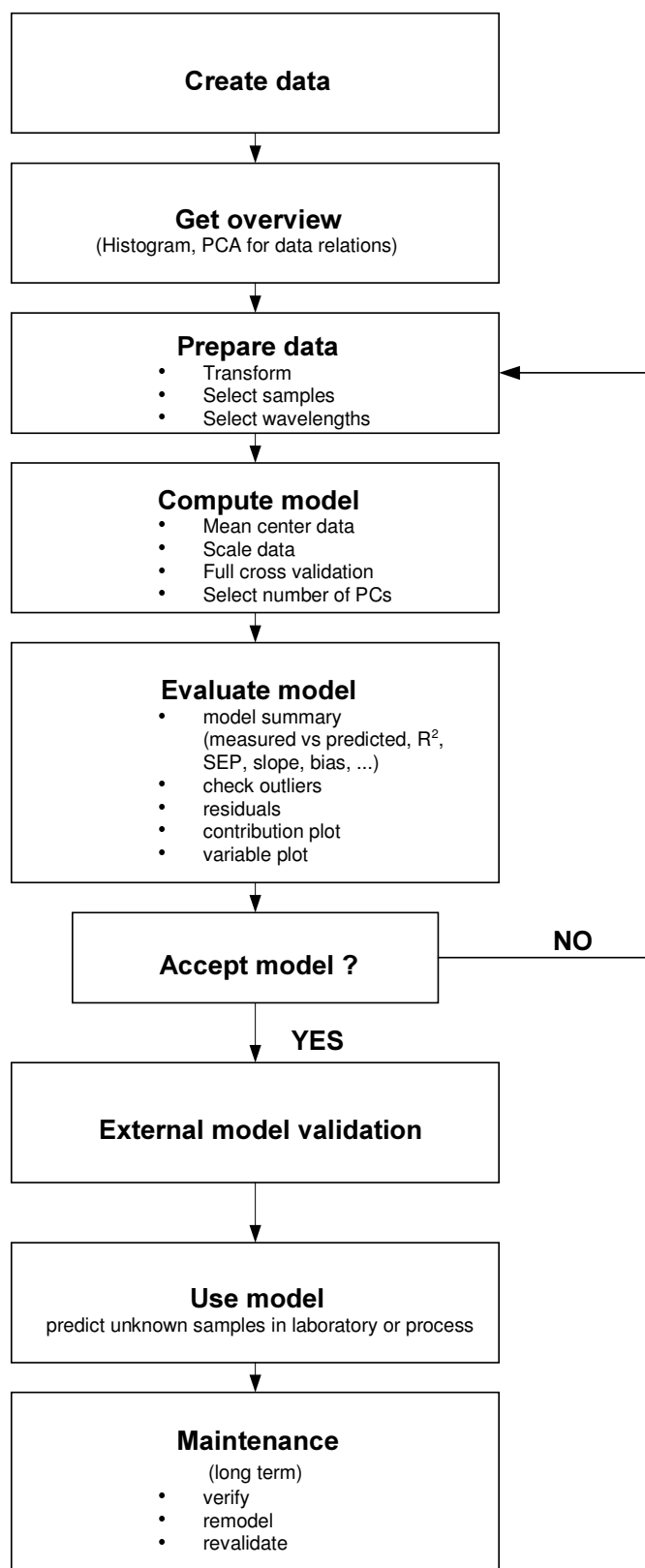


Figure B-34: Flow chart for multivariate calibration of NIR data.

B.3.6 MVDA applied to NIR spectroscopy

The dimensionality of the X-space i.e. the 'spectral' space is given by K, the number of wavelengths. Each variable defines one coordinate axis in the K-dimensional X-space. Points, lines, distances, and other geometrical concepts, have similar properties in K-space to those they have in two- or three-dimensional spaces. Each spectrum (i.e. each row) in a data table corresponds to a point in the K-dimensional X-space.

A data table containing N observations (rows, samples, spectra) corresponds to N points in the K-dimensional X-space. Usually, these points form a swarm with some regularity, which shape and elongation depends on the complexity of the investigated samples. When the series of the investigated samples contain only one analyte, all points are situated on a line, or a smooth curve, with some small deviations caused by noise. Further complexity is introduced in the series when the samples also contain some interacting compounds. Then, the points can be presented by a plane or a hyperplane plus some noise, with one component (dimension) per compound (analyte). The typical procedure of model development in NIR spectroscopy is illustrated in Figure B-34.

B.3.6.1 Common spectral pretreatments

The purpose of a regression model is to extract all the relevant information for the prediction of the response from the available data. Unfortunately observed data such as NIR spectra usually contain some amount of noise, and may also include some irrelevant information. Thus, a good regression model should be able to pick up only relevant information, but all of it. Furthermore, it should avoid overfitting, i.e. distinguish between variation in the response that can be explained by variation in the predictors, and variation caused by mere noise.³²

In these cases some mathematical pretreatment of the spectral data may be useful to filter or reduce secondary effects. In spectroscopy the following transformations are of crucial interest.

➤ Absorbance transformed to reflectance

Spectral data in diffuse reflectance configuration is usually collected in absorbance data format. Thus, prior to Kubelka-Munck based on transmittance T, a spectra

transformation has to be performed. The absorbance A , is represented by Equation B-14.

$$A = -\lg\left(\frac{I}{I_0}\right) \quad \text{or} \quad A = -\lg T = \lg\left(\frac{1}{R}\right)$$

Equation B-14: Formula to compute the absorbance A , with I = intensity of radiation passing through or reflected from the sample, I_0 = intensity of the incident light, T and R = transmittance and reflectance, respectively.

The intensity of the incident light energy from the source, I_0 includes losses due to solvent absorption, refraction, and scattering when the sample is not present. Or in reflectance measurements, it is the intensity of radiation indirectly reflected from the background reference material.

➤ Kubelka-Munck

Kubelka-Munck (1931) states when light penetrates a homogenous scattering material, it will either be absorbed or scattered. By analyzing the light flux in the penetration direction in addition to the flux in the opposite direction, and by applying mathematical techniques, the so-called Kubelka-Munck function was developed:

$$\frac{K}{S} = \frac{(1-R)^2}{2 \cdot R}$$

Equation B-15: The Kubelka-Munck function with K = true absorbance, S = scatter, R = reflected light. R is defined as $R = I / I_0$ intensity of the incident light.

According to this theory the light scatter effect is multiplicative. This means if the spectrum is first properly transformed to the Kubelka-Munck scale, a difference in scatter between two 'equal' samples can be compensated by multiplying the measurement at each wavelength of one of the samples by the same constant.

In diffuse NIR spectroscopy it also sometimes happens that there are clear indications of an additive scatter component.³³ One reason for such an effect may be the following: The theoretical models (e.g. Kubelka-Munck and Beer-Lambert) assume that all or a constant part of the reflected light is detected. But if the instrument is constructed in such a way that only a fraction ($1 / c$) of the reflected light is detected for a particular sample, Equation B-16 is obtained.

$$I_{\text{detected}} = \frac{1}{c \times I_{\text{reflected}}}$$

Equation B-16: If $c' = \lg(c)$ is sample dependent, this will cause an additive baseline difference between the samples, i.e. an additive effect in the absorbance values.³⁴

➤ Multiplicative Scatter Correction (MSC)

Spectroscopic measurements of powders, aggregates of grains or particle sizes, slurries and other particulate-laden solutions often display light scattering effects. This especially applies to NIR data, but is also relevant to other types of spectra. Scatter effects in IR spectra may be caused by background effects, varying optical path lengths, temperature, and pressure variations. Other types of measurement may also suffer from instrument baseline shift, drift, interference effects in mixtures etc. These effects are in general composed both of a so-called multiplicative effect as well as an additive effect.

MSC is a transformation method that can be used to compensate for multiplicative (common amplification) and additive (common offset) effects. MSC was originally designed to deal specifically with light scattering. However, a number of analogous effects can be successfully treated with MSC.

The idea behind MSC is that the two undesired general effects, amplification (multiplicative) and offset (additive), should be removed from the raw spectral signals sometimes dominating over the chemical or other similar signals of lesser magnitude. Thus, one or more PLS components may be saved in the modeling of the relevant Y-phenomena, if it was possible to eliminate (most of) these effects before multivariate calibration.

The Full MSC includes the common offset and common amplification effects as follows: all object spectra are plotted against their average spectrum and a standard regression is fitted to these data, with offset A_i and slope B_i , called the *common amplification* and *common offset* respectively. The MSC function replaces every element in the original X-matrix according to Equation B-17.

$$M_{new} = \frac{M_{i,k} - A_i}{B_i}$$

Equation B-17: The Multiplicative Scatter Correction with offset A, and slope B. The index i stands for all individual objects in the data set.

The whole data set, including the test set, will be corrected using this MSC base. Before any future prediction, the new samples must also be corrected using the same MSC-base.³⁵

➤ Differentiation

The first and second derivatives are common transformations on continuous function data where noise is a problem, and are often applied in spectroscopy. Some local information gets lost in the differentiation but the 'peakedness' is supposed to be amplified and this trade-off is often considered as advantageous. It is always possible to try out differentiated spectra, since it is easy to see if the model gets any better or not.

The first derivative is often used to correct for baseline shifts. The second derivative to handle scatter effects, the other being MSC, which handles the same effects.³⁵ The main difference is that derivatives are processing independently one spectrum after the other while MSC mean centers the entire sample set. Thus it makes sense to perform MSC and a derivation afterwards.

➤ Savitzky-Golay

Savitzky-Golay enables to compute first or higher order derivatives including a smoothing factor which determines how many adjacent variables will be used to estimate the polynomial approximation used for derivation.

This algorithm fits a polynomial to each successive curve segment, thus replacing the original values with more regular variations. The length of the segment and the order of the polynomial are adjustable. A first order polynomial is equivalent to a moving average.

➤ Norris

Norris derivation is an alternative algorithm used to compute first derivatives only. The advantage is that there is no loss of data points at the edges of the spectrum.

B.3.6.2 Neural networks

Artificial neural networks have become very popular for handling non-linear problems. Many implementations somehow lack one or more of the critically important facilities like interpretation, diagnostics, outlier detection, and validation. Hence there are no convenient tools to detect severely overfitted applications.

Preprocessing the data first by ordinary PCR or PLS may be a possibility to correct this, giving access to interpretation of the main variations, outlier detection, diagnostics and transformations. If there are clear signs of remaining non-linearity, the PLS score matrix can be used as input to a neural network.

B.3.7 Discussion

The typical analysis procedure for solid dosage forms is to bring a small random sample of a production batch to a laboratory, prepare (e.g. grind or dissolve) it and proceed with some form of chemical or spectrometric testing. Not only are the tests destructive, the time required is considerable. If the purpose of the testing is to perform quantitative analysis, then in all probability the batch will have been completed before the results become available to production staff. If samples are rare and qualitative testing is to be performed, the loss of the material is an added drawback to the requisite analysis time.

One of the strengths of NIR, i.e. low extinction coefficients, was once considered a major disadvantage. That implied that NIR could not be used for trace analysis as could the mid-IR. This disadvantage became important when considering process measurements. Much of the sample preparation in the mid-IR involves dilution. KBr pellets, mulls, dilute solutions, and thin films compensate for the strong absorbance and weak sources exhibited in midrange IR. The strong sources and weak absorbance in NIR allowed for measurements of intact samples close or in direct contact.²³

NIR radiation penetrates further into the material being scanned, is less absorbed, and is more easily detected through diffuse reflectance compared to the mid-IR. The origins of these phenomena include physical and mechanical reasons: higher intensity lamps, 100 - 1,000 times lower extinction coefficients, and quieter detectors.^{36, 37} As a consequence, the measurements of the samples are more than a surface

measurement. The radiation penetrates well into, and in some cases completely through the sample form. This characteristic allows a more representative sampling than a surface or grazing spectrometric approach might provide. NIR light (app. 1 eV photon energy) passes well through usual window glass or fiber optics and does not cause photo decomposition of the samples. NIR equipment is simple and relatively inexpensive.

NIR is a rapid and non-destructive technique requiring no or reduced sample preparation (no reagents are used), that can be used to monitor concentrations of several chemical species and physical parameters simultaneously. Not only sample component identities and concentrations, but also characteristics such as molecular weight, taste, hardness, and even thermodynamic parameters such as heat can be detected. The speed and ease of NIR measurements is one of the most important criteria for many analytical or monitoring processes. In combination with the field of mathematics dealing with multivariate data analysis in chemistry, a fast and powerful tool for qualitative and quantitative analysis of pharmaceutical materials becomes available. All types of materials are concerned, from solid or liquid raw materials to intermediate (powders, slurries, granulates or pellets) and final products in every form (like capsules, tablets and lyophilized products).

The difficulty in measurement arises from the manner in which the sample is presented to the NIR instrument. Scoring and other surface imprinting causes differential scattering of the impinging light. For example density and hardness differences within and between multiple lots cause different penetration of the light. Moreover, variable polishing of a dosage form can result in non-reproducible levels of specular reflection.

All of this possible variation in practice has to be included in an extensive training set for calibration. As a result usually very time consuming calibration work has to be performed before any valid analysis result can be obtained. In general NIR spectroscopy is only beneficial if after calibration a lot of the same analyses will be performed.

In addition to the rather empirical and somewhat arduous development of NIR applications, when it comes to routine implementation in pharmaceutical industry, full

specification and documentation must be provided, and various regulatory aspects have to be considered carefully.^{38, 39} For example, NIR applications focusing on classification, identification, or quantification methods, require extensive model development and validation, a risk impact study making allowance for possible mistakes, the definition of model variables and measuring parameters, and a comprehensive data analysis. Furthermore, clearly defined working procedures, the training of potential users and usable outputs should be foreseen. To comply with general regulatory requirements, the maintenance of a really serviceable documentation on the lifecycle of the NIR model, the spectrometer and the computer is required.⁴⁰

References B.3 Near-infrared spectroscopy (NIRS)

- ¹ Radtke et al., Nahinfrarot (NIR)-Spektroskopie: Grundlagen und Anwendung aus pharmazeutischer Sicht
- ² Davies A. M. C., Giangiacoimo R., Near Infrared Spectroscopy: Proceeding of the 9th International Conference, NIR Publications, 2000
- ³ Norris K., NIR News, 4, 10, 1993
- ⁴ Norris K., NIR News, 3, 12, 1992
- ⁵ Norris K., Hart J. R., Proceedings of the 1963 International Symposium on Humidity and Moisture, Vol. 4, 19 - 25, Reinhold Publishing Corporation, New York, 1965
- ⁶ Wold S., Albano C., Dunn W.J., Edlund U., Esbensen K., Geladi P., Hellberg S., Johansson E., Lindberg W., Sjöström M., Multivariate Data Analysis in Chemistry, in: Kowalski B.R., Chemometrics: Mathematics and Statistics in Chemistry, D. Reidel Publishing Company, Dodrecht, Holland, 1984
- ⁷ European Pharmacopoeia 4th edition 4.03, 2.2.40, Near-infrared spectrophotometry, Govi-Verlag, Stuttgart, Germany, 2002
- ⁸ Naes T., Isaksson T., Fearn T., Davies T., A User-Friendly Guide to Multivariate Calibration and Classification, NIR Publications, Chichester, UK, p. 324 (2002)
- ⁹ Ingle J. D. Jr., Crouch S. R., Spectrochemical Analysis, Prentice Hall, Englewood Cliffs, NJ, USA, 1988
- ¹⁰ Ciurczak E. W., Drennen J. K., Pharmaceutical and Medical Applications of Near Infrared Spectroscopy, Practical Spectroscopy Series Volume 31, Marcel Dekker, Inc., New York, Basel, 2002
- ¹¹ Siesler H. W., Ozaki K., Kawata S., Heise H. M., Near-Infrared Spectroscopy, Wiley-VCH, Weinheim, Germany, 2002
- ¹² Drago R. S., Physical Methods in Chemistry, W. B. Saunders, Philadelphia, 1977
- ¹³ Documentation to NIRVIS basic course, Büchi Labortechnik AG, Flawil 1999
- ¹⁴ FOSS NIRSystems, A guide to Near Infrared Spectroscopic Analysis of Industrial Manufacturing Processes, Silver Spring, MD, USA
- ¹⁵ Bruker Optics, Guide for Infrared Spectroscopy, 2003
- ¹⁶ ABB Bomem, Québec, Canada
- ¹⁷ Introduction to Acousto-Optics, Brimrose Corporation of America, Baltimore
- ¹⁸ AOTF Spectroscopy: A powerful new tool in near infrared spectroscopy, Brimrose Corporation of America, Baltimore
- ¹⁹ Wang X., Acousto-optic tunable filters spectrally modulate light, Laser Focus World, PennWell Publishing Company, May 1992
- ²⁰ Soos J., Industrial process monitoring requires rugged tools, Laser Focus World, PennWell Publishing Company, August 1994

References B.3 Near-infrared spectroscopy (NIRS) continuation

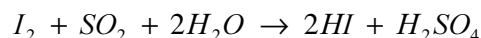
- ²¹ Eilert A. J., Sweat J. A., Wetzel D. L., Parabolic concentration of diffusely transmitted near infrared radiation in an acousto optic tunable filter spectrometer, *Near Infrared Spectroscopy* 8, 239-250, USA, 2000
- ²² McClure W. F., Near-Infrared Spectroscopy - The Giant is Running Strong, *Analytical Chemistry*, Vol. 66, No. 1, 43 - 50, January 1, 1994
- ²³ Ciurczak E. W., A comparison of Near-Infrared Spectrometers for solid dosage form Analysis, *Pharmaceutical Technology, Yearbook 1997*, 18 - 28, 1997
- ²⁴ Pickuth A., Advances in bridging the gap between laboratory and process on- and in-line NIR spectroscopy of liquids by the combined technologies of AOTF (acousto-optical tunable filter) remote sensing probes with fiber optics, sampling point multiplexing, and uses of chemometric software packages, Maihak AG, Germany
- ²⁵ Instrument Performance Test Guide, Part No. 720-780-1000, Version 2.0, FOSS NIRSystems, Inc., Silverspring, MD
- ²⁶ European Pharmacopoeia 4th edition 4.03, 2.2.40, Near-infrared spectrophotometry, Govi-Verlag, Stuttgart, Germany, 2002
- ²⁷ Documentation to NIRVIS basic course, Bühler AG, Anatec, Uzwil, 1997
- ²⁸ Eriksson L., Johansson E., Kettaneh-Wold N., Wold S., Multi and Megavariate Data Analysis, Principles and Applications, Handbook of Umetrics Academy, Umea, Sweden
- ²⁹ Jackson J. E., A User's Guide to Principal Components, John Wiley, New York, 1991
- ³⁰ Wold S., et al, Multivariate Data Analysis in Chemistry, In: B. R. Kowalski (ed.), *Chemometrics: Mathematics and Statistics in Chemistry*, D. Reidel Publishing company, Dordrecht, Holland, 1984
- ³¹ Phatak, A., DeJong S., The Geometry of PLS, *Journal of Chemometrics*, 11, 311-338, 1997
- ³² User Manual The Unscrambler, Camo, Oslo, Norway, 1998
- ³³ Geladi P., Mac Dougall D., Martens H., Linearization and Scatter-correction for Near-infrared Reflectance spectra of Meat, *Applied spectroscopy*, 3, 491 - 500, 1985
- ³⁴ Naes T., Isaksson T., Fearn T., Davies T., *Multivariate Calibration and Classification*, NIR Publications, Chichester, UK, 2002
- ³⁵ Esbensen K. H., *Multivariate Data Analysis - in practice*, 4th edition, 2000
- ³⁶ Williams P., Norris K., *Commercial Near-Infrared Reflectance Analyzers*, Near-Infrared Technology in Agriculture and Food Industries (American Association of Cereal Chemists, St. Paul, MN, 1987
- ³⁷ Ciurczak E. W., Burns D. A., *Principles of Near-Infrared Spectroscopy*, Handbook of Near-Infrared Analysis, Marcel Dekker, New York, 1992
- ³⁸ European Pharmacopoeia, 4th Edition 4.02, chapter 2.2.40, Deutscher Apotheker Verlag, Stuttgart, Govi Verlag - Pharmazeutischer Verlag GmbH, Eschborn, 1997
- ³⁹ TGA Requirements for Use of Near Infra-Red, NIR, Final Version, 22 August 1997
- ⁴⁰ Ulmschneider M., An introduction to near-infrared spectroscopy, 22 December 2000

B.4 Karl Fischer titration

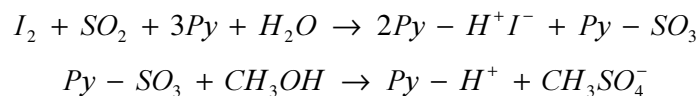
B.4.1 Theoretical background

B.4.1.1 Karl Fischer reaction

The determination of the water content is based on the redox-reaction described by R. W. Bunsen (1853)¹:



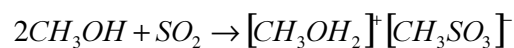
Karl Fischer (KF) discovered that this reaction could be used for water determination in a non-aqueous system containing an excess of sulfur dioxide.² Methanol proved to be a suitable solvent. In order to achieve an equilibrium shift to the right, it is necessary to neutralize the acids that are formed during titration. Smith, Brynaz and Mitchell³ formulated a two step reaction:



According to these equations, methanol not only acts as solvent but also participates directly in the reaction itself. In an alcoholic solution, the reaction between iodine and water takes place in the stoichiometric ratio of 1 : 1. In an alcohol free solution, the reaction between iodine and water occurs in the stoichiometric ratio of 1 : 2.

Further studies conducted by E. Barenrecht and J. C. Verhoff⁴ on the subject of the KF reaction have revealed that pyridine is not directly involved in the reaction, i.e. it only acts as a buffering agent and can therefore be replaced by other organic bases, the rate of the KF reaction depends on the pH value of the medium.

One explanation for this relationship between the pH value and the reaction rate is that it is not the sulfur dioxide itself that is oxidized by iodine under the influence of water, but rather the methyl sulfite ion, which is formed from sulfur dioxide and methanol by solvolysis:

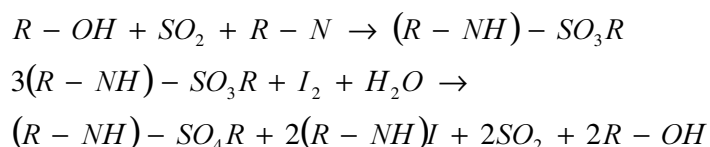


The higher the pH value of the solution, the more methyl sulfite is formed by the capture of protons and the faster the KF reaction. In the pH range from 5.5 to 8, all of

the sulfur dioxide is available as methyl sulfite: the maximum reaction rate is reached here. Due to the side reactions between iodine and hydroxide or methylate ions, the rate rises again at pH values greater than 8.5. This results in a vanishing end point and a higher iodine consumption during the titration.

B.4.1.2 Recent research into the reaction sequence

In 1984 E. Scholz^{5, 6} developed a pyridine-free KF reagent with imidazole (R-N) as base. This reagent not only replaced the toxic, pungent pyridine, but also facilitated faster, more accurate titration, as imidazole buffers in a more favorable pH range than pyridine. The stoichiometric analyses also revealed that other alcohols are capable of improving the titer stability of the reagent. Ethanol, 2-propanol or methoxyethanol (R-OH) can be substituted for methanol. These findings yielded the following equations for the KF titration:



He was also able to confirm the existence of basic methyl sulfite in methanol / SO₂ / I₂ solutions during the titration. In 1988 Seubert⁷ detected methylsulfite in KF solutions with the aid of IR spectroscopy and identified dimethylsulfate as a secondary product of the KF reaction.

Recent studies have postulated that the oxidizing molecules are not I₂ or R-N-I₂ but rather that part of the I₂ in the polar solvents reacts disproportionately to form I⁻ and R-NI⁺ and then reacts further.

B.4.1.3 Consequences for practical applications

➤ pH dependence

Since the maximum speed of the KF titration is in the pH range from 5.5 to 8, values greater than 8 and less than 4 should be avoided in practice. With acidic or basic samples the pH of the titration solution should be adjusted by the addition of buffering agents (with imidazole as the basic buffer and salicylic acid as the acid buffer).

➤ Effect of the solvent

The stoichiometry (molar ratio $\text{H}_2\text{O}:\text{I}_2$) depends on the type of solvent. Investigations by Eberius⁸ have shown that iodine and water react in the ratio of 1 : 1 if the percentage of methanol in the solvent is 20 % or more. Therefore methanol should always be present in the minimum required amount. If a methanol free titrant is required (for ketones or aldehydes), also other primary alcohols can be used.

➤ Effect of the water amount

The molar ratio $\text{H}_2\text{O} : \text{I}_2$ is also influenced by the amount of water in the sample. A rise in the water contents greater than 1 mol / L is observed.⁴ However, this is of no consequence for practical applications, when the water concentration is significantly lower.

B.4.2 Volumetric KF titration

B.4.2.1 Reagents

The KF reagent water equivalent is checked each time before starting any KF measurement. The KF reagent is standardized either with pure water (a water-in-methanol standard) or sodium tartrate with a defined proportion of crystal water ($\text{Na}_2\text{C}_4\text{H}_4\text{O}_6 \times 2 \text{H}_2\text{O}$ containing 15.65 % water)

➤ One-component reagent

A one-component reagent titrant contains iodine, sulfur dioxide and imidazole, dissolved in a suitable alcohol (e.g. methanol). Here the solvent is methanol or a methanolic mixture specially adapted to the sample. The simple handling and the favorable price argue for the one-component reagents, on the other hand the titer is less stable and the titration speed is slower.

➤ Two-component reagents

Two-component reagent titrants contain only iodine and methanol whereas the solvent is composed by sulfur dioxide, imidazole and methanol. A titration speed two or three times higher compared to the one component reagent can be achieved. Both of the components are extremely stable in storage, provided that the bottles are tightly sealed.

Ideally, the titrant should be added as quickly as possible and the addition stopped exactly at the end point. This is the only way to determine the titrant consumption precisely. Control is only possible if the end point is indicated.

B.4.2.2 Principle of bivalentametric indication

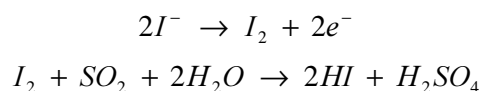
A small, constant current - the polarization current (I_{pol}) - is applied to a double platinum pin electrode. As long as the added iodine reacts with the water, there is no free iodine in the titrating solution. A high voltage is necessary to maintain the specified polarization current at the electrode. As soon as all the water has reacted with iodine, there will be free iodine in the titration solution. This free iodine causes ionic conduction and the voltage needs to be reduced to keep the polarization current constant. When the voltage drops below a defined value, the titration is terminated.

The ionic conduction takes the following course: an iodine molecule is attracted to the cathode platinum pin. The molecule is reduced to iodide ($2 I^-$) anions, which are immediately attracted to the anode, where they donate the electrons and reform an iodine molecule again. The titration solution must be stirred thoroughly to ensure constant ionic conduction.

The titration is terminated when free iodine is detected in the titration solution, i.e. the titration end point is reached when the potential at the polarized, double platinum pin electrode drops below a predefined value. This value depends above all on the polarization current, and to a lesser extent on the type of electrode as well as on the solvent that is used. Electrodes with a large platinum surface result in a smaller potential jump and a lower end point, and vice versa.

B.4.3 Coulometric titration

The term coulometry summarizes methods in which a substance is quantified by either oxidation or reduction at an electrode. For coulometric KF titration a solution of sulfuric dioxide and iodide is required. If water is present a low concentration of iodide is generated electrochemically. As the iodide is generated it reacts stoichiometrically with the water and sulfuric dioxide to sulfuric acid and iodine.



Therefore the potential is kept constant, and the current will decrease as the reactants are consumed. As soon as the reaction is completed, the current is negligible.

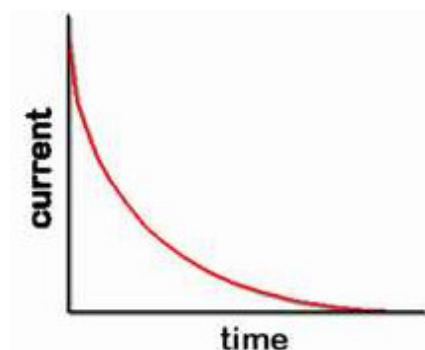


Figure B-35: Course of the current over the time in a coulometric titration.

The area under the curve equals the number of coulombs used and is proportional to the reduced iodine molecules. As the control of currents is highly precise, the water equivalent can be determined by this electrical charge.

$$Q = \int_0^{t_E} I_E dt$$

Equation B-18: Calculation of the required charge by means of the current I_E and the time of analysis t_E .

B.4.4 Sources of error

An overestimation of the true water content is caused by both moisture adhering to walls of the unit and absorption of atmospheric moisture, which is very probable in case of hygroscopic samples, such as lyophilizates. If the stirring speed is too high air bubbles appear in the titration vessel corrupting the conductivity of the solution.

Equally overestimation of moisture is originated by chemical interactions by all of which can reduce iodine; very common is ascorbic acid, hydroxy- and amino-phenols and naphthols. Other chemical interferences can be due to i.e. carbonyl compounds and strong acids reacting with methanol producing water, unsaturated fat binds iodine.⁹

Another source of error could be an incomplete water extraction out of the sample, e.g. due to bad solubility in the solvent or a too short endpoint delay time to allow for

complete extraction. Using too small or too large sample size: both will result in inaccurate readings.

For volumetric determinations it is the most precise to choose a sample size that will titrate within one burette-filling. Equally when wet methanol is used unnecessarily large amounts of titrant are consumed and the system can be blanked. Air bubbles in burette cylinder or delivery lines, caused by too high refill velocities, will result in inaccurate volume delivery.

References B.4 Karl Fischer titration

- ¹ Bunsen R. W., Liebigs Ann Chem. 86, 256, 1853
- ² Fischer K., Neues Verfahren zur Massanalytischen Bestimmung des Wassergehaltes von Flüssigkeiten und festen Körpern, Angew. Chem. 48, 394 – 396, 1935
- ³ Smith D.M., Bryant W.M., Mitchell jr. J., Analytical Procedures Employing Karl Fischer Reagent I. Nature of Reagent, J. Amer. Chem. Soc 61, 2407 – 2412, 1939
- ⁴ Verhoff J. C., Barendrecht E., Mechanism and Reaction Rate of the Karl Fischer Titration Reaction. Part I, Potentiometric measurements, J. Electroanal. Chem. 71, 305 - 315, 1976 and Verhoff J. C., Barendrecht E., Mechanism and Reaction Rate of the Karl Fischer Titration Reaction. Part V. Analytical Implications, Anal. Chem. Acta. 94, 395 - 403, 1977
- ⁵ Scholz E., Karl Fischer Reagenzien ohne Pyridin, Fresenius Z. Anal. Chem., 303, 203 - 207, 1980
- ⁶ Scholz, E., Karl Fischer Reagenzien ohne Pyridin, Einkomponenten Reagenzien, Fresenius Z. Anal. Chem., 309, 30 - 32, 1981
- ⁷ Seubert A., Diplomarbeit an der Universität Hannover, 1988
- ⁸ Eberius E., Wasserbestimmung mit Karl Fischer Lösung, 2nd Edition, Verlag Chemie Weinheim, 1954
- ⁹ Application Brochure 26 of Mettler Toledo GmbH, Fundamentals of the Volumetric Karl Fischer Titration with 10 Selected Applications, October 1998

Chapter C: Experimental Part

C.1 Scope

In view of the financial risk involved, the feasibility of total in-line inspection was to be investigated. The following project plan was compiled:

1. Assessment of the original situation

QC already had a sound knowledge of NIRS and moisture analysis on a laboratory scale. For this reason, attempts were first made to learn as much as possible from earlier experiments. The available knowledge was used to carry out further tests with a view to reducing known uncertainties or to check their validity for other products.

2. Evaluation of the appropriate analytical system

Most of the spectrometer suppliers approached refused to cooperate right from the outset, since their systems could not satisfy the speed requirements. The only two appropriate analytical systems were compared for suitability in a study. The comparison was to include both the spectrometer and the software. The crucial criterion was the quality of the forecast of water content under process conditions.

3. Laboratory-scale feasibility study

As soon as a spectrometer had been selected, the feasibility of determining the residual moisture content was also to be demonstrated with the other products on a laboratory scale. This test included the time-critical parameters. This stage had to be completed successfully before going on to the next phase.

4. Process simulation

An automation concept into which the production line could be integrated had already been designed in collaboration with a mechanical engineer. Using this as a base, only a prototype capable of simulating the dynamic process was initially commissioned. This meant that the initial investment could be limited to a much smaller amount and that an off-line test device would in future be available outside routine production for the development of new calibrations. It also means that other

product validations could be performed in the laboratory. To make the two process units directly comparable, care was taken to ensure that as many matching components were used as possible.

5. Investment accounting

If in-line inspection was feasible, a certain level of investment was needed in order to implement it in the production line. This would cover the analytical equipment and its software, plus automation of the vial feed and vial transport. On the basis of the products investigated, a profitability calculation should show whether this investment was profitable or not.

C.2 Original situation

C.2.1 Measurement parameters

Since NIR measurements are fundamentally temperature-dependent, there was a need to avoid any fluctuations, both in the spectrometer and in the samples. Consequently, all spectrometers were used in continuous operation to obtain conditions that were as constant as possible. The samples were measured only at ambient temperature, regardless of whether they were refrigerated products, since the production environment was climate-controlled to 20 – 25 °C.

As the layer of even the lowest-diameter samples was too thick for study in transmittance, the measurements had to proceed using a diffuse reflection arrangement. Lateral measuring of moving vials was likely to produce further distortions. To avoid further scattering on the round glass surface of the vials, the samples were measured from below, through the bottom of the vial. Defined device-specific distances to the reading window had to be maintained, and these were specified individually for each spectrometer.

All NIR measurements within this project were taken in absorbance mode, against a background spectrum of a 99 % Spectralon reflection standard. PCAs were used for qualitative calibrations, PLSs for quantitative determinations, with both methods based on mean centered data.

C.2.2 Preparation of the samples

This study covered four different freeze-dried products, two of them manufactured in two different concentrations.

As stated above, water contents from 0 to 2 % or 3 %, depending on the product specification, were approved for sale, while levels between 0 and 0.5 % were very unlikely in practice. No samples with higher moisture content may be released. The NIR models therefore had to cover at least this calibration range. In order to avoid inaccurate extrapolations and to set up robust calibrations, samples outside the regular analysis range had also to be used. However, the accuracy of the predictions relating to

these peripheral samples was becoming less and less important, since the only decisive factor for release was whether the actual water content lied above or below the recorded figure.

	Dosage [mg]	Fill mass [mg] (anhydrous)	Max. water content [%]
Product A	20	100	2
	40	100	2
Product B	90	108	3
Product C	150	300	3
	400	500	3
Product D	500	500	3

Table C-1: Overview about the product specifications.

Pharmaceutical industry processes are strictly validated to ensure high levels of product uniformity. Correspondingly, experience has shown that most units of a lyophilized batch were within a very narrow bandwidth. For example, the water content of standard Product A 20 mg vials was between approximately 1 % and 1.5 %. As the acceptance limit for this product was around 2 %, a calibration range from 0.5 % to 3 % was desirable. Since in the normal course of events such samples occurred either not at all or very rarely, they had to be created artificially for the purpose of calibrating the NIR models.

Once a non-destructive analysis method was in place, outliers in routine production could be recognized and collected and then used to improve an existing calibration or set up a new one.

C.2.2.1 Drying

In absolute terms, residual moisture involved very small quantities of water, since the fill masses of the dried vials were relatively low (approx. 100 – 500 mg). Thus in a case of Product A approximately 1 – 1.5 mg of water remained, which now needed to be further extracted without altering the product's chemical composition or its physical characteristics, since those factors also play a role in NIR measurements. At the same time it had to be remembered that these were hygroscopic products: in other words, they had a tendency to absorb ambient moisture once their containers were opened.

As a first step, TGA was used to determine the temperature at which the greatest loss of mass occurs without the product actually decomposing. This finding was then used as a guideline value for further drying of the corresponding samples in a vacuum drying cabinet at around 20 – 30 mbar.

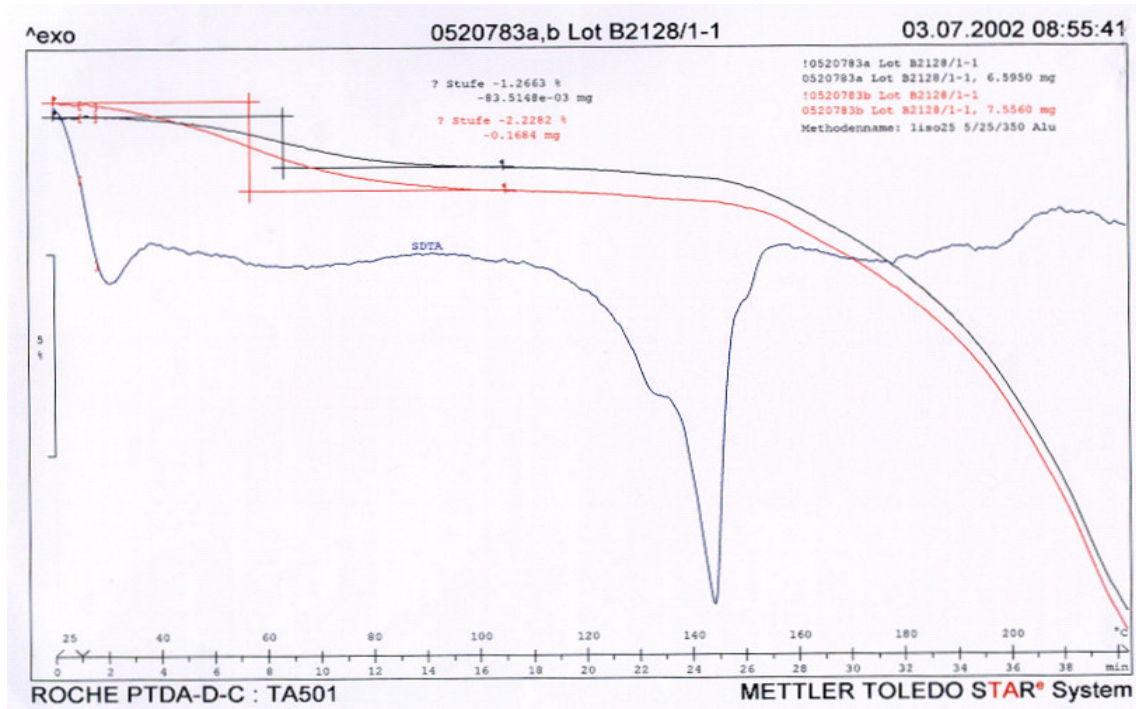


Figure C-1: Duplicate TGA analysis of Product A 20mg. At approx. 60 °C the greatest loss of mass per unit time occurs, while the lyophilizate decomposes above approximately 140 °C (The corresponding plots for the other products are attached in the appendix).

Since the precise water content at the beginning of drying could not be determined with certainty, it was difficult to ascertain the loss of mass per unit time as a constant. In the case of Product A, it proved possible to achieve water contents of < 0.5 % at 80 °C and drying times of approximately 80 hours. In order to avoid any new absorption of moisture by the samples on removal from the drying cabinet, the Teflon stoppers were dried together with the samples and placed on the flasks while these were still hot. The stoppers were then crimped and the vials stored in desiccators over blue silica gel. Dried samples were marked with the number of drying hours (XXh).

Approx. drying temperature [°C]	
Product A	80
Product B	90
Product C	120
Product D	120

Table C-2: Guideline values for drying temperatures.

C.2.2.2 Humidification

Due to the hygroscopic nature of the lyophilizates, it was sufficient to store them opened in DC chambers over water. In order to achieve higher air humidity in the chamber at the same temperature, saturated potassium dihydrogen phosphate solutions were used, increasing the vapor pressure of the water. The humidified samples were marked with the appropriate time in minutes in the DC chamber (XXm).

	Solubility [g / 100g H ₂ O]	Relative air humidity U [%] at T			
		20 °C	23 °C	25 °C	30 °C
KH ₂ PO ₄	23	96	96	96	95

Table C-3: Stated relative air humidity over a saturated potassium dihydrogen phosphate solution at ambient temperature.¹

➤ Theoretical considerations on the targeted humidification of samples

Particularly when certain water values required for uniform distribution across the range were missing during calibration development, it was desirable to humidify samples to a targeted degree. However, it proved difficult to standardize sample humidification, since several parameters were unknown. These included the fill mass, which according to the pharmacopoeia may deviate by ± 10 %. In addition, in some products baseline moisture varied markedly even between samples from the same batch. In reality the intention was that in future samples from unknown new batches could also be conditioned in this way.

Nevertheless, a number of trials were conducted to determine the average water absorption of the lyophilizates per unit time. For this purpose three samples of each product were placed in a DC chamber and weighted every 15 minutes.

$$\text{Mass increase [mg]} = \text{Mass} - \text{Tare}$$

Equation C-1: Computation of the sample mass increase.

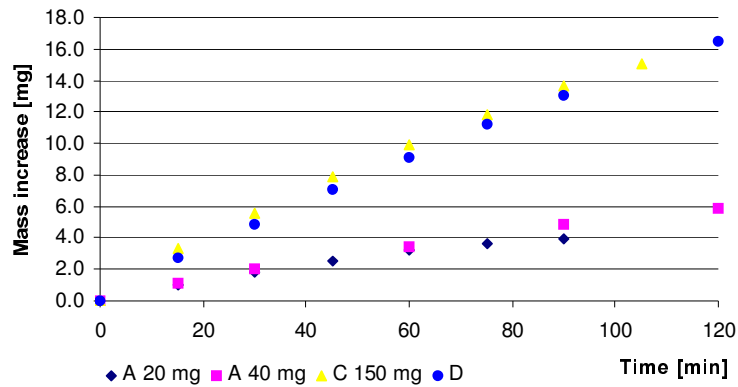


Figure C-2: Absolute mass increase over 2 hours averaged of 3 samples per product. The scale was divergent because the fill mass of Products C and D was a multiple of that of Product A.

In order to make the results for the different products more comparable, the increase in water content (ΔH_2O) needed to be related in percentage terms to the fill mass (M_0). Correct calculation of the content based on KF titration was achieved using Equation C-2:

$$KF \text{ water content } [\%] = \frac{(H_2O_{t=0} + \Delta H_2O) \cdot 100 \%}{M_0 + \Delta H_2O}$$

Equation C-2: Accurate computation of the water content determined by KF titration.

To simplify this equation, it was assumed that all vials corresponded to the target mass of the corresponding products, although this was only the case if a tolerance of $\pm 10 \%$ was allowed:

$$M_0 \pm 10 \% \gg \Delta H_2O$$

Equation C-3: The variation in fill mass was much higher than the mass increase due to the water absorption.

Since this error was approximately ten times greater than the increase in mass resulting from water absorption, the latter addend could be eliminated from the denominator, resulting in the following Equation C-4:

$$\text{Water increase [\%]} \approx \frac{\Delta H_2O \text{ [mg]} \cdot 100 \text{ \%}}{M_0 \text{ [mg]}}$$

Equation C-4: Simplified estimation of the water increase in percent.

Consequently, Figure C-3 permitted only a rough estimation of what actually happened.

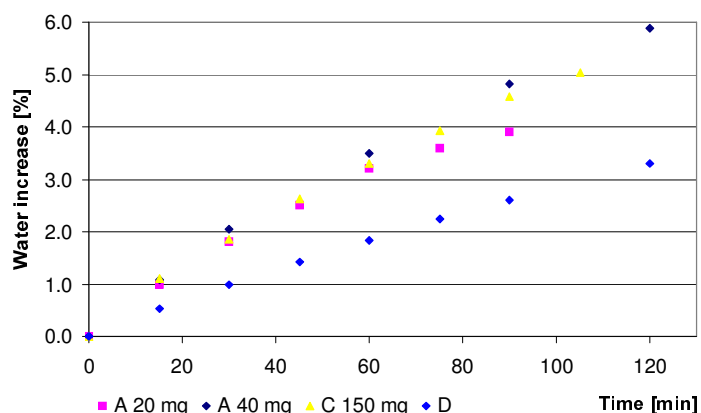


Figure C-3: The mass increase resulting from water absorption was divided by the target fill mass of the product in question.

For the products listed, humidification for 2 hours was sufficient to produce all requisite water contents. Since this trial did not consider the baseline water content of the samples ($H_2O_{t=0}$), this had to be added in order to determine the actual final value. To this end, the QC release value for a given batch or, more simply, the combined average of several batches of a product was used. As the project proceeded, more original samples from different batches were titrated than is normal in QC. Except for Product D, the resulting average values shown in Table C-4 proved to be reliable.

Typical baseline content [%]	
Product A 20 mg	1.0
Product A 40 mg	1.3
Product B	0.7
Product C 150 mg	0.9
Product C 400 mg	0.6
Product D	0.8 – 2

Table C-4: Typical baseline water content of the different dosage forms. The widest variation was found for Product D.

➤ Empirical convention-based method for humidification of samples

On the basis of the experience from a large number of titrations of independent batches over a period of approximately two years it was possible to draw up an empirical relation between humidification time and target content. This is based on the average KF result of a large number of samples, which were averaged as a function of humidification time.

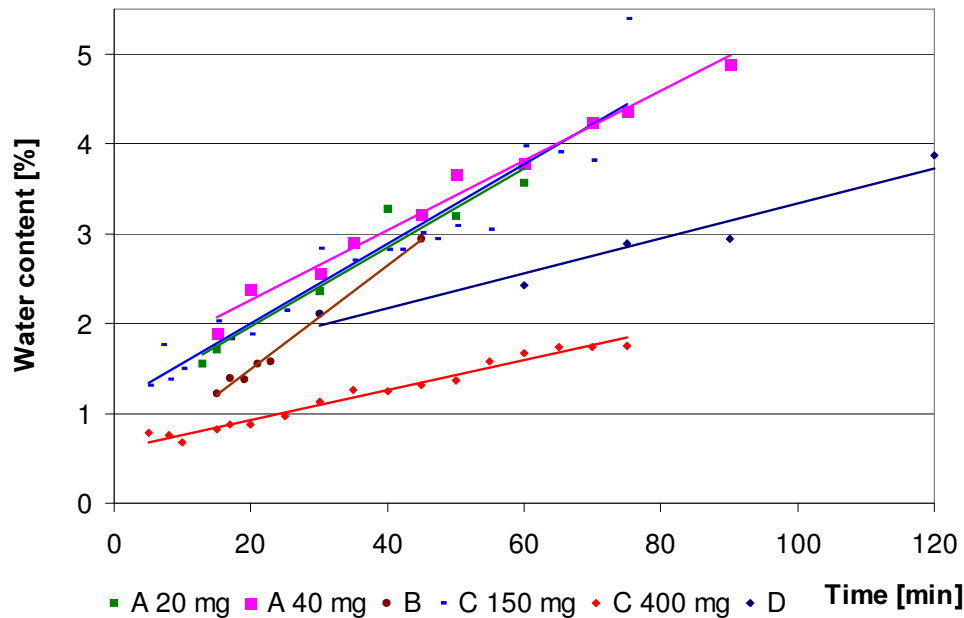


Figure C-4: Empirical relation between the result of the KF titration and the humidification time.

However, the most representative were those samples that came directly from production without subsequent modification. Consequently, where possible, Teflon spacers (2 – 4 mm high) were placed under selected drying trays in the freeze-dryer. As a result of the reduced heat transfer from the trays, these vials were less thoroughly dried and, naturally, damp vials resulted. The most efficient approach proved to be placing spacers 4 mm thick under all 4 corners, in order to achieve significantly higher water contents.

C.2.2.3 Equilibration after humidification

Repeated NIR measurements during the first weeks after manipulation demonstrated that artificially altered samples featured a moisture gradient in the first weeks. Since the cake was measured through the bottom of the vial, the water values determined

were too low in the initial days and gradually approached the actual values as time passed. After a waiting period of three weeks the samples became constant. To be as certain as possible, the manipulated samples were not used for calibration until after a minimum waiting period of four weeks.

C.2.3 Determination of water content

C.2.3.1 Alternative method for water determination

The volumetric KF method had some inherent drawbacks, first of all the time consumption. Once daily the factor of the reagent had to be determined, sometimes several repetitions were required. The opening of the titration vessel involved the risk of introduction of environmental humidity to the water-free system, theoretically balanced by the determination of a blind titration value, added up to the inaccuracy of the method. Some products (especially Product D) demonstrated poor solubility and it could be doubted if really the entire water was released by the sample. In such cases the solvent had to be replaced for each titration. Over time the consumption of expensive reagents was considerable as well.

➤ Coulometric KF oven

A coulometric KF oven could at least avoid some of these drawbacks. In this case the sample is heated so that the contained water evaporates and is discharged by a stream of dry nitrogen into the coulometric cell. The samples do not require dissolution and the vessel is not contaminated. Side reactions and frequent solvent replacement are consequently avoided.



Figure C-5: Coulometric KF oven with sample processor.²

➤ Procedure

It should be assessed if an improvement of both the accuracy of the NIR calibrations and the sample handling could be achieved as an alternative water content determination. To allow good comparability, two products were considered here: Product A 20 mg to be compared to already existing calibrations relying on volumetric KF titration and Product D, being known for an inhomogeneous cake appearance and poor solubility.

In both cases, original and moisturized samples were prepared. Prior to titration they were NIR measured (1,200 - 2,150 nm, 2 nm resolution, 10 scans). The unique pretreatment for all the data was MSC, and a PLS was computed afterwards. As the exact fill-mass of the samples was not known, the net weight had to be determined by filling preferably the entire cake into special sealable glass containers. Heating temperatures superior to 100 °C but inferior to any decomposition were identified according to previous TGA results. Due to the high deliquescence of the product no double determination by the volumetric and coulometric method was feasible.

➤ Product A 20 mg, KF oven as reference method

For Product A 20 mg, initially 60 original samples were analyzed. The KF oven results for these original samples yielded water contents between 0.57 to 1.10 % with a heating temperature of 116 °C.

The Residual Validation Variance plot of the calibration (Figure C-6) did not represent a consistent model performance. The minimum in this plot was found at 3 PCs, although leading to a quite poor correlation. The data points were rather arbitrarily scattered about the entire plot. The correlation values of 0.5 rather indicate no correlation than a good relation between two data sets. The far too low slope but too high offset indicated that the coulometrically detected water contents were usually higher than those predicted by NIR.

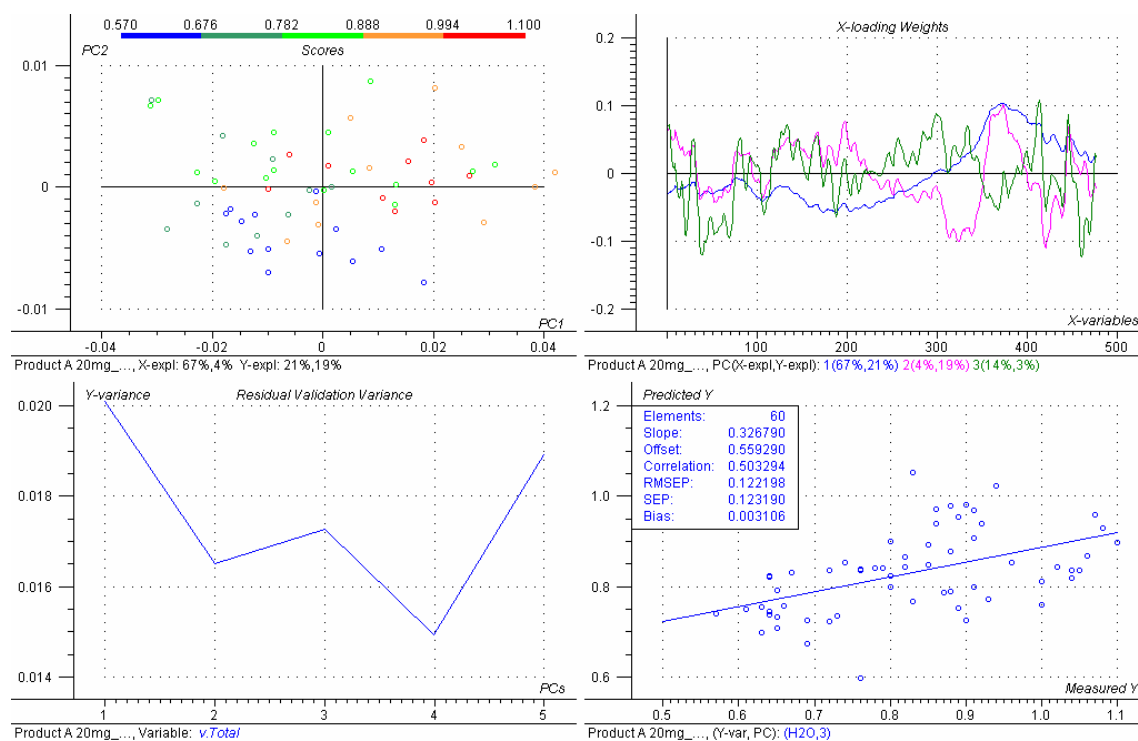


Figure C-6: Model overview of the calibration of exclusively original samples. The residual validation variance plot showed non-consistent correlation results.

Thus, some moisturized samples were added to the set. Ten further samples containing 1.30 to 1.86 % water according to the KF oven were included to the model and the PLS was recalculated.

Apparently, the humidified samples were all predicted approximately to the same water content, but the titration result varied by 0.6 % (Figure C-7). This addition reduced the number of PCs to two and improved all the benchmarks beyond the SECV. But actually, the correlation line was just dominated by the data far apart from the main point swarm. It did not represent true values.

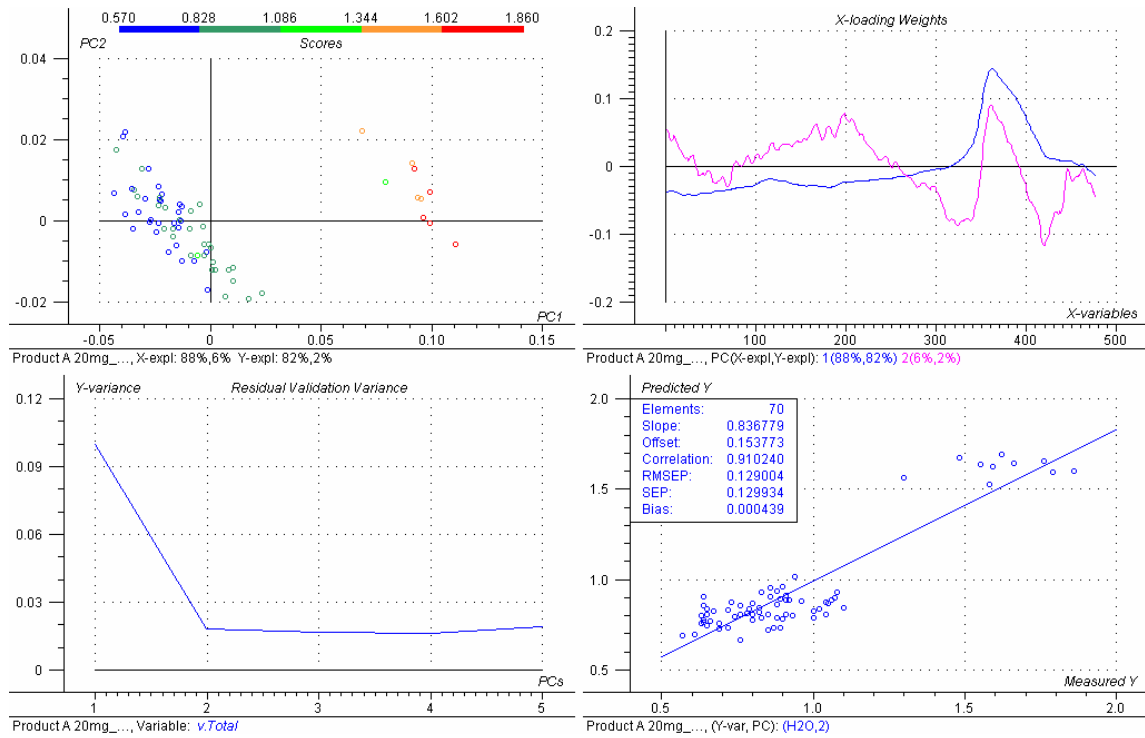


Figure C-7: Model overview of the calibration with 10 artificially moisturized samples added.

➤ Product D, KF oven as reference method

Due to its poor solubility, the potential advantages of the KF oven should become especially manifest in case of Product D. Here from the beginning overlapping sample sets were prepared, 39 original samples from 0.63 to 2.40 % water and 50 manipulated vials in the range of 1.38 to 2.51 % according to the KF oven with heating temperatures of 141 °C. Again a regression of the multiplicative scatter corrected data was computed. 3 PCs were required to obtain weak calibration benchmarks. Not satisfying slope and offset indicated once more the underestimation of the water content by NIRA (Figure C-8).

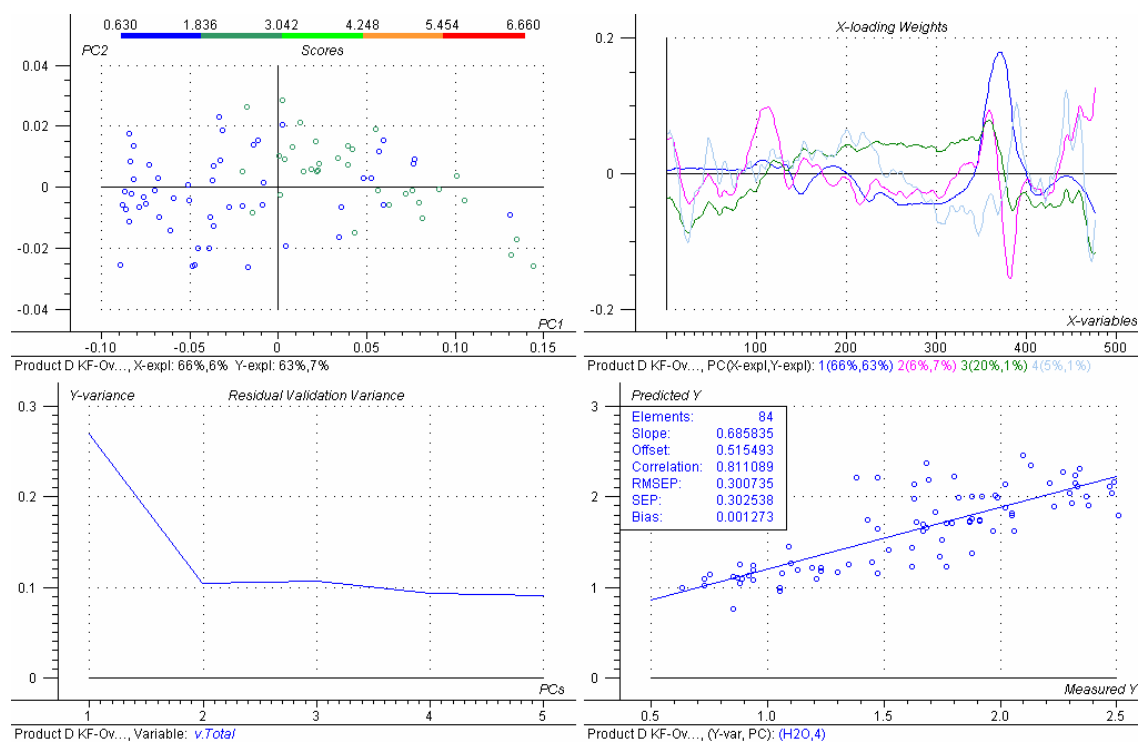


Figure C-8: Model overview of Product D with a mixed calibration sample set.

➤ Discussion and conclusion

The sample handling was comfortable enabling the titration of 32 samples in one run on an auto sampler without intermediate preparation. But the analysis precision did not correspond to the expectations.

Although the sample set of Product D was much more homogeneous in comparison to that of Product A, it was not possible to achieve acceptable regression results. Unreproducible titration results caused a broad scatter on the predicted versus measured plots of the calibrations. Especially, the original samples were underestimated in the NIRA predictions. To transfill the lyophilizates it was necessary to open the hermetically sealed containers. Afterwards, the samples remained a certain time on the sample processor before being heated and analyzed. Very likely the hygroscopic samples absorbed ambient humidity during these preparation steps, and this the more, the drier the samples initially were. According to this assumption, the NIRA prediction value was typically lower than the KF oven result. Thus, the KF oven was not considered as an appropriate alternative to the conventional volumetric KF titration.

C.2.3.2 Volumetric KF titration

➤ Product specific parameters and calculation

To determine the actual water content in the samples, volumetric Karl-Fischer titration was carried out with a Dosimat 701 KF Titrino and Hydranal solvents and titrators by Riedel-de Haën.



Figure C-9: Volumetric KF titration stand.²

For each product a precise titration procedure was legally registered, which results were acknowledged as the true value serving as a reference for the NIR calibrations. Depending on the solubility of the dosage form different solvents were defined. Differing from the official regulation, all samples were titrated with the same reagent concentration to achieve the highest possible accuracy of the method (one-component reagent Hydranal Composite 2; 1 ml \cong 2 mg water). The exact water equivalent of the KF reagent was determined once a day against distilled water in the respective solvent to use.

$$\text{water equivalent [mg/ml]} = \frac{\text{weighted sample [mg]}}{\text{KF volume [ml]}}$$

Equation C-5: Formula to calculate the water-reagent-equivalence.

The drift of the water-free solvent may not be higher than 6 μ l / min. The relative difference of the double determination should not exceed 1.0 %.

$$\frac{(|A_1 - A_2|)}{A_1} \cdot 100 < 1.0 \%$$

Equation C-6: Computation of the variance of two successive determination of the reagent's factor.

In the end of the entire titration the deployed factor was verified by the determination of another drop of pure water. This result gave an estimation of the accuracy of the titrations performed during that series. If the deviation was too high, all the concerned samples were rejected.

$$\text{water } [\% (m/m)] = \frac{KF \text{ volume } [ml] \cdot \text{water equivalent} \cdot 100 \%}{\text{weighted sample } [mg]}$$

Equation C-7: The result of the terminal water determination should be as close as possible to 100 %.

Synonym	Solvent	Weighted sample [mg]	Exchange of the solvent after x determinations
Product A	Hydranal Solvent	~ 100	3
Product B	Methanol	~ 100	3
Product C	Methanol	~ 200	1
Product D	Mixture of Methanol and form amide 1:1	~ 500	1

Table C-5: Overview of the solvents used for the KF titration. For the methanol an HPLC grade should be preferred.

➤ Method validation

NIRS methods to be used for quantification require calibration of the NIR spectral response against verified reference data. Therefore characteristics of the reference method should be considered in the process of the development and validation of the NIRS-method, e.g. accuracy, range, and precision.

Earlier studies in this context raised statistics including up to 150 values that emerged from parallel determinations of NIRA and KF titration. These assays revealed an absolute error of $\pm 0.2 \%$ of NIRA in comparison to KF. This statement was acknowledged with a 95 % confidence interval by use of an official statistical validation tool of the QC-laboratories. This absolute inaccuracy was converted to a relative deviation starting from the mean value of the target band. The rounded up relative

deviation was afterwards adopted as criterion of the method comparison required for any further NIR method validation.

	Target band [%]	Mean value [%]	Relative deviation [%]
Product A	0 - 2	1	± 20
Product B	0 - 3	1.5	± 15
Product C	0 - 3	1.5	± 15
Product D	0 - 3	1.5	± 15

Table C-6: The rounded relative deviations were adopted to assess the method comparison of NIRA to KF titration.

C.2.4 Baseline Situation, Product A

A validated laboratory NIR method for determination of residual water content using the laboratory spectrometer FOSS NIRSystems Rapid Content-Analyzer already existed for Product A 20 mg. Examination of freshly lyophilized samples of this product direct from ongoing production revealed that the water content measured by NIRA slowly increased over the course of the first weeks. In order to quantify this phenomenon, ten newly lyophilized vials were tested several times over five months with the existing laboratory NIR spectrometer. All samples produced comparable measurement profiles, with the predicted water values increasing over the first ten weeks by an average of 0.36 % (Figure C-10).

The same test was then repeated on an AOTF spectrometer with a different batch of the same product. The subsequent KF titration of the samples (in this case using the entire product cake) produced values similar to those obtained at the end of the equilibration phase rather than on the first day after lyophilization. Since in-line analysis is carried out on fresh vials just unloaded from the dryer, this observation was considered significant and was investigated further. This phenomenon was observed only with Product A, in both dosages.

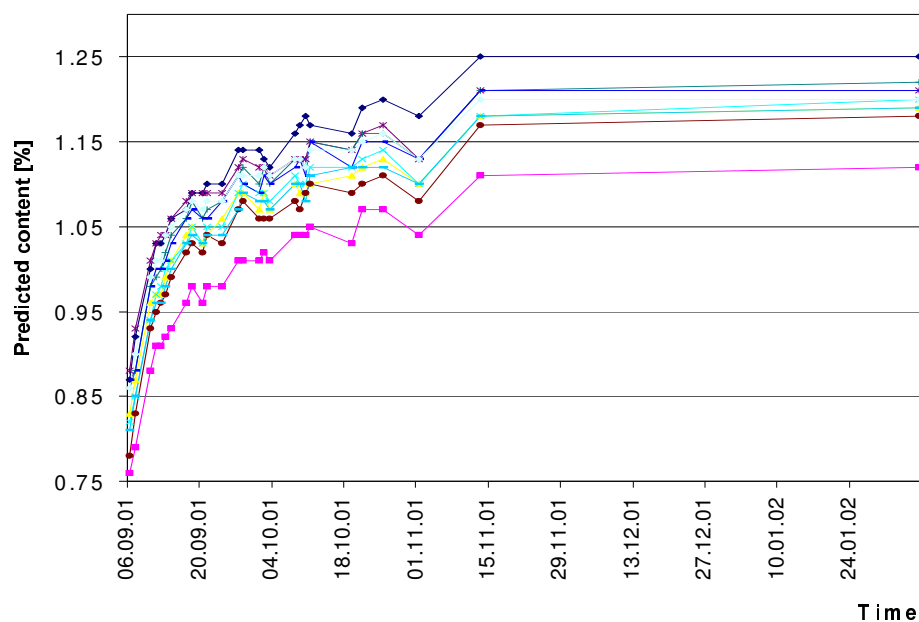


Figure C-10: Moisture content time profile for the parallel determination of 10 samples of Product A 20 mg.

C.2.4.1 Vial sealing

Based on the results of standard tests conducted by Packaging Development at Roche, Kaiseraugst, the vials could be regarded as hermetically sealed. Mass increase over time was determined gravimetrically and a steam permeability test was conducted. In both cases the gas permeability was within the range of accuracy of the best testing methods. This virtually rules out absorption of water from the environment, which in any event was highly improbable, given the homogeneous profiles obtained with several vials.

C.2.4.2 Polymorphism

During lyophilization and also afterwards, transitions between amorphous and crystalline states are possible. The crystal structure is often examined by means of mid-IR and may thus by definition also have an influence on an NIR reading. Since several polymorphous states of the active ingredient of Product A were known, an x-ray-based polymorphism study was undertaken as a next step. The same vial was examined five times (after 1, 8, 15, 33 and 41 days). Within the accuracy limits of the method it was not possible to observe any change in the spectrum over this period. Consequently, a

rearrangement of the crystalline structure of the products was also ruled out as a cause for the changing moisture values.

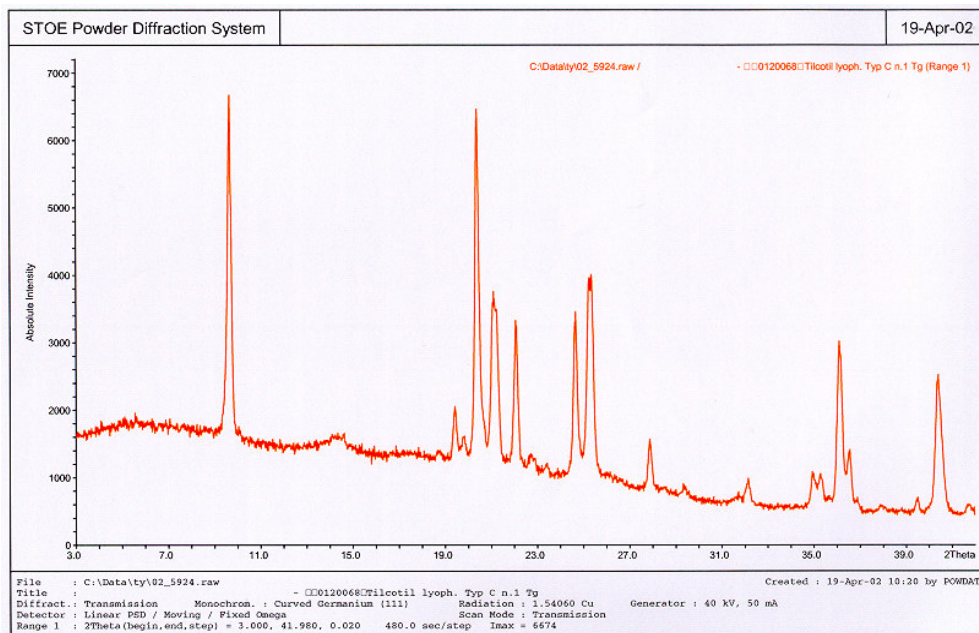


Figure C-11: X-ray spectrum of Product A 20 mg, one day after lyophilization.

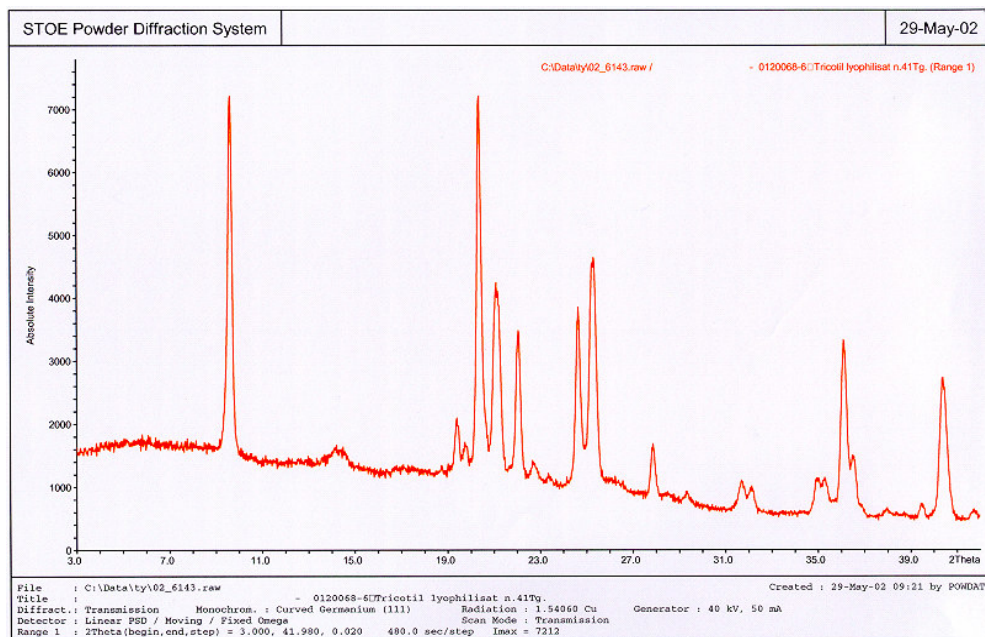


Figure C-12: X-ray spectrum of the same sample of Product A 20 mg, 41 days after lyophilization.

C.2.4.3 Other causes

Theoretically, the lyophilizate could also be absorbing moisture picked up by the stopper during sterilization.³ This assumption, however, is not consistent with the fact that, immediately after lyophilization, it was possible to measure the final water content by volumetric KF titration. Accordingly there had to be another explanation.

As described in the section on lyophilization, sublimation in the lyophilized product cake does not proceed in a horizontal plane from top to bottom, but from all sides towards the centre. Therefore before the start of secondary drying the final traces of ice are at the heart of the cake. It may therefore be assumed that even after completion of the entire freeze-drying process a moisture gradient may exist in the lyophilizate. Pikal and Shah⁴ have confirmed this supposition. They divided different dried cakes into pieces in such a way that the upper and lower and the inner and outer parts could be titrated separately from one another. They concluded that, as drying progresses and interval heterogeneity decreases, intravial heterogeneity increases, as calculated from the ratio of the water content of the outer section to that of the whole vial.

It therefore seemed plausible that at the core of Product A there was a cluster of moisture that diffused outwards only very slowly. Depending on the sample, the low-power NIR radiation penetrates only a few millimeters – but perhaps not deep enough to interact with the core. Furthermore, Product A was a deep yellow and very compact cake that consequently was probably highly absorbent.

C.2.4.4 Action taken

Since the new method in contrast to routine QC analysis was intended to examine fresh vials, it was necessary to take this phenomenon into account. Initially, a challenge set of 120 samples was set up. This contained only original vials from production, NIR measured on an AOTF spectrometer at the first day after production (1,200 - 2,150 nm, 2 nm resolution, 10 scans). This set was then predicted by three PLS models with different set-ups. The unique pretreatment for all these calibrations was MSC again.

➤ PLS model with equilibrated samples only

The prediction for this set was initially made by a calibration that consisted exclusively of already equilibrated samples, original plus artificially dried and humidified ones (Figure C-13).

Quite apart from the gentle slope, the negative bias in particular was a clear indication that the calibration had systematically underestimated the samples (Figure C-14).

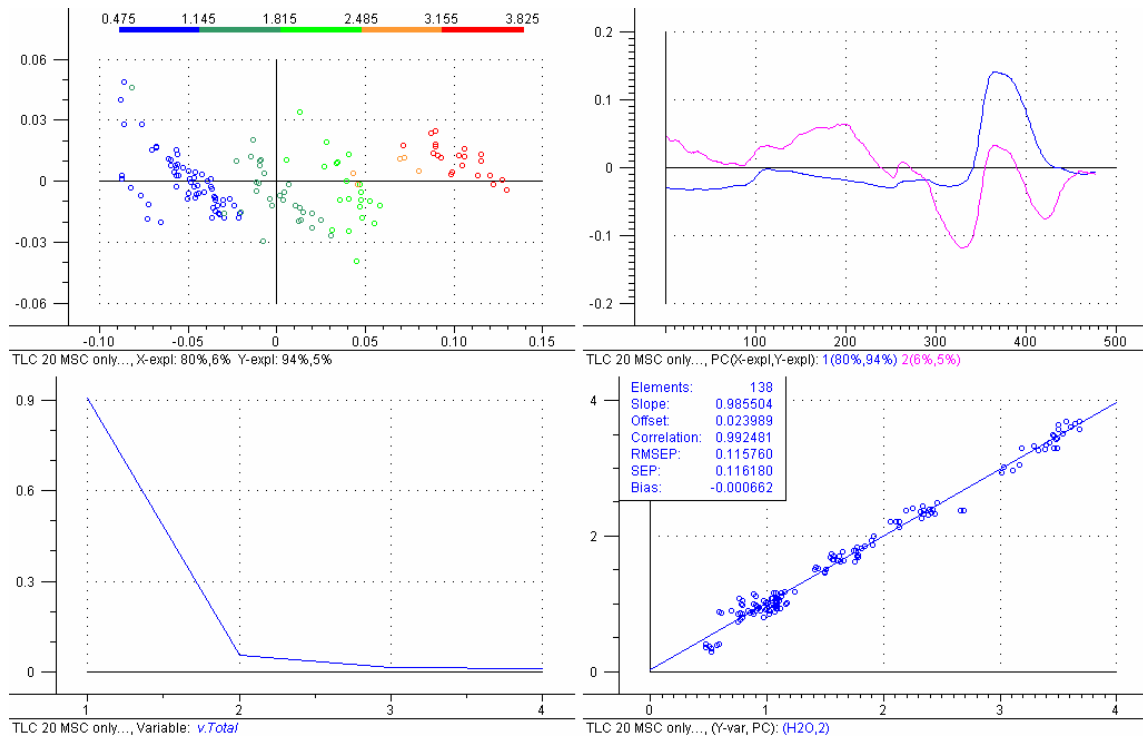


Figure C-13: Calibration overview of the model based on equilibrated samples only.

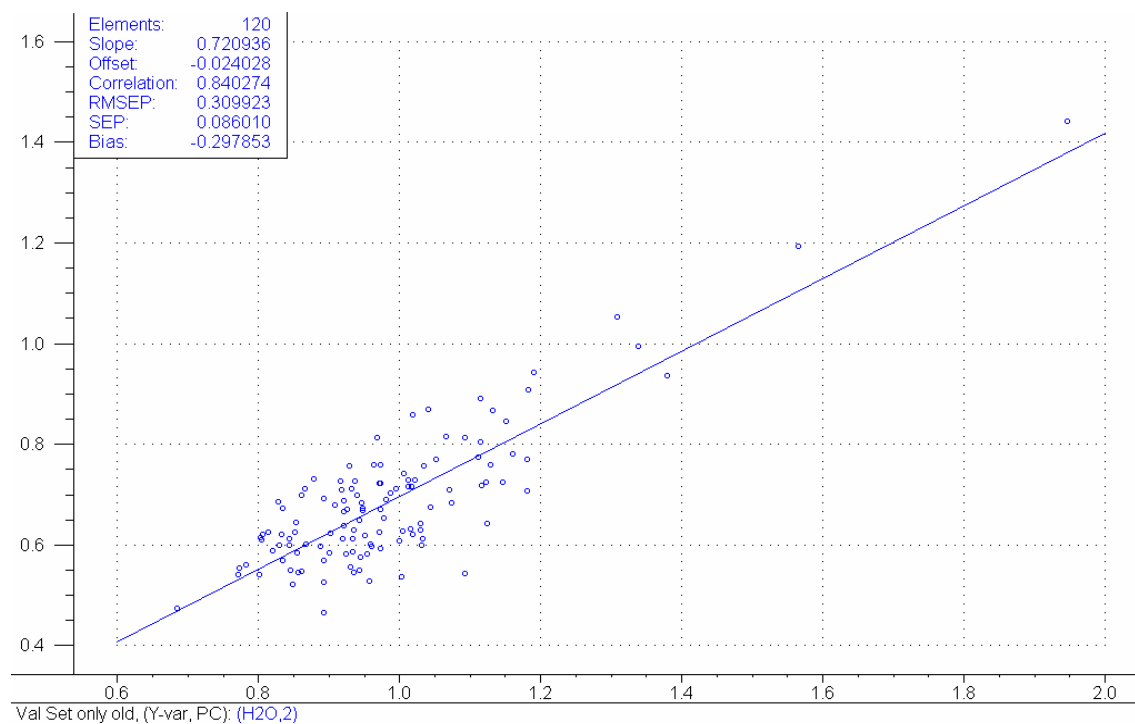


Figure C-14: Prediction results for the challenge set of an initial model based on equilibrated samples only.

➤ Mixed PLS model with equilibrated and fresh samples

In order to additionally include the moisture gradients of fresh samples in the NIRA calibration, initially only fresh original samples were added to the artificially dried or humidified ones.

According to Figure C-15 the calibration parameters remained virtually unchanged. But in the predicted versus measured plot of the external validation set (Figure C-16), RMSEP and bias dropped considerably, but slope and offset deteriorated. The predictions of the low values, therefore, were clearly trending too high and those of the higher values too low.

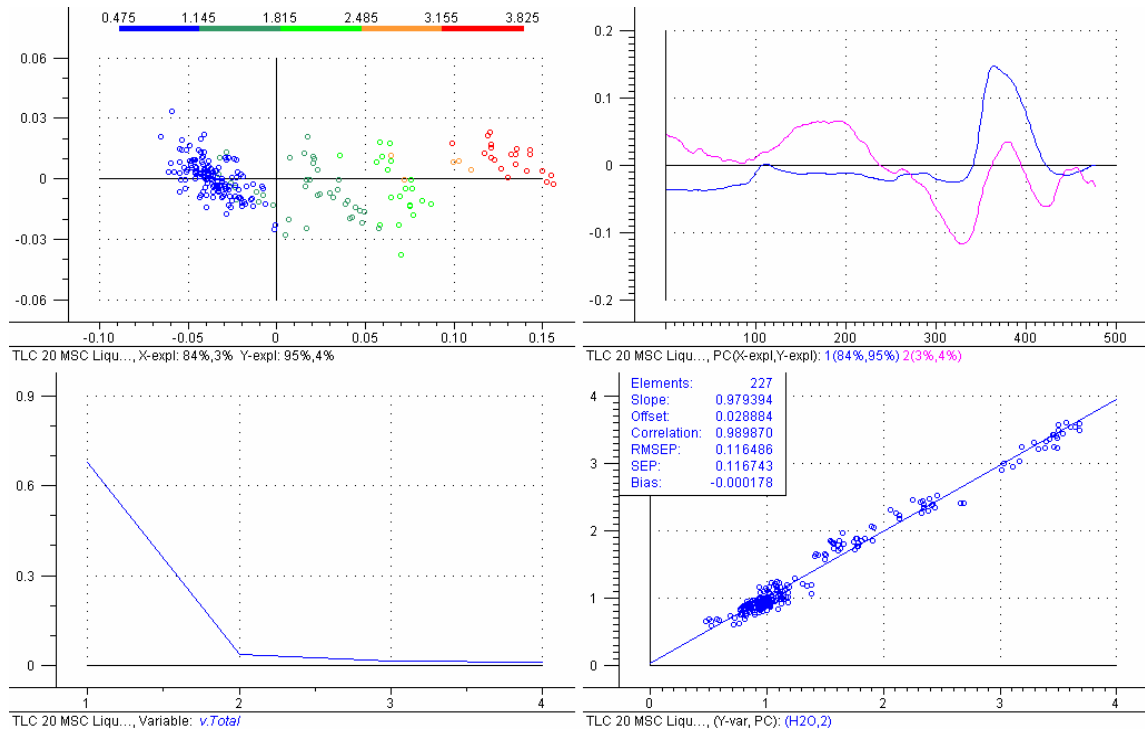


Figure C-15: Model overview of a mixed calibration comprising equilibrated and fresh samples from the production line.

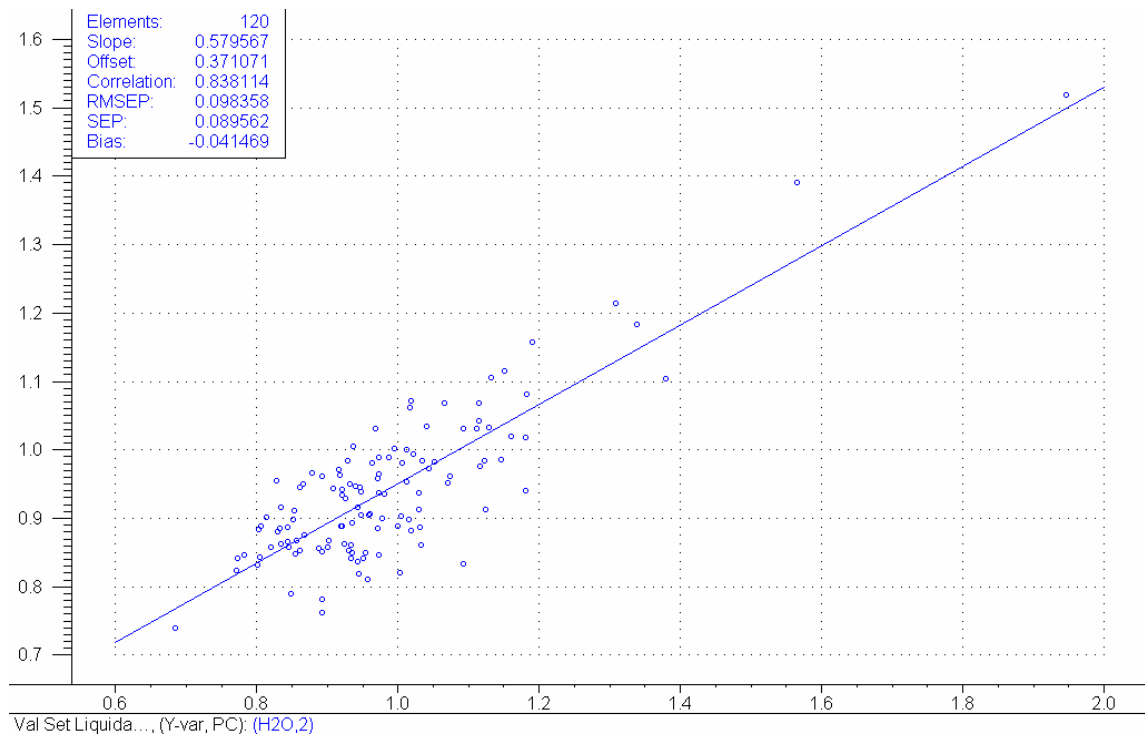


Figure C-16: Predicted versus measured plot of the challenge set predicted by the mixed model, containing fresh and equilibrated samples from the production line.

➤ PLS model with exclusively fresh samples

As last step, all samples were replaced with fresh vials. This naturally required the entire bandwidth, including both wetter and drier samples than usual. Consequently, several experimental lyophilization cycles were run. The vials were sealed at different times before the end of secondary drying in order to retain higher moisture content. Other samples were dried for significantly longer and also at higher temperatures than normal. It was thus possible to cover a moisture range of 0.8 – 2.5 %. An additional problem was due to the fact that the lyophilization cycles in routine production did not always end at the same time. The freeze-drier was thus unloaded at different times at the conclusion of secondary drying. It was thus unclear exactly which sample age should be used for calibration of the NIR models. As a compromise, the samples were subjected to NIR measurement 24 hours after removal.

In spite of this, subsequent NIRA measurements showed severe fluctuations, since the lyophilization cycles could not be adequately reproduced in the experimental system and the intravial distribution effects were particularly marked in the first few hours. The calibration therefore required three PCs (Figure C-17).

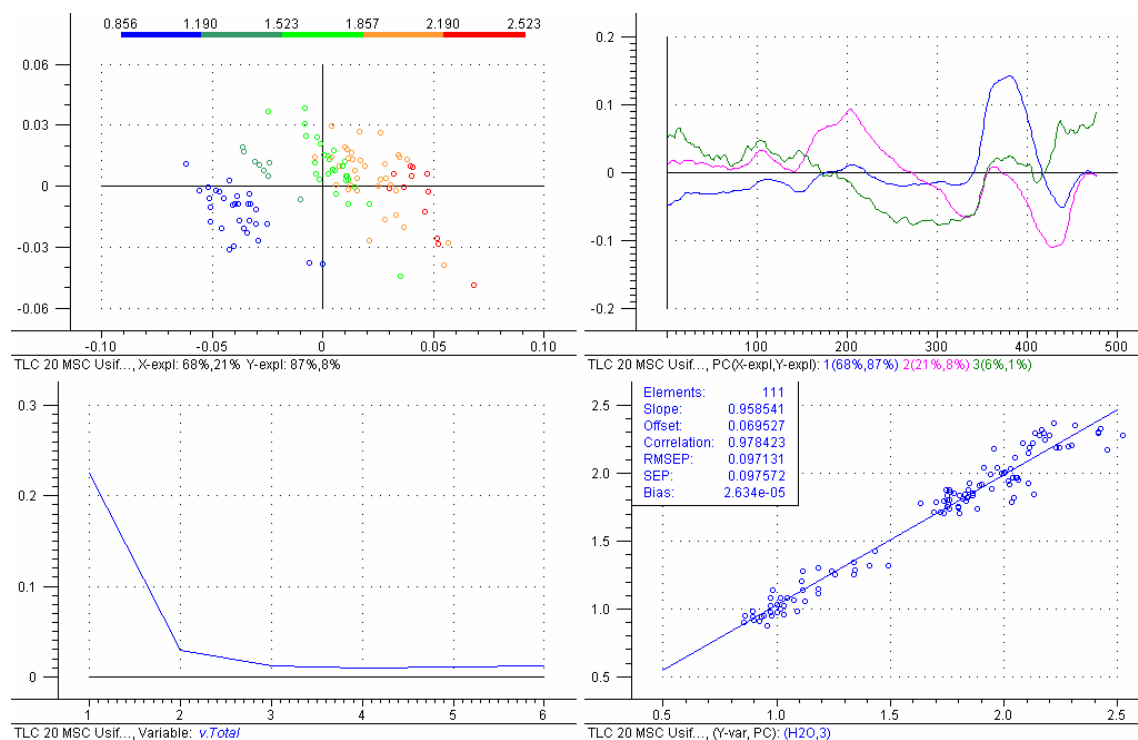


Figure C-17: Model overview based exclusively on samples from the research batches.

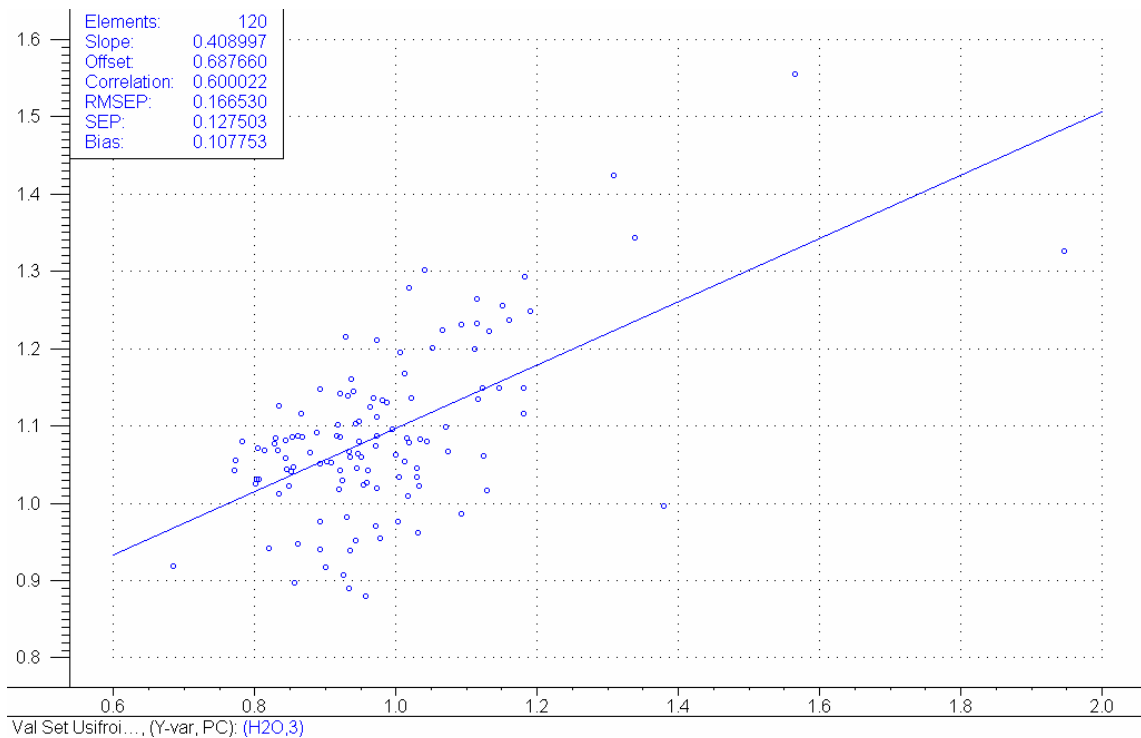


Figure C-18: The model with only fresh samples from the research batches still gave poor prediction results of the challenge set.

Also in this case the scatter of the externally predicted values was far too wide (Figure C-18). Once again, slope and offset did not yield useful results. In addition, this procedure involved a disproportionately large amount of effort, since the lyophilization cycles took several days and in some cases there was a need for unloading at night.

C.2.4.5 Conclusions

Inadequate vial sealing or polymorphism could be ruled out as the cause of the increasing prediction results. Instead, it was concluded that the rise in water content resulted from moisture redistribution within the lyophilized cake.

Alternative calibration procedures and calibration sets did not eliminate the problem of insufficient accuracy in the prediction results. However, as moisture redistribution was a reproducible phenomenon that occurred in a similar manner in several different samples, it should be possible to allow for it by using a correction factor based on sample age. We therefore ultimately decided to use only equilibrated samples for calibration purposes and to validate the method based on conditions encountered

most frequently in production. An alternative would be to lower the acceptance criterion of 2 % accordingly, and thus prevent the release of OOS vials. That could increase the rejection rate, but this would not be significant, since Product A is the least expensive product, and borderline vials would presumably be quite rare.

References C.2 Original situation

- ¹ Konstantklimate über wässrigen Lösungen, DIN 50 008, Beuth Verlag GmbH, Berlin, 1981
- ² Photograph from the Metrohm homepage, Metrohm AG, Herisau, Switzerland
- ³ Rey L., Some Leading Edge Prospects in Lyophilization, Keynote Address from 2002 Lyophilization Conference, 2002
- ⁴ Pikal M.-J., Shah S., Intravial Distribution of Moisture During the Secondary Drying Stage of Freeze Drying, PSINCE journal of Pharmaceutical Science & Technology, Vol. 51, No. 1, 1997

C.3 Evaluation of the appropriate analysis system

These days, equipment vendors are more and more acquainted with the needs of their pharmaceutical clients and aim to provide a complete solution. A standard agreement with a reputable vendor will include the cost of the equipment, manuals, training, installation and operational qualification (IQ / OQ) package, follow up training and consultancy comprising calibration, after sales service and warranty. Usually the devices are automatically delivered with specific and not exchangeable software offering especially adapted tools or limited calibration options. The sum of physical patterns of the spectrometer and the software design ends up in the performance of a spectral device.

The scope was to reflect either the physical spectroscopic or the software performance separately and afterwards both in addition for the decision making of an analytical device in this in-line application.

C.3.1 Preselection of spectrometers

Here a rugged analytical device able to cope with rough environmental conditions was required. The severest challenge for the commercially available NIR spectrometers was the measuring velocity of 300 samples per minute. Thus, less than 200 milliseconds would be available per measurement. Being aware that it would follow up with a compromise between speed and accuracy diode array devices were excluded from the beginning as being known for having a low resolution and low sensitivity, especially at the borders of the wavelength scale.

As most of the vendors from the beginning refused to face this challenge in this study only two spectrometers were considered. On one hand a Bomem MB160 FT spectrometer (abbr. as FT) with 3 m glass fiber and diffuse reflectance probe. A sample to probe distance of 5 mm had to be respected. As interferometers always require an entire movement of the mirror to accomplish a scan and supplementary only start scanning when the mirror is in a zero position, two of these spectrometers would be necessary to achieve the line's performance. It was compared with a Brimrose AOTF Luminar Freespace 3030 (abbr. as AOTF) with a sampling area of 5.3 x 3.1 mm. Its

technique allows the acquisition of roughly 16,000 arbitrarily accessible data points per second, sufficient for five samples a second. All the measurements with this device were performed with samples posed on a support 42 mm from the sensor window. The grating laboratory FOSS Rapid Content-Analyzer (abbr. as REF) with lead-sulfide (PbS) detector served as laboratory reference.

	FOSS Rapid-Content Analyzer	ABB Bomem MB160	Brimrose Luminar Freespace 3030
Spectrometer technique	Grating	FT	AOTF
Wavelength scale	1,100 - 2,500 nm	10,000 - 4,500 cm ⁻¹	1,100 - 2,200 nm
Resolution	2 - 10 nm	4 - 128 cm ⁻¹	2 - 10 nm
Wavelength accuracy*	± 1.3 nm	0.04 cm ⁻¹ at 7300 cm ⁻¹	± 0.5 nm
Wavelength repeatability	< 0.01 nm	0.002 cm ⁻¹ (± 2σ)	± 0.01 nm
Non-linearity	± 1 %	0.1 %	0.1 %
S / N-ratio	< 35 μabs	4 μabs for 1 min data acquisition	40 μabs for 5 s data acquisition

Table C-7: Instrument specifications according to their manuals. The S / N-ratio was determined by deploying an external Spectralon diffuse reflectance standard.

The higher sensitivity of the indium gallium arsenide (InGaAs) detectors, required for high speed measurements and low light intensities, has a negative impact on the wavelength range. Thus in this comparison only a limited scale from 1,100 to 2,150 nm was used in case of the FT and the AOTF device.

Whereas dispersive instruments usually work on wavelength units, FT spectrometers deploy wavenumbers. These measuring units are not linearly transferable so that wavenumbers are corresponding to the reciprocal value in nanometers. This denotes that, in comparison to the wavelength scale, resolution adjusted in wavenumbers decreases in the more significant area of the spectrum but is very high in the area without any useful information. For the same reason one may find the FT spectra always in a separate plot. In some cases they had to be mathematically converted.

C.3.2 Assessment parameters

The first comparison is oriented on the European Pharmacopoeia's recommendations to survey regularly the photometric performance of NIR instrumentation. The USP 25, offers an alternative description recommending the use of low reflectance standards for the determination of spectral noise levels.²

The second approach is based on a practical application as the choice of an instrument should not be based on a theoretical classification figure. Thus, PLS models were computed in two different settings to predict the water content of Product A 40 mg.

Firstly, the spectral information of all the spectrometers was computed only on the Unscrambler and the results were compared. This procedure should help to assess the quality of the acquired spectra only, excluding the impact of the software differences. Secondly, the entire computation was performed on the specific assembly, including spectrometer and software. This represented a real-life situation.

C.3.3 Assessment oriented on the European Pharmacopoeia

The control of instrument performance of the European Pharmacopoeia prescribed for regular verifications was used as a comparison criterion.¹

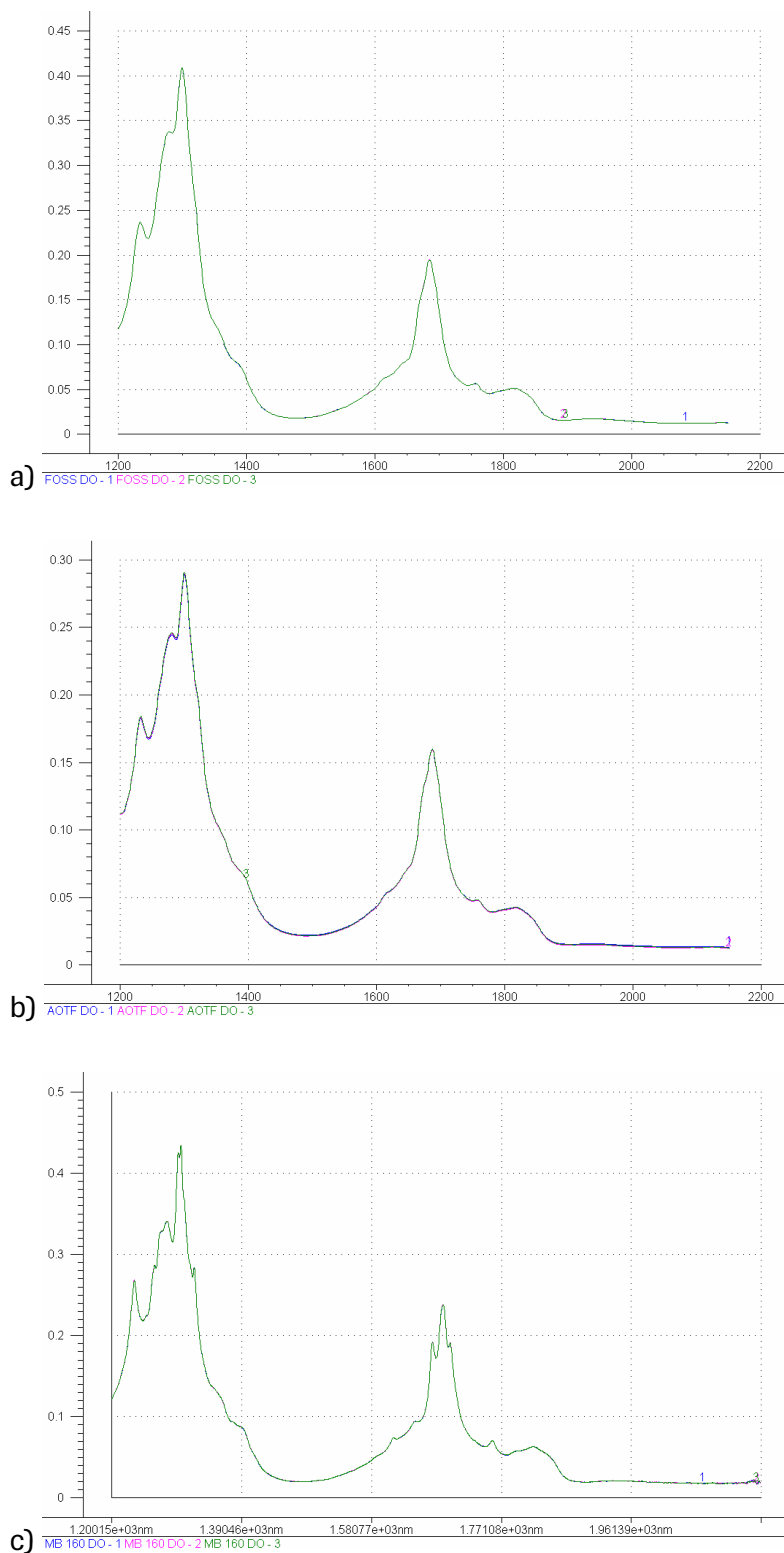


Figure C-19: The plots of the rare earth spectra each with three repetitions a) REF spectrometer (1,200 - 2,150 nm) in maximal resolution of 2 nm, b) AOTF maximal resolution of 1 nm and c) FT with a resolution of 4 cm^{-1} .

C.3.3.1 Verification of the wavelength scale and the wavelength repeatability

The first two comparison criteria 'verification of the wavelength scale' and 'verification of the repeatability (except for filter apparatus)' using suitable wavelength standards with characteristic maxima, for example polystyrene or rare-earth oxides, were summarized. The wavelength repeatability is verified by the standard deviation (SD) of the wavelengths being consistent with the spectrophotometer's specification.¹

➤ Procedure

Always the same NIST traceable rare earth dysprosium oxide wavelength calibration standard was deployed. Three measurements with the highest available resolution were performed and averaged for successive calculations. A visual comparison of the two rare earth plots illustrated the lowest resolution and signal intensity of the AOTF whereas the FT detected the sharpest bands proving a high resolution. The peaks at 1,321 and 1,669 nm did not appear in the spectra of the other devices. However, the peaks at 1,262 and 1,695 nm were even not given in the calibration certificate while the 1,279 nm maximum consisted only out of one sharp apex and not a couple of spikes.

➤ Results and discussion

Each of the spectrometers detected always the same wavelengths by scanning the rare earth standard a couple of times, only signal intensity varied slightly. The adjustable resolution was not high enough to verify the spectrometer specifications in terms of wavelength repeatability.

Remarkable was the change from negative to positive deviation of the AOTF, while the entire wavelength scale of the other two spectrometers was shifted to upper values. The standard deviations of the maxima of the detected rare earth spectra varying between 0.81 and 1.31, did not indicate any severe quality issue as the wavelength intercept was too low and the standard was certified with an accuracy of ± 0.8 nm in the range of 800 to 2,000 nm. FOSS published the lowest requirements but met the best results. Neither the FT nor the AOTF met the high level of their own specifications.

According certificate	Wavelength [nm]	1,232.8	1,279.1	1,299.4	1,684.2	SD
	Relative intensity	0.572	0.761	1.000	0.458	
FOSS NIRSystems						
Rapid Content-Analyzer						
Res. 2 nm						
Wavelength [nm]						
		1,234.0	1,280.0	1,300.0	1,684.0	
Deviation						
		+ 1.2	+ 0.9	+ 0.6	+ 0.2	0.81
Relative Intensity						
		0.589	0.830	1.000	0.489	
Brimrose						
Luminar Freespace AOTF						
Res. 1 nm						
Wavelength [nm]						
		1,232.0	1,280.0	1,300.0	1,686.0	
Deviation						
		- 0.8	+ 0.9	+ 0.6	+ 1.8	1.12
Relative Intensity						
		0.662	0.884	1.000	0.551	
ABB Bomem						
MB160						
Res. 4 cm ⁻¹						
Wavelength [nm]						
		1,233.3	1,279.9	1,301.4	1,685.6	
Deviation						
		+ 0.5	+ 0.8	+ 2.0	+ 1.4	1.31
Relative Intensity						
		0.618	0.798	1.000	0.549	

Table C-8: Maxima of the three rare earth plots and their deviation from the Labsphere certificate.

C.3.3.2 Verification of response repeatability

The 'response repeatability' should be verified by using suitable standards, for example reflective thermoplastic resins doped with carbon black. The SD of the maxima response should be consistent with the spectrophotometer specification.¹

➤ Procedure

Spectra of three different reflectance standards (75 %, 50 %, 10 %) were taken on each one of the test instruments. Regarding the obtained spectra of the same 10 % standard the maximum response area was difficult to determine and furthermore the appearance of the spectra was extremely different (Figure C-20). Instead, the most important area for water analysis from 1,900 to 1,950 nm was chosen to evaluate the response repeatability. Three successive measurements were carried out and the SD for each wavelength was calculated. Again the SD of these results was computed (Table C-9).

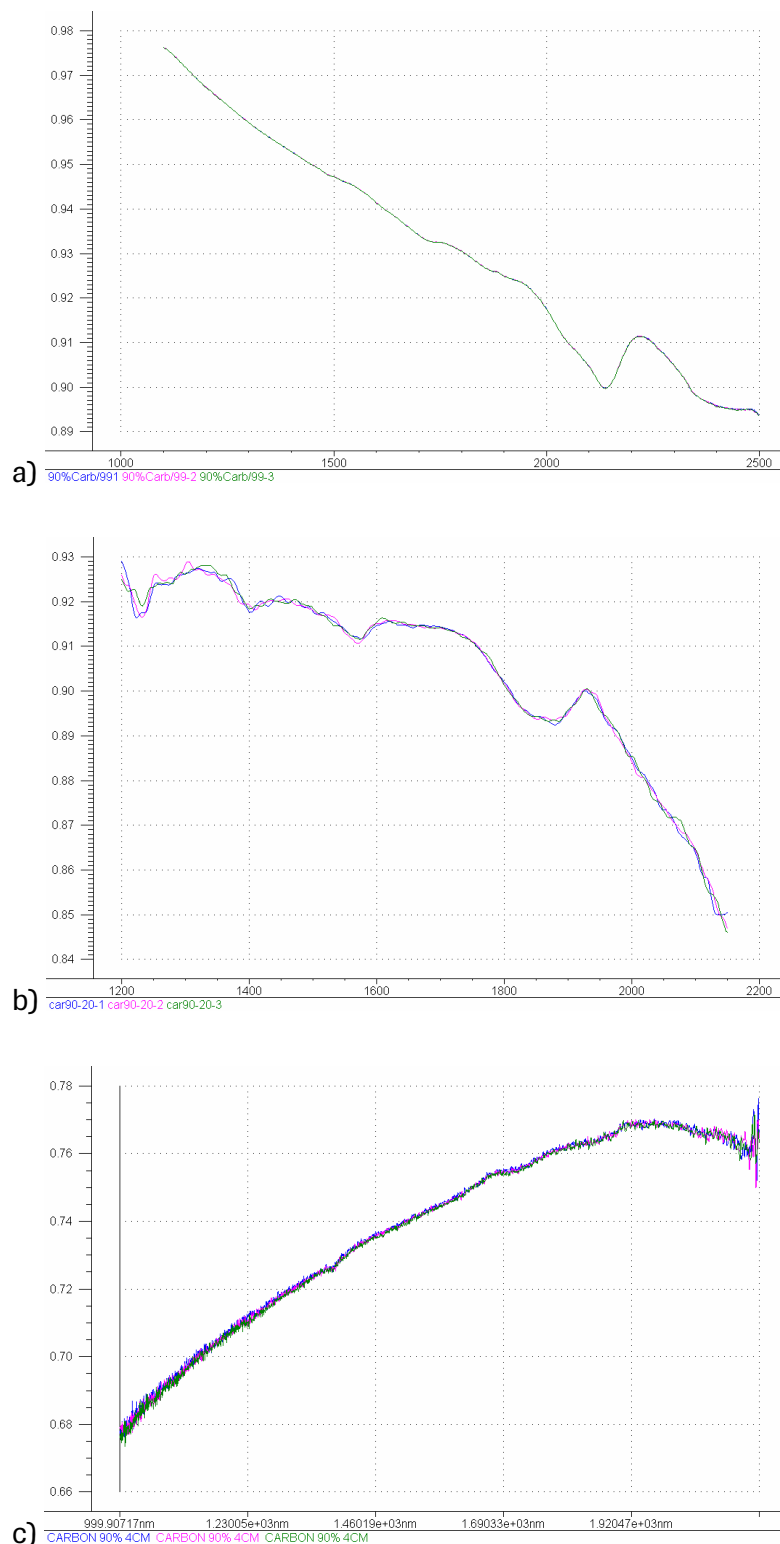


Figure C-20: Photometric response repeatability of three sequenced measurements of a 10 % reflective standard against the 99 % reflectance standard, a) REF (2 nm, 32 scans), b) FT (4 cm⁻¹, 20 scans) c) AOTF (2 nm, 20 scans).

Resp. Repeat. 1900 - 1950 nm	SD of 75 % Refl.	SD of 50 % Refl.	SD of 10 % Refl.
FOSS	4.37E-06	6.57E-06	1.08E-05
Brimrose	4.67E-05	2.95E-05	1.54E-04
Bomem	8.77E-05	1.16E-04	2.98E-04

Table C-9: Standard Deviation of response intensities.

➤ Results and discussion

The appearance of the absorbance spectra of the same reference was completely different from one instrument to the other. In contrast to the REF and the AOTF, the FT spectrum was ascending instead of descending.

The higher the energy absorption the more increases the noise level and the response repeatability decreases. The variation of the individual measurements was large and the spectra were difficult to reproduce. The FT had nonetheless by far the worst repeatability, followed by the AOTF differing still in decimal powers from the laboratory spectrometer.

C.3.3.3 Verification of photometric noise

The 'photometric noise' is determined by using a suitable reflectance standard, for example white reflective ceramic tiles or reflective thermoplastic resins. The standards should be scanned in accordance with the manufacturer's recommendation and calculate the photometric noise, either peak to peak, or for a given wavelength. In the latter case, the photometric noise is represented by the SD of the responses. The photometric noise should be consistent with the spectrophotometer specification.¹

The instrument noise is evaluated at high-light flux by measuring reflectance of the reference standard, the reference standard acting as the sample and the background reference. In a similar procedure, noise measurements with a lower-reflectivity reference material, a 10 % or less reflectance standard being recommended, are obtained to determine system output at reduced light-flux. In practice this occurs when a highly absorbing or very low reflectance sample is measured. The source, optics, detector, and electronics make significant contributions to the noise under these conditions.²

➤ Procedure

It is often stated that FT instruments experience the worst noise levels at the shorter wavelengths. Among other reasons, this may be due to positioning errors or unwanted lateral movements of the mirror being amplified by the shorter wavelengths. At the wavelengths near the distance of any potential tracking error, the noise becomes exacerbated. Dispersive-type monochromators tend to exhibit increased noise at longer wavelengths. This is where the PbS detector begins to lose sensitivity, filament lamps lose energy, and fiber-optic attenuation increases.³

To be fair in noise assessment and to balance the differing detector sensitivities, the noise of the best 70 % of the acquired spectra, respectively between 1,266 – 2,036 nm, were calculated separately.

The REF spectrometer was set to the default configuration (2 nm resolution, 32 scans), while the test spectrometers ran on the same rate of 20 scans per spectra. These configurations did not correspond to the manufacturer's specifications to detect the above mentioned S / N-ratio, but may represent a probable laboratory use. At a time two noise scans were averaged. The intensity scales of the following plots were varying seriously.

➤ Results and discussion

Already a peak-to-peak noise comparison could be carried out by visual inspection of the overlaid plots (Figure C-21). Preferably, a more thorough analysis was performed by tabulating the SD noise level over the spectral segment.

	Wavelength range	Noise-1	Noise-2	Average
FOSS	SD 1,266 - 2,038 nm	1.15E-05	1.22E-05	1.19E-05
	SD overall	1.45E-05	1.59E-05	1.52E-05
Brimrose	SD 1,266 - 2,038 nm	8.02E-05	7.83E-05	7.93E-05
	SD overall	1.11E-04	1.06E-04	1.09E-04
Bomem	SD 1,266 - 2,038 nm	1.50E-04	1.94E-04	1.62E-04
	SD overall	2.60E-04	3.75E-04	2.77E-04

Table C-10: Comparison of the photometric noise.

Using lower reflectance standards like a 90 % carbon black led to about five times higher noise levels whereas the relation between the different spectrometers remained the same. Accordingly the results of these measurements were not shown.

Noise levels are very low values and can easily be influenced by surrounding effects. Consecutive measurements varied already, but measurements on different days anyway. Thus this investigation should be considered as a practical approach to evaluate the influence of noise in real acquisition conditions.

The magnitudes had more expressiveness than the absolute values to estimate the specific results. The lowest and thereby best noise level was, as it should be expected, achieved by the REF spectrometer. AOTF led to almost ten times worse results, whereas the FT's noise level is again two times worse than the AOTF. Also the variation between two consecutive measurements was the highest in case of the FT.

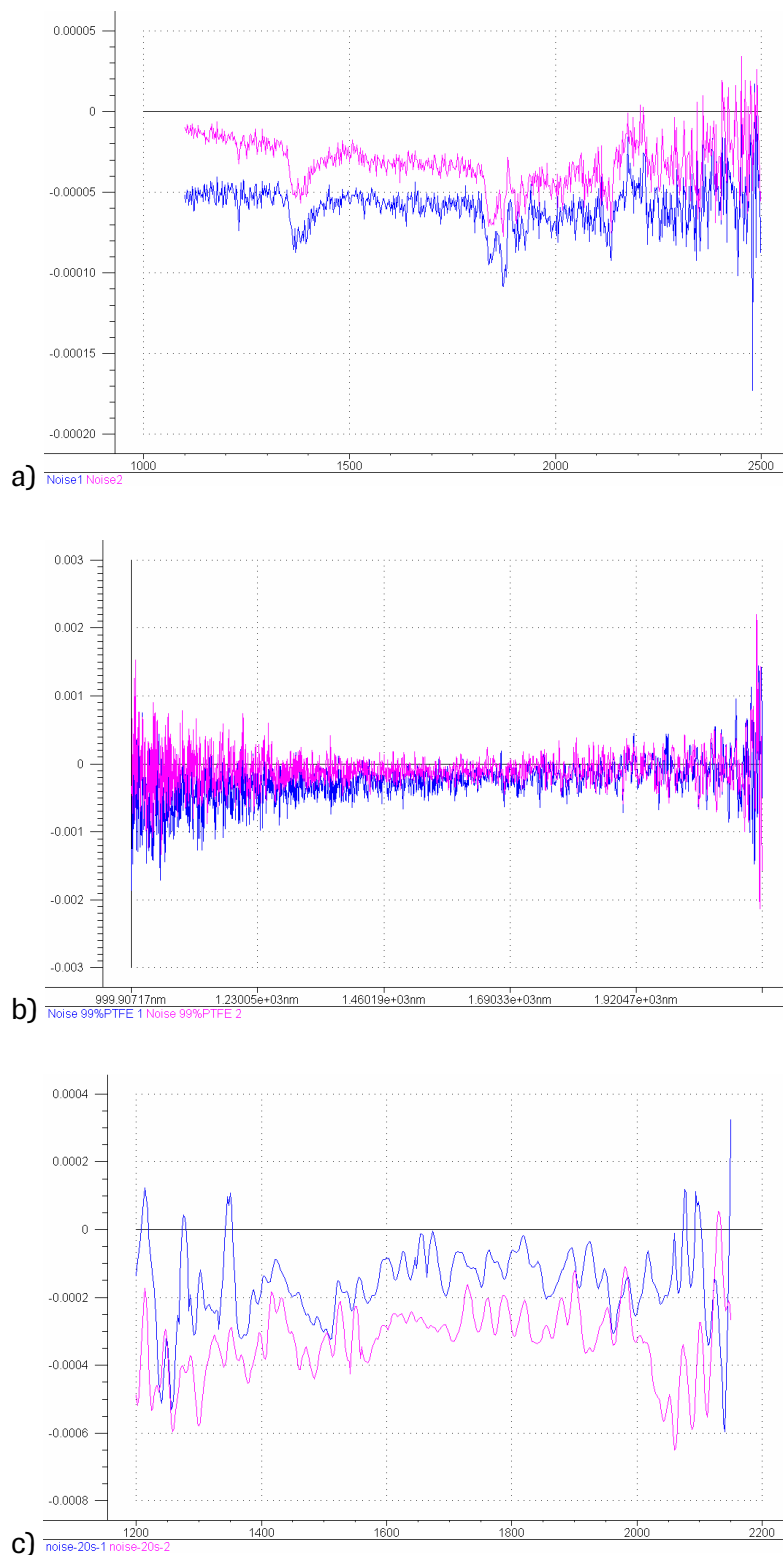


Figure C-21: Each plot with two noise spectra, successively scanned and then superposed: a) REF increased noise level at higher wavelengths, b) FT higher noise levels at short wavelengths, c) AOTF with obviously the lowest resolution.

C.3.4 Comparison of model performance

For the next comparison experiments a set of 60 lyophilized samples Product A 40 mg except of outliers was composed. Some of them were conditioned to cover a broader calibration range. According to the table below 50 samples (0.7 - 3.7 % water content) were chosen as calibration set and 10 (0.7 - 2.5 % water content) as independent validation set, respecting a homogenous distribution over the entire calibration range. All of them were scanned on each of the spectrometers and afterwards titrated by KF method. Correspondingly all the models relied on exactly the same samples and reference data. The readings of the KF titration are given in the appendix.

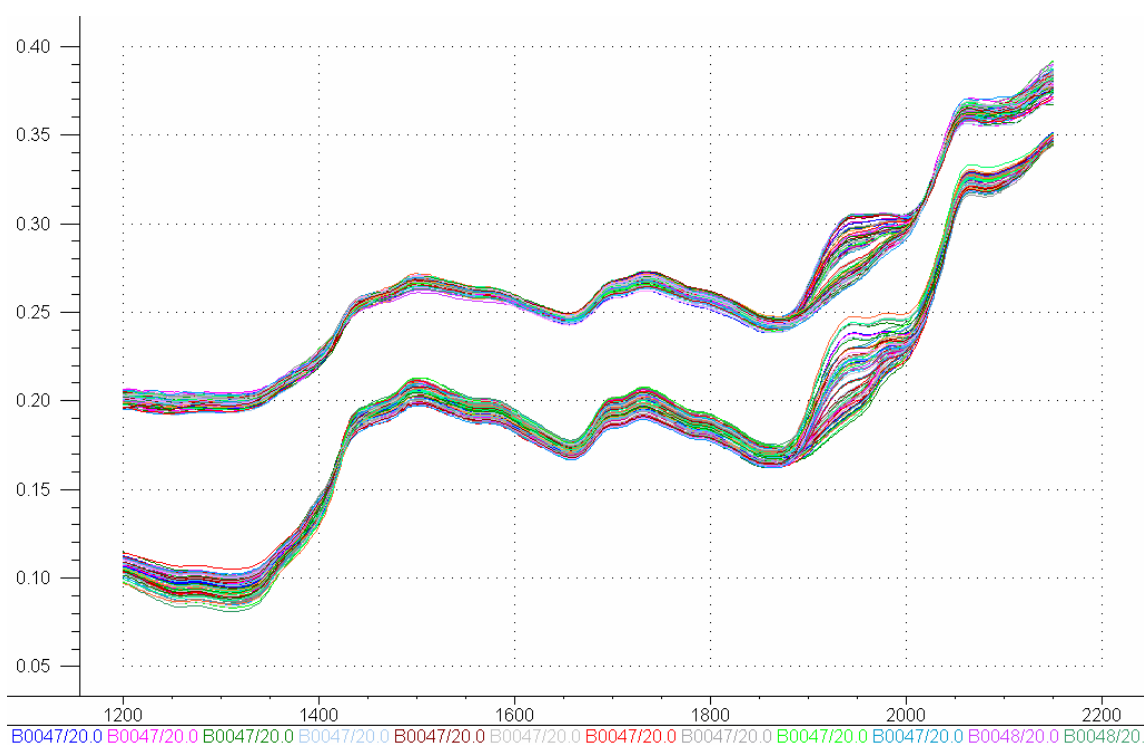


Figure C-22: The MS corrected band of spectra of the AOTF (above; 2 nm, 10 scans) and the REF (below; 2 nm, 32 scans). The higher spectroscopic resolution of the REF spectrometer became evident. The variation in water content was visually recognizable between 1,850 and 2,050 nm.

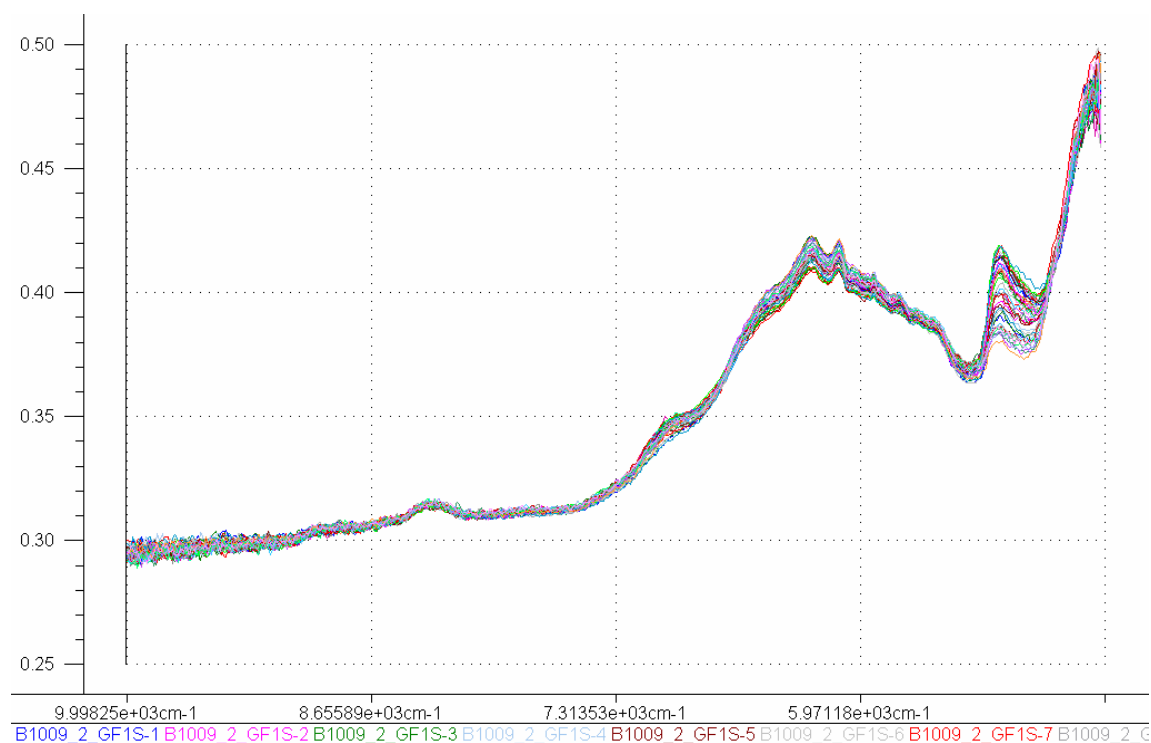


Figure C-23: Exemplary the multiplicative scatter corrected array of the FT spectra acquired with a 16 cm^{-1} resolution and a single scan mode. The high resolution is overlaid by much noise, for FT instruments typically on the edges of the scale in particular.

In the first configuration an optimal setting was chosen assuming an hypothetical laboratory exercise with 32 scans equally to the REF. Afterwards the conditions were adapted to an in-line implementation respecting the time restrictions.

Regarding the AOTF both of these alignments were equally set to 2 nm and 10 scans (~ 3 samples a second). In order to save time, Bomem recommended to use 64 cm^{-1} or higher resolutions which in practice flattened the spectrum. Actually the high resolution strength of this device got lost and no more useful results were obtained. Thus, only resolutions between 64 and 16 cm^{-1} were included in this comparison. In these configurations a semi-scan would require more than the available time and supplementary it only starts scanning from a zero position. Subsequently two spectrometers would be required to achieve the terminal stream velocity. The REF standard configuration was kept without changes, requiring about 30 seconds scanning 32 times the entire wavelength scale from 1,100 - 2,500 nm with a resolution of 2 nm.

In every mode a couple of different chemometric spectral treatments were tried out, but in the following comparison only the best result was shown. For each modification the common benchmarks correlation coefficient, the SECV of full cross validation, and the SEP were raised below. The indicated bias should be close to zero.

C.3.4.1 Comparison of the spectral quality

In this study all the collected data was imported to the Unscrambler. To avoid any alteration of the origin data in case of the FT no abscissa conversion (wavenumbers to nanometers) was performed. As pretreatment the same multiplicative scatter correction (MSC) was computed to guarantee comparability of the benchmarks.

Spectrometer	Resolution	Scans	PCs	1,100 – 2,150 / 2,500 nm	
				Correlation	SECV
FOSS	2 nm	32	2	0.9934	0.11
Brimrose	2 nm	10	2	0.9938	0.11
Bomem	16 cm ⁻¹	1	2	0.9831	0.18
	16 cm ⁻¹	32	2	0.9857	0.17
	32 cm ⁻¹	1	2	0.9854	0.17
	32 cm ⁻¹	32	2	0.9860	0.17
	64 cm ⁻¹	1	2	0.9848	0.17
	64 cm ⁻¹	32	2	0.9845	0.17

Table C-11: The correlation coefficient and SECV out of FCV of the Unscrambler MSC models. Without respect to the source of the spectral data the Unscrambler computed an acceptable correlation with only two PCs.

The FT results were not competitive with neither the REF nor the AOTF. Astonishing was the fact of only slightly different benchmarks of REF and AOTF, whereas the AOTF data was the best modeled in terms of correlation and SECV. Increasing the number of scans of the FT spectrometer did not seriously improve the models.

Unscrambler MSC Sample	KF Ref.	REF 2 nm, 32 scans		AOTF 2 nm, 10 scans		FT 16 cm ⁻¹ , 1 scan		FT 16 cm ⁻¹ , 32 scans	
		Pred.	Dev.	Pred.	Dev.	Pred.	Dev.	Pred.	Dev.
B1021-3-24h-1	0.68	0.49	-0.19	0.66	-0.02	0.56	-0.12	0.61	-0.07
B1021-3-24h-2	0.65	0.45	-0.20	0.60	-0.05	0.48	-0.17	0.50	-0.15
B1009-2-1	1.36	1.37	0.01	1.31	-0.05	1.12	-0.24	1.13	-0.23
B1009-2-2	1.40	1.43	0.03	1.48	0.08	1.67	0.27	1.63	0.23
B1010-3-1	1.92	1.88	-0.04	1.86	-0.06	1.96	0.04	1.96	0.04
B1010-3-2	1.88	1.84	-0.04	1.76	-0.12	2.02	0.14	1.96	0.08
B1021-3-15m-1	1.76	1.71	-0.05	1.84	0.08	1.88	0.12	1.88	0.12
B1021-3-15m-2	1.65	1.64	-0.01	1.53	-0.12	1.80	0.15	1.73	0.08
B1021-2-30m-1	2.45	2.53	0.08	2.60	0.15	2.61	0.16	2.56	0.11
B1021-2-30m-2	2.40	2.34	-0.06	2.48	0.08	2.49	0.09	2.49	0.09
SEP			0.10		0.09		0.17		0.14
Bias			-0.05		0.00		0.04		0.03

Unscrambler MSC Sample	KF Ref.	FT 32 cm ⁻¹ , 1 scan		FT 32 cm ⁻¹ , 32 scans		FT 64 cm ⁻¹ , 1 scan		FT 64 cm ⁻¹ , 32 scans	
		Pred.	Dev.	Pred.	Dev.	Pred.	Dev.	Pred.	Dev.
B1021-3-24h-1	0.68	0.58	-0.10	0.57	-0.11	0.53	-0.15	0.61	-0.07
B1021-3-24h-2	0.65	0.49	-0.16	0.50	-0.15	0.53	-0.12	0.54	-0.11
B1009-2-1	1.36	1.13	-0.23	1.13	-0.23	1.15	-0.21	1.13	-0.23
B1009-2-2	1.40	1.60	0.20	1.63	0.23	1.67	0.27	1.66	0.26
B1010-3-1	1.92	1.95	0.03	1.94	0.02	1.93	0.01	1.93	0.01
B1010-3-2	1.88	1.98	0.10	1.93	0.05	2.00	0.12	1.94	0.06
B1021-3-15m-1	1.76	1.91	0.15	1.91	0.15	1.86	0.10	1.89	0.13
B1021-3-15m-2	1.65	1.71	0.06	1.74	0.09	1.72	0.07	1.72	0.07
B1021-2-30m-1	2.45	2.52	0.07	2.52	0.07	2.55	0.10	2.56	0.11
B1021-2-30m-2	2.40	2.47	0.07	2.43	0.03	2.42	0.02	2.46	0.06
SEP			0.14		0.14		0.15		0.14
Bias			0.02		0.02		0.02		0.03

Table C-12: The prediction results of the external validation set performed by the respective MSC Unscrambler models.

The prediction results were confirming the SECV and correlation values of the models in general, although the SEP was inferior to the SECV.

The REF spectrometer showed in individual cases very precise predictions, but was the most incorrect in dry samples (B1021-3-24h). This was also the main reason for the high bias value indicating the general underestimation of the water content. The AOTF was more equilibrated but showed manifest deviations in higher water content. Although the AOTF's SEP of the validation set was worse than the REF spectrometer, the bias was close to zero confirming the best model benchmarks (Table C-11).

B1009-2 was generally very poorly modeled with the FT data. The lower the adjusted resolution, whereas the higher the number of scans of the FT, the better was the prediction accuracy.

C.3.4.2 Comparison of analysis precision

In a GxP regulated environment it would neither be possible to transfer the spectral data nor even to run a spectrometer with another software than it was validated or delivered with. Sometimes the data collection drivers were directly engineered in the respective software.

The REF spectrometer was running with Vision, the FT with Grams / 32 AI. The AOTF was configured in a modular way so that the choice of software was not restricted. Nevertheless, the Unscrambler was included in the delivery.

In purpose of obtaining models with the best benchmarks available several pretreatments with their combinations and variations were tried out. MSC, automatic baseline correction (ABC), 1st and 2nd derivatives of Savitzky-Golay, and a Norris derivation were applied. Only the model with the best performance was shown below.

Spectrometer	Resolution	Scans	PCs	1,100 – 2,150 / 2,500 nm	
				Correlation	SECV
FOSS	2 nm	32	4	0.9943	0.09
Brimrose	2 nm	10	2	0.9938	0.11
Bomem	16 cm ⁻¹	1	4	0.9783	0.14
	16 cm ⁻¹	32	3	0.9774	0.15
	32 cm ⁻¹	1	4	0.9815	0.13
	32 cm ⁻¹	32	4	0.9816	0.13
	64 cm ⁻¹	1	3	0.9748	0.16
	64 cm ⁻¹	32	4	0.9804	0.14

Table C-13: Correlation and SECV computed with MSC pretreatment performed by the corresponding software.

Corresponding Software MSC Sample	KF Ref.	REF 2 nm, 32 scans		AOTF 2 nm, 10 scans		FT 16 cm ⁻¹ , 1 scan		FT 16 cm ⁻¹ , 32 scans	
		Pred.	Dev.	Pred.	Dev.	Pred.	Dev.	Pred.	Dev.
B1021-3-24h-1	0.68	0.50	-0.18	0.66	-0.02	0.59	-0.09	0.54	-0.14
B1021-3-24h-2	0.65	0.51	-0.14	0.60	-0.05	0.53	-0.12	0.45	-0.20
B1009-2-1	1.36	1.32	-0.04	1.31	-0.05	1.20	-0.16	1.22	-0.14
B1009-2-2	1.40	1.46	0.06	1.48	0.08	1.58	0.18	1.57	0.17
B1010-3-1	1.92	1.85	-0.07	1.86	-0.06	1.80	-0.12	1.91	-0.01
B1010-3-2	1.88	1.82	-0.04	1.76	-0.12	1.80	-0.08	1.92	0.04
B1021-3-15m-1	1.76	1.77	0.01	1.84	0.08	1.90	0.14	1.85	0.09
B1021-3-15m-2	1.65	1.73	0.08	1.53	-0.12	1.77	0.12	1.73	0.08
B1021-2-30m-1	2.45	2.56	0.11	2.60	0.15	2.61	0.16	2.57	0.12
B1021-2-30m-2	2.40	2.44	0.04	2.48	0.08	2.47	0.07	2.49	0.09
SEP			0.10		0.09		0.14		0.13
Bias			-0.02		0.00		0.01		0.01

Corresponding Software MSC Sample	KF Ref.	FT 32 cm ⁻¹ , 1 scan		FT 32 cm ⁻¹ , 32 scans		FT 64 cm ⁻¹ , 1 scan		FT 64 cm ⁻¹ , 32 scans	
		Pred.	Dev.	Pred.	Dev.	Pred.	Dev.	Pred.	Dev.
B1021-3-24h-1	0.68	0.57	-0.11	0.60	-0.08	0.48	-0.20	0.61	-0.07
B1021-3-24h-2	0.65	0.53	-0.12	0.50	-0.15	0.47	-0.18	0.54	-0.11
B1009-2-1	1.36	1.18	-0.18	1.17	-0.19	1.22	-0.14	1.17	-0.19
B1009-2-2	1.40	1.53	0.13	1.56	0.16	1.60	0.20	1.57	0.17
B1010-3-1	1.92	1.81	-0.11	1.81	-0.11	1.88	-0.04	1.80	-0.12
B1010-3-2	1.88	1.81	-0.07	1.79	-0.09	1.97	0.09	1.79	-0.09
B1021-3-15m-1	1.76	1.91	0.15	1.91	0.15	1.83	0.07	1.90	0.14
B1021-3-15m-2	1.65	1.69	0.04	1.70	0.05	1.71	0.06	1.69	0.04
B1021-2-30m-1	2.45	2.58	0.13	2.55	0.10	2.54	0.09	2.59	0.14
B1021-2-30m-2	2.40	2.40	0.00	2.35	-0.05	2.42	0.02	2.41	0.01
SEP			0.12		0.13		0.13		0.13
Bias			-0.01		-0.02		0.00		-0.01

Table C-14: Prediction results referring to the validation set with MSC pretreatment of the corresponding software.

The increase of the number of PCs, and the decrease of correlation in Grams models, indicated that MSC was not the optimal pretreatment in the other chemometric packages. The introduction of a higher number of PCs increased the risk of modeling noise in the meantime. However, the SEP decreased in these models in comparison to what the Unscrambler calculated. This showed that common benchmarks, like the correlation coefficient and SECV, should not be compared in an unrestricted manner over different systems, as the computation of these values varied (refer to the appendix).

Grams dealt a bit better with the problem to predict the two samples of B1009-2. This ability was mainly responsible for the lower SEP. The bias decreased enormously, but a large variability was still remaining in comparison to the competitors. This invalidates the assumption that the samples may have been scanned badly on the FT, which was responsible for worse results. Secondly it is mentioned that the bias of the REF instrument decreased from Unscrambler to Vision remarkably of about 60 %.

C.3.4.3 Discussion

The software had a huge impact on the calibration quality. The implemented algorithms were not the same; pre-treatments were calculated in different manners and with non equivalent options. Knowledge of one assembly was not one by one transferable to another device. Observing only the common benchmarks to estimate the quality of a calibration was insufficient. Comparability was reduced due to slightly different calculation formula.

The corresponding software seemed to be well adapted to the photometric device and treated the spectral data the best. In any combination the best model was calculated with the REF data by Vision, but tightly followed by the AOTF / Unscrambler assembly requiring only two PCs.

The area beyond 2,100 nm did not contribute to any one of the calibrations as water is absorbing at 1,440 and 1,940 nm. Excluding this zone from the REF model did not influence it negatively. But the lower wavelengths down to 1,100 nm were improving the benchmarks. This zone was only well differentiated in the spectra of the REF and the FT spectrometer. In contrast to the AOTF these instruments evidently detected a supplementary variation in this area. For good results generated by the AOTF this range was not required. AOTF technology allows time savings by decreasing the sum of data points what is advantageous for in-line applications with high velocities. Here all the five samples would be predictable by one single spectrometer.

C.3.5 Conclusions

The choice of instrumentation is dependent on the application and should be taken according to the strengths and shortcomings of the various types of equipment and the specific analytical need.

The use of fiber optic probes generally requires a very high detector sensitivity causing on the other hand an increase of the noise level but a decrease in repeatability what probably was the reason for the bad theoretical examination performance of the tested FT. Furthermore, water bands in the spectra can interfere with the high amount of open OH-groups of the silica glass over the whole length of such a probe.

Obviously neither the best spectrum in resolution and intensity nor e.g. the lowest noise level of the equipment ensured imperatively the best prediction results. Referring solely on results of a theoretical evaluation was not directly correlated to the best performance in practice. A calibration of real samples challenged by an independent validation set served for a better basis of assessment. The FT assembly was not able to compete with the performance of the AOTF. The AOTF's prediction results were better in every configuration, requiring even less time for the spectra acquisition. In mean time it was the lower-priced and less complex solution in automation as only one spectrometer was sufficient.

In conclusion, the project was continued with the Brimrose Luminar Freespace AOTF spectrometer combined with the Unscrambler as chemometric software. All the following investigations were based on this assembly. For further in-line calibrations the spectral range could be reduced to a smaller wavelength range, enabling five reliable measurements per second.

References C.3 Evaluation of the appropriate analysis system

- ¹ European Pharmacopoeia, 4th Edition 4.02, chapter 2.2.40, Deutscher Apotheker Verlag, Stuttgart, Govi Verlag - Pharmazeutischer Verlag GmbH, Eschborn, 2000
- ² United States Pharmacopoeia 25, 2nd supplement, general chapter <1119> NEAR-INFRARED SPECTROPHOTOMETRY, 2000
- ³ Ciurczak E. W , A Comparison of Near-Infrared Spectrometers for Solid Dosage Form Analysis, Pharmaceutical Technology Yearbook 1997, pp. 18 - 28, 1997

C.4 Static scan mode evaluation

The AOTF technology allowed to scan 16,000 independent data points per second in an almost random distribution over the wavelength range. With respect to the residual moisture determination, the impact of this distribution on the analysis accuracy should be explored. For water analysis the best scan parameters, in terms of resolution, and number of scans with regard to a static sample presentation, had to be browsed. This setting should include a broad spectral range allowing to identify the most important spectral regions for this purpose.

C.4.1 Procedure

A sample set of Product A 20 mg was prepared, containing 106 original, dried and moisturized vials. All of them were scanned several times, but in different spectrometer settings varying from 1 to 8 nm resolution and 5 to 40 scans. This led to eight independent files each containing the data of one configuration. The terminal KF titration revealed that the comprised samples had water contents in the range of 0.5 to 3.7 %.

The data of the default configuration recommended by the manufacturer (2 nm, 10 scans) was used to find an appropriate spectral pretreatment for an accurate quantitative PLS model. Based on this knowledge the same pretreatment was computed to any of these files to compare nothing but the differences of the spectral quality.

C.4.1.1 Pretreatment evaluation

Many different mathematical pretreatments were applied on the same spectral data, separately and in combination. Possible and reasonable options were MSC, normalization, baseline corrections, and first or second derivatives such as Savitzky-Golay or Norris which could be further varied in their polynomial order. Then a full cross validated PLS model was computed. As valuation criterion of the best model primarily the correlation coefficients and SECV were regarded. It was considered as a secondary advantage if no outliers appeared and, in view of a future in-line analysis, the required spectral region was small.

Pretreatment	Spectral Range [nm]	PCs	Correlation	SECV	Comment
MSC	1,200 - 2,150	2	0.9905	0.13	
MSC	1,814 - 2,036	2	0.9920	0.12	
Norris Segment Size 5	1,200 - 2,150	2	0.9854	0.17	25 an outlier
Norris Segment Size 5	1,854 - 2,024	2	0.9804	0.19	25 an outlier
MSC Norris Segment Size 5	1,200 - 2,150	2	0.9910	0.13	
MSC Norris Segment Size 5	1,362 - 2,038	2	0.9923	0.12	still large spectral area
Savitzky-Golay 1st	1,200 - 2,150	2	0.9852	0.17	25 an outlier
Savitzky-Golay 1st	1,628 - 2,014	2	0.9876	0.15	25 an outlier
Savitzky-Golay 2nd	1,200 - 2,150	3	0.9771	0.21	increased no. of PCs
Savitzky-Golay 2nd	1,768 - 2,068	3	0.9855	0.17	increased no. of PCs

Table C-15: Results of a selection of the computed example PLS models.

In all cases the correlation coefficients were remarkably high. Equivalently low SECVs were achieved with both the MSC pretreated data (spectral region 1,814 - 2,036 nm) and the MSC Norris combination (1,362 - 2,038 nm). MSC required a smaller spectral range and was simpler to compute. Accordingly, MSC was considered as the most adequate treatment.

C.4.1.2 Scan-mode comparison

For all the resolutions there was a setting with 10 scans. The second one was adapted in such a way, that the number of scans compensated the lower amount of data points. Reference was the standard setting of 2 nm and 10 scans, which led equally to 4 nm / 20 scans and 8 nm / 40 scans to 5,250 data points. The same MSC was computed on each of these 8 files created and the model benchmarks were plotted here. The best model performance was situated in the upper right section of the scatter plots (Figure C-24 and Figure C-25).

Resolution [nm]	Scans	1,100 – 2,150 nm		1,814 – 2,036 nm	
		Correlation	SECV	Correlation	SECV
1	5	0.9864	0.1596	0.9911	0.1291
1	10	0.9908	0.1315	0.9915	0.1265
2	10	0.9900	0.1374	0.9920	0.1225
2	15	0.9905	0.1335	0.9920	0.1230
4	10	0.9893	0.1420	0.9920	0.1230
4	20	0.9919	0.1233	0.9915	0.1265
8	10	0.9907	0.1319	0.9894	0.1410
8	40	0.9888	0.1452	0.9914	0.1274

Table C-16: Overview of the benchmarks of the 8 models.

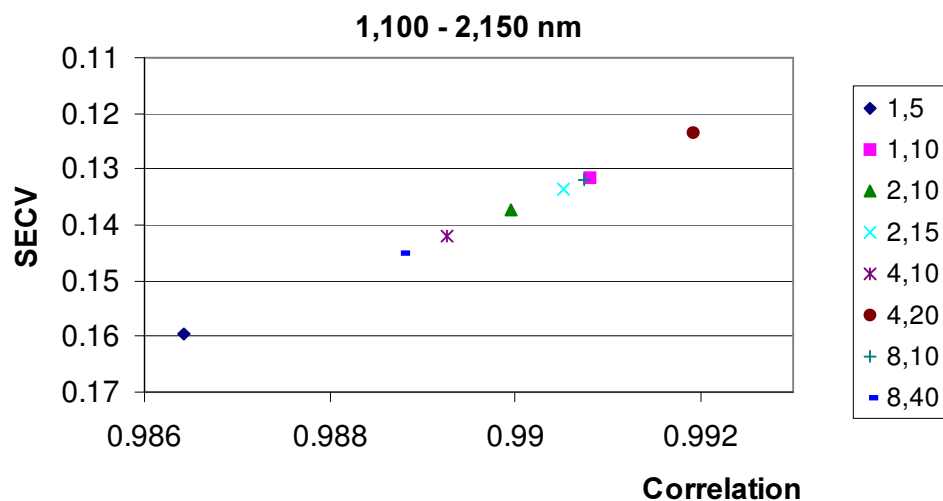


Figure C-24: Scatter plot of the correlation versus SECV of the models with the entire spectral range from 1,100 - 2,150 nm.

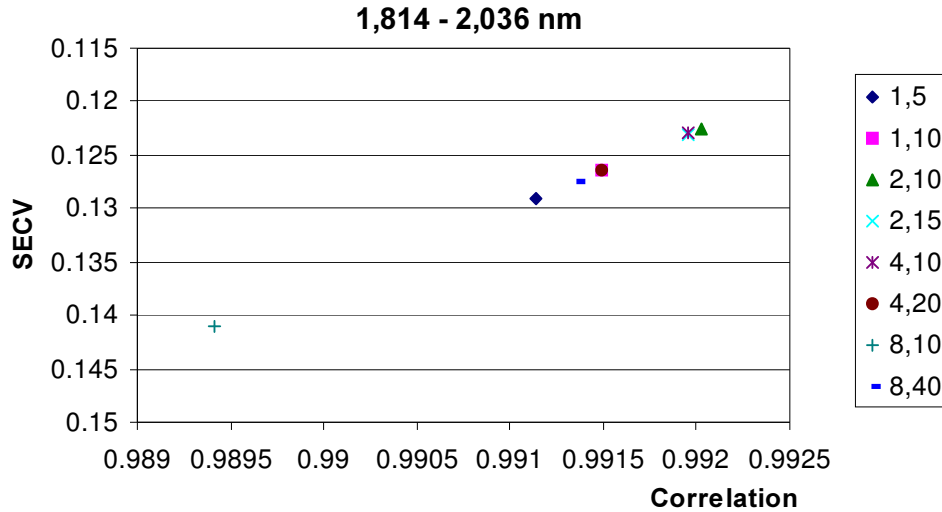


Figure C-25: Scatter plot of the correlation versus SECV of the models with the reduced spectral range from 1,814 - 2,036 nm.

C.4.2 Discussion and conclusions

The influence on the model benchmarks due to the applied scan number or resolution was quite weak. Increasing the number of scans should compensate a decreased resolution. In case of the calibrations using the entire spectral range this assumption was confirmed beyond in case of 8 nm. However, considering the columns of reduced range this statement was even not true. Apparently, there was a kind of optimum depending on the resolution.

Regarding the highlighted rows of equivalent number of scans in the reduced spectral range the highest correlation but lowest SECV was found at 2 nm and 10 scans. In this scan mode only 1,110 data points per spectrum were acquired, requiring less than 70 milliseconds. With regard to the future in-line application of the same spectrometer this configuration seemed to offer a good opportunity. Some more time for the container transport, data transfer, and calculation would remain. Thus, this setting was considered as a standard for successive static measurement.

C.5 Validated qualification of Product B vials

This chapter was published in Ref.¹ and partially in Ref.²

Quantitative specifications may also be considered from a broader qualitative point of view. Moreover, in production it is not just the values of these few samples that are of interest, but the homogeneity of the batch as a whole.

Whenever the objective is to test if a certain acceptance limit is respected or not, and this is mainly the case in practice, a classification result is largely sufficient and forms the basis for a 'reject' or 'accept' decision. If an evidence of the whole batch is required a total inspection is preferable. NIR in combination with chemometrics even allows approaching quantitative problems by a qualitative definition. Accordingly, a NIR calibration was developed to provide a rapid and precise technique for the classification of batches into quality groups.

C.5.1 Control and calibration

NIRS and principal component analysis (PCA)³ were applied to classify Product B vials into two groups of 'good' and 'bad' samples. The acceptance limit for the NIR calibration was set to $< 2.0 \%$ to define the group of 'good' samples. Samples with water contents between 2 and 4 % were considered to belong to the group of 'bad' samples which had to be rejected. Any higher values were characterized as 'outliers' and were also rejected.

The method was validated using an extensive set of samples covering a broad moisture range. A qualitative two class model was easy to create and to handle and provided the basis for a 100 % batch control as an alternative to the KF titration of selected samples.

Both the samples for calibration and validation of the NIR model were titrated by KF method. The readings of the results are given in the appendix.

C.5.1.1 Data acquisition

The sealed glass vials were placed directly on a support 42 mm from the sensor window in order to measure through the bottom of the colorless glass vials. The diffuse reflectance spectra were collected in absorbance mode with a resolution of 2 nm and

10 scans from 1,200 to 2,150 nm. To compensate for surface phenomena, the majority of the samples were measured 3 times. The samples were rotated between each measurement. All the measurements were performed at room temperature.

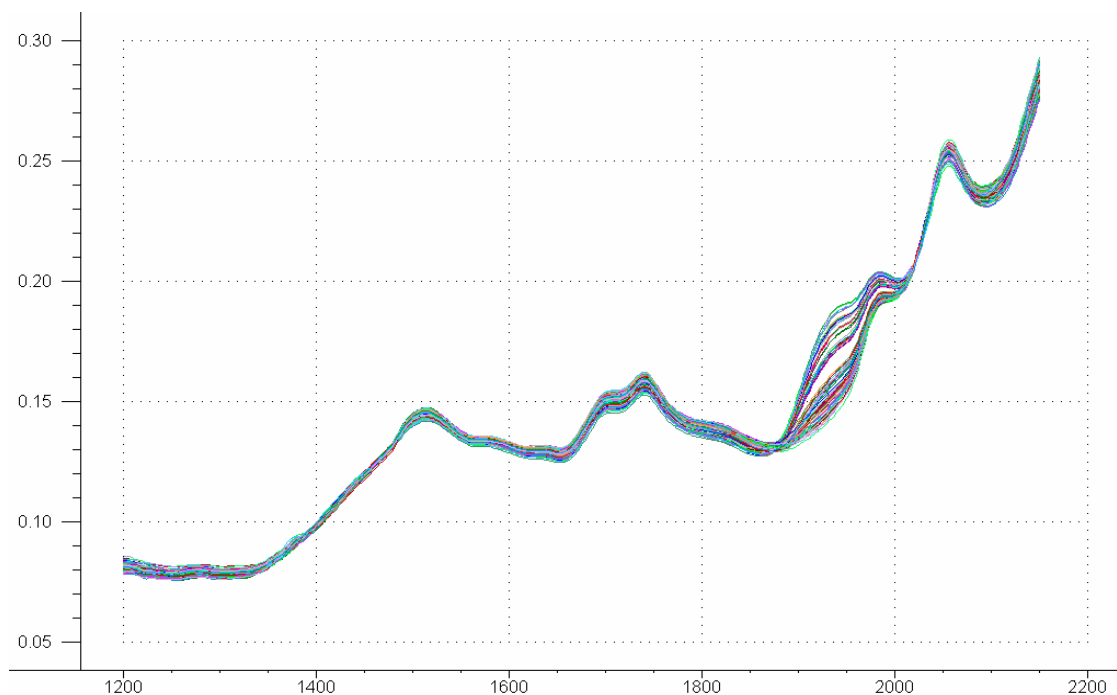


Figure C-26: NIR spectra of 'good' and 'bad' samples. The distinction at the position of the water band (1,940 nm) is clear. The lower group of spectra corresponds to samples with less than 1.4 % water, the upper group to samples with more than 2.0 %.

C.5.1.2 Sample selection and calibration

To establish the alternative qualitative calibration, two classification groups of samples were required. In a first step, samples were prepared from different batches with an extended range of water contents. Afterwards the corresponding NIR spectra were divided into two groups: spectra of 'good' samples containing less than 2 % and spectra of 'bad' samples with more than 2 and less than 4 % water. The 'good' database comprised 69 samples with water contents between 0.3 and 1.4 %. The 'bad' database contained 43 spectra corresponding to water values between 2.0 and 3.5 %. In total a set of only 113 samples was required for modeling.

The gap between these groups was intended to avoid decision uncertainties caused by overlapping analysis results. The size of this interval was defined with respect to the standard error of prediction ($SEP = 0.1 \%$) which would be at least required for an

equivalent quantitative NIR method. The SEP here was a statistical parameter that indicated the upper limit of accuracy of the NIR method.³

It was considered reasonable to use three times the SEP of the quantitative prediction method to have 99 % confidence. Assuming a normal distribution of the samples included in the calculation, 99 % of them would have an actual water content of y_i .

$$y_i \leq \pm 3 \cdot SEP$$

Equation C-8: Computation of y_i

For the qualitative prediction model the difference between the two groups was set to twice this value. Accordingly only calibration samples with water contents of 0.6 % below the acceptance limit were acknowledged, as it was very important to avoid any false good decisions resulting in a lack of quality.

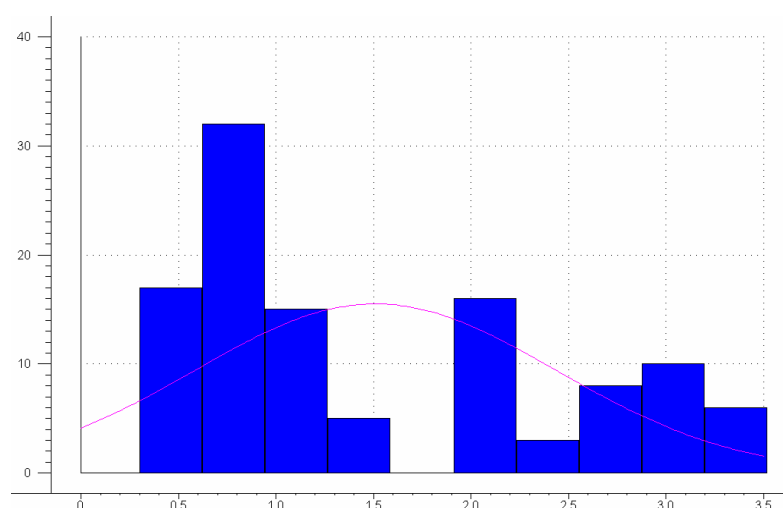


Figure C-27: This histogram of the sample distribution illustrates the two distinct calibration sets.

C.5.1.3 Calibration

In a first step, the feasibility of the calibration was explored by using third party chemometric software. To carry out the calculation, all the spectra were assembled in one Unscrambler file and a multiplicative scatter correction (MSC) was applied to filter out sampling variations. A PCA was then computed to analyze the correlation between the spectra and the water values. The results showed that differentiation of the qualitative groups of 'good' and 'bad' samples was possible with one single PC.

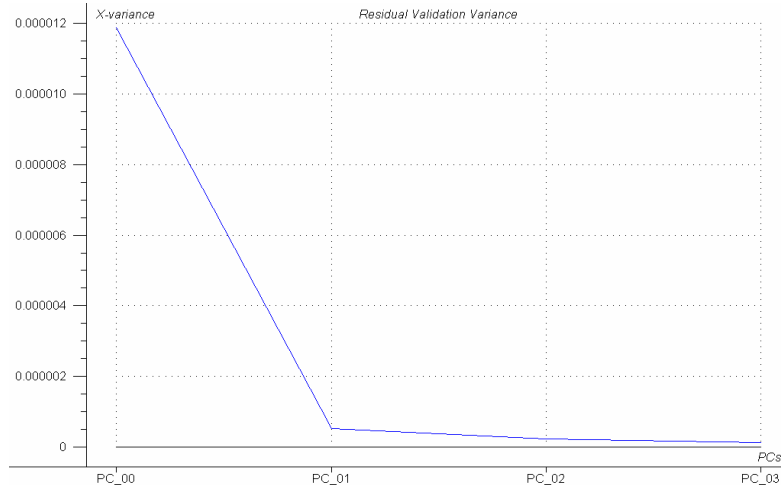


Figure C-28: The residual validation variance plot shows that only one PC is required for this calibration.

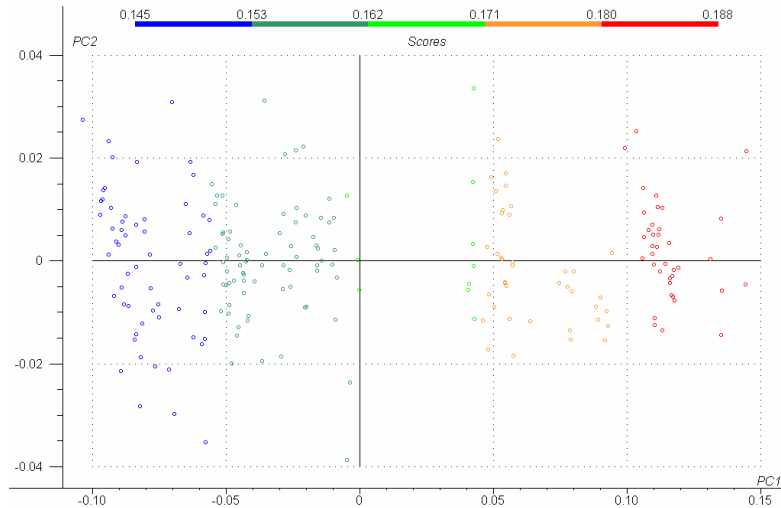


Figure C-29: The scores plot confirms the validation variance plot and shows the two separate groups as distinguished by the first principal component.

The second step was the transfer of the calibration to the on-line software Snap!. The 'Prediction Profile Compiler' was used to create the on-line prediction operation interface. The two group files were imported to form the basis for the MSC and the qualitative classification. The Mahalanobis distance was fixed to 1.5 to comply with a collection of samples of known water content. To run the prediction, this calibration file was loaded in the 'Predict' module of the Snap! software.

C.5.2 External validation

Further samples from different batches of the lyophilized product were used for validation. The objective was to challenge the calibration with marginal samples. They were first measured with the 'Predict' on-line monitor, classified on the basis of the NIR analysis result and then titrated by the KF method.

A total of 150 samples were measured; 75 'good' samples had less than 2 % water (max. 1.7 %), 45 'bad' vials more than 2 % (2.1 - 4.1 %), and 30 'outliers' more than 4 % (4.3 - 10.1 %). All the results were within the specified ranges. The corresponding KF water values confirmed the qualitative NIR calibration.

C.5.3 Results and discussion

A non-invasive NIR reflectance method to carry out a good vs. bad quality assessment with respect to the water content of lyophilized vials was developed and validated. After mathematical pretreatment, a classification method with an acceptance limit set to 2 % was computed. The calibration set composed of 113 samples was challenged by classifying 150 more samples which were not included into the initial calibration set.

The GMP rules relating to pharmaceutical quality control set high standards for quantitative methods. After general system suitability testing, calibration-specific parameters need to be verified.^{4, 5} In particular, the validation e.g. in terms of accuracy, linearity and repeatability with narrow statistic confidence intervals requires considerable work. In NIR assays, the accuracy is indicated by the standard error of prediction. Substantial validation sets over the entire calibration range are used to prove accuracy in the short term and parallel test sets are used to validate the assay over time at regular intervals. Linearity is proven by a straight calibration line over the working range of the assay with correlation coefficients of more than 99 %, slopes close to unity and offsets theoretically equal to zero. These parameters should be submitted to regulatory authorities for registration. Repeatability is demonstrated using several determinations of one or more samples, intermediate precision by conducting assays e.g. on different days and with different analysts.⁶ Especially in case of low contents, even minimal deviations lead to high relative standard errors and unacceptable calibrations.

However, only the specificity and robustness need to be validated for qualitative modeling. Accuracy, linearity, and repeatability do not need to be evaluated, simplifying the validation effort. On the other hand, potential challenges (e.g. different batches, blends) should be presented to the reference library, but not used for calibration, must be tested and shown to give current results. Thus a new test should be established. Here the threshold situation in particular should be challenged, using samples in the range just above and below the acceptance limit (Table C-17), to demonstrate correct assignment by the system.

Traditionally the predicted water value of a quantitative method is compared with an acceptance limit, but the summary of results in the batch record only needs to indicate 'conform' if the sample meets the requirements or 'non-conform' if it does not. However, current regulations require the storage of all the raw data – including the water values. The qualitative method also provides the basis for a release decision but does not generate this kind of data. An additional advantage would then be the smaller amount of resulting data for storage in the case of large sample quantities possibly reducing the demand of statement by the regulatory authorities.

Validation	Quantitative	Qualitative
Specificity	+	+
Robustness	+	+
Accuracy	+	--
Precision	+	--
Linearity	+	--
Threshold challenge	--	++

Table C-17: Assessment of validation work relating to quantitative or qualitative calibrations in practice.

In future, new calibrations for new products or changed compositions requiring re-calibration can be performed on a second equivalent spectrometer in the laboratory environment. These models need to be transferred to the plant spectrometer afterwards, assuming good agreement between the two devices in terms of spectral quality. As calibration transfer from one spectrometer to the other within one type series including method modification and revalidation still remains an issue, simple and

robust calibration techniques are of interest.⁷ If the required calibration work is limited the product could be remodeled independently on a second or third device.

C.5.4 Conclusions

A qualitative two-class model is easy to create and to handle compared with quantitative determinations. No large-scale data treatment is necessary, the sample sets can be kept very small, but the calibration remains fast and robust. This NIRA method was non-destructive and fast. Each analysis took less than one second.

For these reasons, the NIR application could be used not just for laboratory quality control, but also for the screening of large numbers of samples or even for a total quality control of entire batches. Samples deviating from the quality parameters could be rejected simultaneously and a homogeneous in-specification batch would result. This was exemplarily performed at-line with an entire batch Product B. The outcome of this inspection formed the basis for an investment accounting reported below in Chapter D: Business case.

References C.5 Validated qualification of Product B vials

- ¹ Sukowski L., Ulmschneider M., Near-Infrared Spectroscopy: High Speed Noninvasive Qualification of Lyophilized vials, in Davies A. M. C., Giangiaco R., Near Infrared Spectroscopy: Proceeding of the 11th International Conference, NIR Publications, 2004
- ² Sukowski L., Ulmschneider M., Leuenberger H., Near-Infrared Spectroscopy: Non-Invasive Qualification of Lyophilized Vials, Poster on the Pharmaday, Basel, 11 July 2003
- ³ Esbensen K. H., Multivariate Data Analysis - In Practice, 4th Edition, CAMO, Oslo, Norway, 2000
- ⁴ United States Pharmacopoeia, Edition 25, Validation of compendial Methods, Chapter <1225>, 2000
- ⁵ Röttele J., Benda S., Rau B., Determination of residual moisture in lyophilized pharmaceutical products through intact glass vials: validation of the NIR-method, Proceedings of the International Conference on Near Infrared Spectroscopy, 6th, 1995
- ⁶ Ritchie G.E., Ciurczak E.W., Validating a Near-Infrared Spectroscopic Method, Proceedings of Spectroscopy in Process and Quality Control Conference, New Brunswick, NJ, 1999
- ⁷ McGonigle R., Development and Validation of Analytical Method Programs in Pharmaceutical and Biomedical Analysis, Vol. 3, Pergamon Press, Elsevier Science, New York, USA, 1996

C.6 The process simulator

The feasibility of a total in-line inspection in a lyophilization production line running with a maximum velocity of almost 300 samples per minute was evaluated in a further step. A process simulator was designed to perform all the calibration and validation work off-line in a laboratory environment without disturbing the routine procedures.

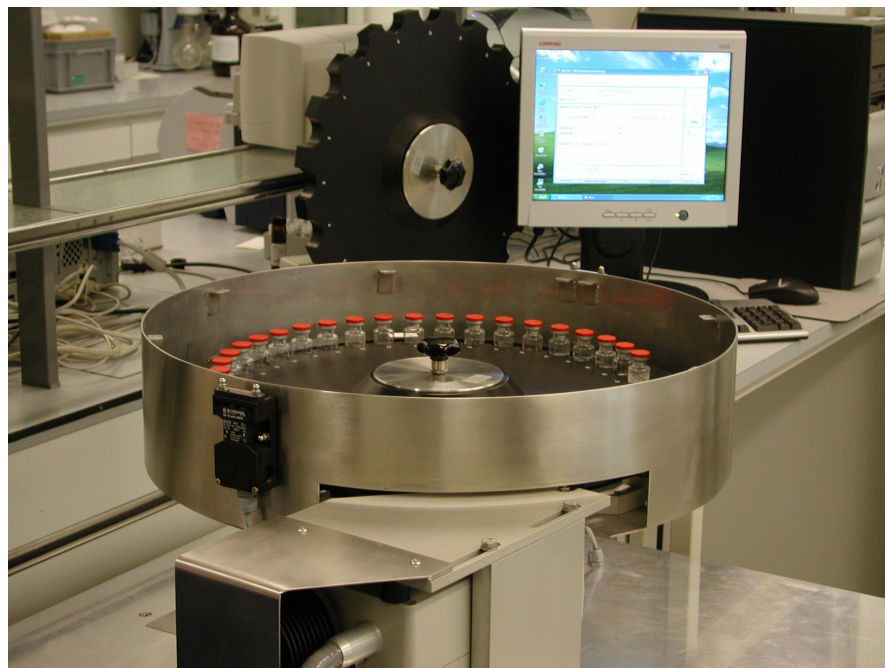


Figure C-30: Simulation of an in-line total quality inspection of lyophilized vials by NIRS.

The simulator was a custom-built prototype conceptually designed to imitate the real production conditions as closely as possible. This unit was mainly composed of a stepless controllable servo-motor, with respect to the units' format exchangeable starwheels, and a rotary encoder similar to an auto sampler. The optical measuring head of the spectrometer was mounted below the starwheel, in order to irradiate the samples through the vials' bottom. It was possible to select different velocities between 0 and 300 vials per minute. When the motor was started, the rotary encoder generated automatically a trigger signal whenever a sample-position of the starwheel was located above the sensor. Activated by the trigger signal a scan on the continuously moving samples was excited. The trigger signal was a function of the starwheel position and was therefore time independent. Consequently the measurement always started on the same spot on the bottom of the vials, irrespective of the rotation speed.

With regard to the in-line application in the production, parallelly a 21 CFR Part 11 compliant process software was developed, allowing the spectra acquisition with the same velocity and a prediction according to a predefined calibration simultaneously. The results were displayed on the screen and optionally stored on the hard-disk together with the entire spectra. By means of these data, a batch record could be printed e.g. in the end of the analysis of an entire lot.

C.6.1 Dynamic scan mode evaluation

As the NIR spectra were acquired while the bottles were moving continuously, there was only a limited time available for scanning. Nevertheless the scan parameters should be independent of the rotary speed. To filter local surface phenomena or temporary influences like vibrations several scans should be averaged to one spectrum. On one hand the entire bottle bottom surface should be exploited for scanning, but on the other hand there should be no light energy missing the bottle. Already touching the curvature of its border caused unwanted scattering or disturbing signals from the periphery.

By computing PCA models the optimal measurement parameters of the highest velocity of the respective format were searched. Successively, only these parameters were applied for all rotary speeds.

C.6.1.1 Procedure dynamic scan mode evaluation

Ten selected vials of a specific diameter were measured at different rotary speeds covering the range of reasonable operation. All of these measurements were performed with a 2 nm resolution in the range from 1,500 to 2,150 nm representing a robust calibration range. At a time five of the ten spectra corresponding to one velocity were averaged. First the shape of the spectra was visually estimated, then a PCA was computed to explore if there was a velocity dependent shift in the data. This procedure is presented in detail only for one vial format. The corresponding plots for the other container diameters are given in the appendix.

C.6.1.2 Example diameter 16.25 mm, 2 and 3 ml

For vials with a diameter of 16.25 mm velocities between 100 and 300 samples per minute were considered. The initial number of 8 scans was successively reduced one by one.

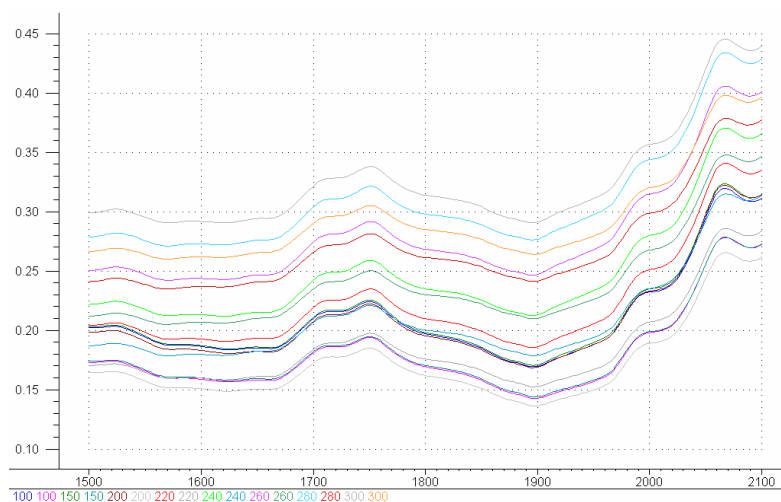


Figure C-31 : The averaged raw spectra of 8 scans taken with velocities between 100 and 300 vials per minute.

Already the spectra plot (Figure C-31) illustrated a shift in absorbance depending on the rotary speed. The faster the starwheel turned the higher was the absorbance or, with other words, the more light got lost. Furthermore the spectra looked much undifferentiated in comparison to statically acquired ones or spectra of a lower number of scans with the same velocity (compare to Figure C-32). Apparently the course was corrupted when too many scans were taken.

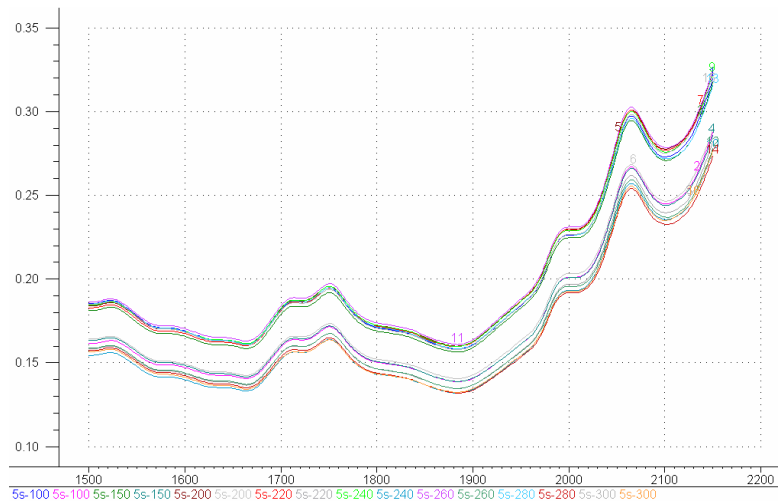


Figure C-32: The average raw spectra of 5 scans taken with velocities between 100 to 300 vials per minute.

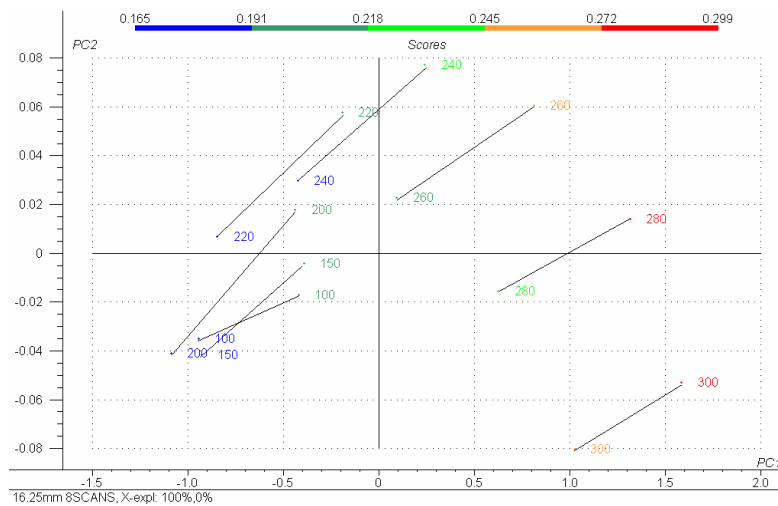


Figure C-33: With 8 scans per sample the lines were arranged in a clockwise manner. Already the spectra taken with velocities superior to 220 samples per minute were weighted differently in comparison to the other ones.

The faster the moving speed the higher was the weight of the scores. Actually, there appeared to be a causal relation between the rotary speed and the scores as the spectra are separated according to this order.

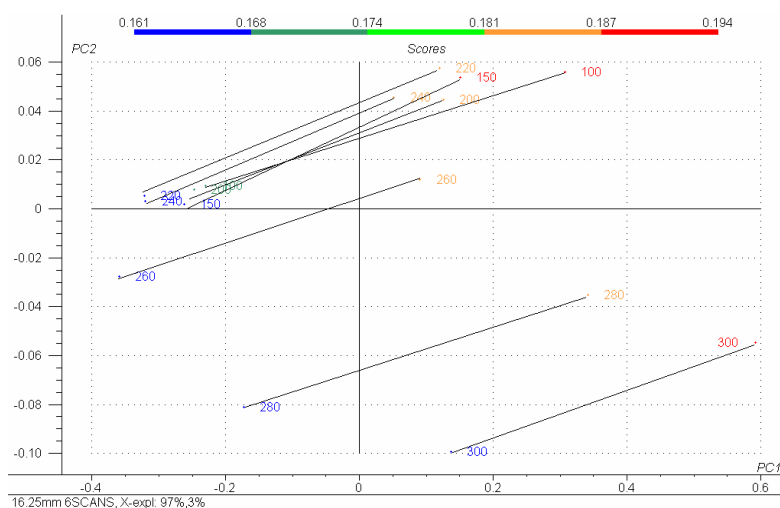


Figure C-34: The PCA computed with spectra based on 6 scans reduced the scores scale to about the half. The sample sets measured with more than 260 per minute still showed the separation effect like in the setting with 8 scans.

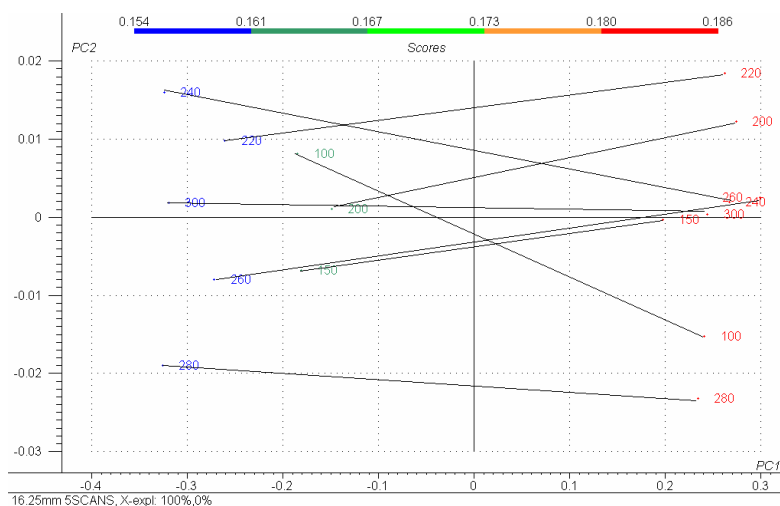


Figure C-35: With 5 scans the scale dimension was reduced again. As all the lines were superposed the velocity influence seemed to have disappeared. The distinctive quality found was now the water variation within one velocity series.

When only 5 scans per spectrum were taken the influence of the velocity appeared to be negligible. The same experiment was performed with the other vial diameters as well.

C.6.2 Conclusions

If the spectra acquisition was time independent, resulting calibrations would be applicable for all the velocities. Thus, for each vial diameter the number of scans was set according to the computed PCAs. Later on, all the dynamic spectra of a certain vial diameter were always taken with the same number of scans and the same spectral range from 1,500 to 2,150 nm.

Diameter	16.25 mm	22.0 mm	26.5 mm	42.5 mm
Max rotary speed [vials per minute]	300	150	150	75
Max. number of scans per average	5	6	8	16

Table C-18: Summary of the number of scans applied in the future with regard to the respective vial diameter, but without respect of the rotary speed.

C.7 Validated quantitative model Product B

Quantitative calibrations require exhaustive validation, including tests for accuracy, precision, linearity and robustness. The extend of the regulatory demands should be demonstrated at the example of Product B for a dynamic analysis at a default velocity of 270 samples per minute.

The qualitative model for Product B enabled the inspection of entire lots from routine production and development. Afterwards, the rejected vials became available for further modeling work. As original vials were considered as being more representative than artificially manipulated ones, it was tried to avoid as far as possible the use of prepared samples. For the method development samples out of five batches of the routine production and 6 batches of the scale up department were included to enhance variability. In order to complete a homogeneous distribution only 39 moisturized samples were added in the range of 1.1 to 2.5 % water content.

C.7.1 Preconditions

A NIRS quantification should always include a qualification of the suitability of the sample to be quantified with the proposed method. This qualification method should reject samples that are either out of range or out of the specifications of the calibration.

Thus, prior to any quantification sample identification should be performed, i.e. a PCA could be computed on the basis of the entire calibration set. The range of similarity to the identification set could be adjusted with the Mahalanobis distance and should be validated according with regard to specificity.

To introduce new methods deployed prospectively as alternative to established procedures, specific statistical testing is required in the validated environment. Although the model development of PLS features internal validation tools, it was followed by further generally accepted statistical test methods. The detailed test tables are given in the appendix.

C.7.2 Method development

All the samples in this section were measured under the same conditions. A reduced spectral range from 1,500 to 2,100 nm was scanned 5 times and averaged for one spectrum. After intermediate rotation all the samples measured either three times or for repeatability tests 10 times by NIR. The standard velocity on the simulator was set to 270 samples per minute, with respect to the validated product conditions in the routine production. For the robustness testing only, the speed of the starwheel was changed.

C.7.2.1 Calibration

The calibration range should be wider than the specified range (max. 3.0 %) and not too small in view of the accuracy of the laboratory reference method. Accordingly, a calibration range from 0.3 - 5.2 % water content was covered by the calibration set. The 506 samples were selected in such a way, that the major population was concentrated in the range of highest precision requirements. This concerned especially the values below 4 % water content, because the exact quantification of higher OOS samples was considered being of minor importance.

➤ PLS: model performance by full cross validation

The spectra were derived with a 1st order Savitzky-Golay and nine averaged data points. Then, a PLS was calculated on the centered data. For each iterative step of the SSCV, all the three measurements of one sample were taken out.

The reduction of the spectral range to 1,700 to 2,082 nm improved the model performance. One PC was sufficient for the calibration benchmarks plotted in Table C-19.

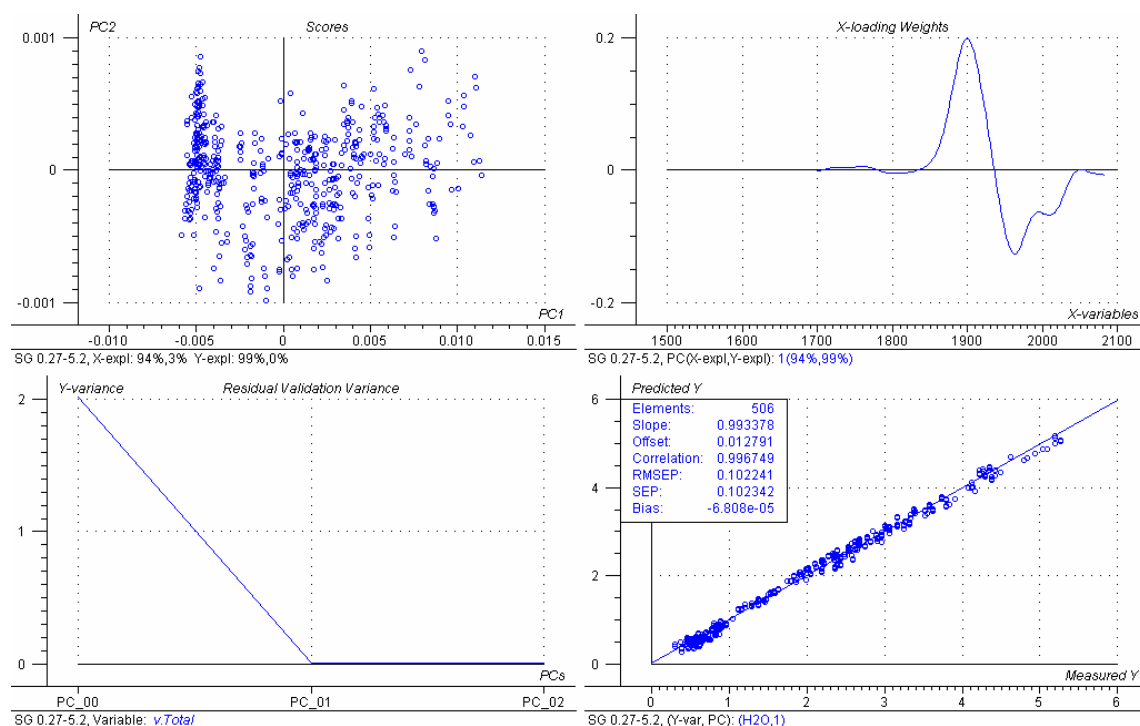


Figure C-36: Overview of the full cross validated calibration set for the quantitative model Product B.

Calibration set for Product B	
Spectral range	1,700 - 2,082
Elements	506
Moisture range	0.3 - 5.2
No. of PCs	1
Slope	0.9933
Offset	0.0128
Correlation	0.9967
SECV	0.1023
Bias	-6.81E-5

Table C-19: Summary of the calibration of Product B.

➤ Accuracy by method comparison

This validation criterion defines that the mean values of the measurements obtained with both the method under validation and an already validated reference method using the same samples must be equivalent. Equivalence is proven with a statistical probability of 95 % one sided confidence band Student's t-test. The difference between the two means should be within the acceptance limits. As explained in a previous

chapter the acceptance limit of the relative method difference between KF and NIRA for Product B was set to $\pm 15.0\%$.

The predicted and the KF titrated water values were compared by a paired Student's t-test. The accuracy by method comparison led to the results presented in Table C-20.

The result of the one sided paired t-test was inferior to the corresponding limit for a 95 % confidence interval. The relative method difference corresponded to the acceptance limit, as the difference of the means was below $\pm 15.0\%$. Therefore it could be estimated with a 95 % probability that the NIRA-prediction was equivalent to the KF titration.

	KF results	NIR prediction
Means [%]	1.942	1.942
Sample SD	1.266	1.270
Sample SD _{rel} [%]	65.19	65.41
Pooled SD	1.268	
One sided paired t-test	0.493	
t-Test acceptance limit for 95 % confidence interval	0.675	
Difference of means	-7.510E-05	
Acceptance limit for the difference ($\pm 15.0\%$ of NIR prediction)	-0.291 to 0.291	

Table C-20: Statistical summary of the accuracy by method comparison assay.

C.7.2.2 Validation

➤ External linearity test

The linearity test compares the results of two methods by plotting them against each other in a scatter plot. If the plot forms a straight line relationship, then it can be assumed that y depends linearly on x. The linearity is assessed by the method of linear regression. The closer the points to the straight line, the higher the linearity expressed in terms of the coefficient of correlation. The PLS is by definition a linear calibration method and comprises automatically a corresponding test by computing the correlation, slope and offset, as given above. Thus, a verification of the linearity during

the validation was not considered as being beneficial. Alternatively, this pattern was verified in the validation set as an additional feature.

The concentration range for evaluation of linearity should cover the prospectively expected concentration level. Accordingly, for this validation step of the model an independent set was composed embracing 300 elements in the range of 0.5 - 3.8 % water content. The spectra of these samples were mathematically pretreated in the same way as the calibration set.

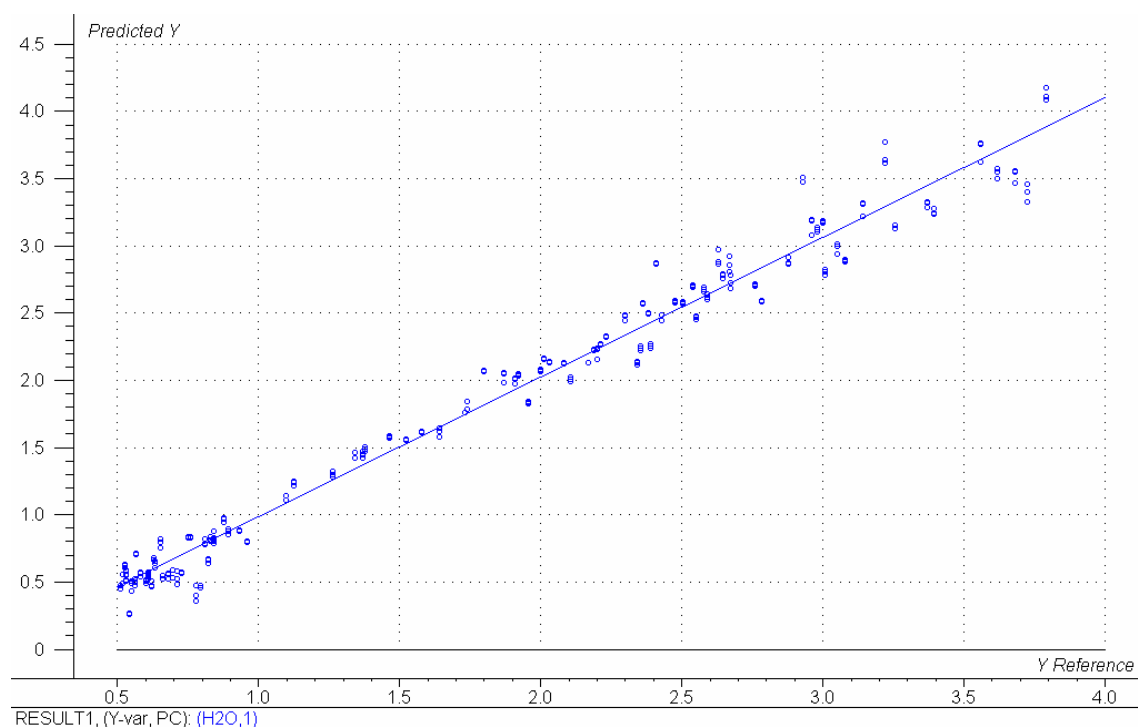


Figure C-37: KF measured versus NIR predicted water values of the external validation set.

The prediction of the unknown samples resulted in the readings given in Table C-21. The trend-line Figure C-37 had a slope slightly above one, indicating rather an over- than an underestimation of the real water content. Consequently, false bad decisions were more likely than false good predictions.

Validation set for Product B	
Elements	300
Moisture range	0.5 - 3.8
Slope	1.039
Offset	- 0.051
Correlation	0.989
SEP	0.155
Bias	0.017

Table C-21: Summary of the prediction results of the external validation set of Product B.

The SEP of 0.155 would require a rounded readjustment of the acceptance limit (AL) to 2.5 % according to the following formula:

$$AL = 3 \% - 3 \cdot SEP = 2.5 \%$$

Equation C-9: Computation of the acceptance limit (AL) with a statistical 99 % confidence interval.

In this case, the accept or reject decision of this quantitative prediction method would have a 99 % confidence interval.

➤ Precision by repeatability

The precision of a method is a degree of reproducibility and is expressed by the SD of a number of repeated measurements. The test parameters should correspond to the actual analysis conditions.

The first test was to prove the repeatability on one sample measured 10 times. For this assay three vials with different moisture contents were selected. One in the area of the most often occurrence (~ 0.7 %), another one close to the mean of calibration (~ 2 %), and the third one at the acceptance limit (~3 %). For the second assay, the repeatability on several samples, three measuring repetitions on 10 different samples were performed. To cover again a broad distribution, 10 vials from 0.6 to 3.5 % were selected. For both tests the relative sample SD should not exceed 2.0 %.

Sample	Mean predicted x_i [%]	SD $x_i - \bar{x}$	Mean SD_{rel} [%]
1	0.655	1.25E-02	1.91 %
2	2.075	1.10E-02	0.53 %
3	3.026	3.77E-02	1.25 %

Table C-22: Repeatability results of 10 measurements each performed on one sample of regular, intermediate, or high moisture content.

Samples	Mean predicted x_i [%]	SD $x_i - \bar{x}$	Mean SD_{rel} within sample [%]
1 - 10	2.374 %	1.47E-02	0.76 %

Table C-23: Precision by repeatability assay of 3 measurements of 10 different samples spread over the calibration range.

In all the cases the average SD_{rel} was below 2.0 % and thereby corresponded to the acceptance limit. As it should be expected, the relative variation was the greatest for low water values, although the absolute SD was even lower.

C.7.3 Robustness testing

It is required to minimize the system's sensitivity to changes in certain critical factors. The objective of robustness testing is to design a model, so that its performance remains satisfactory even when some influential factors are allowed to vary. A robustness test is usually carried out before the release of an almost finished analytical system, as an ultimate test to ensure quality.

Different critical factors of variability were considered, such as batch to batch product variation, temperature and measuring velocity changes and deviations in the spectrometer performance. During the period of calibration, once weekly a performance test was run to ensure the integrity of the spectrometer. This test included a wavelength accuracy and repeatability test, a spectral noise test and the verification of the internal sensors, controlling beyond others the enclosure temperature and the lamp intensity. Only if the specified criteria were met, further data acquisition was performed. The batch to batch variation was already covered by the procedure of sample selection for either, the calibration and the validation set. The NIR measurements were carried out about a time period of 6 months, so that environmental

e.g. seasonal changes should be calibrated into the model. A potential drift of the spectrometer or the influence of an aging lamp was included equally.

C.7.3.1 Temperature influence

NIR is a warmth radiation. By definition the radiation is warming up the analyte but the temperature of the sample and the environment can reasonably have an influence on the acquired spectrum as well.¹

For the lyophilizates in question two scenarios were possible. If the product was unloaded immediately after the end of secondary drying, the samples would have the process end temperature. But depending on the daytime of the endpoint of the lyophilization cycle the dryers were unloaded a couple of hours up to two days later. For this case, each product had a defined storage temperature, varying from 5 to 23 °C.

	Product A	Product B	Product C	Product D
Shelf temperature secondary drying [°C]	30	30	25	42
Shelf temperature storage [°C]	15	5	5	23

Table C-24: Dryer-shelf temperatures according to the products.

Following to the discharge of the trays of products, they were either first put onto metal trolleys or directly transferred to a turning table. This table fed the vials to the crimping machine and after being capped the containers followed the conveyer belt for any further quality control. Here, in future the NIR inspection should be introduced. Depending on the preconditions the samples theoretically could arrive with different temperatures. Actual temperature measurements on the respective conveyor belt demonstrated that during the handling time the samples were already adapted to the ambient temperature. Through winter and summer the rooms were air conditioned to 20 to 25 °C, so that no serious deviation should ever appear. Nevertheless, it was tried to quantify the impact of temperature variations on the precision of the NIR analysis.

➤ Procedure

Ten vials were stored for at least three days in a usual refrigerator at about 2 - 8 °C to assure they were completely chilled. The samples were taken off and immediately

charged on the simulator's starwheel. The samples were measured continuously until they took ambient temperature, what took a period of about 15 minutes. The sample temperature was determined by a contactless infrared thermometer (Lutron TM-919). The accurate temperature determination appeared to be difficult, as the re-warming time of the vials was short and the starwheel was always in rotation.

Time [min]	Measurement	Temperature [°C]
0	1	2
5	17	6
10	34	20
15	50	24

Table C-25: Approximate re-warming time and the corresponding number of measurements.

➤ Results

During the 15 minutes the 10 samples were measured 50 times. The variation of the corresponding prediction values showed slightly higher results compared to those obtained in usual repeatability tests with a constant rotation velocity (average SD 1.99E-02). The low correlation coefficient of the regression lines in Figure C-38 indicated the negligible relevance of the apparent slope seemingly due to the temperature.

To identify a potential drift in the data depending on the temperature increase, an ANOVA test with 5 % uncertainty was first performed on all 50 measurements. Here only the results of a reduced data set (every 5th measurement) were plotted. None of them indicated any relevant difference between the successive measurements of one sample as the value F was inferior to F_{critical} (Table C-26).

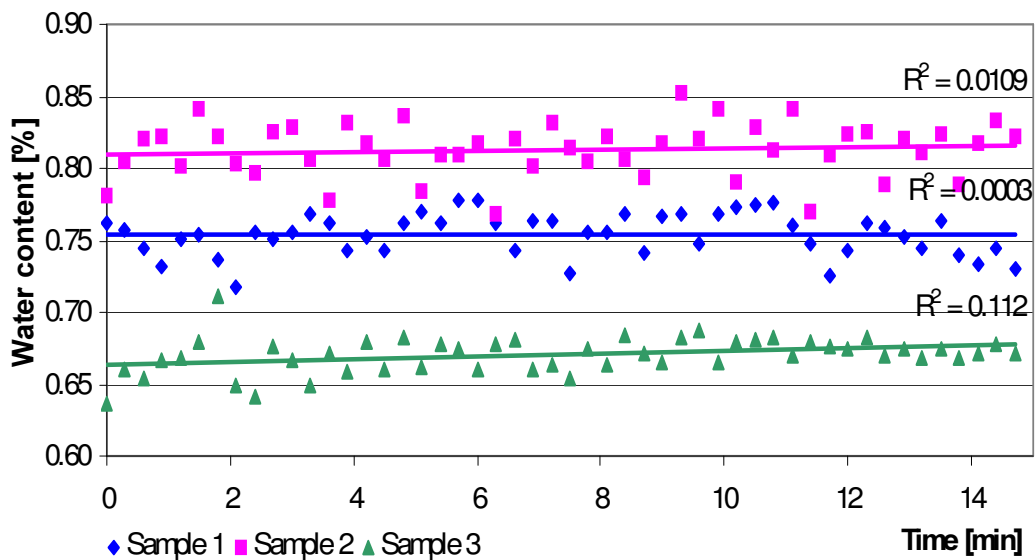


Figure C-38: The water content of three representative samples was plotted against the 50 measurements taken within 15 minutes. The lines may suggest a slight upward trend, but the low correlation indicated a very poor significance.

SUMMARY

Groups	Count	Sum	Average	Variance
Measurement 1	10	7.603	0.7603	0.003032
Measurement 6	10	7.638	0.7638	0.002570
Measurement 11	10	7.679	0.7679	0.002546
Measurement 16	10	7.562	0.7562	0.002292
Measurement 21	10	7.652	0.7652	0.002507
Measurement 26	10	7.648	0.7648	0.002885
Measurement 31	10	7.657	0.7657	0.003187
Measurement 36	10	7.744	0.7744	0.002887
Measurement 41	10	7.621	0.7621	0.002413
Measurement 46	10	7.767	0.7767	0.002214

ANOVA results

Source of Variation	SS	df	MS	F	P-value	F _{critical}
Between Measurements	0.003386	9	0.000376	0.141788	0.998296	1.985594

Table C-26: The ANOVA analysis results with a single variation factor performed for 10 of the 50 measurements of 10 samples. With SS = sum of squares, df = degrees of freedom, MS = mean sum of squares, F = test statistic, P-value = correlation coefficient, and F_{critical} = acceptance limit of the test statistic.

➤ Discussion

At least 15 minutes elapsed for the handling of the samples from the product discharge in the sterile room to the conveyor belt outside. Furthermore, the samples would be in contact with warm plant parts and subject to some mechanical stress when they were standing on the rotating table and were crimped afterwards. Thus, the re-warming time was in real life much shorter than in the experiment.

However, it could be shown by the experiment with an error probability of 5 % that there was no relation between the sample temperature within 2 and 24 °C and the NIR predictions on the simulator. Temperature variations were even lower in reality and thus a consideration of this impact factor was negligible for this application.

C.7.3.2 Measuring velocity

Within one product the production stream speed could vary depending on the following inspections or due to any other technical deviation. Then, the in-line NIR inspection should not be influenced by this parameter, but within a certain range still give the same results.

➤ Procedure

In case of a manual visual inspection the line velocity would only be 100 samples per minute. The validated speed for the automated inspection instead, was 270 per minute. Nevertheless this method should still have some potential for further acceleration. For these reasons 4 different velocities, 100, 200, 270 and 300 vials per minute were investigated. To give representative results, the same 10 vials as in the repeatability study on several samples with water contents distributed over the calibration range were utilized. Accessorily, the containers were rotated between the measurements.

➤ Results

The different velocities could be regarded as a reproducibility study. Reproducibility is defined as a repeatability test, whereas one or several analysis parameters are varied. Thus, the same method as in the validation section of the repeatability on several samples was applied. The acceptance limit was equally a maximal mean relative standard deviation of 2.0 %. If the deviation between the predictions was the same as

in the upper section, the influence of changing the turning speed would be equivalent to the repeated measurement on a rotated sample at a constant speed.

Sample	Mean predicted x_i [%]	SD $x_i - \bar{x}_i$	SD _{rel} within sample [%]
1- 10	2.205	2.79E-02	1.47

Table C-27: All the 10 samples were measured at each of the 4 velocities from 100 to 300 samples per minute and then predicted. The plotted SD is the average of the within sample SDs.

➤ Discussion

Although the same samples as in the precision by repeatability section (Table C-23) were considered the predicted mean content as well as the SD and SD_{rel} were higher in the velocity trial. The highest SD appeared within the measurements on samples with predicted water contents below 1 %.

The mean of the SD_{rel} was 1.47 % and thereby still fulfilled the acceptance limit of 2.0 %. Nevertheless they were not equivalent to the readings of the previous repeatability test with a constant speed. Mostly, it was the measurement with the highest velocity (300 / min) that resulted in the highest SD. If only these values were left out, the SD would reduce to 1.68E-02 and the SD_{rel} to 1.08 %, sufficient to comply with a t-test. Under these limited conditions with a 95 % confidence interval no significant deviations could be identified between a usual repeatability and the velocity trial.

Sample	Mean predicted x_i [%]	SD $x_i - \bar{x}_i$	SD _{rel} within sample [%]
1 - 10	2.364	1.68E-02	1.08

Table C-28: Table equivalent to Table C-27 without the highest measurement velocity of 300 samples per minute.

	Repeatability	Robustness
Means [%]	2.374	2.364
Sample SD	1.47E-02	1.68E-2
Sample SD _{rel} [%]	0.76	1.08
Pooled SD	1.58E-02	
One sided paired t-test	1.74E-02	
t-Test acceptance limit for 95 % confidence interval	0.683	
Difference of means	-1.0E-02	
Acceptance limit for the difference (± 15.0 % of NIR prediction)	-4.728E-02 to 4.728E-02	

Table C-29: The results of the repeatability test at a constant rotational speed with 270 / min were assessed with those of the velocity trial. The corresponding SDs were compared by a Student's t-test with 95 % confidence interval, and the means with an acceptance limit for the difference of maximal 2.0 %. Both results matched to the requirements.

C.7.4 Conclusions

By use of virtually only original samples collected during several months it was possible to compute a quantitative NIR model requiring only one PC showing good performance in the PLS validation tools. Furthermore, generally recognized statistic methods were applied to verify the integrity of the calibration. First of all, the accuracy was shown by the comparison of KF titration and NIRA. The system was then challenged by an external validation set demonstrating both linearity and precision by repeatability.

For robustness testing temperature variations and changes in measuring velocity were considered. It could be demonstrated that under regular controlled process conditions there was no impact on the accuracy of the NIR determination expected. The within sample deviation of measuring speeds between 100 and 270 samples per minute was comparable to a usual repeatability assay at constant circumstances. But the excess of this range could not be included to the validation.

It turned out that low moisture contents led to high relative deviations, potentially corrupting this validation step. This effect could be circumvented if the validation was reduced to a scale of water contents e.g. above 0.7 %. As the accurate determination of

the values below 1 % were not of essential importance in this application, this would not reduce the usefulness of the method.

All together, the quantitative model Product B was fast and robust, but required enormous efforts in both calibration and validation work over a long time scale. This investment did not seem to be justified in every application area, but only if imperatively an exact quantitative value was required.

References C.7 Validated quantitative model Product B

- ¹ Young C.A., Knutson K., Miller J.D. Significance of Temperature Control in FT-NIR Spectrometers, *Applied spectroscopy*, 47, No. 1, 1993

C.8 Quantitative model Product C 150 mg

C.8.1 Scope

The performance of the process simulator and the in-line software should be evaluated in real life conditions with a total at-line inspection of a regular batch in production environment. Furthermore a better insight in the water distribution over an entire lot of another product could be gained.

C.8.2 Control and calibration

Original and artificially modified samples of Product C 150 mg were prepared. To compensate for surface phenomena, all of them were measured 3 times by NIR. The range of 1,500 - 2,100 nm was scanned 8 times on each moving vial with an increment of 2 nm. Between the measurements the samples were rotated, so that 480 spectra were obtained. These spectra were divided into two groups; for calibration a set with initially 87 equally distributed samples with water contents ranging from 0.3 to 4.7 %, and for validation, a set comprised 73 samples with water contents between 0.8 to 4.0 % according to KF titration. During the evaluation phase eight outliers appearing in the calibration set were excluded, so that 253 spectra remained. The results of the reference analysis are given in the appendix.

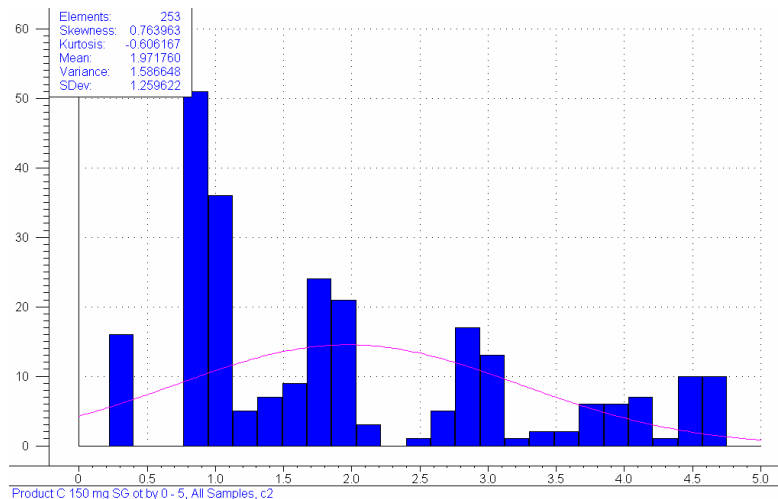


Figure C-39: Histogram of the calibration set.

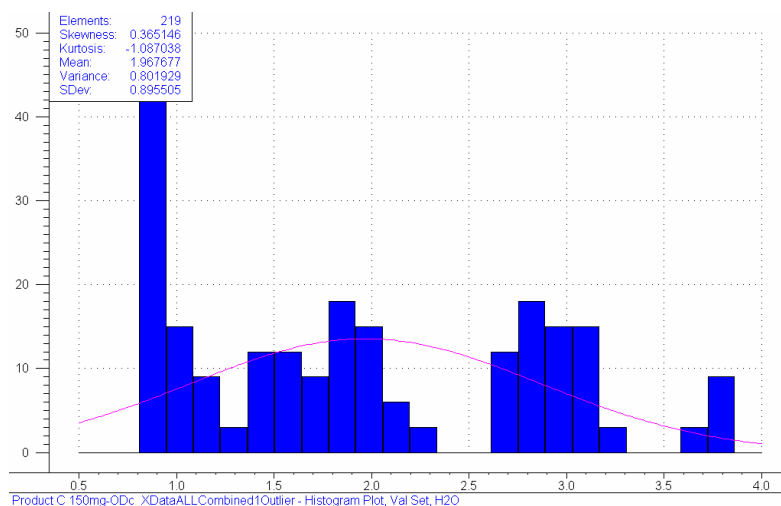


Figure C-40: Histogram of the validation set.

As quantification should always include a qualification of the suitability of the sample to be quantified, prior to any water determination by a PLS model a sample identification by a PCA had to be performed. Both of them would require a mathematical pretreatment of the spectral data. To obtain robust sample recognition patterns a sample independent pretreatment was preferred.

For the quantitative PLS model a SSCV was selected, taking out always all of the three spectra corresponding to one sample out. A 1st order Savitzky-Golay derivative with a smoothing over 9 data points gave the best benchmarks. Afterwards, this most promising model was challenged by the independent validation set. The SEP and the included bias were calculated.

The PCA was computed similar to the PLS with the same data pretreatment but relying on the entire spectra data base. The PCA was loaded to an on-line software and the Mahalanobis distance for the identification was adjusted to 0.15.

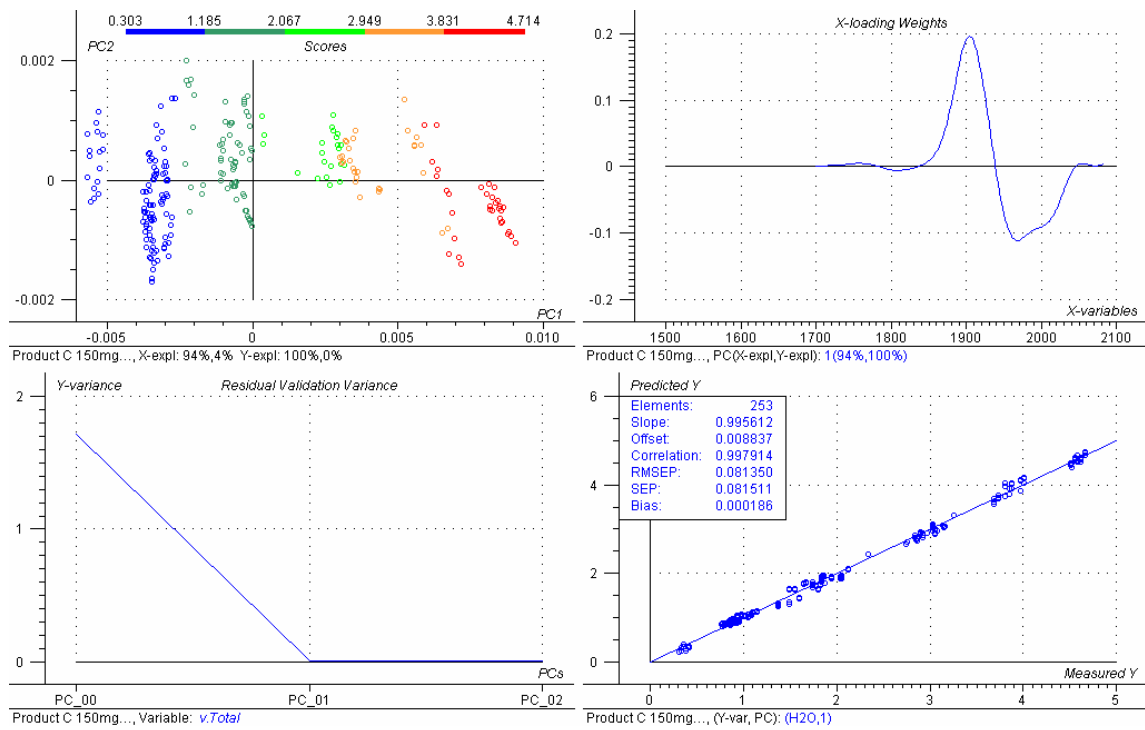


Figure C-41: Model overview for Product C quantification.

Calibration set for Product C	
Spectral range	1,700 - 2,082
Elements	253
Moisture range	0.3 - 4.7
No. of PCs	1
Slope	0.9956
Offset	0.0088
Correlation	0.9979
SECV	0.0815
Bias	1.86e-4
External validation set	
SEP	0.1606
Bias	0.0061

Table C-30: Summary of the experimental model of Product C 150 mg.

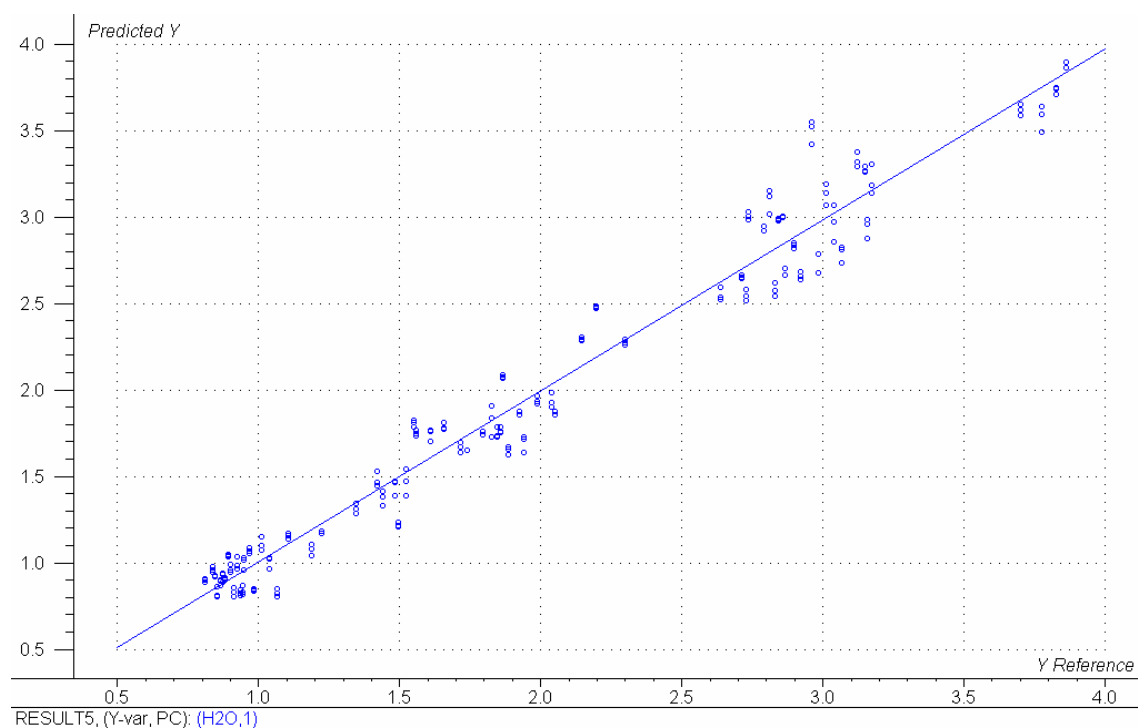


Figure C-42: Predicted versus measured plot of the independent validation set.

C.8.3 At-line inspection

C.8.3.1 Procedure

Usually, the acceptance limit is calculated according to the SEP of the used calibration (see C.5 Validated qualification of Product B vials). Reducing the official release limit of 3 % by 3 times the SEP would correspond to a 99 % confidence interval. Thus, the acceptance limit was reduced to 2.5 %. Frequent titrations of original Product C 150 mg samples demonstrated typical water content below 1 %. Actually, only few unusual vials were expected at higher values, being of particular interest to learn more about the product.

The target of a future in-line control was primarily the detection of samples with moisture contents higher than 3 % that could not be recognized visually. Externally dirty or broken vials, as well as meltbacks did not belong to this target. Nevertheless, glass breakage was detected because of an increased water content of the hygroscopic lyophilized cake. Usually, meltbacks were rejected as well, since this phenomenon is proportional to the moisture content in the transition of the primary to the secondary drying step.

C.8.3.2 Results of the at-line inspection

During the at-line inspection altogether 13,324 samples were measured by NIR. 98.90 % (equivalent to 13,246 samples) of the analyzed vials were detected as Product C 150 mg within the acceptance limits, which was a proof for a robust lyophilization cycle.

97.91 % of the 13,246 predicted water contents were values between 0.6 and 0.9 %, and the overall average was 0.8 %. The thereby included 69 rejects were visually grouped into meltbacks and glass breakage, the rest was checked by the professional visual inspectors for any distinctive feature. As there was nothing objected, it was assumed they normally would not be noticed. To confirm the NIR results they were finally KF titrated.

78 of the inspected samples were not detected as belonging to the qualitative group of Product C 150 mg, but were assigned to the outliers. This was mainly due to meltbacks and glass breakage. One more vial was completely pyrolyzed and almost empty. Three of the outliers were exceptionally crystallized on the bottom of the product cake.

	Number	Amount in [%]
Inspected vials in total	13,324	100.00
Recognized as Product C in total	13,246	99.41
Water content < 2.5 %	13,177	98.90
Water content > 2.5 % rejected:	69	0.52
• Good visual appearance	10	0.08
• Meltback	45	0.34
• Breakage of glass	13	0.10
Average predicted water content		0.80 %

Table C-31: Summary of all the vials being detected as Product C 150 mg.

	Number	Amount in [%]
Outliers in total:	78	0.59
• Meltback	68	0.51
• Breakage of glass	6	0.05
• Crystallized bottom	3	0.02
Pyrolyzed	1	0.01

Table C-32: Summary of all the outliers being detected during the inspection.

	NIRA predicted [%]	KF titrated [%]	Deviation
Rejected > 2.5 % good visual appearance			
Reject 2-2.7	2.8	2.5	0.3
Reject 12-4.0	4.0	4.0	0.0
Reject 15-2.6	2.6	2.5	0.1
Reject 19-2.7	2.7	2.4	0.3
Reject 30-3.1	3.1	2.8	0.3
Reject 31-2.5	2.6	2.5	0.1
Reject 47-3.5	3.5	3.4	0.1
Reject 60-2.9	3.0	2.7	0.3
Reject 62-3.4	3.4	3.5	- 0.1
Reject 82-4.0	4.0	3.2	0.8
Outliers with crystallized bottom			
Outlier 2-1	--	0.84	
Outlier 10-1	--	1.14	
Outlier 63-1	--	0.91	

Table C-33: Results of the KF titration of the rejected and crystallized vials.

The samples being predicted with higher water content than 2.5 % and the outliers with a crystallized bottom were KF titrated to verify the NIRA result.

According to the KF titration the water content of the rejected samples was exceptionally high. Almost invariably, the reference method yielded lower results than the NIRA, in one case even below the acceptance limit. Considering the accuracy of the KF method, this value was within the tolerances and did not constitute any issue for the alternative spectroscopic method itself, but illustrated rather an additive security level.

C.8.4 Discussion

This total inspection confirmed the robustness of the lyophilization cycle of this product. On the other hand the existence of only few OOS samples that would not be discovered showed the usefulness of a total inspection by innovative techniques. The product quality and security level could be increased by NIRA.

Due to a certain fuzziness of the identification of the product the production staff would need to reckon on an increased number of unrectifiable rejects.

A quantitative model was not required for a routine application, as there was no real even distribution over an extended range, but one median with only few outliers.

Chapter D: Business case

D.1 Investment accounting in pharmaceutical production

Different developments have led in these last years to an increasing pressure on the pharmaceutical industry. Drivers of a market which has become more and more competitive are factors such as an insufficient productivity of R&D, products going off patent and an upcoming generics industry, faster innovation cycles or state-aided price prescriptions. New products are usually expensive biotech developments in innovative dosage forms with increased handling complexity.

For years patients, top management or capital markets focused their interest on the research and development, as well as on the marketing and sales units. An increasingly strict inspection practice by the drug regulatory authorities has strengthened the importance of the GMP-regulated departments for the commercial success of pharmaceutical companies. All the departments are explored by independent cost centers with the focus on commercial effectiveness. Credit applications need to be filed and expenditures have to be justified by an investment accounting.

The term investment is defined as the expenditure of means of payment that consequently will be bound over long term. Future revenue is expected to be higher than the present investment. There is expenditure with different purposes: Typically, investment is made for the foundation of a company, the replacement for worn-out and aged equipment, the expansion or rationalization (economization and modernization). Very often investment can not be assigned definitely to one of these subgroups.

D.1.1 Methods of investment appraisal

By means of the investment accounting the profitability of an investment project should be estimated. This method considers only quantitative (monetary), but no qualitative reflections (such as flexibility, quality, working conditions). Nevertheless it is useful for the preparation of decisions.

The accounting systems can be classified in static and dynamic procedures. Dynamic methods such as the net present value (NPV) and the internal rate of return (IRR) are more complex, whereas the static payback accounting is a quick and rough calculation easy to understand.

All these methods have in common that they are oriented to the future, and thus relying on partly incorrect forecasts. Consequently, the uncertainty of the accounting is not hidden in the computation steps but the preliminary assumptions. The period under review must be in either case shorter than the expected useful life of the acquirement. Money that was spend for e.g. survey, to make these estimations more reliable, are so-called 'sunk costs' and can not be included in the accounting.¹

D.1.1.1 Dynamic accounting

➤ Net present value (NPV)

The NPV identifies the total excess of the investment, the amount, which exceeds the amortization of the capital expenditure and the costing-based interests.

The NPV is defined as the sum of all the net cash-flows discounted to a reference date to an interest i , which appears supplementary due to the investment.

$$NPV = -G_0 + \frac{G_1}{(1+i)^1} + \frac{G_2}{(1+i)^2} + \frac{G_3}{(1+i)^3} + \dots + \frac{G_n}{(1+i)^n}$$

Equation D-1: Computation of the NPV, with the interest i , the net cash-flow G_0 of the year 1 and the years 1 to n .

An investment is economic, if the sum of the discounted yearly net cash-flows is positive (> 0). The earlier this happens (for small n), the more profitable is the investment including a lower risk. For the determination of the discounting rate the average capital cost-effectiveness is an orientation for the companies.

This method does not allow any statement about the profitability of a project but constitutes a base for the comparison of alternative projects.

➤ Internal rate of return (IRR)

The internal rate of return indicates the percentage of interest the invested capital is bearing. Accordingly, the IRR calculates the cost-effectiveness of an investment.

In order to calculate the IRR, the NPV is set to zero. The multiplication of this equation by $(1+i)^n$ leads to a polynomial without unique elemental solution for $n > 3$.

$$G_1(1+i)^{n-1} + G_2(1+i)^{n-2} + \dots + G_n - G_0(1+i)^n = 0$$

Equation D-2: The computation only leads to unique results if the cash-flow leads to exactly one change of a leading sign. Most likely this is the case.

In practice the management of a company usually demands a minimum interest return, and the IRR should be higher than this threshold.

D.1.1.2 Static accounting - Payback method

The payback method is a static measure without respect to timely capital flow. The payback calculates the time required until the invested capital is balanced by net receipts. Neither the expenditure nor the receipts are discounted in this case.

For expansion the payback periods usually vary between 3 - 5 years whereas rationalization should be amortized in 2 - 4 years. In general, projects with shorter payback times are preferred, as the longer the period the higher is the impact on the company's liquidity and the more risky is the investment. The payback accounting does not supply any information about the actuarial rate of return.

D.1.2 Business case in-line PAT

Prior to any investment appraisal and credit application certain preliminary structural steps have to be respected. Especially long term projects should be conform to the strategy of the business area. First, the current situation and the reason for this capital expenditure are assessed. Only qualitative benefits will convince to pursue the project. Alternatives should be reviewed and reasons for rejection are requested. Then the financial analysis follows considering the resources, operating costs and profitability.

Due to a confidentiality agreement with Roche, all the financial values in this chapter are only given in a relative figure represented as money equivalents (ME) without indication of the detailed cash flows.

D.1.2.1 Estimated expenditure

The realization of an in-line NIRA involves some required equipment such as spectrometer and automation but a lot of preparatory work as well. As this amount of

work was difficult to quantify and sometimes performed alongside to routine this part was not considered here. In the cost estimate all the hardware was accounted including the pilot phase and the implementation. The items are roughly given in Table D-1 what led to a total expense of about 125,000 ME.

Buildings incl. external works	adaptations of: infrastructure (electricity, vacuum, air pressure) existing line parts
Machines and apparatus	spectrometers and automation including: documentation qualification
Plant installations incl. engineering fees	transport connection to resources and stream startup qualification documentation
Software and equipment	control of: spectrometer automation reference standards for calibration
Reserve	unforeseen items
Total	~ 125,000 ME

Table D-1: Composition of the estimated capital expenditure costs for the in-line project. The sum of expenditure is given in money equivalents (ME).

D.1.2.2 Benefit accounting

The quality costs that incur in the manufacture of pharmaceuticals can be structured in three sub-groups: the required cost of testing, and external and internal costs of defects. A benefit accounting would obviously try to find the domains in which savings would be achieved by a certain investment (Figure D-2).

As in short term the in-line PAT initiative would not replace the traditional registered release analysis performed by the QC, the cost of testing could not directly be considered. External costs of defects may be extremely high especially if e.g. product recalls were involved. The related loss of image would be even worse but hard to quantify in cash. As these incidents never took place due to the residual moisture in the lyophilizates in question, these potential costs were left out and were only summarized as qualitative arguments. But the internal costs of quality were more transparent and cost factors such as IRs and DRs, extended quarantine, restricted batch release or product destruction were realistic scenarios concerning these products. The main cost driver in this group was the

abolishment of product, and this more and more as the products became more valuable. Accordingly, this chapter focused on the probability of such a case and the potential consequences thereby incurred. The benefit accounting refers to the results of the two total inspections of the current work performed off-line. A rather conservative moderate appraisal of the scenario was adopted.

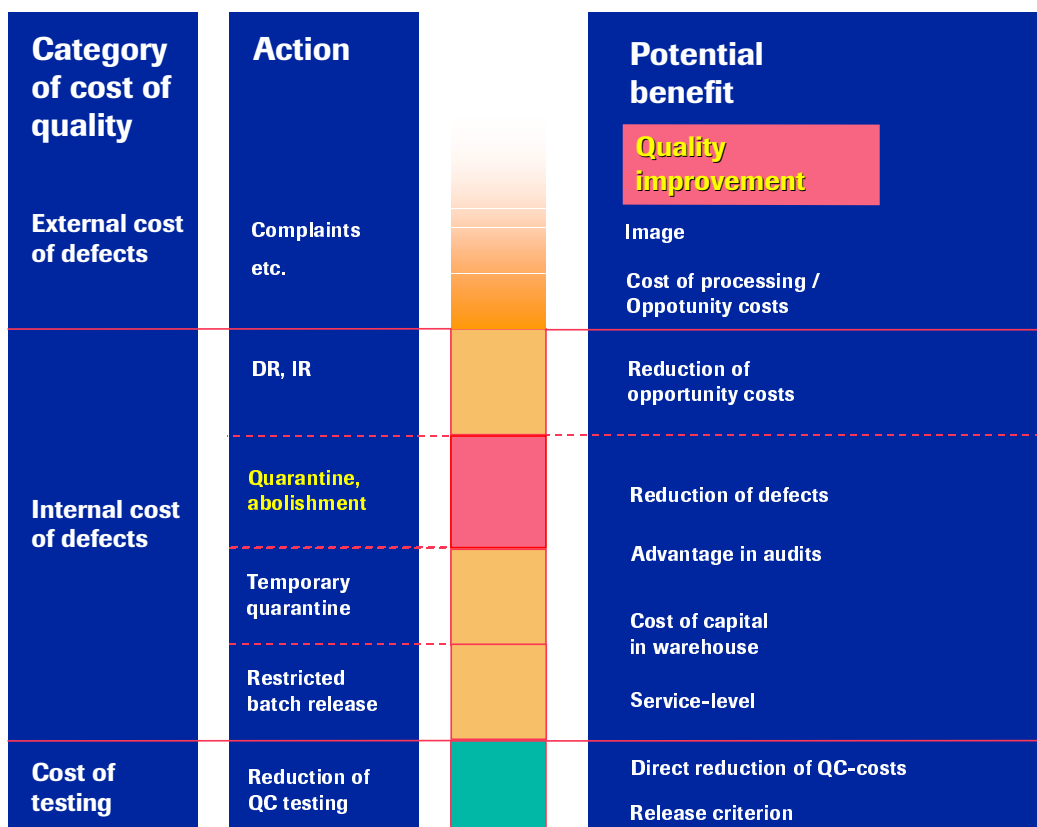


Figure D-1: Illustration of the different categories of cost of quality.

Product	Units per dryer	Price per unit [ME]	Price per dryer [ME]
Product A 20 mg	37,000	0.10	3,700
Product A 40 mg	37,000	0.11	4,070
Product B	37,000	1.00	37,000
Product C 150 mg	14,000	5.08	71,120
Product C 400 mg	NN	NN	NN
Product D	14,000	0,30	4,200

Table D-2: Manufacturing prices of the lyophilized Products A – D in money equivalents (ME).

➤ Product B

During the inspection of one batch of Product B in the total of 26,000 vials 150 OOS samples with higher water contents than 3 % were detected. These results were confirmed by successive KF titration. The OOS samples could be rejected and the rest of the batch released as it was within the specifications. This was equivalent to a saving of ca. 26,000 ME, since the actual market demand could not be supplied yet.

It could be assumed that in any produced batch of Product B 0.6 % of the vials contained more than 3 % residual moisture. In the routine release analysis the QC sampled 3 vials in 'worst case' positions of the freeze-dryer. According to the hypogeometrical distribution the probability was here 1.7 %, that one of these 3 QC samples would be by coincidence an OOS vial (for $x = 1$, $n = 3$, $M = 213 = 0.6 \%$ of $N = 37,000$). The consequence in this case would be the destruction of the entire batch in question. This corresponded to the so-called 'write off risk'. In purpose of increasing the product quality or due to the in-line inspection regularly roughly 200 additional vials per batch would be rejected. To readjust the accounting this increased loss of product had to be subtracted from the potential savings (rejects due to total inspection).

Year	2003	2004	2005	2006	2007
Product B batch forecast	~ 172	~ 307	~ 350	~ 281	~ 350
Potentially affected batches	3	> 5	6	5	6
Write off risk [ME]	> 111,000	> 185,000	222,000	> 185,000	222,000
Rejects due to total inspection [ME]	~ 34,000	~ 61,000	~ 70,000	~ 56,000	70,000
Readjusted potential savings by NIRA [ME]	77,000	124,000	152,000	129,000	152,000

Table D-3: Readjusted benefit accounting based on the volume forecast March, 2003. All the monetary values are given in money equivalents (ME).

➤ Product C 150 mg

By use of a quantitative model an entire lot of Product C 150 mg was inspected. This analysis comprised roughly 13,000 vials prior to the visual control. Here 4 OOS vials with water contents superior to 3 % were detected. As the visual control could not find any deviation, it was assumed they would normally not be noticed.

The probability to hit on one of these four is close to zero (hypergeometric distribution = 0.01 %, for $x = 1$, $n = 3$, $M = 4 = 0.03 \%$ of $N = 13,000$). With respect to the production forecast this would appear once in 150 years, what was negligible. However, if this incident ever happened, a loss of more than 71,000 ME would appear. Though, the increase of product quality and homogeneity seemed to come to the fore, since water contents up to 4 % were observed. At least in case of stability tests of such a vial deviations were supposable. Furthermore, the visual control could be relieved by a total NIRA inspection, as meltbacks and glass breakage were detected as defects as well.

D.1.2.3 Investment accounting

According to the findings of the total inspection of one lot of Product B a future prognosis based on facts was made, and a potential of considerable savings was determined. Only the cost of defects of Product B was included to the calculation of the NPV, IRR, and payback period. The standard period under consideration was 10 years which was conform to the expected useful life time of the plant. With a discount rate of 12 % and a tax rate of 30 %, the Roche management expectation of the IRR was $> 10 \%$.

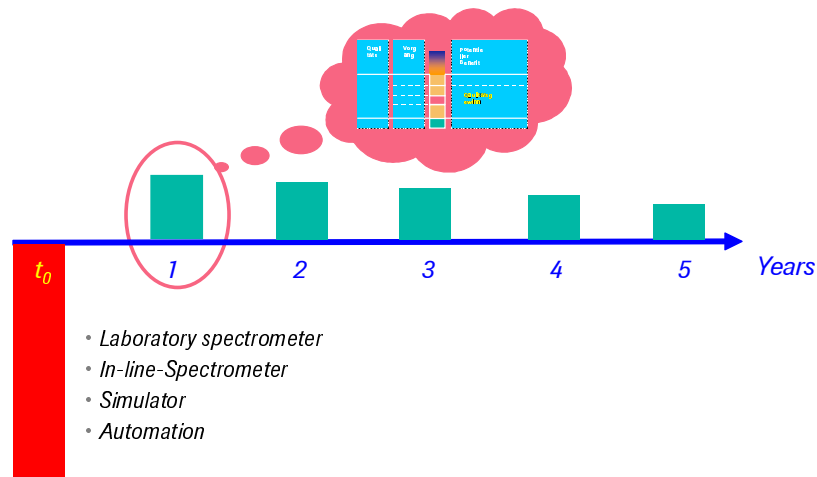


Figure D-2: Illustration of the discounted investment at t_0 about a limited payback period.

Net present value (NPV)	Internal rate of return (IRR)	Payback period
~ 375,000 ME	75 %	<1.5 years

Table D-4: Results of the business accounting regarding NPV, IRR, and the payback period.

The result of the NPV was positive, the IRR 75 % and thereby $> 10 \%$. The sum of the gross profit after tax was after less than 1.5 years equal to the capital of investment. This time corresponded to the payback period, which should be below 3 years. Investments are

in general exceptionally profitable and bear less risk if high cash-flows appear in the early periods of a project. The short payback time assured the results of the NPV and IRR.

All the requirements in terms of NPV, IRR, and payback period were met by the in-line PAT project. Monetarily it could be assumed that this investment would be profitable.

D.1.3 Conclusions

In practice it could be shown that the NIR method was useful. In the application for Product B savings of about 26,000 ME could be generated. A loss of product was practically equal with a loss of sales, since the actual production volume could not supply the demands of the market. An increase of the service level was thus essential. Product C featured some few OOS vials in moisture content as well. Nevertheless the calculated likelihood was low that ever a batch should be rejected, the risk was due to the high value of the product disproportionately high.

The entire investment accounting based exclusively on the most important product at that time and could thus be considered as moderate: Product A and Product D were even not regarded. The commercial benchmarks were calculated by a moderate appraisal adjusting the potential savings by the increased number of rejects. Although this qualitative improvement was calculated as a financial loss of product already 1 ½ years would be sufficient for the payback period.

Qualitative arguments were not regarded yet. In this context the increase of product quality and homogeneity due to the NIRA inspection should be mentioned. Simultaneously the theoretical financial risk of a product recall and a damaged image of the company could be reduced. Furthermore the visual inspection performed by man power could be eased by the application of the NIR method. Besides, the inspection machine could be used as a tool for process optimization of the lyophilization cycles. The potential benefit could be an increased capacity of the production line if the cycle time was reduced. In a future step the in-line data could also be taken over for the release analytic and reduce the service costs and work load of the QC-department.

In conclusion of quantitative and qualitative reasons the in-line PAT project was considered as being profitable and was pursued further.

References D.1 Investment accounting in pharmaceutical production

- ¹ Seiler A., Financial Management, BWL in der Praxis II, Orell Füssli, Zürich, 1999

Chapter E: Overall conclusions

E.1 Discussion and conclusions

E.1.1 Scope

The current work presented a NIR based application of PAT in case of a lyophilization line. The critical attribute of a lyophilized product was identified as the residual moisture content. Former batch records indicated deviations in the QC analysis performed by KF titration. The consequence was periodically the severe loss of end-product, and thereby the decreased service level. Different studies in production and scale-up did not manage to resolve these phenomena, although the process was in terms of validation fully under control. A complete batch inspection was desirable providing the opportunity to reject the vials out of specification only, but assuring the compliance of the remaining lot.

Thus, a study was conducted to reveal under consideration of financial aspects if an in-line control was feasible without constraining the process stream. NIRS was identified as a non-destructive and fast method for water determination.

E.1.2 Original situation

The QC-department already disposed of experiences in the field of water analysis for Product A 20 mg in a laboratory scale. Such a model was approved and in routine use. This knowledge base in terms of sample preparation and specific patterns was extended to the other products as well and a possibility of a targeted humidification was developed. The reassessment of the reference method yielded the preference of volumetric KF titration as an absolute accuracy of $\pm 0.2\%$ according to a statistical inquiry.

The rise of the NIRA results of fresh Product A was contributed to a redistribution of the higher moisture level in the core of the product cake during the first weeks. The relief was either the introduction of a correction factor for the predicted value or a reduction of the acceptance limit according to the average age of the analyzed samples.

E.1.3 Evaluation of the appropriate analysis system

The analysis performance under time restrictions of an FT and an AOTF spectrometer was compared. A theoretical approach according to the current pharmacopoeias did not provide satisfactory results. Only a comparison relying on the real analysis problem showed evidence. The product related case study revealed a worse analysis result for the FT spectrometer. Furthermore it required a longer measuring time causing a more complex and more expensive plant design. Consequently, out of both analytical and economic reasons it was decided to continue the project with the AOTF device.

E.1.3.1 Static scan mode evaluation

In AOTF technology almost arbitrarily accessible wavelengths required a comparison of different spectrometer set-ups. The evaluation of a different number of scans with a successively decreased resolution did not show any extraordinary impact on the analysis performance of a reference product. However, the experiment showed best results with 2 nm resolution and a reduced spectral range. Finally, it was concluded for static laboratory analysis to continue measurements with 10 scans in a resolution of 2 nm over the entire wavelength range from 1,100 - 2,150 nm. The raw spectra could easily be truncated later according to individual preferences.

E.1.3.2 Statically validated qualitative model Product B

Whenever the objective is to test if a certain acceptance limit is respected or not, a classification result is largely sufficient. The feasibility of this approach was proven with a small sample set of a new protein product. The method validation was simplified as it was possible to renounce on the complex parameters such as accuracy, precision, and linearity. Instead the threshold was challenged to test the classification method.

Transferability issues, prevalent in NIRS, could be avoided by remodeling a comparable calibration on a second device without extensive efforts.

Due to the rapidity of this analysis it was applicable at-line for a manual total quality control of an entire batch performed manually. This produced serious savings providing the base for a payback accounting.

E.1.4 The process simulator

In order to limit the financial risk of investment, a prototype was designed in allusion to a final plant to simulate the real process conditions. All the formats could be fed to the NIR sensor in the original velocity and NIR measured simultaneously. Alongside, a 21 CFR Part 11 compliant in-line software was programmed according to customer specific requirements to survey the process stream. In the prospective plant integration a similar system should be realized with the additional feature of an automated supply and rejection of non-compliant samples.

E.1.4.1 Dynamic scan mode evaluation

The NIR measurements were performed on continuously moving vials. The higher the rotary speed of the starwheel, the shorter the time the samples remained above the sensor window. Nevertheless, the scan parameters should stay independent on velocity changes. Thus, for each vial format a configuration was defined by a PCA, which allowed NIR measurements without respect to the current speed. In order to increase the number of possible scans the wavelength range was reduced to 1,500 to 2,150 nm. Later on all the dynamic spectra were taken according to these settings.

E.1.4.2 Dynamically validated quantitative model Product B

The batch inspection with the statically validated qualitative model Product B rejected representative samples originating out of routine batches. Mainly these samples were deployed to compose an extended sample set for the demonstration of a GMP conform calibration and validation of a quantitative NIR model. The substantial statistical test of general recognition proved the method comparability to KF titration and system suitability for a dynamic analysis.

The robustness testing showed no significant impact on the NIR measurement within a realistic temperature interval. A reproducibility test proved velocity independence in the range of 100 - 270 samples per minute.

The shortcoming of the method was the analysis of samples with moisture contents below 0.7 %. The impact of the absolute failure of the reference method and the relative deviation of repeated measurements was exceptionally high. For future calibrations this feature should be regarded more closely.

However, this fast and robust NIR model required enormous calibration and validation efforts. Prior to any commitment a serious assessment about the usefulness should be performed. The implementation of such a model would only be beneficial if a large number of samples was analyzed afterwards.

E.1.4.3 Dynamic quantitative model Product C 150 mg

A complete Product C 150 mg batch inspection was investigated at-line in order to challenge both the simulator and the in-line software under real conditions. Few OOS samples were detected and rejected that could otherwise not be discovered by traditional optical methods. The overall quality of this batch was improved and could be confirmed as complying with the specifications.

The narrow distribution of the water content (0.6 - 0.9 %) of the majority of the vials approved the process control. The representation of the quantitative results did not provide any additive information and thus, was not considered as being useful for the routine production. The results of this complete inspection added qualitative arguments to the estimation of the potential benefit.

E.1.5 Investment accounting

The results of the two inspections of entire batches formed the basis of the business case calculation. The potential benefit was itemized in different cost categories considering the external and internal cost of quality as well as the cost of testing. For the calculation of the investment amortization, only the risk of product destruction as part of the internal costs of quality were regarded. Due to the short time scale of the investment accounting the more complex dynamic methods were not required. Nevertheless, both the discounted NPV and IRR confirmed the result of the static payback calculation.

As the payback period was below 2 years, the in-line PAT project was assumed as being highly profitable. The cost of testing, external cost of defects, and qualitative arguments provided further reasons for a prosecution of the project.

E.2 Outlook

Only the use of an in-line PAT would really give the desired information about the global quality of a complete lot and represent the proper understanding of cGMP. With NIRS, the pharmaceutical industry could move one step closer to 'zero-defect' quality control, making the costs associated with the method's development well spent. But, prior to a consistent implementation several further questions should be answered.

➤ Which kind of calibration strategy should be followed?

The main interest of the in-line NIRA is to know whether the specification limit is met or not. Thus, the highest accuracy of prediction should be achieved at this threshold value. For research investigations and freeze-drying validation purposes the exact reading of the analyte of interest may be interesting. But for the routine analysis the quantitative analysis results will always be summarized in the terms 'conform' or 'non-conform'. If this was the case, a qualitative prediction assignment would be largely sufficient. This could avoid important calibration and validation work as well as the problem of extended data handling accumulated over long term. The challenge of calibration transfers could be reduced.

➤ How to calibrate new products?

There are two options for the calibration of new products. The best analysis results are usually met if all the conditions were equal to those of the final analysis. Thus, for in-line calibrations it would be optimal to perform the calibration work on the final spectrometer integrated in the production stream. Once the plant is installed, the access will be limited for preparatory work. In this case either timesaving calibration strategies should be preferred (e.g. qualitative models) or it will be required to transfer the models from an off-line laboratory environment.

➤ How to increase the performance of the dynamic analysis,
in terms of velocity or accuracy respectively?

By nature there will always be a compromise between speed and accuracy. The measurement velocity is dependent on the amount of scans and the number of wavelengths. As a standard, the range from 1,500 to 2,150 nm was covered to increase the degree of freedom for the calibration. But the models showed better performance if

the spectra were truncated to 1,700 to 2,100 nm or a even more narrow range. A reduction of the wavelengths would decrease the required scan time. Accordingly, either more scans could be performed to increase accuracy and repeatability or the measurement could be accelerated. With electronic modifications the maximal rotary speed of the simulator could be increased to about 400 samples per minute.

➤ What does transferability signify and how could it be achieved?

In this context transferability denotes the use of an NIR model on another device or different conditions than it was designed. This procedure will be required e.g. in case of a breakdown of equipment or when the same analysis is supposed to be applied at multiple locations. The term transferability can refer to different NIR spectrometers of the same model series, the automation the spectrometer is installed on, or the work environment, i.e. laboratory and production.

For the model transfer between spectrometers different approaches are feasible. Probably the easiest is the use of correction factors in order to adapt an already computed to a further spectrometer. The second option is to generate mixed models with spectra from different apparatus or measurement conditions. At least with time the periodic model adjustment will introduce more and more inaccuracy to these models. Thus, the manufacturers offer software tools for the alignment of different spectrometers to improve transferability. Usually they are working in a two step procedure, whereas in the first the wavelength accuracy is balanced and then the corresponding absorption coefficient is adjusted.

During this project NIR measurements were performed in a static laboratory set up, and a dynamic process simulation. Prospectively, the same analysis will be explored on an industrial plant. According to the validated quantitative model Product B there is no impact of the surrounding work conditions expected. But, especially the equality of analysis between the simulator and a future in-line plant still remains to be proven.

➤ What are the critical factors of the in-line PAT project?

NIR is a complex analysis technique assuming at least basic knowledge in various domains, such as chemistry and mathematics. Good skills in general spectroscopy, specific statistics, and chemometrics are necessary. For the in-line application the requirements of computer skills and technical understanding increase. Accordingly, the

extend of training for development and maintenance personnel is important. First the orientation phase and then the method development is time consuming. Thus, the successful implementation is dependent on continuously employed labor.

The apparatus and calibrations need to be maintained regularly by these NIR specialists. The maintenance should concern the proper spectrometer functionalities (wavelength accuracy, repeatability, noise level, light source, etc.), but also the models' performance. This means that the prediction accuracy of a representative number of samples should be verified by a comparison with the results of the reference method. To assure the realization of these periodic verifications strict time periods have to be defined.

Due to the elaborate preparative work, including beyond others the sample selection and preparation, the reference method as well as the all embracing validation, NIR calibrations can only be profitable if a great amount of analyses will be performed afterwards. Whenever the sample is modified in terms of chemical or physical pattern, e.g. the formulation or the packaging of the product, the NIR response may be affected. This requires a verification of the model suitability.

F.1 Glossary of terms

F.1.1 Spectroscopic definitions

➤ Absorbance

Absorbance A, is represented by the following equation.

$$A = -\lg\left(\frac{I}{I_0}\right) \quad \text{or} \quad A = -\lg T = \lg\left(\frac{1}{r}\right)$$

Equation F-1: Computation of the absorbance, with I = intensity of radiation passing through or reflected from the sample, I₀ = intensity of the incident light energy from the source, and T and r = transmittance and reflectance, respectively.

The intensity includes losses due to solvent absorption, refraction, and scattering when the sample is not present. In reflectance measurements, it is the intensity of radiation indirectly reflected from the background reference material.

➤ Accuracy

The accuracy of a measurement method is its faithfulness, i.e. how close the measured value is to the actual value. Accuracy differs from precision, which indicates the spread of successive measurements performed on the same object.

➤ Collinearity

The term collinearity means the linear relationship between variables. Two variables are collinear if the value of one variable can be computed from the other, using a linear relation. Three or more variables are collinear if one of them can be expressed as a linear function of the others. Variables which are not collinear are said to be linearly independent. Collinearity is the major cause of trouble for MLR models, whereas projection methods like PCA, PCR, and PLS handle collinearity well.

➤ Diffuse Reflectance

Diffuse Reflectance is that portion of radiated light penetrating the sample surface, interacting with the analyte material, and being reflected back to the detector. This is the part of the overall reflectance that produces the absorbance spectrum of the sample.

➤ Loadings

Loadings are estimated in bilinear modeling methods where information carried by several variables is concentrated onto a few components. Each variable has a loading along each model component. The loadings show how well a variable is taken into account by the model components. They are used to understand how much each variable contributes to the meaningful variation in the data, and to interpret variable relationships. They are also useful to understand the meaning of each model component.

➤ Mahalanobis distance

Multivariate techniques are often based on the measurements of distances between objects. One of the most commonly used distance measure is the Mahalanobis distance calculated in the original variable or in the principal component space.

➤ Model

Mathematical equation summarizing variations in a data set. Models are built to understand the structure of a data table better than by looking at all raw data values. Statistical models consist of a structured part and an error part. The structure part (information) is intended to be used for interpretation or prediction, and the error part (noise) should be as small as possible for the model to be reliable.

➤ Noise

Noise is defined as random variation that does not contain any information. The purpose of multivariate modeling is to separate information from noise.

➤ Peak to peak noise

Peak to peak noise is the difference between the maximum and the minimum values of absorbance defined within a restricted wavelength or energy range of a noise spectrum.

➤ Resolution

Data Resolution is the spacing, in nm or cm^{-1} , between the data points collected in a spectrum.

Spectral Resolution, also called instrument bandwidth, is a measure of the ability of a spectrometer to separate adjacent narrow spectral lines. Spectral resolution of an instrument is affected by all optical elements in the system, namely, the source geometry, apertures, lenses, mirrors, detector elements, diffraction grating, etc. The line width at half-intensity of a narrow-band laser source or a very sharp absorption peak can be used to measure resolution.

➤ Scores

Scores are estimated in bilinear modeling methods where information carried by several variables is concentrated onto a few underlying variables. Each sample has a score along each model component. The scores show the locations along each model component, and can be used to detect sample patterns, groupings, similarities or differences.

➤ Transflectance

Transflectance is a transmittance measurement technique where the radiation crosses the sample twice, the second time after being reflected from a surface behind the sample, e.g. a 100 % reflectance standard.

➤ Transmittance

Transmittance is represented by the following equation.

$$T = \frac{I}{I_0}$$

Equation F-2: Computation of the transmittance T, with I = intensity of the radiation transmitted through the sample; I_0 = intensity of the radiant energy incident on the sample including losses due to solvent absorption, refraction, and scattering.

F.1.2 Statistics

➤ Bias

Bias is the average value of residuals calculated from constituent values of a prediction set. A bias value close to zero (0) indicates that the deviations are distributed randomly. A bias value (either positive or negative) that is large compared with typical constituent values indicates systematic error, e.g. changes in the instrument, the condition of samples or the system being analyzed, or in the reference analysis. In some cases, simple bias correction can be used to address this problem.

$$Bias = \frac{\sum_{i=1}^N (\hat{y}_i - y_i)}{N}$$

Equation F-3: Computation of the bias, with y_i = predicted constituent value, \hat{y}_i = true constituent value of the respective y_p and N = population size.

➤ Correlation

The multiple correlation coefficient (r) is a measure of how well the spectral data fits the constituent values. This statistical quantity, also called coefficient of multiple determination, is equal to zero when spectral response is unrelated to constituent data (relationship is statistically random). A value of one signifies that the constituent values fit spectral data perfectly and all residuals are equal to zero. Formally the correlation indicates the fraction of total variance in the data set modeled by the equation. The correlation coefficient is a dimensionless characteristic of the strength of the linear relationship between two variables x and y.

$$r = \frac{\sum_{i=1}^n (x_i - \bar{x})(y_i - \bar{y})}{\sqrt{\sum_{i=1}^n (x_i - \bar{x})^2 \sum_{i=1}^n (y_i - \bar{y})^2}}$$

Equation F-4: General formula of the computation of the correlation coefficient (r) between two variables x and y.

➤ Cross validation

Cross validation is a validation method where some samples are kept out of the calibration and used for prediction. This is repeated until all samples have been kept out once. Validation residual variance can be computed from the prediction residuals.

In full cross validation (FCV) only one sample at a time is kept out of the calibration.

In segmented sample cross validation (SSCV), the samples are divided into subgroups of relative readings. Each subgroup contains for example repeated measurements on only one sample. For validation, at a time an entire segment is kept out of the calibration. A final calibration is then performed with all samples.

➤ Hypogeometric distribution

The hypogeometric distribution computes the probability of a given number of sample successes, given the sample size, population successes, and population size. This function should be used for problems with a finite population, where each observation is either a success or a failure, and where each subset of a given size is chosen with equal likelihood.

$$P(X = x) = h(x; n, M, N) = \frac{\binom{M}{x} \binom{N - M}{n - x}}{\binom{N}{n}}$$

Equation F-5: Formula of the hypogemoetric distribution, with x = number of success in the sample, n = size of the sample, M = number of success in the population, and N = population size.

➤ Mean

The mean describes the average value of a population.

$$\bar{x} = \frac{\sum_{i=1}^N x_i}{N}$$

Equation F-6: Computation of the mean of a population N.

➤ Root Mean Square Error of Prediction (RMSEP) and
Root Mean Square Error of Calibration (RMSEC)

RMSEP and RMSEC are direct estimates of the prediction error and the modeling error in y respectively, expressed in original measurement units. If one measures a concentration in %, say, RMSEP will be in %.

RMSEP is defined as the square root of the average of the squared differences between predicted and measured y -values of the validation objects:

$$RMSEP = \sqrt{\frac{\sum_{i=1}^N (\hat{y}_i - y_i)^2}{N}}$$

Equation F-7: Calculation of the RMSEP, with \hat{y}_i = true constituent value, y_i = predicted constituent value; and N = population size.

RMSEP is also the square root of the validation variance for y , divided by the weights used at calibration (scaling). RMSEC is the corresponding measure for the model fit, calculated from the calibration objects only.

RMSEP expresses the average error to be expected associated with the future predictions. Therefore one may conveniently give predicted Y -values using $2 \times RMSEP$ as the estimated precision; e.g. the concentration in a new samples is $2 \% \pm 0.3 \%$, where 0.3% would be $2 \times RMSEP$.

Because bilinear projection modeling makes no assumptions about the statistical distribution of errors, we cannot give the prediction error as proper statistical interval estimates (such as twice the standard deviation etc.). In fact with this data analytical approach it is not possible to make any statistical inferences at all. RMSEP is the practical average prediction error as estimated by the validation set. So, a good model validation was performed, and both the calibration set and the validation set were representative of future prediction sets, then RMSEP should serve as a valid empirical error estimate.

➤ Standard Deviation (SD) and Relative Standard Deviation (SD_{rel})

Typically, the SD is a measure of how widely values are dispersed from the average value (the mean).

$$SD = \sqrt{\frac{\sum_{i=1}^N (\bar{x} - x_i)^2}{(N-1)}}$$

Equation F-8: Computation of the Standard Deviation (SD), with \bar{x} = mean of the population, x_i = value of a specific sample i, and N = size of the population.

The SD_{rel} is related to the mean value \bar{x} and is computed according to Equation F-9.

$$SD_{rel} [\%] = \frac{SD \cdot 100 \%}{\bar{x}}$$

Equation F-9: Computation of the SD_{rel}.

If the true values are known or the same samples are tested twice, not the sample dispersion from the overall mean is of interest, but the deviation of the paired analysis results from each other. In this case the SD is computed according to Equation F-10. This appraisal is equal to the Standard Error of Prediction (SEP).

$$SD_{paired} = \sqrt{\frac{\sum_{i=1}^N (\hat{x}_i - x_i)^2}{(N-1)}}$$

Equation F-10: Paired computation of the Standard Deviation (SD_{paired}), with \hat{x}_i = true value of a sample i, x_i = assumed value of the same sample i, and N = size of the population.

➤ Standard Error of Prediction (SEP) and
Standard Error of Cross Validation (SECV)

SEP is a statistical parameter that indicates the upper limit of accuracy in the prediction of samples not used in the calibration, i.e. a validation sample set. If Full Cross Validation (FCV) is applied SEP is also called SECV and refers to the standard error of the successively excepted samples belonging to the calibration and not to an external sample set. The SECV is computed according to the same equation.

The generally accepted formula for the SEP is represented in Equation F-11 and is also adopted as definition for the present work.

$$SEP = \sqrt{\frac{\sum_{i=1}^N (\hat{y}_i - y_i)^2}{N-1}}$$

Equation F-11: The generally accepted formula for the computation of the SEP, with \hat{y}_i = true constituent value, y_i = predicted constituent value; and N = population size.

In case of a normal distribution of the samples included in the calculation of the bias,

95 % of them will have $\hat{y}_i - y_i \leq 2 \cdot SEP$

5 % of them will have $\hat{y}_i - y_i \geq 2 \cdot SEP$.

Therefore 2 times SEP may be considered as a 95 % confidence interval. This also means that the uncertainty of the bias is directly dependent on the SEP. The value of the SEP increases when the Y-values (the reference values) are inaccurate.

The relationship between RMSEP, SEP and bias is statistically well known.

$$RMSEP^2 \approx SEP^2 + Bias^2$$

Equation F-12: Relationship between RMSEP and SEP.

Normally there is no bias which then leads to $RMSEP = SEP$.

If RMSEP is unusually high, given an otherwise reasonable data structure, the reason may either be a bad model specification or a non-representative validation set. The latter is the case if the bias is large.

Some software manufacturer adopted different approaches for the definition and correct the SEP by either the bias or the degrees of freedom. With respect to certain limits, the influence of these adaptations is negligible.

$$SEP_{Unscrambler} = \sqrt{\frac{\sum_{i=1}^N (\hat{y}_i - y_i - Bias)^2}{N-1}}$$

Equation F-13: Computation of the SEP according to the Unscrambler, with \hat{y}_i = true constituent value, y_i = predicted constituent value, N = population size; corrected by the respective bias.

If the bias is low, and this is mainly the case if a consistent calibration was computed, its influence on the numerator can be neglected and the $SEP_{\text{Unscrambler}}$ becomes equal to the general SEP.

$$SEP_{\text{Vision}} = \sqrt{\frac{\sum_{i=1}^N (\hat{y}_i - y_i)^2}{N - K - 1}}$$

Equation F-14: Computation of the SEP according to Vision 2.51, with \hat{y}_i = true constituent value, y_i = predicted constituent value, N = population size; corrected by K = number of Principal Components (PC) for the respective calibration.

In the present work usually large sample sets were used to compute calibrations with low numbers of PCs, so that the influence of K was negligible. Under these conditions SEP_{Vision} could be considered as being equal to the general definition of the SEP.

➤ Paired Student's t-test

The paired Student's t-test or paired t-test is a tool to determine whether two samples are likely to have come from the same two underlying populations that have the same mean. The paired t-test is used when a sample group is tested twice – e.g. before and after an experiment or with two different test methods. Accordingly, a paired t-test is only possible if both populations have the same size.

$$t = |\bar{x}_1 - \bar{x}_2| \sqrt{\frac{N}{SD_{\text{paired } 1}^2 + SD_{\text{paired } 2}^2}}$$

Equation F-15: The formula returns the probability t associated with a paired Student's t-test, with N = size of the population, and $SD_{\text{paired } x}^2$ = squared paired SD of the corresponding underlying population.

$$f = 2 \cdot N - 2$$

Equation F-16: Computation of f = degrees of freedom.

If the calculated value t is inferior to the corresponding tabulated value respecting the degrees of freedom, the difference between the two compared means is with an error probability α not significant and vice versa.

F.2 Tables and figures

F.2.1 Sample preparation

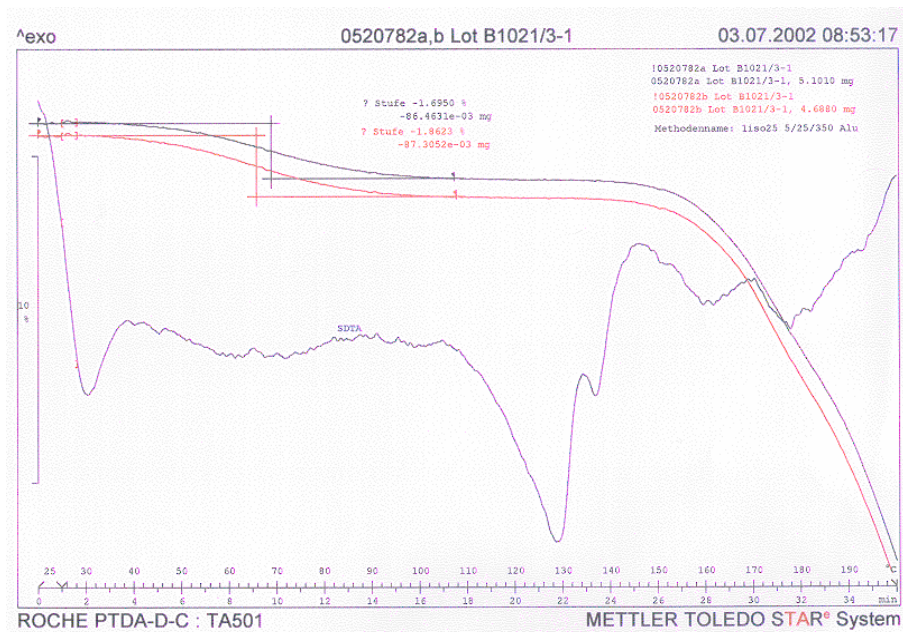


Figure F-1: TGA Product A 40 mg.

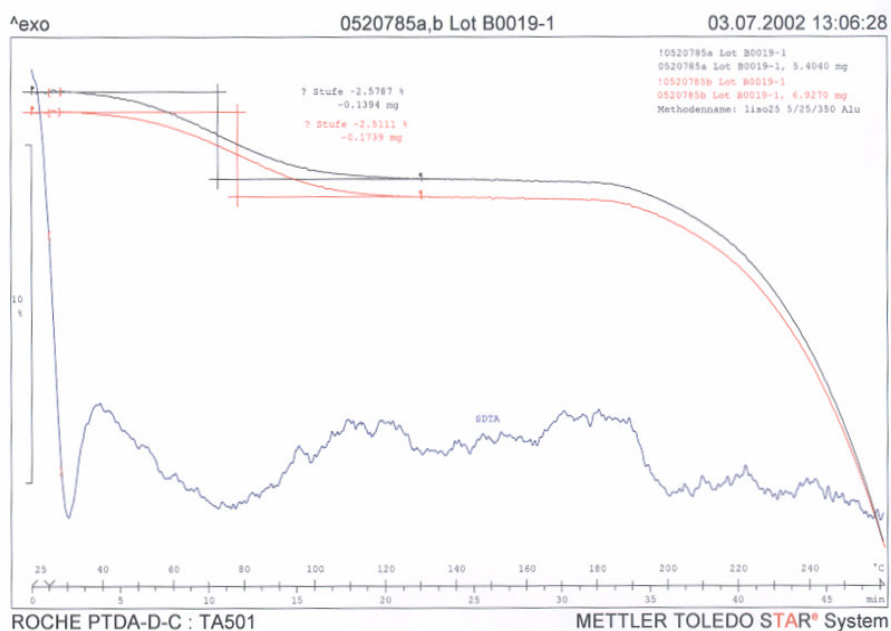


Figure F-2: TGA Product B.

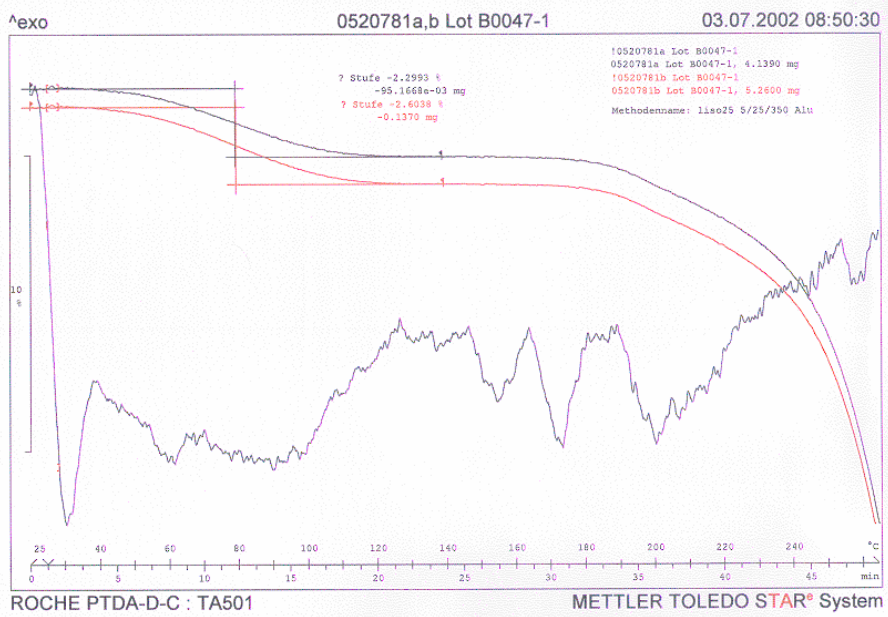


Figure F-3: TGA Product C 150 mg.

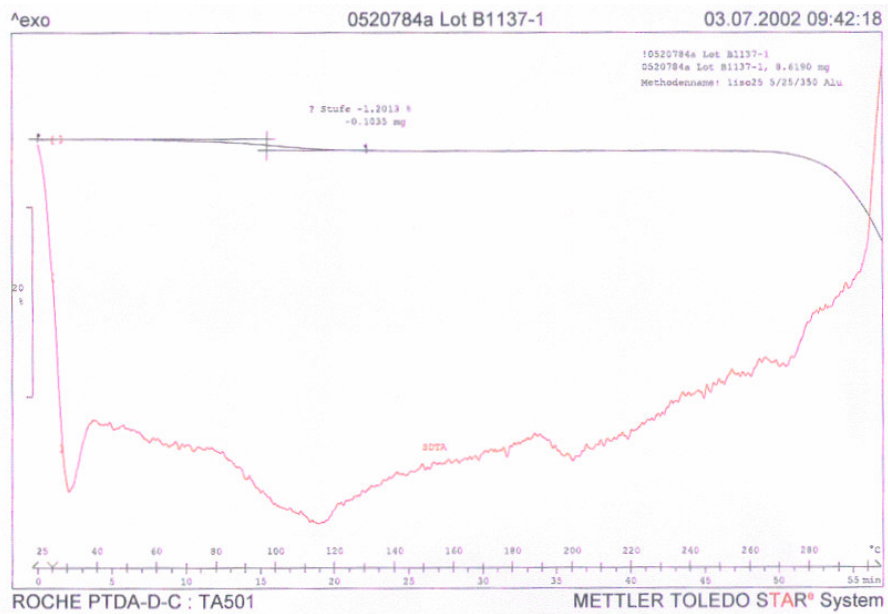


Figure F-4: TGA Product D.

F.2.2 Evaluation of the appropriate analysis system

Calibration sample name	KF [%]	Calibration sample name	KF [%]	Validation sample name	KF [%]
B1021-3-24h-3	0.56	B1021-3-15m-4	1.76	B1021-3-24h-1	0.68
B1021-3-24h-4	0.60	B1021-3-15m-5	1.86	B1021-3-24h-2	0.65
B1021-3-24h-5	0.65	B1021-2-30m-3	2.34	B1009-2-1	1.36
B1021-3-24h-6	0.61	B1021-2-30m-4	2.52	B1009-2-2	1.40
B1021-3-24h-7	0.57	B1021-2-30m-5	2.40	B1010-3-1	1.92
B1021-3-24h-8	0.59	B1021-3-30m-1	2.37	B1010-3-2	1.88
B1021-3-24h-9	0.58	B1021-3-30m-2	2.80	B1021-3-15m-1	1.76
B1021-3-24h-10	0.64	B1021-3-30m-3	2.41	B1021-3-15m-2	1.65
B1009-2-3	1.32	B1021-3-30m-4	2.48	B1021-2-30m-1	2.45
B1009-2-4	1.42	B1021-3-30m-5	2.43	B1021-2-30m-2	2.40
B1009-2-5	1.31	B1021-2-45m-1	3.13		
B1009-2-6	1.53	B1021-2-45m-2	3.16		
B1009-2-7	1.43	B1021-2-45m-3	3.09		
B1009-2-8	1.71	B1021-2-45m-4	3.15		
B1009-2-9	2.42	B1021-2-45m-5	3.14		
B1009-2-10	1.53	B1021-3-45m-1	3.12		
B1010-3-3	1.38	B1021-3-45m-2	2.96		
B1010-3-4	1.59	B1021-3-45m-3	3.29		
B1010-3-5	1.78	B1021-3-45m-4	3.05		
B1010-3-6	1.12	B1021-3-45m-5	3.02		
B1010-3-7	1.28	B1021-2-60m-1	3.63		
B1010-3-8	1.28	B1021-2-60m-2	3.64		
B1010-3-9	1.79	B1021-2-60m-3	3.66		
B1010-3-1	2.16	B1021-2-60m-4	3.71		
B1021-3-15m-3	1.78	B1021-2-60m-5	3.69		

Table F-1: Calibration and validation sample sets of evaluation of the appropriate analysis system.

F.2.3 Static scan mode evaluation

Sample name	KF [%]	Sample name	KF [%]	Sample name	KF [%]
B2128/1-15m-1	1.7	B2132/2-8	1.0	B2131/1-30m-5	2.4
B2128/1-15m-2	1.6	B2132/2-9	1.0	B2131/1-30m-6	2.7
B2128/1-15m-3	1.8	B2132/2-10	1.4	B2131/1-30m-7	2.4
B2128/1-15m-4	1.6	B2132/6-1	0.9	B2131/1-30m-8	2.7
B2128/1-15m-5	1.6	B2132/6-2	1.1	B2131/1-30m-9	2.8
B2128/1-15m-6	1.6	B2132/6-3	1.0	B2131/1-30m-10	2.4
B2128/1-15m-7	1.6	B2132/6-4	1.1	B2132/3-40m-1	3.2
B2128/1-15m-8	1.5	B2132/6-5	1.1	B2132/3-40m-2	3.1
B2128/1-15m-9	1.6	B2132/6-6	1.0	B2132/3-40m-4	3.3
B2128/1-15m-10	1.6	B2132/6-7	1.2	B2132/3-40m-5	3.0
B2127/1-30m-1	2.3	B2132/6-8	1.1	B2132/3-40m-6	3.4
B2127/1-30m-2	2.3	B2132/6-9	1.1	B2132/3-40m-7	3.2
B2127/1-30m-3	2.1	B2132/6-10	1.1	B2132/3-40m-9	3.0
B2127/1-30m-4	2.1	B2132/5-13m-1	1.5	B2132/3-40m-10	3.2
B2127/1-30m-5	2.1	B2132/5-13m-2	1.8	B2133/4-50m-1	3.3
B2127/1-30m-6	2.1	B2132/5-13m-3	1.5	B2133/4-50m-2	3.4
B2127/1-30m-7	2.2	B2132/5-13m-4	1.4	B2133/4-50m-3	3.5
B2127/1-30m-8	2.3	B2132/5-13m-5	1.6	B2133/4-50m-4	3.2
B2127/1-30m-9	2.3	B2132/5-13m-6	1.8	B2133/4-50m-5	3.5
B2127/1-30m-10	2.3	B2132/5-13m-7	1.4	B2133/4-50m-6	3.3
B2131/4-24h-1	0.5	B2132/5-13m-8	1.4	B2133/4-50m-7	3.5
B2131/4-24h-2	0.7	B2132/5-13m-9	1.5	B2133/4-50m-8	3.5
B2131/4-24h-3	0.7	B2132/5-15m-1	1.8	B2133/4-50m-9	3.4
B2131/4-24h-4	0.5	B2132/5-15m-2	1.6	B2133/4-50m-10	3.4
B2131/4-24h-5	0.5	B2132/5-15m-3	1.9	B2131/5-60m-1	3.7
B2131/4-24h-6	0.8	B2132/5-15m-4	1.8	B2131/5-60m-2	3.5
B2131/4-24h-7	0.6	B2132/5-15m-5	1.8	B2131/5-60m-3	3.7
B2131/4-24h-8	0.5	B2132/5-15m-6	1.9	B2131/5-60m-4	3.5
B2131/4-24h-9	0.5	B2132/5-15m-7	1.8	B2131/5-60m-5	3.6
B2131/4-24h-10	0.6	B2132/5-15m-8	1.8	B2131/5-60m-6	3.6
B2132/2-1	1.0	B2132/5-15m-9	1.9	B2131/5-60m-7	3.5
B2132/2-2	1.1	B2132/5-15m-10	1.7	B2131/5-60m-8	3.6
B2132/2-3	0.9	B2131/1-30m-1	2.4	B2131/5-60m-9	3.4
B2132/2-4	1.2	B2131/1-30m-2	2.3	B2131/5-60m-10	3.5
B2132/2-5	1.0	B2131/1-30m-3	2.5		
B2132/2-6	1.1	B2131/1-30m-4	2.4		

Table F-2: Sample set Product A 20 mg, static scan mode evaluation.

F.2.4 Qualitative model Product B

F.2.4.1 Calibration samples class 'Good' (< 2 %)

Sample name	turned	KF [%]	Sample name	turned	KF [%]
B1007-1	x	0.3	B0019-1	-	1.1
B1007-2	x	0.4	B0019-2	-	0.9
B1007-3	x	0.3	B0019-3	-	0.7
B1007-4	x	0.4	B0019-4	-	0.6
B1007-5	x	0.4	B0019-5	-	0.6
B1007-6	x	0.4	B0019-6	-	0.6
B1007-7	x	1.2	B0019-7	-	0.6
B1007-8	x	0.5	B0019-8	-	0.6
B1007-9	x	0.4	B0019-9	-	0.6
B1007-10	x	0.4	B0019-10	-	0.7
B1011-1	x	0.7	B0021-1	-	0.8
B1011-2	x	0.8	B0021-2	-	0.6
B1011-3	x	0.9	B0021-3	-	0.6
B1011-4	x	0.8	B0021-4	-	0.6
B1011-5	x	0.9	B0021-5	-	1.4
B1011-6	x	0.6	B0021-6	-	0.6
B1011-7	x	0.9	B0021-7	-	1.4
B1011-8	x	0.8	B0021-8	-	0.7
B1011-9	x	0.6	B0021-9	-	0.9
B1011-10	x	1.0	B0021-10	-	0.8
B1011-11	x	1.0	B0021-71h-1	-	1.0
B1011-12	x	0.7	B0021-71h-2	-	0.9
B1011-13	x	0.9	B0021-71h-3	-	0.9
B1011-14	x	0.9	B0021-71h-4	-	0.9
B1011-15	x	0.9	B0021-71h-5	-	0.9
F1000-15m-1	x	1.3	B0021-71h-6	-	0.9
F1000-15m-2	x	1.2	B0021-71h-7	-	0.8
F1000-15m-3	x	1.1	B0021-71h-8	-	0.9
F1000-15m-4	x	1.1	B0021-71h-9	-	0.9
F1000-15m-5	x	1.3	B0021-71h-10	-	0.9
F1000-15m-6	x	1.2	F0012-15m-1	-	1.1
F1000-15m-7	x	1.3	F0012-15m-2	-	1.2
F1000-15m-8	x	1.4	F0012-15m-3	-	1.2
F1000-15m-10	x	1.1	F0012-15m-4	-	1.2
			F0012-15m-5	-	1.2

Table F-3: The spectra of all samples marked with an x were recorded three times. Between the measurements the samples were rotated.

F.2.4.2 Calibration samples class 'Bad' ($\geq 2\%$)

Sample name	turned	KF [%]	Sample name	turned	KF [%]
F0019-30m-1	-	2.0	F1003-30m-1	x	2.1
F0019-30m-2	-	2.0	F1003-30m-2	x	2.4
F0019-30m-3	-	2.0	F1003-30m-3	x	2.4
F0019-30m-4	-	2.0	F1003-30m-4	x	2.1
F0019-30m-5	-	2.0	F1003-30m-5	x	2.0
F0019-30m-5	-	2.0	F1003-30m-7	x	2.0
F0019-30m-7	-	3.2	F1003-30m-8	x	2.1
F0019-30m-8	-	2.0	F1003-30m-9	x	2.0
F0019-30m-9	-	2.0	F1003-30m-10	x	2.0
F0019-30m-10	-	2.0	F1006-45m-1	x	2.9
F0021-45m-1	-	2.5	F1006-45m-2	x	2.9
F0021-45m-2	-	3.0	F1006-45m-3	x	2.9
F0021-45m-3	-	2.6	F1006-45m-4	x	2.9
F0021-45m-4	-	2.6	F1006-45m-5	x	3.0
F0021-45m-5	-	2.6	F1006-45m-6	x	3.0
F0021-45m-6	-	2.6	F1006-45m-7	x	3.0
F0021-45m-7	-	2.6	F1006-45m-8	x	2.9
F0021-45m-8	-	2.7	F1006-45m-9	x	3.0
F0021-45m-9	-	2.7	F1006-45m-10	x	3.0
F0011-60m-1	-	3.4			
F0011-60m-2	-	3.3			
F0011-60m-3	-	3.4			
F0011-60m-4	-	3.5			
F0011-60m-5	-	3.4			

Table F-4: The spectra of all samples marked with an x were recorded three times. Between the measurements the samples were rotated.

F.2.4.3 Validation samples classified as 'Good' (< 2 %)

Sample name	KF [%]	Sample name	KF [%]
PT3618H61a-58	1.1	PT3618H67d-213	0.8
PT3618H61a-72	0.7	PT3618H67d-214	0.9
PT3618H61a-120	0.6	PT3618H67d-215	0.8
PT3618H61a-131	0.6	PT3618H67d-240	1.0
PT3618H61a-200	0.7	PT3618H67d-241	0.9
PT3618H61a-232	1.0	PT3618H67d-242	1.0
PT3618H61a-343	0.7	PT3618H67d-243	0.8
PT3618H61a-254	0.7	PT3618H67d-244	0.8
PT3618H61a-376	0.8	PT3618H67d-269	0.8
PT3618H61a-394	0.8	PT3618H67d-270	0.8
PT3618H67c-190	0.4	PT3618H67d-271	0.8
PT3618H67c-191	0.5	PT3618H67d-272	0.9
PT3618H67c-220	0.5	PT3618H67d-298	0.8
PT3618H67c-229	0.5	PT3618H67d-299	0.8
PT3618H67c-244	0.5	PT3618H67d-300	0.8
PT3618H67c-245	0.6	PT3618H67d-442	0.8
PT3618H67c-246	0.5	PT3618H67d-444	0.8
PT3618H67c-247	0.5	PT3618H67e-52	0.5
PT3618H67c-248	0.7	PT3618H67e-53	0.5
PT3618H67c-249	0.6	PT3618H67e-54	0.6
PT3618H67c-275	0.6	PT3618H67e-55	0.5
PT3618H67c-276	0.6	PT3618H67e-56	0.6
PT3618H67c-277	0.6	PT3618H67e-57	0.5
PT3618H67c-278	0.7	PT3618H67e-80	0.5
PT3618H67c-305	0.7	PT3618H67e-81	0.6
PT3618H67c-307	0.7	PT3618H67e-82	0.6
PT3618H67c-334	0.7	PT3618H67e-82	0.6
PT3618H67c-335	0.5	PT3618H67e-84	0.6
PT3618H67c-445	0.6	PT3618H67e-85	0.6
PT3618H67c-446	0.6	PT3618H67e-112	0.6
PT3618H71a-58	0.6	PT3618H67e-113	0.6
PT3618H71a-173	0.5	PT3618H67e-140	0.5
PT3618H71a-408	1.8	PT3618H67e-141	0.5
PT3618H71a-442	1.7	PT3618H67e-168	0.5
PT3618H71a-443	1.7	PT3618H67e-169	0.6
PT3618H67d-184	0.8	PT3618H67e-196	0.7
PT3618H67d-185	0.8	PT3618H67e-197	0.8
PT3618H67d-212	1.0		

F.2.4.4 Validation samples classified as 'Bad' (> 2 %)

Sample name	KF [%]	Sample name	KF [%]
PT3618H61c-1	2.6	PT3618H61e-25	3.5
PT3618H61c-30	3.0	PT3618H61e-26	3.2
PT3618H61c-58	2.7	PT3618H61e-27	3.1
PT3618H61c-115	3.6	PT3618H61e-28	2.8
PT3618H61c-144	2.8	PT3618H61e-29	2.5
PT3618H61c-145	3.4	PT3618H61e-56	3.8
PT3618H61c-172	2.9	PT3618H61e-57	3.1
PT3618H61c-229	3.1	PT3618H61e-85	3.7
PT3618H61c-282	3.1	PT3618H61e-86	2.9
PT3618H61c-315	4.0	PT3618H61e-114	2.6
PT3618H61c-343	2.9	PT3618H61e-143	2.8
PT3618H61c-372	3.5	PT3618H61e-171	3.2
PT3618H61c-400	2.7	PT3618H61e-369	3.8
PT3618H61c-401	4.0	PT3618H61e-370	3.2
PT3618H61c-429	3.1	PT3618H61e-371	2.6
PT3618H61c-430	3.0	PT3618H61e-399	2.4
PT3618H61c-431	3.5	PT3618H61e-426	2.8
PT3618H61c-432	3.8	PT3618H61e-427	2.5
PT3618H61c-433	4.1	PT3618H61e-428	2.4
PT3618H61c-435	4.0	PT3618H61e-455	2.2
PT3618H71a-5	2.6		
PT3618H71a-63	3.0		
PT3618H71a-313	3.7		
PT3618H71a-371	3.1		
PT3618H71a-401	2.1		

F.2.4.5 Validation samples classified as 'Outlier' (> 4 %)

Sample name	KF [%]	Sample name	KF [%]
PT3618H61c-344	5.3	PT3618H71a-15	4.3
PT3618H61c-402	6.0	PT3618H71a-61	6.3
PT3618H61c-404	7.1	PT3618H71a-108	5.3
PT3618H61c-407	9.2	PT3618H71a-164	6.9
PT3618H61c-434	4.8	PT3618H71a-176	5.8
PT3618H61c-436	4.7	PT3618H71a-208	4.9
PT3618H61c-437	4.3	PT3618H71a-245	4.4
PT3618H61e-53	7.0	PT3618H71a-266	6.3
PT3618H61e-54	5.6	PT3618H71a-309	5.3
PT3618H61e-55	5.3	PT3618H71a-395	4.5
PT3618H61e-82	7.4		
PT3618H61e-83	6.2		
PT3618H61e-84	4.5		
PT3618H61e-110	5.6		
PT3618H61e-113	4.5		
PT3618H61e-134	7.7		
PT3618H61e-136	6.1		
PT3618H61e-137	6.9		
PT3618H61e-161	10.1		
PT3618H61e-162	7.0		

F.2.5 Dynamic scan mode evaluation

F.2.5.1 Diameter 22.0 mm, 10 ml vials

For the vial diameter of 22.0 mm velocities up to 150 samples per minute were feasible and were analyzed.

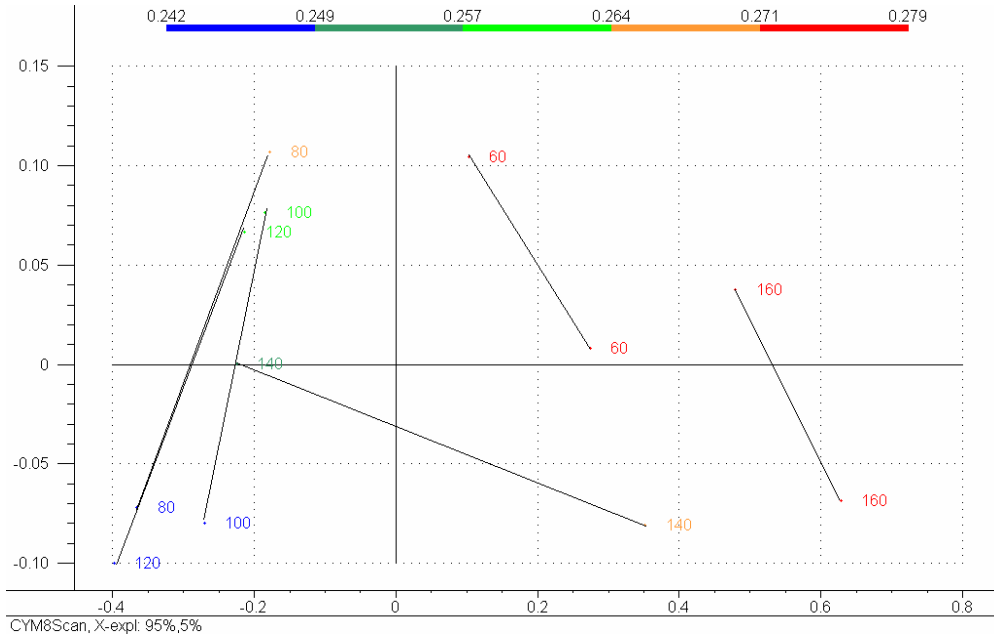


Figure F-5: Diameter 22.0 mm, 60 – 150 samples per minute, 8 scans.

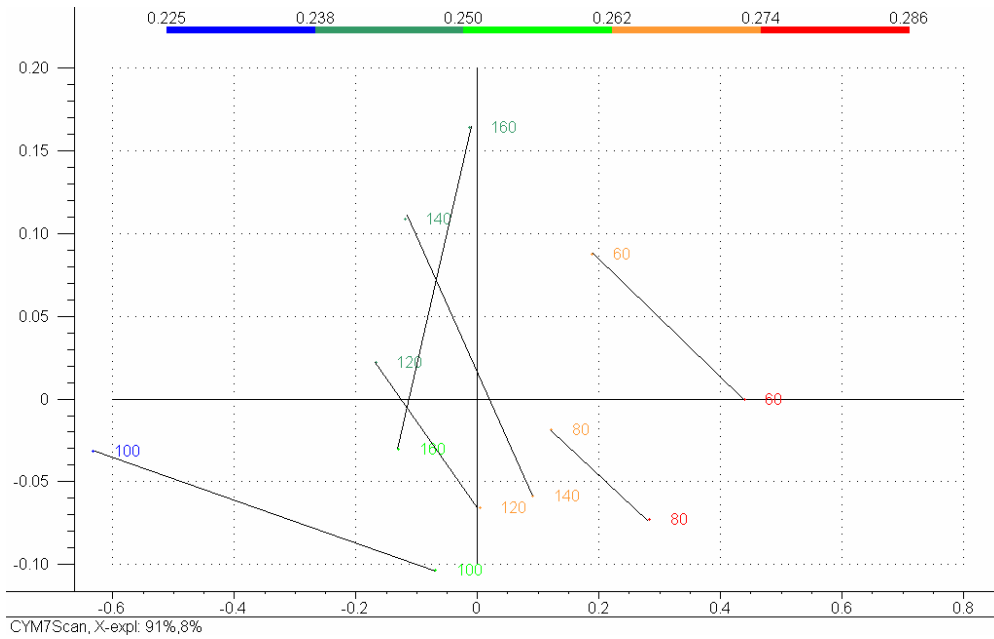


Figure F-6: Diameter 22.0 mm, 60 – 150 samples per minute, 7 scans.

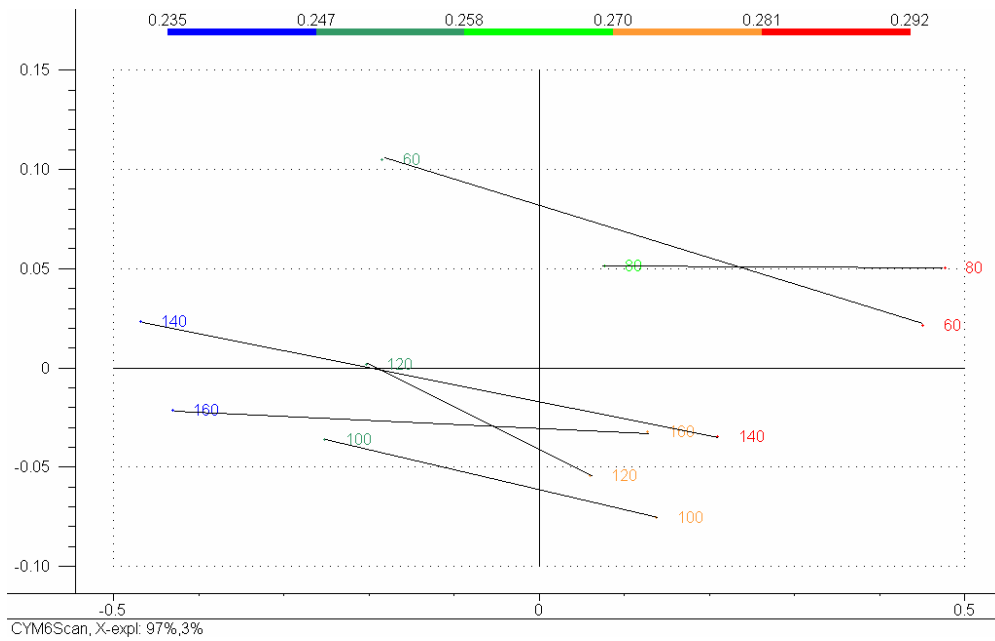


Figure F-7: Diameter 22.0 mm, 60 – 150 samples per minute, 6 scans.

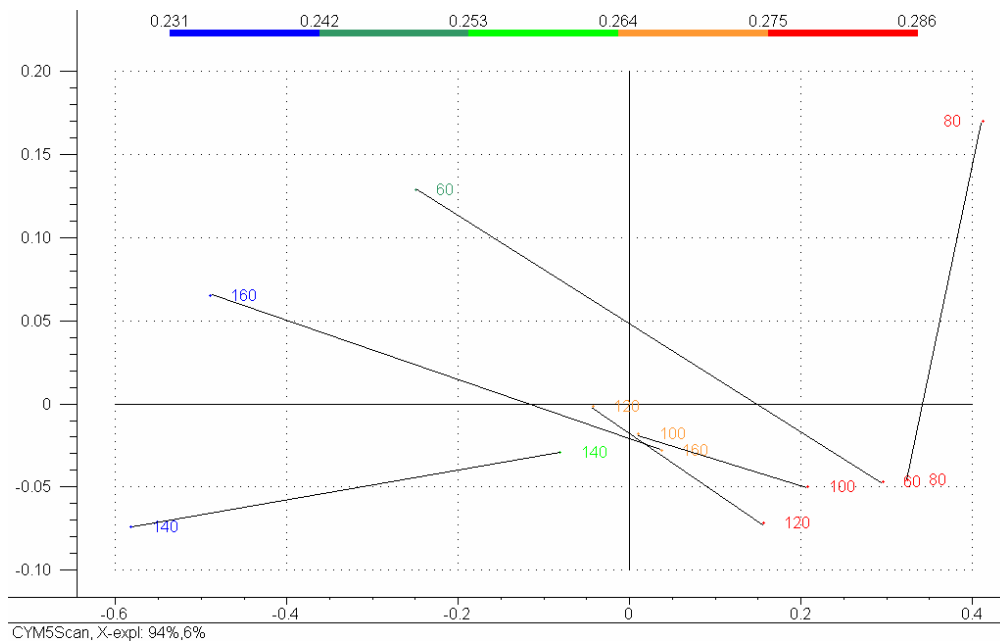


Figure F-8: Diameter 22.0 mm, 60 – 150 samples per minute, 5 scans.

F.2.5.2 Diameter 26.5 mm, 15 ml vials

For the vial diameter of 26.5 mm velocities up to 150 samples per minute were feasible and were analyzed.

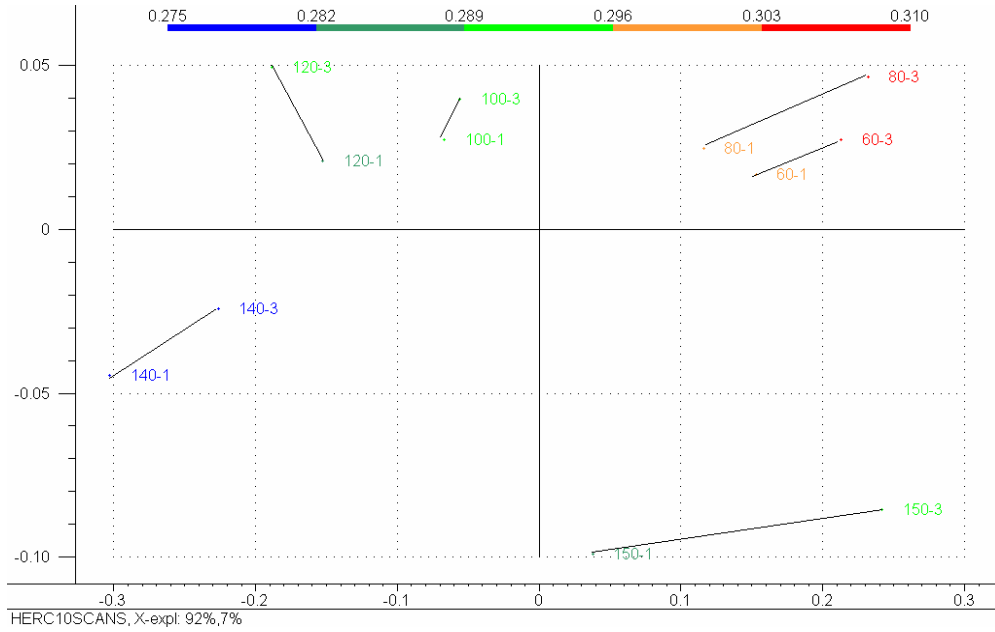


Figure F-9: Diameter 26.5 mm, 60 – 150 samples per minute, 10 scans

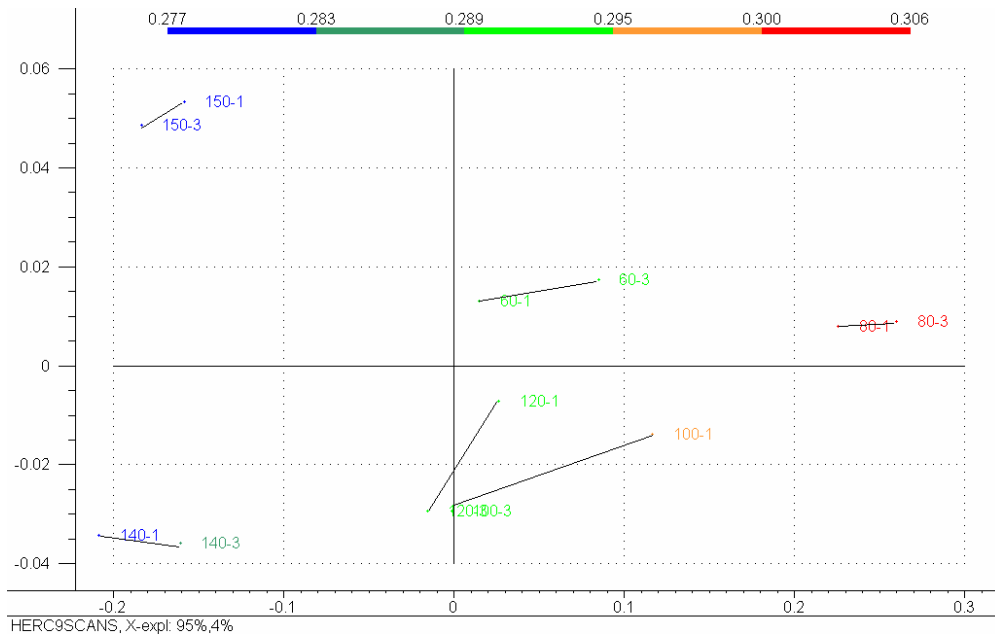


Figure F-10: Diameter 26.5 mm, 60 – 150 samples per minute, 9 scans.

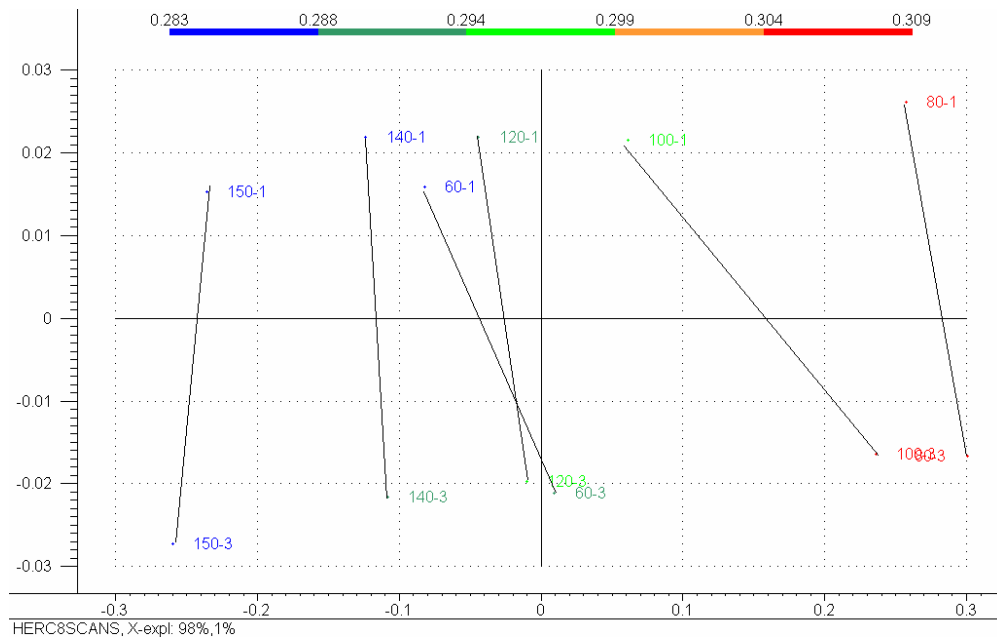


Figure F-11: Diameter 26.5 mm, 60 – 150 samples per minute, 8 scans.

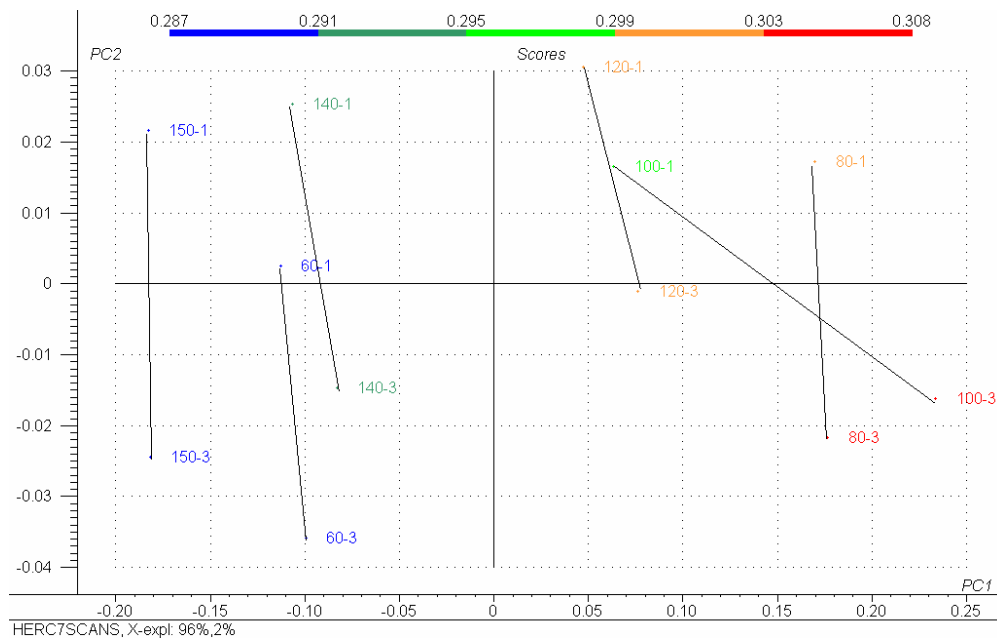


Figure F-12: Diameter 26.5 mm, 60 – 150 samples per minute, 7 scans.

F.2.5.3 Diameter 42.5 mm, 50 ml vials

For the vial diameter of 42.5 mm velocities up to 70 samples per minute were feasible and were analyzed.

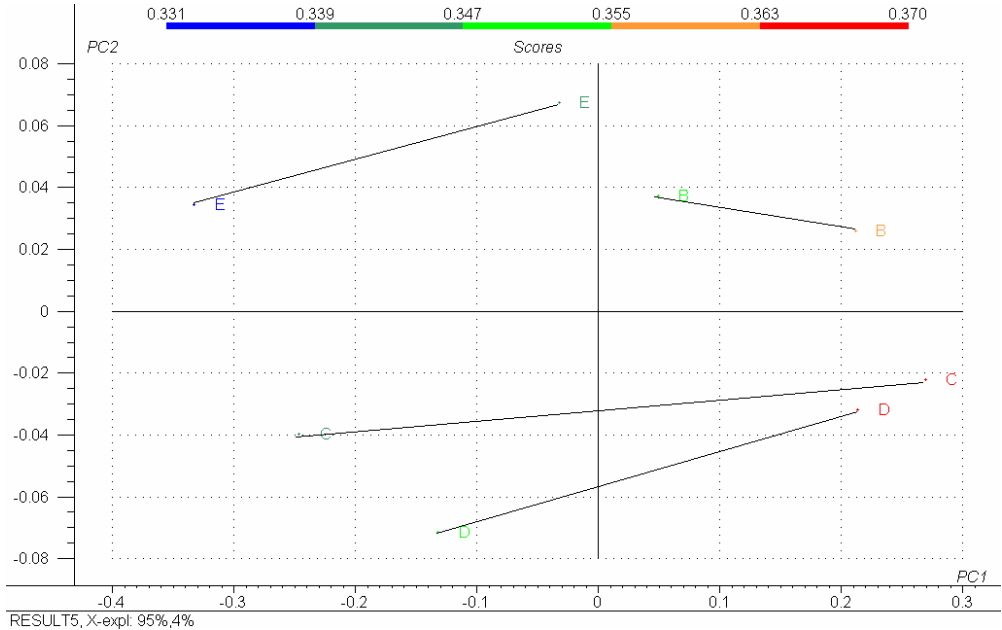


Figure F-1: Diameter 42.5 mm, 26 – 70 samples per minute, 16 scans.

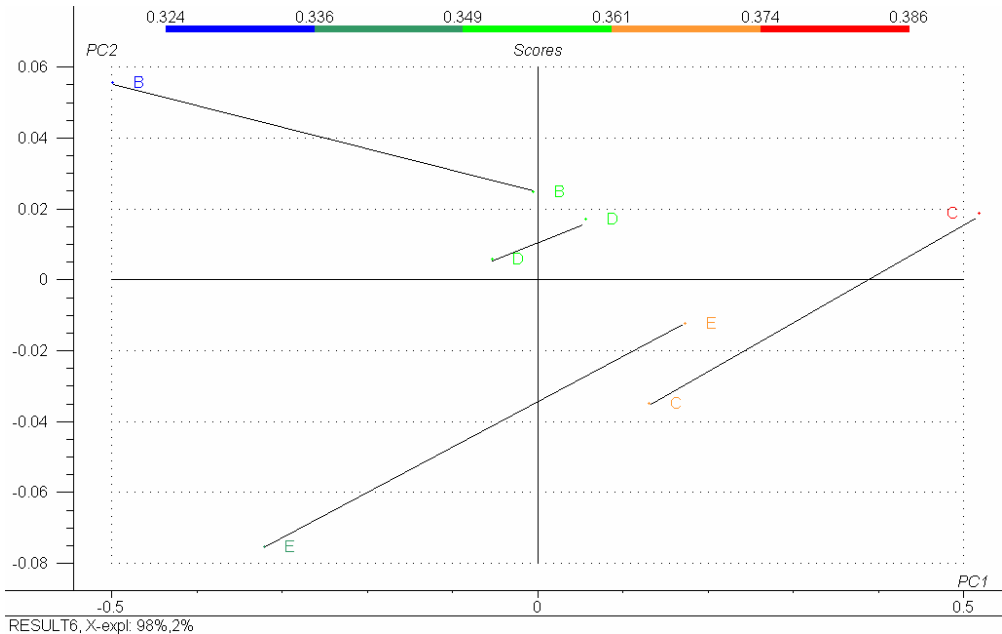


Figure F-2: Diameter 42.5 mm, 26 – 70 samples per minute, 14 scans.

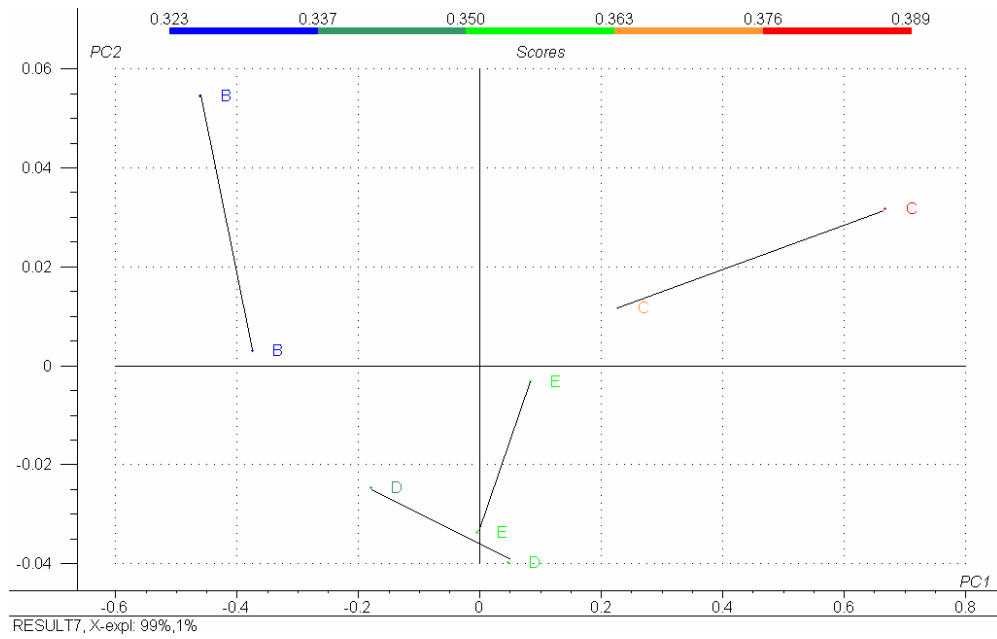


Figure F-3: Diameter 42.5 mm, 26 – 70 samples per minute, 12 scans.

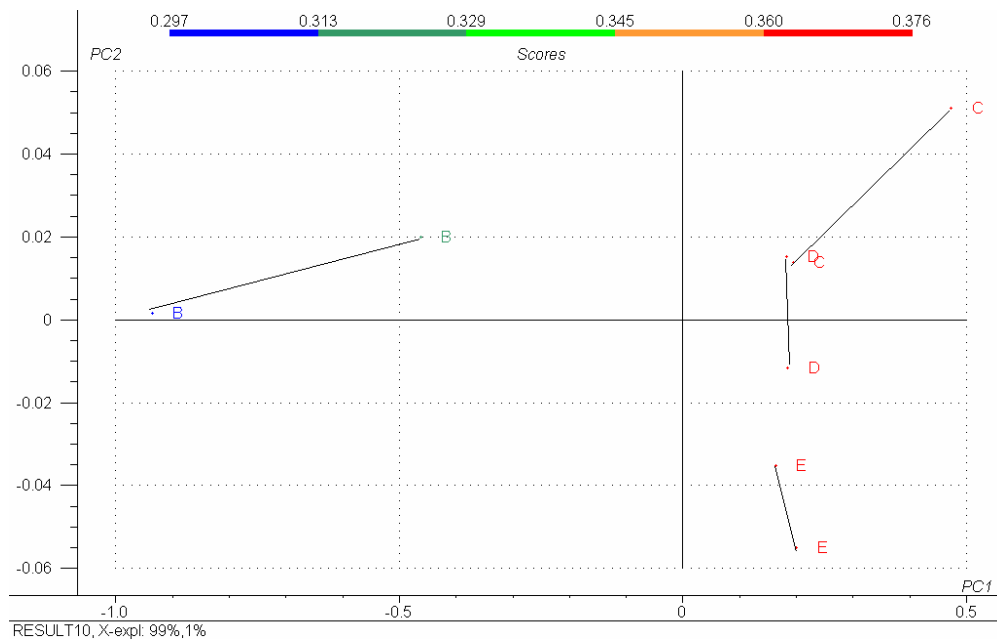


Figure F-4: Diameter 42.5 mm, 26 – 70 samples per minute, 10 scans.

F.2.6 Validated quantitative model Product B

F.2.6.1 Repeatability validation

Repetition	Predicted x_i [%]	$x_i - \bar{x}$	$\frac{(x_i - \bar{x}) \cdot 100}{\bar{x}}$
1	0.661	6.50E-03	0.99
2	0.653	-1.50E-03	-0.23
3	0.642	-1.25E-02	-1.91
4	0.655	5.00E-04	0.08
5	0.631	-2.35E-02	-3.59
6	0.661	6.50E-03	0.99
7	0.654	-5.00E-04	-0.08
8	0.652	-2.50E-03	-0.38
9	0.679	2.45E-02	3.74
10	0.657	2.50E-03	0.38
Mean	0.655	SD 1.25E-02	SD_{rel} 1.91 %

Table F-5: Repeatability results of 10 measurements performed on one sample with a typical moisture content.

Repetition	Predicted x_i [%]	$x_i - \bar{x}$	$\frac{(x_i - \bar{x}) \cdot 100}{\bar{x}}$
1	2.068	-7.40E-03	-0.36
2	2.071	-4.40E-03	-0.21
3	2.081	5.60E-03	0.27
4	2.061	-1.44E-02	-0.69
5	2.087	1.16E-02	0.56
6	2.075	-4.00E-04	-0.02
7	2.091	1.56E-02	0.75
8	2.063	-1.24E-02	-0.60
9	2.089	1.36E-02	0.66
10	2.068	-7.40E-03	-0.36
Mean	2.075	SD 1.10E-02	SD_{rel} .53 %

Table F-6: Repeatability results of 10 measurements performed on one sample of average moisture content.

Repetition	Predicted x_i [%]	$x_i - \bar{x}$	$\frac{(x_i - \bar{x}) \cdot 100}{\bar{x}}$
1	3.054	2.76E-02	0.91
2	3.053	2.66E-02	0.88
3	3.075	4.86E-02	1.61
4	2.970	-5.64E-02	-1.86
5	2.981	-4.54E-02	-1.50
6	2.982	-4.44E-02	-1.47
7	3.062	3.56E-02	1.18
8	3.044	1.76E-02	0.58
9	3.014	-1.24E-02	-0.41
10	3.029	2.60E-03	0.09
Mean	3.026	SD 3.77E-02	SD_{rel} 1.25 %

Table F-7: Repeatability results of 10 measurements performed on one sample of high moisture content.

Repetition	Predicted x_i [%]	$x_i - \bar{x}_i$	$\frac{(x_i - \bar{x}_i) \cdot 100}{\bar{x}_i}$	SD_{rel} within sample [%]
1	0.634	1.13E-02	1.82	
1	0.624	1.33E-03	0.21	
1	0.610	-1.27E-02	-2.03	1.94
2	0.661	9.00E-03	1.38	
2	0.653	1.00E-03	0.15	
2	0.642	-1.00E-02	-1.53	1.46
3	2.068	-5.33E-03	-0.26	
3	2.071	-2.33E-03	-0.11	
3	2.081	7.67E-03	0.37	0.33
4	2.318	-4.00E-03	-0.17	
4	2.326	4.00E-03	0.17	
4	2.322	0.00E+00	0.00	0.17
5	2.580	-4.67E-03	-0.18	
5	2.584	-6.67E-04	-0.03	
5	2.590	5.33E-03	0.21	0.19
6	2.754	-2.13E-02	-0.77	
6	2.785	9.67E-03	0.35	
6	2.787	1.17E-02	0.42	0.67
7	2.863	-2.03E-02	-0.71	
7	2.876	-7.33E-03	-0.25	
7	2.911	2.77E-02	0.96	0.86
8	3.054	-6.67E-03	-0.22	
8	3.053	-7.67E-03	-0.25	
8	3.075	1.43E-02	0.47	0.41
9	3.210	-1.87E-02	-0.58	
9	3.230	1.33E-03	0.04	
9	3.246	1.73E-02	0.54	0.56
10	3.502	-4.00E-02	-1.13	
10	3.572	3.00E-02	0.85	
10	3.552	1.00E-02	0.28	1.02
Mean	2.374 %	SD 1.47E-02		SD_{rel} 0.76 %

Table F-8: Precision by repeatability assay of 3 measurements of 10 different samples spread over the calibration range.

F.2.6.2 Reproducibility

Repetition	Predicted x_i [%]	$x_i - \bar{x}_i$	$\frac{(x_i - \bar{x}_i) \cdot 100}{\bar{x}_i}$	SDrel within sample [%]
1 _{100/min}	0.590	-1.90E-02	-3.12	
1 _{200/min}	0.615	6.00E-03	0.99	
1 _{270/min}	0.634	2.50E-02	4.11	
1 _{300/min}	0.597	-1.20E-02	-1.97	3.24
2 _{100/min}	0.634	-1.47E-02	-2.27	
2 _{200/min}	0.629	-1.97E-02	-3.04	
2 _{270/min}	0.661	1.23E-02	1.89	
2 _{300/min}	0.671	2.23E-02	3.43	3.15
3 _{100/min}	2.048	-1.80E-02	-0.87	
3 _{200/min}	2.079	1.30E-02	0.63	
3 _{270/min}	2.068	2.00E-03	0.10	
3 _{300/min}	2.069	3.00E-03	0.15	0.63
4 _{100/min}	2.318	8.25E-03	0.36	
4 _{200/min}	2.316	6.25E-03	0.27	
4 _{270/min}	2.318	8.25E-03	0.36	
4 _{300/min}	2.287	-2.28E-02	-0.98	0.66
5 _{100/min}	2.579	0.00E+00	0.00	
5 _{200/min}	2.596	1.70E-02	0.66	
5 _{270/min}	2.580	1.00E-03	0.04	
5 _{300/min}	2.561	-1.80E-02	-0.70	0.55
6 _{100/min}	2.744	1.40E-02	0.51	
6 _{200/min}	2.765	3.50E-02	1.28	
6 _{270/min}	2.754	2.40E-02	0.88	
6 _{300/min}	2.657	-7.30E-02	-2.67	1.81
7 _{100/min}	2.851	2.50E-04	0.01	
7 _{200/min}	2.890	3.93E-02	1.38	
7 _{270/min}	2.863	1.23E-02	0.43	
7 _{300/min}	2.799	-5.17E-02	-1.82	1.34
8 _{100/min}	3.085	3.03E-02	0.99	
8 _{200/min}	3.089	3.43E-02	1.12	
8 _{270/min}	3.054	-7.50E-04	-0.02	
8 _{300/min}	2.991	-6.37E-02	-2.09	1.48
9 _{100/min}	3.160	-3.10E-02	-0.97	
9 _{200/min}	3.214	2.30E-02	0.72	
9 _{270/min}	3.210	1.90E-02	0.60	
9 _{300/min}	3.180	-1.10E-02	-0.34	0.80
10 _{100/min}	3.543	3.13E-02	0.89	
10 _{200/min}	3.540	2.82E-02	0.80	
10 _{270/min}	3.502	-9.75E-03	-0.28	
10 _{300/min}	3.462	-4.98E-02	-1.42	1.08
Mean	2.205 %	SD 2.79E-02		SDrel 1.47 %

Table F-9: All the 10 samples were measured at each of the 4 velocities and then predicted. The plotted SD is the average of the within sample SDs.

Repetition	Predicted x_i [%]	$x_i - \bar{x}_i$	$\frac{(x_i - \bar{x}_i) \cdot 100}{\bar{x}_i}$	SD_{rel} within sample [%]
1 _{100/min}	0.590	-2.30E-02	-3.75	
1 _{200/min}	0.615	2.00E-03	0.33	
1 _{270/min}	0.634	2.10E-02	3.43	3.60
2 _{100/min}	0.634	-7.33E-03	-1.14	
2 _{200/min}	0.629	-1.23E-02	-1.92	
2 _{270/min}	0.661	1.97E-02	3.07	2.68
3 _{100/min}	2.048	-1.70E-02	-0.82	
3 _{200/min}	2.079	1.40E-02	0.68	
3 _{270/min}	2.068	3.00E-03	0.15	0.76
4 _{100/min}	2.318	6.67E-04	0.03	
4 _{200/min}	2.316	-1.33E-03	-0.06	
4 _{270/min}	2.318	6.67E-04	0.03	0.05
5 _{100/min}	2.579	-6.00E-03	-0.23	
5 _{200/min}	2.596	1.10E-02	0.43	
5 _{270/min}	2.580	-5.00E-03	-0.19	0.37
6 _{100/min}	2.744	-1.03E-02	-0.38	
6 _{200/min}	2.765	1.07E-02	0.39	
6 _{270/min}	2.754	-3.33E-04	-0.01	0.38
7 _{100/min}	2.851	-1.70E-02	-0.59	
7 _{200/min}	2.890	2.20E-02	0.77	
7 _{270/min}	2.863	-5.00E-03	-0.17	0.70
8 _{100/min}	3.085	9.00E-03	0.29	
8 _{200/min}	3.089	1.30E-02	0.42	
8 _{270/min}	3.054	-2.20E-02	-0.72	0.62
9 _{100/min}	3.160	-3.47E-02	-1.09	
9 _{200/min}	3.214	1.93E-02	0.61	
9 _{270/min}	3.210	1.53E-02	0.48	0.94
10 _{100/min}	3.543	1.47E-02	0.42	
10 _{200/min}	3.540	1.17E-02	0.33	
10 _{270/min}	3.502	-2.63E-02	-0.75	0.65
Mean	2.364 %	SD 1.68E-02		SD_{rel} 1.08 %

Table F-10: Table equivalent to Table C-27 without the highest measurement velocity of 300 samples per minute.

F.2.7 Quantitative model Product C 150 mg

F.2.7.1 Calibration set

Sample name	NIR [%]	KF [%]	Sample name	NIR [%]	KF [%]
T0051-3h-ODc-4	0.2	0.3	F0006-15min-ODd-8	1.8	1.6
T0051-3h-ODc-4	0.2	0.3	F0006-15min-ODd-8	1.8	1.6
B0052-3h-ODc-8s-3	0.3	0.3	F0006-15min-ODd-1	1.8	1.7
B0052-3h-ODc-8s-3	0.3	0.3	F0006-15min-ODd-1	1.8	1.7
B0052-3h-ODc-8s-3	0.2	0.3	F0006-15min-ODd-1	1.8	1.7
T0053-2h-ODc-1	0.4	0.4	F0048-41h-ODc-8s-4	1.7	1.7
T0053-2h-ODc-1	0.3	0.4	F0048-41h-ODc-8s-4	1.7	1.7
T0053-2h-ODc-1	0.4	0.4	F0048-41h-ODc-8s-4	1.7	1.7
T0053-2h-ODc-3	0.3	0.4	F0066-ODc-17min-1	1.8	1.7
T0053-2h-ODc-3	0.3	0.4	F0066-ODc-17min-1	1.7	1.7
T0053-2h-ODc-3	0.3	0.4	F0066-ODc-17min-1	1.8	1.7
T0051-3h-ODc-5	0.3	0.4	F0048-41h-ODc-8s-10	1.7	1.8
T0051-3h-ODc-5	0.4	0.4	F0048-41h-ODc-8s-6	1.6	1.8
T0053-2h-ODc-2	0.4	0.4	F0048-41h-ODc-8s-6	1.7	1.8
T0053-2h-ODc-2	0.3	0.4	F0048-41h-ODc-8s-6	1.6	1.8
T0053-2h-ODc-2	0.3	0.4	F0005-ODc-20min-5	1.8	1.8
B0005-ODc-2	0.8	0.8	F0005-ODc-20min-5	1.7	1.8
B0005-ODc-2	0.8	0.8	F0005-ODc-20min-5	1.7	1.8
B0005-ODc-2	0.9	0.8	F0066-ODc-17min-5	1.9	1.8
B1019-ODc-8s-2	0.9	0.8	F0066-ODc-17min-5	1.9	1.8
B1019-ODc-8s-2	0.8	0.8	B1007-15m-ODc-8s-2	1.8	1.8
B1019-ODc-8s-2	0.9	0.8	B1007-15m-ODc-8s-2	1.8	1.8
B0005-ODd-5	0.8	0.8	B1007-15m-ODc-8s-2	1.9	1.8
B0005-ODd-5	0.8	0.8	B1007-15m-ODc-8s-1	1.9	1.9
B0005-ODd-5	0.8	0.8	B1007-15m-ODc-8s-1	2.0	1.9
B0005-ODc-1	0.8	0.8	B1007-15m-ODc-8s-1	1.9	1.9
B0005-ODc-1	0.9	0.8	F0066-ODc-17min-3	2.0	1.9
B0005-ODc-1	0.9	0.8	B1007-15m-ODc-8s-4	1.9	1.9
B0005-ODd-6	0.9	0.8	B1007-15m-ODc-8s-4	2.0	1.9
B0005-ODd-6	0.8	0.8	B1007-15m-ODc-8s-4	1.9	1.9
B0005-ODd-6	0.8	0.8	F0005-ODc-20min-1	1.8	1.9
T0066-72h-ODc-4	0.9	0.8	F0005-ODc-20min-1	1.8	1.9
T0066-72h-ODc-4	0.9	0.8	F0005-ODc-20min-1	1.8	1.9
T0066-72h-ODc-4	0.9	0.8	B1007-15m-ODc-8s-5	1.9	1.9
B1019-ODc-8s-1	0.9	0.9	B1007-15m-ODc-8s-5	1.9	1.9
B1019-ODc-8s-1	0.8	0.9	B1007-15m-ODc-8s-5	1.9	1.9
B1019-ODc-8s-1	0.8	0.9	F0008-ODc-25min-4	1.9	2.0
B0008-ODc-1	1.0	0.9	F0008-ODc-25min-4	1.9	2.0
B0008-ODc-1	0.9	0.9	F0008-ODc-25min-4	1.9	2.0
B0008-ODc-1	1.0	0.9	F0008-ODc-25min-5	1.9	2.0
B0008-ODd-7	0.9	0.9	F0008-ODc-25min-5	1.9	2.0
B0008-ODd-7	0.9	0.9	F0008-ODc-25min-5	1.9	2.0
B0008-ODd-7	0.9	0.9	F0046-48h-ODc-8s-6	2.0	2.1
B0008-ODd-8	0.9	0.9	F0046-48h-ODc-8s-6	1.9	2.1

Sample name	NIR [%]	KF [%]	Sample name	NIR [%]	KF [%]
B0008-ODd-8	0.9	0.9	F0008-ODc-25min-1	2.1	2.1
B0008-ODd-8	0.9	0.9	F0008-ODc-25min-1	2.1	2.1
B0005-ODd-2	0.9	0.9	F0008-ODc-25min-1	2.1	2.1
B0005-ODd-2	0.9	0.9	F0066-25min-ODc-4	2.4	2.3
B0005-ODd-2	0.9	0.9	F1019-42m-ODc-8s-4	2.7	2.7
T0066-72h-ODc-8	1.0	0.9	F1019-42m-ODc-8s-1	2.7	2.8
T0066-72h-ODc-8	1.0	0.9	F1019-42m-ODc-8s-1	2.7	2.8
T0066-72h-ODc-8	1.0	0.9	F0005-45min-ODd-5	2.9	2.8
B0008-ODc-2	0.9	0.9	F0005-45min-ODd-5	2.8	2.8
B0008-ODc-2	1.0	0.9	F0005-45min-ODd-5	2.9	2.8
B0008-ODc-2	0.9	0.9	F1019-42m-ODc-8s-2	2.8	2.8
B0008-ODd-6	0.9	0.9	F1018-45m-ODc-8s-2	2.7	2.9
B0008-ODd-6	0.9	0.9	F1018-45m-ODc-8s-2	2.8	2.9
B0008-ODd-6	0.9	0.9	F1018-45m-ODc-8s-2	2.8	2.9
B0008-ODd-2	0.9	0.9	F0005-45min-ODd-8	2.9	2.9
B0008-ODd-2	0.9	0.9	F0005-45min-ODd-8	2.9	2.9
B0008-ODd-2	0.9	0.9	F0005-45min-ODd-8	2.9	2.9
T0066-72h-ODc-2	0.9	0.9	F1018-47m-ODc-8s-4	2.8	2.9
T0066-72h-ODc-2	0.9	0.9	F1018-47m-ODc-8s-4	2.9	2.9
T0066-72h-ODc-2	0.9	0.9	F0005-45min-ODd-6	2.9	2.9
B0007-ODd-3	1.1	0.9	F0005-45min-ODd-6	2.9	2.9
B0007-ODd-3	1.0	0.9	F0005-45min-ODd-6	2.8	2.9
B0007-ODd-3	1.0	0.9	F1018-47m-ODc-8s-2	2.9	3.0
T0066-72h-ODc-7	1.0	0.9	B0008-45m-ODc-8s-1	2.9	3.0
T0066-72h-ODc-7	1.0	0.9	B0008-45m-ODc-8s-1	3.0	3.0
T0066-72h-ODc-3	0.9	0.9	B0008-45m-ODc-8s-4	3.1	3.0
T0066-72h-ODc-3	0.9	0.9	B0008-45m-ODc-8s-4	3.1	3.0
T0066-72h-ODc-3	0.9	0.9	B0008-45m-ODc-8s-4	3.1	3.0
B0008-ODd-4	0.9	0.9	F1016-55m-ODc-8s-3	3.0	3.1
B0008-ODd-4	0.9	0.9	F1016-55m-ODc-8s-3	3.0	3.1
B0008-ODd-4	0.9	0.9	F1016-55m-ODc-8s-3	3.0	3.1
T0066-72h-ODc-1	0.9	1.0	F1018-45m-ODc-8s-1	2.9	3.1
T0066-72h-ODc-1	0.9	1.0	F1018-45m-ODc-8s-1	2.9	3.1
T0066-72h-ODc-1	0.9	1.0	F1018-45m-ODc-8s-1	2.9	3.1
B0007-ODd-7	1.0	1.0	F0007-ODc-50min-3	3.0	3.1
B0007-ODd-7	1.0	1.0	B0008-45m-ODc-8s-5	3.1	3.1
B0007-ODd-7	1.0	1.0	F1016-55m-ODc-8s-5	3.1	3.2
B0007-ODd-5	1.1	1.0	F1016-55m-ODc-8s-5	3.0	3.2
B0007-ODd-5	1.1	1.0	F1016-55m-ODc-8s-2	3.1	3.2
B0007-ODd-5	1.1	1.0	F1016-55m-ODc-8s-4	3.3	3.3
B0007-ODd-2	1.0	1.0	F1016-55m-ODc-8s-4	3.3	3.3
B0007-ODd-2	1.0	1.0	F1016-55m-ODc-8s-4	3.3	3.3
B0007-ODd-2	1.0	1.0	F0043-45min-ODd-9	3.6	3.7
B0007-ODd-10	1.0	1.0	F0043-45min-ODd-9	3.7	3.7
B0007-ODd-10	1.0	1.0	F0043-45min-ODd-9	3.6	3.7
B0007-ODd-10	1.0	1.0	F0052-70min-ODc-3	3.7	3.7
B0007-ODc-4	1.0	1.0	F0052-70min-ODc-3	3.7	3.7
B0007-ODc-4	1.0	1.0	F0052-70min-ODc-3	3.8	3.7

Sample name	NIR [%]	KF [%]	Sample name	NIR [%]	KF [%]
B0007-ODc-4	1.0	1.0	F0069-60m-ODc-8s-2	4.0	3.8
B0007-ODd-6	1.1	1.1	F0069-60m-ODc-8s-2	3.7	3.8
B0007-ODd-6	1.1	1.1	F0069-60m-ODc-8s-2	4.0	3.8
B0007-ODd-6	1.1	1.1	F0049-65min-ODc-3	3.9	3.8
B0007-ODd-9	1.1	1.1	F0049-65min-ODc-3	3.8	3.8
B0007-ODd-9	1.1	1.1	F0049-65min-ODc-3	3.9	3.8
B0007-ODd-9	1.1	1.1	F0052-70min-ODc-1	4.0	3.9
B0007-ODd-8	1.1	1.1	F0052-70min-ODc-1	4.0	3.9
B0007-ODd-8	1.1	1.1	F0052-70min-ODc-1	3.9	3.9
B0007-ODd-8	1.1	1.1	F0049-65min-ODc-1	4.1	4.0
F0048-ODc-5min-3	1.1	1.1	F0049-65min-ODc-1	4.1	4.0
F0048-ODc-5min-3	1.2	1.1	F0049-65min-ODc-1	3.9	4.0
F0006-ODc-8min-4	1.3	1.4	F0069-60m-ODc-8s-1	4.2	4.0
F0006-ODc-8min-4	1.3	1.4	F0069-60m-ODc-8s-1	4.0	4.0
F0006-ODc-8min-4	1.3	1.4	F0069-60m-ODc-8s-1	4.2	4.0
F0006-ODc-8min-3	1.3	1.4	F1052-60min-ODd-1	4.5	4.5
F0006-ODc-8min-3	1.3	1.4	F1052-60min-ODd-1	4.4	4.5
F0006-ODc-8min-3	1.3	1.4	F1052-60min-ODd-1	4.5	4.5
F0050-ODc-10min-1	1.4	1.5	F1052-60min-ODd-8	4.4	4.5
F0050-ODc-10min-1	1.3	1.5	F1052-60min-ODd-8	4.5	4.5
F0050-ODc-10min-1	1.3	1.5	F1052-60min-ODd-8	4.5	4.5
F0008-10min-ODc-4	1.7	1.5	F0047-75min-ODd-4	4.6	4.6
F0008-10min-ODc-4	1.7	1.5	F0047-75min-ODd-4	4.6	4.6
F0008-10min-ODc-4	1.6	1.5	F0047-75min-ODd-4	4.6	4.6
F0008-10min-ODc-2	1.7	1.5	F0047-75min-ODd-8	4.7	4.6
F0008-10min-ODc-2	1.6	1.5	F0047-75min-ODd-8	4.5	4.6
F0008-10min-ODc-2	1.6	1.5	F0047-75min-ODd-8	4.5	4.6
F0050-ODc-10min-3	1.4	1.6	F0047-75min-ODd-2	4.6	4.6
F0050-ODc-10min-3	1.4	1.6	F0047-75min-ODd-2	4.6	4.6
F0006-15min-ODd-6	1.8	1.6	F0047-75min-ODd-2	4.6	4.6
F0006-15min-ODd-6	1.8	1.6	F0047-75min-ODd-3	4.6	4.6
F0006-15min-ODd-6	1.8	1.6	F0047-75min-ODd-3	4.5	4.6
F0006-15min-ODd-8	1.8	1.6			

F.2.7.2 External validation set

Sample name	NIR	KF [%]	Dev.	Sample name	NIR	KF [%]	Dev.
B0005-ODd-4	0.9	0.8	0.1	F0048-41h-ODc-8s-2	1.8	1.8	-0.1
B0005-ODd-4	0.9	0.8	0.1	F0048-41h-ODc-8s-2	1.7	1.8	-0.1
B0005-ODd-4	0.9	0.8	0.1	F0048-41h-ODc-8s-5	1.8	1.9	-0.1
B0005-ODd-7	1.0	0.8	0.1	F0048-41h-ODc-8s-5	1.8	1.9	-0.1
B0005-ODd-7	1.0	0.8	0.1	F0048-41h-ODc-8s-5	1.8	1.9	-0.1
B0005-ODd-7	0.9	0.8	0.1	F0050-20min-ODc-5	2.1	1.9	0.2
B0008-ODd-5	0.9	0.8	0.1	F0050-20min-ODc-5	2.1	1.9	0.2
B0008-ODd-5	0.9	0.8	0.1	F0050-20min-ODc-5	2.1	1.9	0.2
B0008-ODd-5	0.9	0.8	0.1	F0066-ODc-17min-2	1.6	1.9	-0.3
B1019-ODc-8s-4	0.8	0.9	0.0	F0066-ODc-17min-2	1.7	1.9	-0.2
B1019-ODc-8s-4	0.8	0.9	0.0	F0066-ODc-17min-2	1.7	1.9	-0.2
B1019-ODc-8s-4	0.9	0.9	0.0	F0046-48h-ODc-8s-3	1.9	1.9	0.0
B0005-ODc-3	0.9	0.9	0.0	F0046-48h-ODc-8s-3	1.9	1.9	-0.1
B0005-ODc-3	0.9	0.9	0.0	F0046-48h-ODc-8s-3	1.9	1.9	-0.1
B0005-ODc-3	0.9	0.9	0.0	F0005-ODc-20min-3	1.7	1.9	-0.2
B0005-ODd-3	0.9	0.9	0.1	F0005-ODc-20min-3	1.6	1.9	-0.3
B0005-ODd-3	0.9	0.9	0.0	F0005-ODc-20min-3	1.7	1.9	-0.2
B0005-ODd-3	0.9	0.9	0.1	F0046-48h-ODc-8s-1	1.9	2.0	-0.1
B0008-ODd-3	0.9	0.9	0.0	F0046-48h-ODc-8s-1	2.0	2.0	0.0
B0008-ODd-3	0.9	0.9	0.0	F0046-48h-ODc-8s-1	1.9	2.0	-0.1
B0008-ODd-3	0.9	0.9	0.0	F0008-ODc-25min-3	1.9	2.0	-0.1
B0008-ODd-9	1.0	0.9	0.2	F0008-ODc-25min-3	2.0	2.0	-0.1
B0008-ODd-9	1.0	0.9	0.2	F0008-ODc-25min-3	1.9	2.0	-0.1
B0008-ODd-9	1.0	0.9	0.1	F0046-48h-ODc-8s-7	1.9	2.1	-0.2
T0066-72h-ODc-10	1.0	0.9	0.1	F0046-48h-ODc-8s-7	1.9	2.1	-0.2
T0066-72h-ODc-10	1.0	0.9	0.1	F0046-48h-ODc-8s-7	1.9	2.1	-0.2
T0066-72h-ODc-10	0.9	0.9	0.0	F0066-25min-ODc-2	2.3	2.1	0.2
B0005-ODd-8	0.8	0.9	-0.1	F0066-25min-ODc-2	2.3	2.1	0.1
B0005-ODd-8	0.8	0.9	-0.1	F0066-25min-ODc-2	2.3	2.1	0.1
B0005-ODd-8	0.9	0.9	-0.1	F0066-25min-ODc-5	2.5	2.2	0.3
T0066-72h-ODc-5	1.0	0.9	0.0	F0066-25min-ODc-5	2.5	2.2	0.3
T0066-72h-ODc-5	1.0	0.9	0.1	F0066-25min-ODc-5	2.5	2.2	0.3
T0066-72h-ODc-5	1.0	0.9	0.1	F0066-25min-ODc-1	2.3	2.3	0.0
B1016-ODc-8s-1	0.8	0.9	-0.1	F0066-25min-ODc-1	2.3	2.3	0.0
B1016-ODc-8s-1	0.8	0.9	-0.1	F0066-25min-ODc-1	2.3	2.3	0.0
B1016-ODc-8s-1	0.8	0.9	-0.1	F1018-35m-ODc-8s-4	2.5	2.6	-0.1
B1018-ODc-8s-2	0.9	0.9	-0.1	F1018-35m-ODc-8s-4	2.6	2.6	0.0
B1018-ODc-8s-2	0.8	0.9	-0.1	F1018-35m-ODc-8s-4	2.5	2.6	-0.1
B1018-ODc-8s-2	0.8	0.9	-0.1	F1018-35m-ODc-8s-5	2.6	2.7	-0.1
T0066-72h-ODc-9	1.0	0.9	0.1	F1018-35m-ODc-8s-5	2.7	2.7	0.0
T0066-72h-ODc-9	1.0	0.9	0.1	F1018-35m-ODc-8s-5	2.7	2.7	-0.1
T0066-72h-ODc-9	1.0	0.9	0.0	F1018-35m-ODc-8s-2	2.5	2.7	-0.2
B0007-ODd-1	1.1	1.0	0.1	F1018-35m-ODc-8s-2	2.6	2.7	-0.1
B0007-ODd-1	1.1	1.0	0.1	F1018-35m-ODc-8s-2	2.5	2.7	-0.2
B0007-ODd-1	1.1	1.0	0.1	F0005-45min-ODd-4	3.0	2.7	0.3
B1016-ODc-8s-3	0.8	1.0	-0.1	F0005-45min-ODd-4	3.0	2.7	0.2

Sample name	NIR	KF [%]	Dev.	Sample name	NIR	KF [%]	Dev.
B1016-ODc-8s-3	0.8	1.0	-0.1	F0005-45min-ODd-4	3.0	2.7	0.3
B1016-ODc-8s-3	0.8	1.0	-0.1	F0005-45min-ODd-9	2.9	2.8	0.1
B0007-ODd-4	1.2	1.0	0.1	F0005-45min-ODd-9	2.9	2.8	0.2
B0007-ODd-4	1.1	1.0	0.1	F0005-45min-ODd-9	2.9	2.8	0.2
B0007-ODd-4	1.1	1.0	0.1	F0005-45min-ODd-10	3.0	2.8	0.2
B0007-ODc-3	1.0	1.0	0.0	F0005-45min-ODd-10	3.1	2.8	0.3
B0007-ODc-3	1.0	1.0	-0.1	F0005-45min-ODd-10	3.2	2.8	0.3
B0007-ODc-3	1.0	1.0	0.0	F1019-42m-ODc-8s-5	2.6	2.8	-0.3
B1018-ODc-8s-4	0.9	1.1	-0.2	F1019-42m-ODc-8s-5	2.6	2.8	-0.2
B1018-ODc-8s-4	0.8	1.1	-0.3	F1019-42m-ODc-8s-5	2.5	2.8	-0.3
B1018-ODc-8s-4	0.8	1.1	-0.2	F0069-30m-ODc-8s-2	3.0	2.8	0.1
B0007-ODc-2	1.1	1.1	0.0	F0069-30m-ODc-8s-2	3.0	2.8	0.1
B0007-ODc-2	1.2	1.1	0.1	F0069-30m-ODc-8s-2	3.0	2.8	0.2
B0007-ODc-2	1.2	1.1	0.1	F0049-40min-ODc-1	3.0	2.9	0.1
F0048-ODc-5min-1	1.1	1.2	-0.1	F0049-40min-ODc-1	3.0	2.9	0.1
F0048-ODc-5min-1	1.1	1.2	-0.1	F0049-40min-ODc-1	3.0	2.9	0.1
F0048-ODc-5min-1	1.0	1.2	-0.1	F0005-45min-ODd-2	2.7	2.9	-0.2
F1016-7m-ODc-8s-2	1.2	1.2	0.0	F0005-45min-ODd-2	2.7	2.9	-0.2
F1016-7m-ODc-8s-2	1.2	1.2	-0.1	F0005-45min-ODd-2	2.7	2.9	-0.2
F1016-7m-ODc-8s-2	1.2	1.2	-0.1	F0005-45min-ODd-3	2.8	2.9	-0.1
F0006-ODc-8min-5	1.3	1.3	0.0	F0005-45min-ODd-3	2.8	2.9	-0.1
F0006-ODc-8min-5	1.3	1.3	-0.1	F0005-45min-ODd-3	2.8	2.9	-0.1
F0006-ODc-8min-5	1.3	1.3	0.0	F1018-45m-ODc-8s-5	2.7	2.9	-0.2
F0006-ODc-8min-2	1.5	1.4	0.1	F1018-45m-ODc-8s-5	2.7	2.9	-0.3
F0006-ODc-8min-2	1.4	1.4	0.0	F1018-45m-ODc-8s-5	2.6	2.9	-0.3
F0006-ODc-8min-2	1.5	1.4	0.0	F0005-45min-ODd-1	3.4	3.0	0.5
F0050-ODc-10min-4	1.3	1.4	-0.1	F0005-45min-ODd-1	3.6	3.0	0.6
F0050-ODc-10min-4	1.4	1.4	-0.1	F0005-45min-ODd-1	3.5	3.0	0.6
F0050-ODc-10min-4	1.4	1.4	0.0	F1019-42m-ODc-8s-3	2.8	3.0	-0.2
F1016-7m-ODc-8s-4	1.5	1.5	0.0	F1019-42m-ODc-8s-3	2.7	3.0	-0.3
F1016-7m-ODc-8s-4	1.4	1.5	-0.1	F1019-42m-ODc-8s-3	2.8	3.0	-0.2
F1016-7m-ODc-8s-4	1.5	1.5	0.0	F0007-ODc-50min-2	3.2	3.0	0.2
F1016-5m-ODc-8s-4	1.2	1.5	-0.3	F0007-ODc-50min-2	3.1	3.0	0.1
F1016-5m-ODc-8s-4	1.2	1.5	-0.3	F0007-ODc-50min-2	3.1	3.0	0.1
F1016-5m-ODc-8s-4	1.2	1.5	-0.3	F1018-45m-ODc-8s-3	2.9	3.0	-0.2
F0050-ODc-10min-2	1.5	1.5	0.0	F1018-45m-ODc-8s-3	3.0	3.0	-0.1
F0050-ODc-10min-2	1.4	1.5	-0.1	F1018-45m-ODc-8s-3	3.1	3.0	0.0
F0050-ODc-10min-2	1.5	1.5	0.0	F0007-ODc-50min-4	2.7	3.1	-0.3
F0008-10min-ODc-3	1.8	1.6	0.3	F0007-ODc-50min-4	2.8	3.1	-0.3
F0008-10min-ODc-3	1.8	1.6	0.2	F0007-ODc-50min-4	2.8	3.1	-0.2
F0008-10min-ODc-3	1.8	1.6	0.3	F0006-55min-ODc-3	3.4	3.1	0.3
F0006-15min-ODd-3	1.8	1.6	0.2	F0006-55min-ODc-3	3.3	3.1	0.2
F0006-15min-ODd-3	1.7	1.6	0.2	F0006-55min-ODc-3	3.3	3.1	0.2
F0006-15min-ODd-3	1.7	1.6	0.2	F0006-55min-ODc-1	3.3	3.1	0.1
F0006-15min-ODd-2	1.8	1.6	0.2	F0006-55min-ODc-1	3.3	3.1	0.1
F0006-15min-ODd-2	1.7	1.6	0.1	F0006-55min-ODc-1	3.3	3.1	0.1
F0006-15min-ODd-2	1.8	1.6	0.2	F0007-ODc-50min-5	3.0	3.2	-0.2
F0006-15min-ODd-4	1.8	1.7	0.2	F0007-ODc-50min-5	2.9	3.2	-0.3

Sample name	NIR	KF [%]	Dev.	Sample name	NIR	KF [%]	Dev.
F0006-15min-ODd-4	1.8	1.7	0.1	F0007-ODc-50min-5	3.0	3.2	-0.2
F0006-15min-ODd-4	1.8	1.7	0.1	F1016-55m-ODc-8s-1	3.1	3.2	0.0
F0048-41h-ODc-8s-1	1.7	1.7	0.0	F1016-55m-ODc-8s-1	3.2	3.2	0.0
F0048-41h-ODc-8s-1	1.6	1.7	-0.1	F1016-55m-ODc-8s-1	3.3	3.2	0.1
F0048-41h-ODc-8s-1	1.7	1.7	0.0	F0043-45min-ODd-6	3.7	3.7	0.0
F0048-41h-ODc-8s-3	1.7	1.7	-0.1	F0043-45min-ODd-6	3.6	3.7	-0.1
F0048-41h-ODc-8s-3	1.7	1.7	-0.1	F0043-45min-ODd-6	3.6	3.7	-0.1
F0048-41h-ODc-8s-3	1.7	1.7	-0.1	F0052-70min-ODc-4	3.5	3.8	-0.3
F0048-41h-ODc-8s-7	1.7	1.8	-0.1	F0052-70min-ODc-4	3.6	3.8	-0.1
F0048-41h-ODc-8s-7	1.8	1.8	0.0	F0052-70min-ODc-4	3.6	3.8	-0.2
F0048-41h-ODc-8s-7	1.8	1.8	0.0	F0052-70min-ODc-5	3.7	3.8	-0.1
F0005-ODc-20min-4	1.7	1.8	-0.1	F0052-70min-ODc-5	3.7	3.8	-0.1
F0005-ODc-20min-4	1.9	1.8	0.1	F0052-70min-ODc-5	3.7	3.8	-0.1
F0005-ODc-20min-4	1.8	1.8	0.0	F0049-65min-ODc-2	3.9	3.9	0.0
F0048-41h-ODc-8s-2	1.7	1.8	-0.1	F0049-65min-ODc-2	3.9	3.9	0.0
						Bias = 0.00611	

F.3 Conversion of wavelength units

$$\text{Wavelength [nm]} = \frac{10,000,000}{\text{Wavenumber [cm}^{-1}\text{]}}$$

Equation F-17: Conversion formula for wavenumbers to wavelength units.

Wavelength [nm]	Wavenumbers [cm ⁻¹]
800.0	12,500.0
900.0	11,111.1
1,000.0	10,000.0
1,100.0	9,090.9
1,200.0	8,333.3
1,300.0	7,692.3
1,400.0	7,142.9
1,500.0	6,666.7
1,600.0	6,250.0
1,700.0	5,882.4
1,800.0	5,555.6
1,900.0	5,263.2
2,000.0	5,000.0
2,100.0	4,761.9
2,200.0	4,545.5
2,300.0	4,347.8
2,400.0	4,166.7
2,500.0	4,000.0

Equation F-18: Conversion table of wavelengths to wavenumbers.

Curriculum vitae

Personal information

Name	Lars Sukowski
Date of birth	June 10, 1976
Place of birth	Tubingen, Germany
Parents	Ingolf Sukowski Heide Sukowski

Education

2001 - 2003	Ph.D. Program at F. Hoffmann-La Roche Ltd., Basel, in collaboration with the Institute of Pharmaceutical Technology, Pharmacenter University of Basel, Switzerland
1996 - 2001	Institute of Pharmacy, University of Hamburg, Germany Studies in pharmaceutical sciences (3 state examinations with University degree of 'Approbierter Apotheker')
1986 - 1995	Gymnasium Harksheider Strasse, High School, Hamburg, Germany
1982 - 1986	Ludwig Frahm Schule, Elementary School, Hamburg, Germany

Work Experience

August 2001 - present	F. Hoffmann-La Roche Ltd., Basel, Switzerland Project Manager, conduction of analytics, automation, administrative requirements and investment procurement
March 1999 - April 2001	Privilegierte Adler Apotheke, Hamburg, Germany Practical experience in Hamburg's first ISO 9001 certified public pharmacy with sterile room, participated at special

activities at external exhibitions with intense, regular patient contact

- May – October 2000 F. Hoffmann-La Roche Ltd., Basel, Switzerland
Pharmaceutical liquids production, introduced new sterile filter model, installed appropriate test station and trained employees, planned in-line integrity testing
- August – October 1999 F. Hoffmann-La Roche Ltd., Basel, Switzerland
Internship in pharmaceutical liquids production, improved handling procedures of sterile filtration, assisted line manager in technical and organizational issues
- August 1997 Zentralapotheke Kreiskrankenhaus Starnberg,
Community of Munich, Germany
Offered technical support in laboratory and electronic data processing for a central pharmacy which supplied all hospitals in a Bavarian district

Training and Seminars (selection)

- Multivariate Data Analysis, Principle Component Analysis and Partial Least Squares, Umetrics UK Ltd., Bath, UK, November 6 - 8, 2001
- Multivariate Data Analysis and Modeling - Advanced Course by Svante Wold and Nouna Kettaneh-Wold, Umetrics UK Ltd., Englefield Green, UK, February 4 - 6, 2003
- Operation and Calibration Training, ABB Bomem, Basel, Switzerland, March 12, 2002
- NIR Spectroscopy and Chemometrics, Training Chemometrics on the base of CAMO Unscrambler for NIR Spectroscopy, Labor Chemie, Vienna, Austria, 10 - 11 June, 2002

- Der Pharma Experte mit APV-Diplom: Qualitätskontrolle, Pharmazeutische entwicklung: Basistraining Qualifizierung und Kalibrierung analytischer Geräte (Course No. 528), Arbeitsgemeinschaft für Pharmazeutische Verfahrenstechnik e. V. (APV), Darmstadt, Germany, November 14, 2001
- NIR Spektroskopie in der pharmazeutischen Praxis: Applikationsbeispiele aus Qualitätskontrolle, Entwicklung und Produktion, Arbeitsgemeinschaft für Pharmazeutische Verfahrenstechnik e. V. (APV), Nuremberg, Germany, October 8 - 9, 2002
- Pharma-Business and Pharma-Marketing for Beginners, Pharmacenter, Center of Pharmaceutical Sciences Basel-Zürich, Basel/Zurich, Switzerland, September 12 - 13 and 19 - 20, 2002

Conferences and Meetings

- NIR 2003, 11th International Conference on Near Infrared Spectroscopy, Stretching the NIR Spectrum to the Limit, University of Cordoba, Cordoba, Spain, April 6 - 11, 2003
- 12. NIR Meeting, Büchi Labortechnik GmbH, Basel, Switzerland, September 17 - 18, 2002
- Pharma Seminar: The Use of 'On-Line Analysis' to Increase Plant Capacity and Improve Product Quality in Pharmaceutical Production, Carl Zeiss Jena GmbH, Freiburg, Germany, May 16, 2002
- 4th World Meeting on Pharmaceutics, Biopharmaceutics and Pharmaceutical Technology, ADTRITELF, APGI and APV, Florence, Italy, April 8 - 11, 2002
- State of the Art Process Analytics: A Practical View, in cooperation of Solvias AG and Bruker Optics, Basel, Switzerland, November 21, 2001
- 11th NIR Meeting, Büchi Labortechnik GmbH, Frankfurt, Germany, September 25 - 26, 2001

Others

- Active Compliance Document Manager, Roche IT Training Center, Kaiseraugst, Switzerland, December 12 and 13, 2001
- Excel 97 Workshop - Statistische Funktionen, Roche IT Training Center, Kaiseraugst, Switzerland, April 5, 2002
- English conversation course, NSH Bildungszentrum Basel and F. Hoffmann-La Roche Ltd., Basel, Switzerland, Spring/Summer, 2002
- Spanish beginner's course, NSH Bildungszentrum Basel and F. Hoffmann-La Roche Ltd., Basel, Switzerland, Autumn/Winter, 2003

Publication and Presentation

- Sukowski L., Ulmschneider M., Near Infrared Spectroscopy: High Speed Noninvasive Qualification of Lyophilized Vials, NIR 2003, 11th International Conference on Near Infrared Spectroscopy, Stretching the NIR Spectrum to the Limit, University of Cordoba, Cordoba, Spain, April 6 - 11, 2003
- The orally presented paper will appear in the proceedings of the NIR 2003, Near Infrared Spectroscopy: Proceedings of the 11th International Conference, NIR Publications, 2003

Posters

- Sukowski L., Ulmschneider M., Marrer S., Leuenberger H., Online Near-Infrared Spectroscopy: Noninvasive Determination of Residual Moisture in Entire Batches of Lyophilized Pharmaceutical Products, poster presentation at 12th NIR Meeting, Büchi Labortechnik GmbH, Basel, Switzerland, September 17 - 18, 2002
- Sukowski L., Ulmschneider M., Leuenberger H., Near-Infrared Spectroscopy: Non-Invasive Qualification of Lyophilized Vials, Pharmaday, Pharmacenter University of Basel, Switzerland, July 11, 2003

Supervision of Internals

February - June 2003	Pascal Chalus, Ecole Nationale Supérieur de Chimie de Mulhouse (ENSCM), France, targeted degree: Chemistry Engineer, DEA
April - July 2003	Florence Piétrain, Ecole Nationale Supérieur de Chimie de Lille (ENSCL), France, targeted degree: Chemistry Engineer
July - October 2003	Aurélie Edmond, Brevet de Technicien Supérieur Agricole (BTSA), France

Language Skills

German	mother-tongue
English	very good
French	excellent